GEOLOGICAL SURVEY OF CANADA
COMMISSION GÉOLOGIQUE DU CANADA

PAPER 78-1C

This document was produced
by scanning the original publication.

Ce document est le produit d'une
numérisation par balayage
de la publication originale.

CURRENT RESEARCH
PART C

Energy, Mines and Resources Canada
Énergie, Mines et Ressources Canada

1978

Notice to Librarians and Indexers

The Geological Survey's thrice-yearly "Current Research" series contains many reports comparable in scope and subject matter to those appearing in scientific journals and other serials. All contributions to the Scientific and Technical Report section of "Current Research" include an abstract and bibliographic citation. It is hoped that these will assist you in cataloguing and indexing these reports and that this will result in a still wider dissemination of the results of the Geological Survey's research activities.

Technical editing and compilation
R.G. Blackadar
P.J. Griffin
H. Dumych
E.R.W. Neale

Production editing and layout
Leona R. Mahoney
Lorna A. Firth
Michael J. Kiel

Typed and checked by
Debby Busby
Janet Gilliland
Suzanne Lalonde
Janet Legere
Sharon Parnham



GEOLOGICAL SURVEY
PAPER 78-1C

CURRENT RESEARCH
PART C

1978

© Minister of Supply and Services Canada 1978

available by mail from

Printing and Publishing
Supply and Services Canada,
Hull, Québec, Canada K1A 0S9,

and

The Geological Survey of Canada
601 Booth St., Ottawa, K1A 0E8

or

Through your bookseller.

Catalogue No. M44-78/1C
ISBN - 0-660-10031-2

Price: Canada: $3.00
Other Countries: $3.60

Price subject to change without notice

I : SCIENTIFIC AND TECHNICAL REPORTS

Page

1. W.F. FAHRIG, K.W. CHRISTIE, and G. FREDA: The paleolatitude and paleomagnetic age of the Athabasca Formation, northern Saskatchewan 1

2. SUBHAS TELLA and K.E. EADE: Coexisting cordierite-gedrite-cummingtonite from Edehon Lake map area, Churchill Structural Province, District of Keewatin 7

3. K.G. NEAVE, A.S. JUDGE, J.A. HUNTER, and H.A. MACAULAY: Offshore permafrost distribution in the Beaufort Sea as determined from temperature and seismic observations 13

4. JOHN. G. CONAWAY: Problems in gamma-ray logging: Thin zone correction factors 19

5. S.H. RICHARD: Age of Champlain Sea and "Lampsilis Lake" episode in the Ottawa-St. Lawrence Lowlands 23

6. R.M. CLOWES, A.J. THORLEIFSON, and S. LYNCH: Interpretation of a marine deep seismic sounding survey in Winona Basin off the West Coast of Canada 29

7. H.R. BALKWILL and N.E. HAIMILA: K/Ar ages and significance of mafic rocks, Sabine Peninsula, Melville Island, District of Franklin 35

8. T.P. POULTON: Correlation of the Jurassic Bug Creek Formation in the subsurface of the Mackenzie Delta, District of Mackenzie 39

9. H.H.J. GELDSETZER: The Windsor Group in Atlantic Canada – An update 43

10. A.C.ROBERTS: Mineralogical study of an unnamed barium calcium carbonate from the Cave-in-Rock District, Illinois 49

11. JEAN-SERGE VINCENT: Limits of ice advance, glacial lakes, and marine transgressions on Banks Island, District of Franklin: A preliminary interpretation 53

12. J.T. TAN and L.V. HILLS: Oxfordian-Kimmeridgian dinoflagellate assemblage, Ringnes Formation, Arctic Canada 63

13. R.S. TIPNIS: Early Middle Ordovician conodonts of North Atlantic Province from northeastern Ellesmere Island, Arctic Canada 75

14. SUBHAS TELLA and W.W. HEYWOOD: The structural history of the Amer Mylonite Zone, Churchill Structural Province, District of Keewatin 79

15. R.A. FRITH and J.A. PERCIVAL: Stratigraphy of the Yellowknife supergroup in the Mara-Back rivers area, District of Mackenzie 89

II : SCIENTIFIC AND TECHNICAL NOTES

Page

G. VILKS and S.A. SWIFT: Sampling of Bottom sediments in the Equatorial Pacific following test manganese mining 99

S. CREANEY: Spores fluorescence colouration - A rapid microscopic method of maturation assessment 101

A.C. ROBERTS: An orthorhombic unit cell for tlalocite 104

R.J. RICHARDSON: Observations on the paleomagnetism of some sediments from Ellesmere and Devon islands, District of Franklin 105

B.D. BORNHOLD: Carbon/Nitrogen (C/N) ratios in surficial marine sediments of British Columbia 108

J.W.H. MONGER, M. BONARDI, and A.G. PLANT: Composition of pyroxene phenocrysts from Lower Mesozoic volcanics, north-central British Columbia ... 113

K. HINZ, H.-U. SCHLUTER, A.C. GRANT, S.P. SRIVASTAVA, D. UMPLEBY, and J. WOODSIDE: Multichannel reflection seismic survey in the Labrador Sea 118

W. BLAKE, JR.: Coring of Holocene pond sediments at Cape Herschel, Ellesmere Island, Arctic Archipelago 119

A.G. FABBRI, T. KASVAND, and J.H. STRAY: Implementation of an interactive system for computer processing of geological images 123

D.L. MARCHIONI: The effect on vitrinite reflectance of elevated temperatures during sample preparation 125

III : DISCUSSIONS AND COMMUNICATIONS

W.D. BRUCKNER: Carmanville map area, Newfoundland; the northeastern end of the Appalachians – Discussion 127

R.K. PICKERILL and G.E. PAJARI: Carmanville map area, Newfoundland; the northeastern end of the Appalachians – Reply 129

AUTHOR INDEX 133

The Geological Survey of Canada

D.J. McLAREN, Director General

J.O. WHEELER, Deputy Director General

E. HALL, Scientific Executive Officer

M.J. KEEN, Director, Atlantic Geoscience Centre, Dartmouth, Nova Scotia

J.A. MAXWELL, Director, Central Laboratories and Administrative Services Division

PETER HARKER, Director, Geological Information Division

D.F. STOTT, Director, Institute of Sedimentary and Petroleum Geology, Calgary, Alberta

J.E. REESOR, Director, Regional and Economic Geology Division

A.G. DARNLEY, Director, Resource Geophysics and Geochemistry Division

J.S. SCOTT, Director, Terrain Sciences Division

Separates

A limited number of separates of the papers that appear in this volume are available by direct request to the individual authors. The addresses of the Geological Survey of Canada offices follow:

601 Booth Street,
OTTAWA, Ontario
K1A 0E8

Institute of Sedimentary and Petroleum Geology,
3303-33rd Street N.W.,
CALGARY, Alberta
T2L 2A7

British Columbia Office,
100 West Pender Street,
VANCOUVER, B.C.
V6B 1R8

Atlantic Geoscience Centre,
Bedford Institute of Oceanography,
P.O. Box 1006,
DARTMOUTH, N.S.
B2Y 4A2

When no location accompanies an author's name in the title of a paper, the Ottawa address should be used.

1. THE PALEOLATITUDE AND PALEOMAGNETIC AGE OF THE ATHABASCA FORMATION, NORTHERN SASKATCHEWAN

Project 680135

W.F. Fahrig, K.W. Christie, and G. Freda
Regional and Economic Geology Division

Fahrig, W.F., Christie, K.W., and Freda, G., The paleolatitude and paleomagnetic age of the Athabasca Formation, northern Saskatchewan; in Current Research, Part C, Geol. Surv. Can., Paper 78-1C, p. 1-6, 1978.

Abstract

Paleomagnetic study indicates that the Athabasca Formation of northern Saskatchewan, Canada, was deposited about 1550 or about 1700 Ma ago at a latitude of 39°. A Rb/Sr isochron on regolith from below the Athabasca (R.K. Wanless, pers. comm., 1977) suggests that the younger age is correct. Reversals in the polarity of the earth's field occurred a number of times during deposition of the formation and these promise to be of value in the chronostratigraphic correlation of redbed units within the formation.

Introduction

The Athabasca Formation (Fahrig, 1961; Fraser et al., 1970) overlies approximately 77 700 km^2 of crystalline basement rocks of the Churchill Orogen in northern Saskatchewan. It is composed chiefly of orthoquartzite and has a maximum preserved thickness of about 1525 m. In recent years three significant uranium deposits have been discovered at or near the unconformity between the Athabasca and the underlying gneissic rocks. Two of these are on the eastern and southeastern margin of the basin, the third is exposed in the Carswell structure as a result of meteorite impact (Innis, 1964; Robertson et al., 1968). The close association of these deposits with the unconformity has led to speculation that vast uranium deposits may occur at this surface elsewhere within the basin, or possibly in suitable traps within the formation itself. There is special interest then in determining the age of sedimentation, the correlation of units within the Athabasca, and the depositional environment of the formation.

The first discovery of a significant uranium deposit (Rabbit Lake) at or near the unconformity initiated an extensive exploratory drilling program within the basin in the late 1960s and early 1970s. Sections were obtained from a number of essentially vertical drill cores and paleomagnetic study has been carried out on suitable material (chiefly dark maroon siltstone, or silty sandstone) from a number of the cores. These cores are not oriented in the horizontal plane; however, knowledge of the Middle and Upper Proterozoic North American Precambrian polar wandering path has reached the stage where paleomagnetic inclinations alone can provide significant data on the age, as well as on the paleolatitude of sedimentation.

Paleomagnetic Results

Figure 1.1 shows the location of the drill sites from which material was obtained for paleomagnetic study, and Table 1.1 and Figure 1.3, the results obtained from detailed thermal demagnetization of the 31 samples. The dominant carrier of magnetization is hematite, and 29 of the 31 samples proved to be stably magnetized.

The 29 samples fall into two groups, by far the larger of which (21 samples) is Group I of Table 1.1. The samples of this group are well distributed throughout the basin, both areally and vertically. They include hematized regolith from below the sediments, and have a mean inclination of 58°, with k=18, using the statistical method of Briden and Ward (1966) for borehole data. Nine of these specimens have a north-seeking up direction, and 12 a north-seeking down direction.

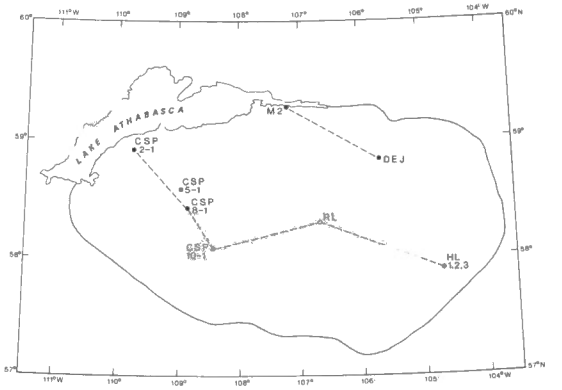


Figure 1.1. Index map showing the extent of the Athabasca Formation and the locations of drillholes from which core was obtained for paleomagnetic study.

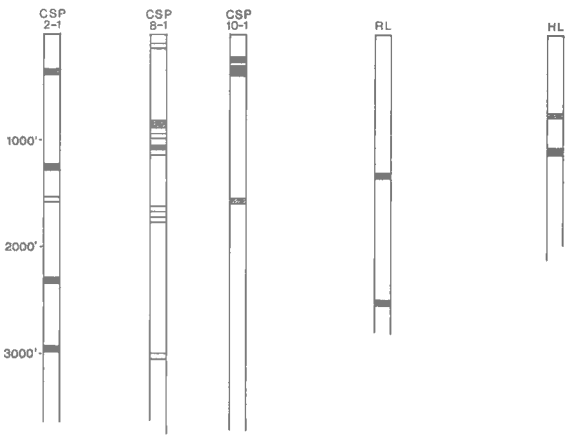


Figure 1.2. Depths of reversely magnetized layers of Group I, Table 1.1 (open rectangles), normally magnetized layers of Group I, Table 1.1 (solid rectangles) and layers of Group II, Table 1.1, whose magnetization is near the horizontal (cross-hatched rectangles).

Table 1.1

Thermal Demagnetization Results

Temperature °C	20°	300°	350°	450°	560°	610°	635°	660°	670°	675°
				INCLINATION AND CHANGE IN DECLINATION						
				GROUP I						
Sample Number										
CSP 1269	+58	+57(+17)	+56(-4)	+61(-1)	+62(-3)	+63(+1)	+64(0)	+64(+1)	+64(+2)	
2-1 1556	-50	-49(+4)	-50(-2)	-51(-2)	-56(+2)	-58(0)	-58(0)	-58(+1)	-58(0)	
2316	+74	+71(+105)	+68(-44)	+80(+30)	+81(-41)	+79(+36)	+80(-14)	+80(+3)	+77(+2)	+33(+44)
2953	+62	+60(+3)	+61(+6)	+60(-3)	+61(+1)	+59(+1)	+58(-1)	+60(-3)	+57(+9)	
CSP 117	-31	-34(+4)	-34(+3)	-33(+1)	-07(+3)	-16(-13)	-50(+8)	-37(+12)	-37(-31)	-09(+32)
8-1 973	+67	+39(-139)	+03(+24)	-35(-38)	-45(+3)	-52(0)	-44(+3)	-47(-3)	-15(+46)	
1093	-10	-16(-8)	-26(+8)	-33(-4)	-36(-2)	-53(-10)	-41(+11)	-37(-3)	-61(-27)	
1122	+65	+76(+51)	+48(-27)	-25(-98)	-31(+17)	-40(+1)	-29(+1)	-31(+11)	-24(+13)	
1635	+55	-34(+58)	-30(-65)	-63(+46)	-55(+8)	-57(-2)	-57(-4)	-57(-1)	-61(+12)	
1760	-17	-37(+14)	-40(-2)	-45(-5)	-43(+3)	-43(-5)	-42(+3)	-43(-3)	-43(+1)	-48(+125)
3006	+01	-26(-8)	-26(+19)	-35(-9)	-38(+2)	-39(+1)	-38(+1)	-39(+1)	-38(0)	
CSP 215	+67	+62(-7)	+66(+3)	+62(+7)	+49(+55)	+54(-25)	+31(+51)	-	-	
10-1 305	+72	+74(+10)	+80(+15)	+86(+30)	+88(+66)	+79(54)	+37(+141)	-06(-52)	+45(+71)	
RL 1323	+72	+63(-9)	+66(+43)	+60(-25)	+60(0)	+61(-3)	+60(+1)	+54(-6)	+62(-21)	
2496	+55	+55(-10)	+53(+4)	+55(+4)	+52(+2)	+45(+8)	+46(+2)	+47(+2)	+47(-2)	+57(-132)
HL 1 1092	+51	+50(-1)	+50(-2)	+49(0)	+50(-2)	+49(0)	+49(+1)	+23(-66)	+35(-17)	
HL 3 1064	+61	+60(+3)	+61(-2)	+61(+1)	+61(0)	+61(+2)	+62(-3)	+61(+6)	+62(0)	+18(+96)
1072	+60	+58(-1)	+58(0)	+57(0)	+57(0)	+57(+2)	+58(-2)	+59(+5)	+60(+12)	
M 2 1051*	-65	-70(+9)	-68(+4)	-64(-2)	-62(+8)	-62(+12)	-64(-2)	-63(0)	-63(+4)	
1053*	+69	+60(+5)	+60(-3)	+65(-13)	+62(-17)	+65(-1)	+64(-4)	+60(+1)	+66(+4)	+62(-14)
1056*	+76	+71(-7)	+70(-2)	+69(-16)	+66(-11)	+66(+2)	+66(0)	-03(+98)	+14(-53)	
				GROUP II						
CSP 2-1 385	+04	+03(+2)	+03(-1)	+03(+1)	+03(+1)	+02(-1)	-01(+3)	+65(-78)	+06(+28)	
CSP 8-1 832	+02	+01(0)	-02(-5)	+01(+2)	-01(+1)	00(+1)	-01(-1)	+05(-3)	-52(-179)	
840	+08	+07(-1)	+07(0)	+07(0)	+06(0)	+6(0)	+04(0)	-13(-29)	-22(+172)	
1087	+35	+25(+44)	+34(-60)	-06(+43)	+4(+1)	+19(-3)	+10(+14)	00(-6)	-17(-32)	
CSP 334	-48	+19(+18)	+20(-8)	+13(+5)	-04(+16)	-09(+4)	+16(-12)	00(+58)	-03(-48)	
10-1 1540	+56	+28(+5)	+25(+7)	+21(+5)	-12(+174)	00(-164)	+01(+41)	-05(-143)	-16(+128)	
DEJ 573	+04	+03(0)	+03(-1)	+03(0)	+03(0)	+02(-1)	+08(+6)	+29(+25)	-03(+24)	
HL 2 762	-15	-17(0)	-18(-1)	-18(0)	-19(0)	-18(0)	-19(0)	00(-8)	-19(+111)	
				UNSTABLE GROUP						
RL 4105	+66	+57(-17)	46(-100)	+33(+73)	+43(+119)	-19(+4)	+25(-97)	+03(+36)	+47(-29)	
CSP 5-1 388	+52	+18(+1)	+19(+1)	+10(-20)	-23(-47)	-01(+46)	-59(+18)			

Sample letters identify drillholes in Figure 1.1 and the numbers indicate depths of samples from the surface. Inclinations of north-seeking directions are shown as positive if below the horizontal, and negative if above. Changes in declination from the previous heating (numbers in brackets) are shown as positive if clockwise, negative if counter-clockwise.

The underlined figures are the ones used in calculating mean inclinations and samples indicated by an asterisk are from regolith below the Athabasca. The underlined inclinations were selected because directions appeared to have reached an end point. Note that in many cases there were no directional changes over a wide range of temperatures after the end point direction was attained.

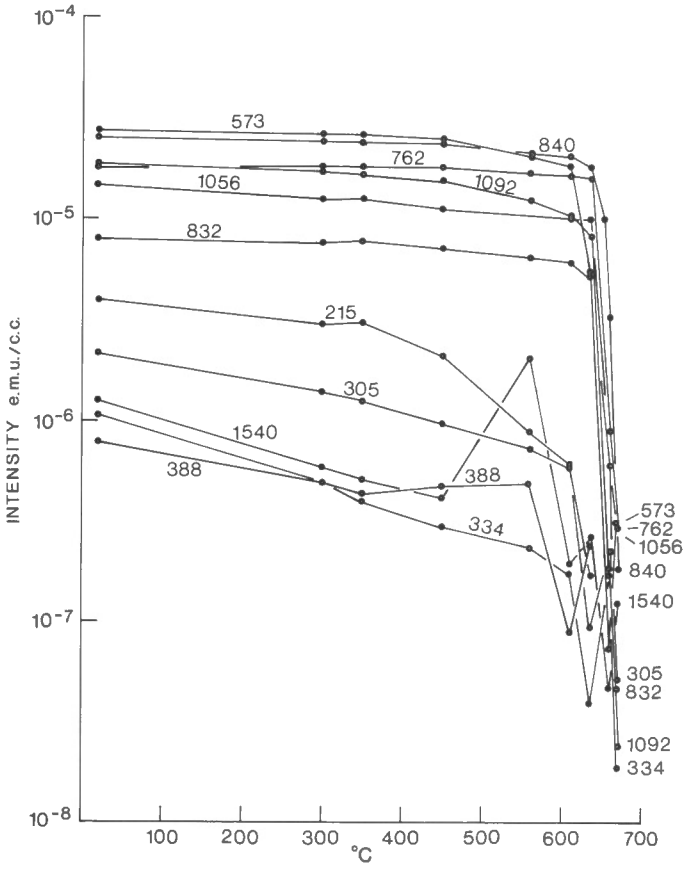


Figure 1.3

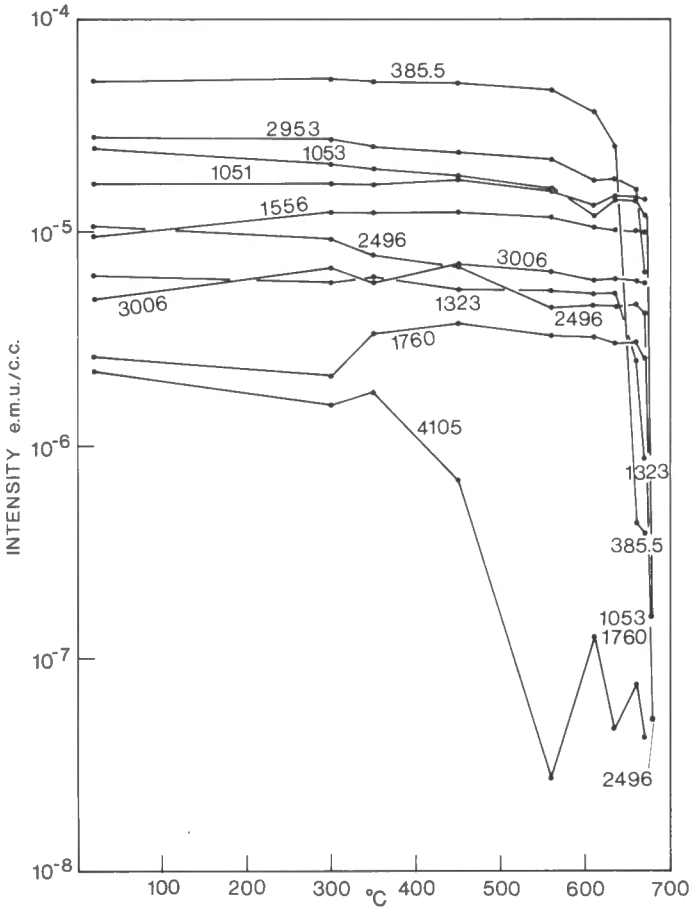


Figure 1.3. Thermal demagnetization curves for samples of Table 1.1.

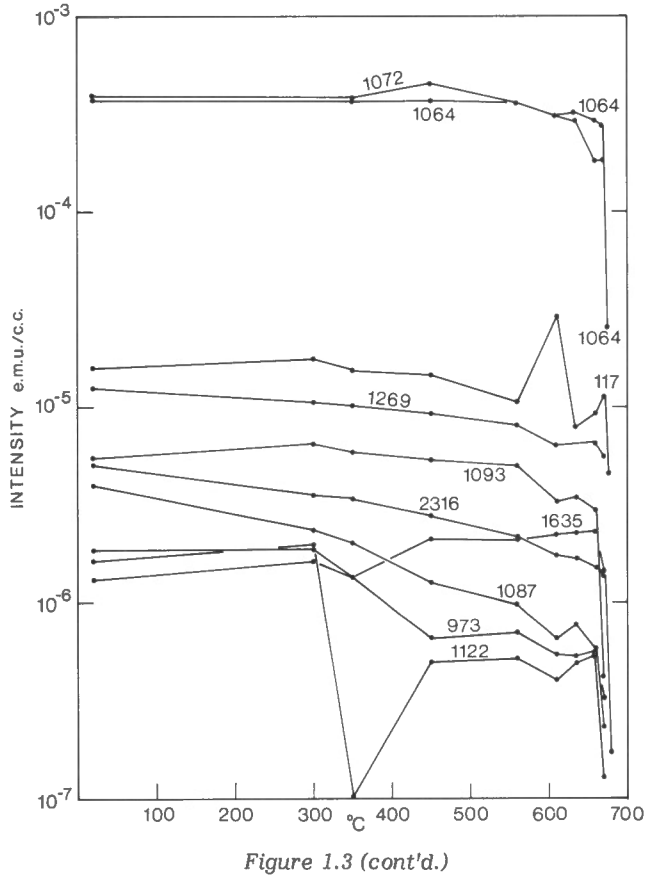


Figure 1.3 (cont'd.)

Because of age limits (the Athabasca lies on the Churchill Orogen and is cut by Mackenzie dykes) the up directions indicate reversed polarity. The specimens from CSP 2-1 indicate that a minimum of two reversals occur in the sequence, and if the polarities of samples from CSP 2-1 are compared with those of CSP 8-1 (Fig. 1.2) it appears likely that a minimum of four polarity reversals took place during deposition of the formation. In some cases (for example, sample 973, Table 1.1) the inclination changed from a north-seeking down direction to a north-seeking up direction, indicating elimination by thermal cleaning of an unstable down component, probably related to the present earth's field.

The discovery of a number of reversals within the sequence was surprising, as it has been argued that most of the Athabasca was rapidly deposited (Fraser et al., 1970) and may represent only a few million years. Polarity reversals during this period may, then, have been as frequent as during the past few million years (Cox, 1969; McElhinny, 1973). It is likely then that magnetostratigraphy will eventually play a role in the chronostratigraphic correlation of redbeds throughout the Athabasca basin.

Eight of the 29 stably magnetized samples have an inclination of magnetization which is significantly shallower than that of Group I. These are listed as Group II in Table 1.1 and their mean inclination irrespective of sign is 08° with k=67. This mean inclination may not be strictly correct, however, because there is no way of knowing whether any of the specimens are reversely magnetized. The origin of this flat magnetization is puzzling. It is unlikely to be secondary as there is no petrographic evidence of deep burial with heating and remagnetization of the Athabasca. Furthermore, samples with flat inclination occur towards the upper parts of

Table 1.2

Saturation Magnetization Results

Sample	Number	Inclination 20°C	Inclination 200°C	Intensity (200°C)	Intensity (6000 oe)	Change
HL 2	0764	-21.4	-21.1	$.12 \times 10^{-4}$	$.10 \times 10^{-1}$	x 830
CSP 2-1	0385	-05.6	-05.6	$.37 \times 10^{-4}$	$.19 \times 10^{-1}$	x 510
M 2	1058	+77.5	+68.2	$.74 \times 10^{-5}$	$.11 \times 10^{-1}$	x1490
CSP 2-1	1269	+45.9	+44.4	$.32 \times 10^{-5}$	$.15 \times 10^{-1}$	x4680

The intensity is given in e.m.u./c.c. Note that the inclinations at 20°C and 200°C are not the same as those given for specimens of the same number in Table 1.1 because they represent fresh specimens taken from the same core only a few centimetres higher or lower. Their inclinations are in good agreement with those of Table 1.1.

a number of holes and sample 1087 is overlain and closely underlain by material with steeper inclination. The flat inclination cannot be ascribed to deflection of the drillhole from the vertical, as some samples contain parallel laminations, indicating that the hole was drilled at 90° to bedding. The same relationship was also observed in cores which are close to other flatly magnetized samples which do not themselves exhibit good parallel bedding.

The paleolatitude of deposition of the Athabasca Formation as calculated from the 21 samples (Group I, Table 1.1) is 39°. This is consistent with the red nature of much of the shale, the local presence of gypsum filling joints in the sandstone, and the presence of stromatolites in the overlying Carswell Formation (Fahrig, 1961; Currie, 1969).

Saturation Remanent Magnetization

An experiment was carried out in an attempt to explain the presence of both shallow and steep magnetic inclinations within the cores. Four samples, two with steep and two with shallow magnetic inclinations, were exposed to a constant field of 6000 oe. The results of this experiment are given in Table 1.2 and Figure 1.4. It was thought that the samples with shallow inclination might contain both normal and reversed components and the increase in their total moment would be much greater than in the steeply magnetized samples if the abundance of the hematite does not vary substantially. Such is not the case, indeed the increase in intensity is much greater for the two more steeply magnetized samples. It seems unlikely that the steep magnetization (involving three-quarters of the samples) would be the resultant of shallow normal and shallow reversed magnetizations. To check this, however, six cylinders with steep stable magnetic inclinations were cut horizontally and the halves were measured. None showed evidence of transition from one polarity to the other.

The same procedure was carried out on six samples exhibiting shallow magnetization. These also showed no evidence of transition from one polarity to the other.

With regard to the above experiment, it should be pointed out that the domains whose magnetization was aligned in a field of 6000 oe may not be the same domains aligned in a field of 0.5 oe.

Age of Magnetization and Sedimentation

A line composed of all possible central Pacific pole positions derived from the mean paleomagnetic inclination of 21 Athabasca hematitic layers after cleaning at optimum temperatures is shown on Figure 1.5, along with part of the North American Precambrian polar wandering curve. The age of the paleomagnetism (sedimentation) should be given by some point at which this line intersects the polar wandering curve. The most westerly intersection of possible interest occurs at a point on the Logan Loop. This would make the Athabasca younger than the 1250 Ma Mackenzie igneous events (Fahrig and Jones, 1969; Van Schmus, 1975), a possibility eliminated by the fact that the sandstone is intersected by a Mackenzie dyke on the south shore of Lake Athabasca. The intersection immediately to the east would make the formation at least 1500 Ma old, probably about 1550 Ma. The third intersection (on the western limb of the Sudbury Loop) at about 1850 Ma would make the formation about the same age as the Dubawnt volcanics (Wanless and Loveridge, 1972; Park et al., 1973). However, the pole for the Martin Formation (Evans and Bingham, 1973) is farther south along the Sudbury Loop (and therefore younger than the Dubawnt pole) and the Athabasca is known to postdate the Martin. This appears to eliminate the third intersection. The fourth, and most easterly intersection, is about 15° north of, and therefore younger than, the pole for the Et Then Formation (Irving et al., 1972). The Et Then is lithologically similar to the pre-Athabasca Martin Formation and for this reason has been correlated with other Late Aphebian-Early Helikian redbed sequences of the western Shield (Fraser et al., 1970). This most easterly intersection could therefore indicate the age of the Athabasca Formation. We are left then with two intersections indicating possible ages of sedimentation, namely 1550 Ma and 1700 Ma.

Ramaekers and Dunn (1976) have reported a 1350 Ma ± 50 Ma whole-rock Rb/Sr age from shales of the formation. This does not agree with the paleomagnetic age. Two poles from rocks of the Canadian Shield, the Michikamau (Murthy et al., 1968) and the Croker Island (Palmer, 1969), lie less than 15° of arc away from the more westerly (≃1550 Ma) Athabasca polar wandering curve intersection. However, these poles have ages between 1400 and 1500 Ma. On the other hand, two rock units, the Sibley Group (Robertson, 1973) and the Mistastin pluton (Fahrig and Jones, 1976), which have Rb/Sr ages close to that suggested by Ramaekers and Dunn for the Athabasca Formation have poles at least 25° distant from the western intersection. This suggests that the paleomagnetism of the Athabasca is significantly greater in age, and Athabasca sedimentation is significantly greater in age than the 1350 Ma suggested by Ramaekers and Dunn.

After the paleomagnetic work on the Athabasca was completed, Wanless reported that a Rb/Sr isochron age of 1633 ± 30 Ma (pers. comm., May, 1977) had been obtained on deeply weathered material which is basement to the Athabasca Formation (decay constant $1.42 \times 10^{-11} y^{-1}$). If this does indeed date the pre-Athabasca weathering, it is unlikely to be more than 250 Ma older than Athabasca sedimentation; a situation required by the 1350 Ma age. It is much more consistent with the 1550 Ma age suggested by paleomagnetic results.

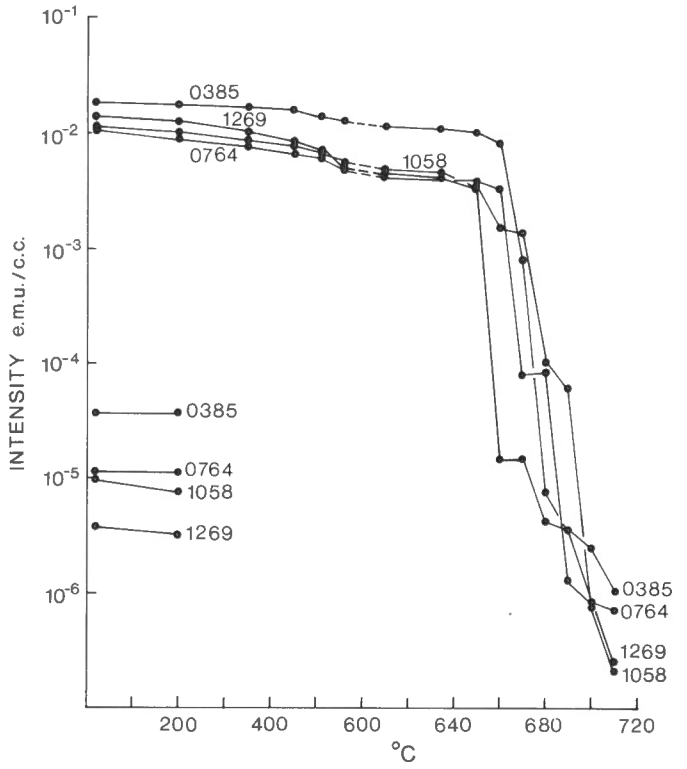


Figure 1.4. The main curves show the thermal demagnetization of two Group I and two Group II samples after magnetization in a 6000 oe field. Curves in lower left give the N.R.M. intensities and intensities after thermal demagnetization at 200°C. See Table 1.2. Note that the horizontal scale above 600°C is expanded.

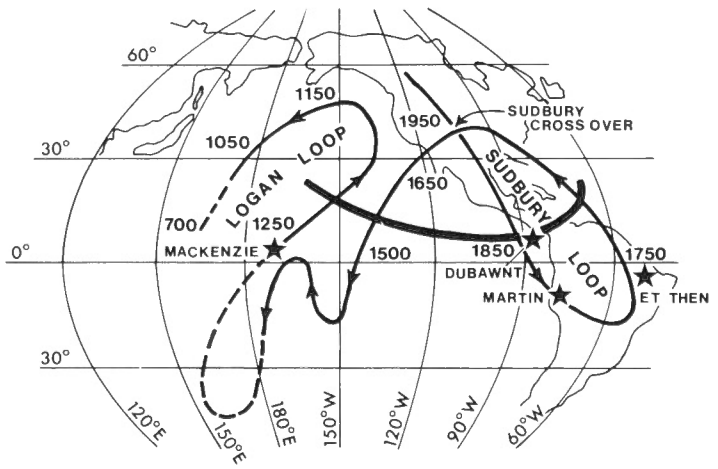


Figure 1.5. North American Middle and Upper Proterozoic polar wandering curve, slightly modified from Christie et al. (1975) and Fahrig (1977). Numbers along the curve are estimated ages of various parts of the curve. The heavy line indicates possible pole positions derived from the mean inclination of magnetization of 21 Group I samples of Table 1.1 of Athabasca Formation after cleaning at optimum temperature.

The Thelon Formation of the Dubawnt Group is generally thought to be a correlative of the Athabasca Formation (Fraser et al., 1970). It unconformably overlies a redbed and volcanic sequence. The latter has yielded a Rb/Sr age of about 1800 Ma, using the decay constants indicated above. If the Athabasca and Thelon are indeed correlatives, the unconformity between the lower Dubawnt redbed volcanic sequences and the overlying Thelon represents at least 200 Ma.

Acknowledgments

We wish to thank Dr. M.E. Evans for bringing to our attention the paper by Briden and Ward for estimating the mean and its variance for inclinations obtained from drill cores, and we wish to thank him, E.J. Schwarz and K. Buchan for critical comments that materially improved the manuscript.

References

Briden, J.C. and Ward, M.A.
1966: Analysis of magnetic inclination in borecores. Pure App. Geophys; v. 63, p. 133-152.

Christie, K.W., Davidson, A., and Fahrig, W.F.
1975: The paleomagnetism of Kaminak dikes — no evidence of significant Hudsonian plate motion; Can. J. Earth Sci., v. 12, p. 2048-2064.

Cox, A.
1969: Geomagnetic reversals; Science, v. 163, p. 237-245.

Currie, K.L.
1969: Geological notes on the Carswell circular structures; Geol. Surv. Can., Paper 67-32.

Evans, M.E. and Bingham, D.K.
1973: Paleomagnetism of the Precambrian Martin Formation, Saskatchewan; Can. J. Earth Sci., v. 10, p. 1485-1495.

Fahrig, W.F.
1961: The geology of the Athabasca Formation; Geol. Surv. Can., Bull. 68.

1977: Paleomagnetic correlation of the Riphean of North America. Correlation of the Precambrian; Volume 2; Publishing office "Nauka", Moscow. Edited by A.V. Sidorenko.

Fahrig, W.F. and Jones, D.L.
1969: Paleomagnetic evidence for the extent of Mackenzie igneous events; Can. J. Earth Sci., v. 6, p. 679-688.

1976: The paleomagnetism of the Helikian Mistastin pluton, Labrador, Canada; Can. J. Earth Sci., v. 13, p. 832-837.

Fraser, J.A., Donaldson, J.A., Fahrig, W.F., and Tremblay, L.P.
1970: Helikian basins and geosynclines of the northwestern Canadian Shield; In Symposium on basins and geosynclines of the Canadian Shield; Geol. Surv. Can., Paper 70-40, p. 213-231.

Innis, M.J.S.
1964: Recent advances in meteorite crater research at the Dominion Observatory, Ottawa, Canada; Meteoritics, v. 2, p. 219-241.

Irving, E., Park, J.K., and McGlynn, J.C.
1972: Paleomagnetism of the Et-Then Group and Mackenzie diabase in the Great Slave area; Can. J. Earth Sci., v. 9, p. 744-755.

McElhinny, M.W.
1973: Paleomagnetism and Plate Tectonics; Cambridge University Press, p. 114-138.

Murthy, G.S., Fahrig, W.F., and Jones, D.L.
1968: The paleomagnetism of the Michikamau anorthositic intrusion, Labrador; Can. J. Earth Sci., v. 5, p. 1139-1144.

Palmer, H.C.
1969: The paleomagnetism of the Croker Island Complex, Ontario, Canada; Can. J. Earth Sci., v. 6, p. 213-218.

Park, J.K., Irving, E., and Donaldson, J.A.
1973: Paleomagnetism of the Precambrian Dubawnt Group; Geol. Soc. Am., Bull., v. 84, p. 859-870.

Ramaekers, P.P. and Dunn, C.G.
1976: In Uranium in Saskatchewan, Symposium of the Saskatchewan Geological Society (abst.).

Robertson, P.B., Dence, M.R., and Vos, M.A.
1968: In Shock Metamorphism of Natural Materials (edit. by B.M. French and N.M. Short), Mono Book Corp., Baltimore, Md., p. 433-452.

Robertson, W.A.
1973: Pole positions from thermally cleaned Sibley Group sediments and its relevance to Proterozoic magnetic stratigraphy; Can. J. Earth Sci., v. 10, p. 180-193.

Van Schmus, W.R.
1975: On the age of the Sudbury dike swarm. Can. J. Earth Sci., v. 12, p. 1690-1692.

Wanless, R.K. and Loveridge, W.D.
1972: Rubidium-Strontium isochron age studies, Report 1; Geol. Surv. Can., Paper 72-23, p. 25-27.

2. COEXISTING CORDIERITE-GEDRITE-CUMMINGTONITE FROM EDEHON LAKE MAP AREA, CHURCHILL STRUCTURAL PROVINCE, DISTRICT OF KEEWATIN

Project 750102

Subhas Tella and K.E. Eade
Regional and Economic Geology Division

Tella, Subhas and Eade, K.E., Coexisting cordierite-gedrite-cummingtonite from Edehon Lake map area, Churchill Structural Province, District of Keewatin; in Current Research, Part C, Geol. Surv. Can., Paper 78-1C, p. 7-12, 1978.

Abstract

An assemblage of garnet-biotite-cordierite-gedrite-cummingtonite in a specimen from the Aphebian Hurwitz Group metasediments is described and discussed. Gedrite invariably occurs as rims around cummingtonite, and is in turn partially surrounded by cordierite. The mineral assemblage and textural relationships are interpreted as having been evolved during syntectonic regional metamorphism of the rocks. The growth of amphiboles, however, occurred during the late- to post-tectonic stage, as is indicated by their random arrangement, and may have been influenced by a coeval, thermal doming caused by late Aphebian plutons.

The Ca/Mn ratios in garnet, and the distribution coefficient (K_D^{Fe-Mg}) data between garnet-biotite and garnet-cordierite mineral pairs indicate middle to upper amphibolite facies conditions of metamorphism. The temperatures are estimated to have been in the range 585°C to 620°C, and the total pressures in the order of 2 to 3.7 kb.

Introduction

The mineral associations, the textural aspects, and the chemistry of mineral phases in one specimen (7c133) from the vicinity of Downer Lake, District of Keewatin (NTS 65A) are described (Fig. 2.1). The mineralogy and texture of a second specimen (7c131) is also described as part of the general geological background. The following associations are present:

1. Garnet-Biotite-Cordierite-Gedrite-Cummingtonite (7c133)
2. Biotite-Cordierite-Muscovite-Sillimanite (fibrolite) (7c131)

To the writers' knowledge the cordierite-gedrite-cummingtonite association in specimen 7c133 is the first reported occurrence in the Churchill Structural Province of the Canadian Shield.

The geological setting of the specimens is shown in Figure 2.1, the geology of which is after Eade (1973). The two specimens represent the mica schist unit (Unit 2) of the Aphebian Hurwitz Group which was deformed and regionally metamorphosed during the 'Hudsonian Orogeny' (Eade, 1973). Post-Hurwitz Group plutons of Aphebian age are widely exposed in the area (Unit 4, Fig. 2.1) and may have thermally affected the Hurwitz Group and older rocks of the region.

Mineralogy and texture

The specimens are mesoscopically medium grained and strongly foliated, with an overall hornfelsic appearance. They are generally fresh with a weak to well-developed schistosity. Microscopically these rocks are fine- to medium-grained and show varying proportions of cordierite ± garnet ± amphibole (both gedrite and cummingtonite) in a relatively fine grained and crystalloblastic matrix composed of quartz, biotite ± feldspar ± muscovite, and ± fibrolite. Muscovite, feldspar, and fibrolite, however, are restricted to one section (7c131). Other accessory minerals include magnetite, ilmenite, apatite, tourmaline and zircon. The estimated modal compositions are listed in Table 2.1.

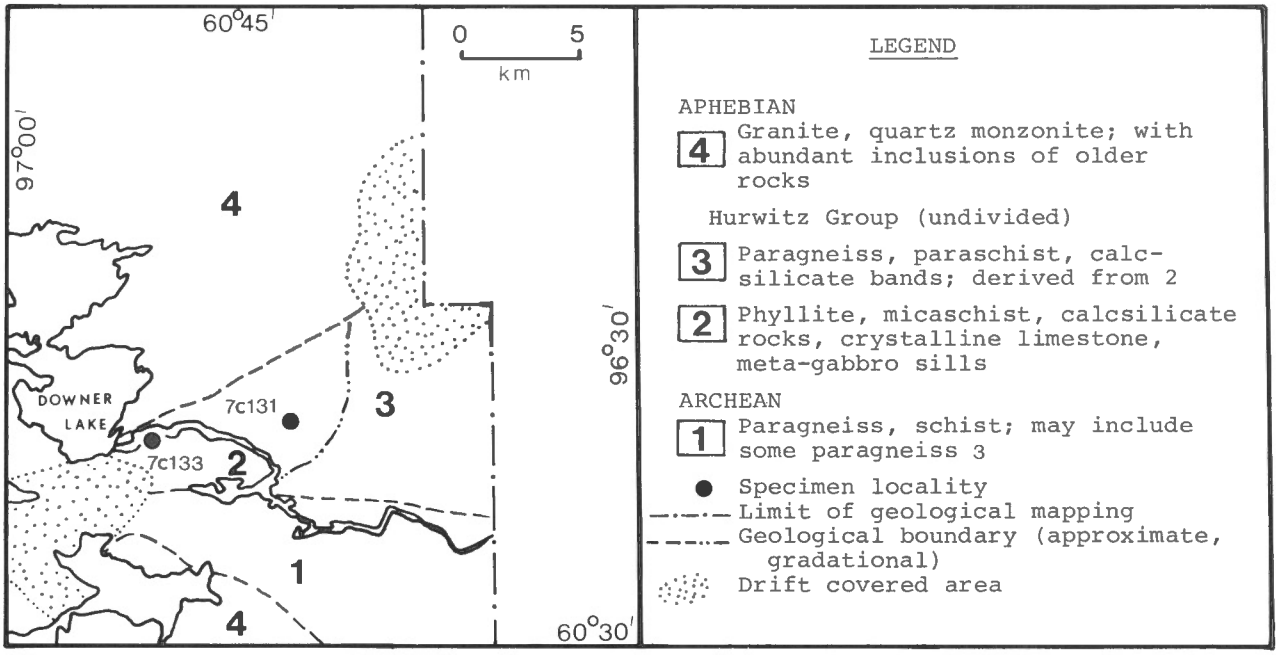


Figure 2.1. Map showing the specimen localities in the Aphebian Hurwitz Group. The geology is after Eade (1973); parts of Edehon Lake map area (NTS 65A E1/2).

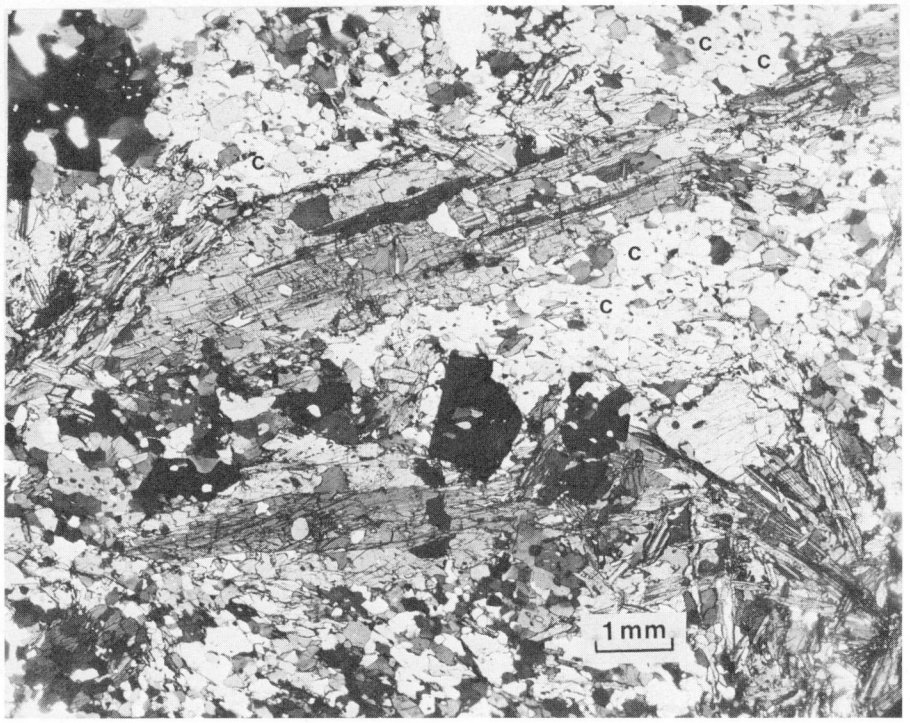


Figure 2.2a

Acicular to sheaf-like amphibole porphyroblasts in 7c133. Cummingtonite core rimmed by gedrite. Matrix minerals include garnet, cordierite (c), biotite, and quartz. Crossed polars. (GSC 203308-C)

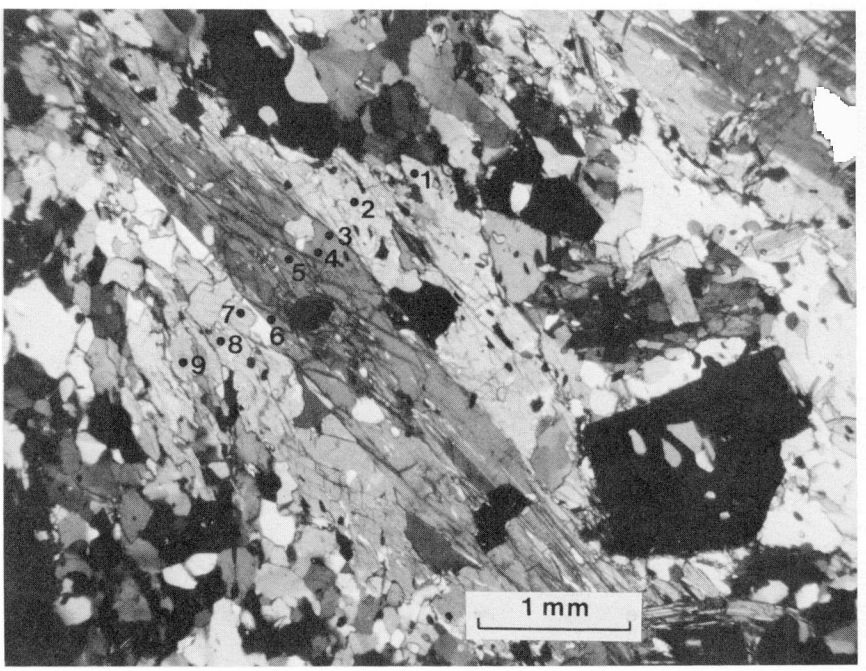


Figure 2.2b

Photomicrograph showing core-rim relations between cummingtonite and gedrite. The numbers refer to the spots analyzed for chemistry of mineral phases (grain 1, Table 2.2). Crossed polars. (GSC 203405-E)

In specimen 7c133, biotite commonly defines a weak planar fabric that has been overgrown by large porphyroblasts of cordierite with numerous inclusions of quartz, opaques, and zircon. Cordierite grain boundaries are rather irregular and show diffusive nature in relation to the surrounding matrix. Pinite alteration is common along the grain margins. Garnet is present as subhedral to anhedral porphyroblasts which contain numerous unoriented quartz inclusions. The garnet appears to be unstable, showing replacement by chlorite along boundaries and fractures. Their boundaries are commonly corroded with numerous embayments. One of the interesting textures in this section is the growth of large amphibole grains (Fig. 2.2), both ortho- and clino-, some of which grew across the planar fabric and others parallel to it. The amphiboles invariably contain a core of cummingtonite (optically positive with an inclined extinction and a large 2V) that shows multiple twins and is nonpleochroic to weakly pleochroic. They are rimmed by a clean orthoamphibole (gedrite – optically positive, parallel extinction, colourless to pale brown pleochroism, and a 2V of approximately 80°). The Mg/Mg+Fe+Mn ratio of the rim suggests that its composition is intermediate between that of anthophyllite and gedrite. Cordierite grains partially surrounded the clinoamphibole blades and most often the two are separated by a rim of gedrite (Fig. 2.2).

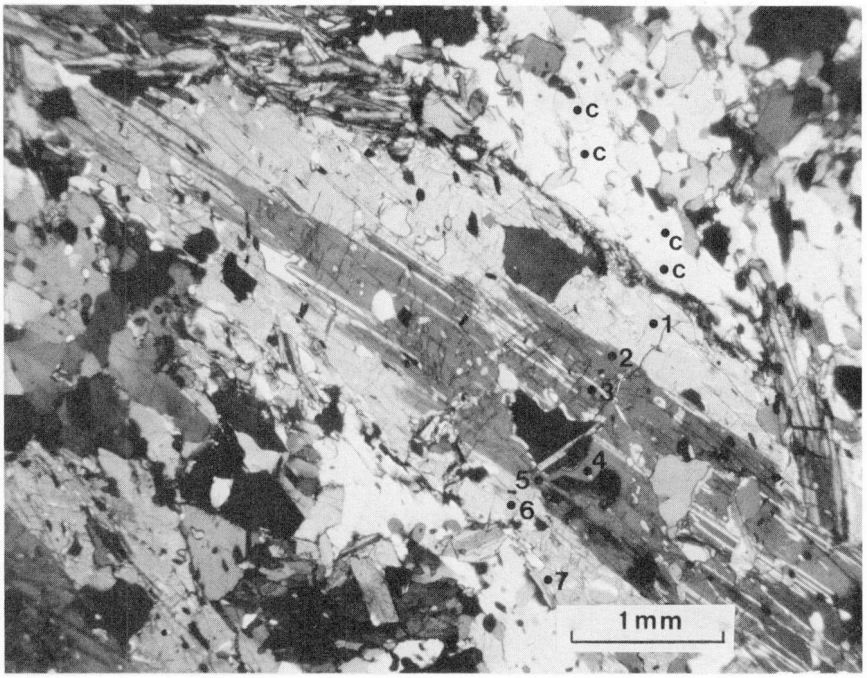


Figure 2.2c

Photomicrograph of an amphibole grain (grain 2, Table 2.2) in contact with cordierite (c). The numbers refer to the spots analyzed. Crossed polars. (GSC 203405-F)

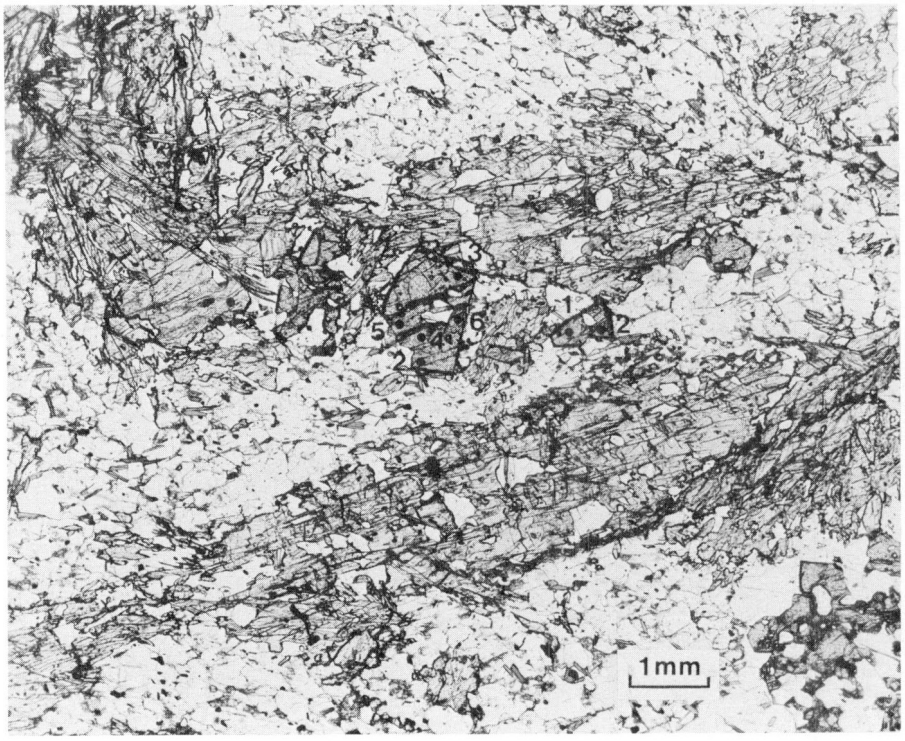


Figure 2.2d

Photomicrograph showing the porphyroblasts of garnet with number of spots analyzed. Crossed polars. (GSC 203308-D)

In specimen 7c131, the typical mineral assemblage is biotite + cordierite + sillimanite + muscovite + quartz + microcline + plagioclase. The amount of biotite is higher compared to specimen (7c133) and that of cordierite very low (3%). Amphibole and garnet are absent. Anhedral to subhedral porphyroblasts of cordierite have overgrown the biotite planar fabric. Mats of fibrolite are extensively developed within and outside the porphyroblasts. The sillimanite fibres outside the porphyroblasts are aligned parallel to the biotite fabric, together with plates of muscovite. Late chlorite alteration is present, especially within and in the vicinity of cordierite porphyroblasts.

The textural relationships between various mineral phases suggest the following time relations between deformation, metamorphism, and mineral growth at the specific study localities.

1. Development of penetrative planar fabric defined by an alignment of biotite ± muscovite during a syntectonic metamorphic event.
2. Growth of garnet followed by cordierite in specimen 7c133, and growth of muscovite, cordierite, followed by fibrolite in specimen 7c131 during syn- to late-tectonic metamorphism.

Table 2.1

Estimated modal compositions

	7c131	*7c133
Quartz	35	40
Plagioclase	11	
Microcline	21	
Amphibole+		25
Garnet		7
Biotite	20	5
Chlorite		tr
Cordierite	5	20
Muscovite	3	
Sillimanite	3	
Tourmaline	tr	
Apatite	1	tr
Zircon	tr	tr
Opaques	1	3

*specimen selected for probe analysis
+contain two amphiboles (Gedrite - Cummingtonite)

3. Possible posttectonic growth of amphiboles during the waning stages of regional metamorphism, probably influenced by the thermal updoming of plutons of Unit 4, or growth of amphibole blades during a contact metamorphic event postdating the regional metamorphism and deformation. Further field data are required to establish these relations on a regional scale.

Electron microprobe analyses

The electron microprobe chemical analyses of mineral phases from specimen 7c133 are presented in Tables 2.2 and 2.3. The spot analyses (Table 2.2) represent two amphibole grains (Fig. 2.2). The optically distinct core and rim areas (cummingtonite-gedrite respectively) clearly show a corresponding chemical difference. The rims have higher Al and lower Mg compared to the core compositions. The Fe content is slightly higher in the core than in the rims.

Biotite, cordierite, and garnet analyses shown in Table 2.3 represent the average analyses of spots on different grains. The three minerals are rich in FeO, MgO, Al_2O_3, and SiO_2, and poor in other oxides. In general, these mineral phases appear to have been derived from parent rocks having high Fe and Mg initial bulk composition. The Mg/Fe ratio in the mineral phases, as determined from the analyses, was found to be in the following order:

Cordierite > biotite > gedrite > cummingtonite > garnet

Mineral reactions

Limited data preclude the possibility of proposing any specific reactions for the observed mineral assemblages although some generalizations may be made by comparing the assemblage data with that from other regions. Lal and Shukla (1975) described cordierite-gedrite-cummingtonite assemblages from Khetri Copper Belt, Rajasthan, India, and discussed metamorphic reactions in terms of the major components SiO_2, Al_2O_3, MgO, FeO, and H_2O. They suggested a discontinuous reaction of the type:

Almandine + Al-chlorite + quartz
$\rightleftharpoons$ Gedrite + Cordierite + H_2O

They also reported the common occurrence of composite prisms of gedrite-cummingtonite (with rim-core relationships as described in the present study) in the product assemblages. Such an association was interpreted, following the experimental results of Akella (1971), as due to the sluggish nature of the conversion of high temperature gedrite to the low temperature cummingtonite. It is conceivable that a similar reaction resulted in the cordierite-gedrite-cummingtonite association described in this paper.

Coexisting cordierite-anthophyllite(gedrite)-cummingtonite assemblages have also been reported by Robinson and Jaffe (1969) from the 'Amphibole Hill' area, central Massachusetts, by Stout (1972) from Telemark, Norway, by Tilley (1937) from Trelease Mill, Lizard, and by Eskola (1914) from Orijarvi District, southwestern Finland. The occurrence of anthophyllite as rims around cummingtonite has been well documented in these studies, and Robinson and Jaffe (1969) implied an equilibrium relationship between cordierite-gedrite and cummingtonite. The assemblages of the present study (in specimen 7c133) have mineralogical, textural, and chemical similarities to the above and a similar equilibrium relation may be suggested. The possibility that the amphiboles developed as late-stage contact metamorphic minerals postdating cordierite, however, cannot be ruled out completely. A complete or partial re-equilibration of constituents between cordierite and cummingtonite is possible under such conditions and may result in the formation of gedrite rims around cummingtonite. Alignment of some amphibole blades parallel to the planar fabric appears to suggest the former relationship, i.e. the assemblages were in equilibrium. The random growth of some of the amphiboles may be explained by proposing that the regional metamorphism outlasted the deformation, resulting in an overgrowth of late minerals (such as cordierite and amphiboles) across the planes of fabric. The thermal doming caused by adjacent plutons (Unit 4) may have influenced the mineral growth to a certain extent, but further data are needed to qualify such statements.

Physical conditions of metamorphism

Sen and Chakraborty (1968), based on Ca/Mn ratios in garnet and on distribution coefficients K_D^{Mg-Fe} in garnet-biotite mineral pairs, formulated a general equation—

$$(Ca/Mn)^G = -10.44\ K_{D\ (Mg-Fe)}^{Gar.-Biot.} + C$$

and have shown that the numerical value of C varies systematically with metamorphic grade. The value of C (= 2.32) determined from the present chemical analyses for the garnet-biotite pair suggests that the metamorphic grade at the specimen locality (7c133) was within the garnet-staurolite zone of the amphibolite facies conditions of metamorphism. Moreover, a comparison of the K_D^{Fe-Mg} values determined for the mineral pairs garnet-cordierite and garnet-biotite (Table 2.4) to those experimentally determined values (Thompson, 1976; Ferry and Spear, 1977), indicates that the temperatures were in the order of 585°C to 620°C. The stability fields of garnet coexisting with cordierite (Thompson, 1976) limit the total pressure range between 2 to 3.7 kb at the above temperature range. However, the occurrence of fibrolite coexisting with muscovite and cordierite seems to indicate that the pressures were in the upper end of the range. These P-T conditions and the mineral assemblages are typical of Abakuma-type facies series of Miyashiro (1961).

Table 2.2

Electron probe spot analyses of coexisting amphiboles

	Grain 1									Grain 2						
	Rim (1-2)			Core (3-6)				Rim (7-9)		Rim		Core (2-5)			Rim (6-7)	
	1	2	3	4	5	6	7	8	9	1	2	3	4	5	6	7
SiO_2	51.20	51.64	52.09	51.67	52.24	51.86	50.91	51.50	50.72	51.75	52.34	52.21	52.15	52.13	51.26	50.47
TiO_2	0.14	0.07	0.09	0.10	0.05	0.13	0.05	0.16	0.12	0.22	0.15	0.10	0.05	0.11	0.13	0.12
Al_2O_3	4.29	3.87	2.68	2.46	2.37	2.48	4.07	3.68	4.45	4.22	2.50	2.41	2.29	2.63	4.00	4.09
Cr_2O_3	0.12	0.11	0.00	0.00	0.05	0.09	0.02	0.13	0.14	0.10	0.05	0.05	0.00	0.00	0.08	0.09
FeO	27.67	27.87	27.29	28.36	28.61	28.67	28.32	28.64	28.73	27.56	28.47	28.24	28.32	28.13	28.46	28.17
MnO	0.09	0.06	0.07	0.13	0.02	0.12	0.11	0.08	0.09	0.08	0.06	0.11	0.01	0.11	0.08	0.10
MgO	15.02	15.18	15.81	15.33	14.86	14.70	14.47	14.16	14.23	14.79	15.16	15.07	15.25	14.95	14.54	14.29
CaO	0.04	0.02	0.03	0.07	0.06	0.10	0.00	0.03	0.05	0.04	0.04	0.06	0.01	0.07	0.07	0.04
Na_2O	0.00	0.15	0.16	0.12	0.00	0.00	0.00	0.00	0.00	0.00	0.00	0.00	0.00	0.00	0.00	0.00
K_2O	0.00	0.00	0.00	0.00	0.00	0.00	0.00	0.00	0.00	0.00	0.00	0.00	0.00	0.00	0.00	0.00
Total	98.57	98.97	98.22	98.24	98.26	98.15	97.95	98.38	98.53	98.76	98.77	98.25	98.08	98.13	98.62	97.37

Analyst: M. Bonardi, Mineralogy Section, Central Laboratories and Administrative Services, Geological Survey of Canada, Ottawa.

Table 2.3

Electron probe analyses of Garnet, Biotite, and Cordierite

	Garnet	Biotite	Cordierite
SiO_2	37.76	36.93	49.40
TiO_2	0.07	2.08	0.01
Al_2O_3	20.46	17.42	32.01
Cr_2O_3	0.08	0.21	0.00
FeO	36.20	19.93	7.66
MnO	0.57	0.00	0.02
MgO	4.47	11.69	9.01
CaO	0.63	0.01	0.00
Na_2O	0.13	0.15	0.63
K_2O	0.00	8.37	0.00
Total	100.36	96.79	98.74

Garnet — Average of 8 spot analyses on two different grains

Biotite — Average of 4 spot analyses on four grains

Cordierite — Average of 4 spot analyses on two grains

Analyst: M. Bonardi, Mineralogy Section, Central Laboratories and Administrative Services, Geological Survey of Canada, Ottawa.

Table 2.4

Average K_D values between Garnet-Biotite and Garnet-Cordierite mineral pairs, and estimated temperatures of metamorphism

Mineral pair	$\ln K_D^{Fe-Mg}$	T°C	
Garnet-Cordierite	2.254	585	Thompson (1976)
Garnet-Biotite	1.558	610	Thompson (1976)
		620	Ferry and Spear (1977)

Acknowledgments

We wish to thank C. Cunningham of the Terrain Sciences Division for donating the two specimens, M. Bonardi and A.G. Plant for the electron microprobe analyses, E. Froese and D.C. Kamineni for critical reading of the manuscript, and several members of the Precambrian Subdivision for valuable suggestions.

References

Akella, J.
1971: The compatibility of cummingtonite $(Fe,Mg)_7 Si_8 O_{22}(OH)_2$ with gedrite $(Mg,Fe)_5 Al_2Si_8O_{22} (OH)_2$ and cordierite $Mg_2 Al_4Si_5O_{18}$; Studies in Earth Sciences, W.D. West Volume, University of Saugar, India, p. 337-344.

Eade, K.E.
1973: Geology of Nueltin Lake and Edehon Lake (west-half) map-areas, District of Keewatin; Geol. Surv. Can., Paper 72-21, 29 p.

Eskola, P.
1914: On the petrology of the Orijärvi region in south-western Finland; Bull. Comm. Geol. Finlande, 40.

Ferry, J.M. and Spear, F.S.
1977: Experimental calibration of the partitioning of Fe and Mg between biotite and garnet; in Annual Report of the Director, Geophysical Laboratory, Carnegie Institution, 1976-77, p. 579-581.

Lal, R.K. and Shukla, R.S.
1975: Genesis of cordierite-gedrite-cummingtonite rocks of the northern portion of the Khetri Copper Belt, Rajasthan, India; Lithos, v. 8, p. 175-186.

Miyashiro, A.
1961: Evolution of metamorphic belts; J. Petrol., v. 2, p. 277.

Robinson, P. and Jaffe, H.W.
1969: Chemographic exploration of amphibole assemblages from central Massachusetts and southwestern New Hampshire; Mineral. Soc. Am., Spec. Paper 2, p. 251-274.

Sen, S.K. and Chakraborty, K.R.
1968: Magnesium-iron exchange equilibrium in garnet-biotite and metamorphic grade; N. Jb. Miner. Abh., v. 108, p. 181-207.

Stout, J.H.
1972: Phase petrology and mineral chemistry of coexisting amphiboles from Telemark, Norway; J. Petrol., v. 13, p. 99-145.

Thompson, A.B.
1976: Mineral reactions in pelitic rocks: II, Calculation of some P-T-X (Fe-Mg) phase relations; Am. J. Sci., v. 276, p. 425-454.

Tilley, C.B.
1937: Anthophyllite-cordierite-granulites of the Lizard; Geol. Mag., v. 74, p. 300-309.

3.

OFFSHORE PERMAFROST DISTRIBUTION IN THE BEAUFORT SEA AS DETERMINED FROM TEMPERATURE AND SEISMIC OBSERVATIONS

K.G. Neave[1], A.S. Judge[2], J.A. Hunter[3], and H.A. MacAulay[3]
Resource Geophysics and Geochemistry Division

Neave, K.G., Judge, A.S., Hunter, J.A., and MacAulay, H.A., Offshore permafrost distribution in the Beaufort Sea as determined from temperature and seismic observations; in Current Research, Part C, Geol. Surv. Can., Paper 78-1C, p. 13-18, 1978.

Abstract

Ice-bonded sediments are found over much of the Beaufort Sea continental shelf but are absent from most parts of Mackenzie Bay. They reflect Pleistocene climatic conditions which resulted in the growth of permafrost to depths of 600 m or more. The study made use of oil industry reflection records to determine the distribution of these sediments.

Introduction

For long periods of time during the Pleistocene, part of the Beaufort Sea continental shelf was exposed to subzero air temperatures and as a consequence permafrost grew in the sediments to a thickness in excess of 600 m. These conditions are reflected today in the ice-bonded sediments which are found over a large percentage of the shelf area.

Seismic Studies

The extent of ice-bonded sediments is determined by analyzing the "front ends" of oil industry reflection records in terms of refracted arrivals. Figure 3.1 shows the extensive distribution of high seismic velocities which are interpreted as ice-bonded sediments.

An examination of the variation of seismic velocity with depth reveals considerably more detail in the results. The shelf has been divided into different regions with different velocity – depth functions. In Mackenzie Bay, a linear increase of velocity with depth (Fig. 3.2) similar to that observed for unbonded marine sediments (Hofer and Varga, 1972), is noted. North of Garry Island and below a depth of 120 m, the rate of increase of velocity with depth is nonlinear and significantly greater than for Mackenzie Bay (Fig. 3.3): a condition, which has been termed the "Netserk anomaly", and is probably due to partial bonding of the sediments. The distribution of this velocity anomaly lies between the high-velocity ice-rich sediments and the ice-free sediments (Fig. 3.4). East of 135°W, high velocities consistent with an ice-rich medium or coarse grained sediments are found (Hunter et al., 1976). The velocity data (Fig. 3.5) is

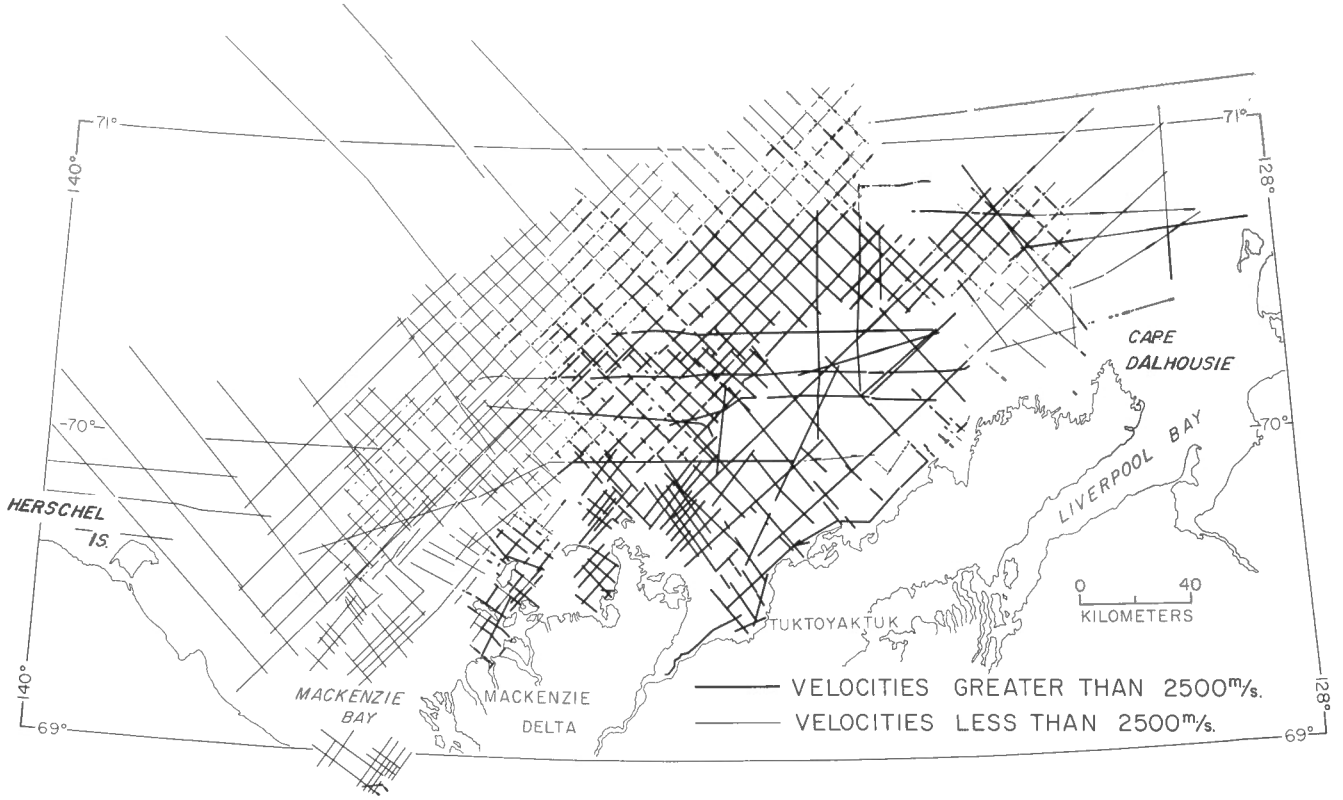


Figure 3.1. Distribution of high seismic velocities from Beaufort Sea reflection records.

[1]Polar Continental Shelf Project

[2]Earth Physics Branch

[3]Geological Survey of Canada

Earth Physics Branch Contribution No. 710

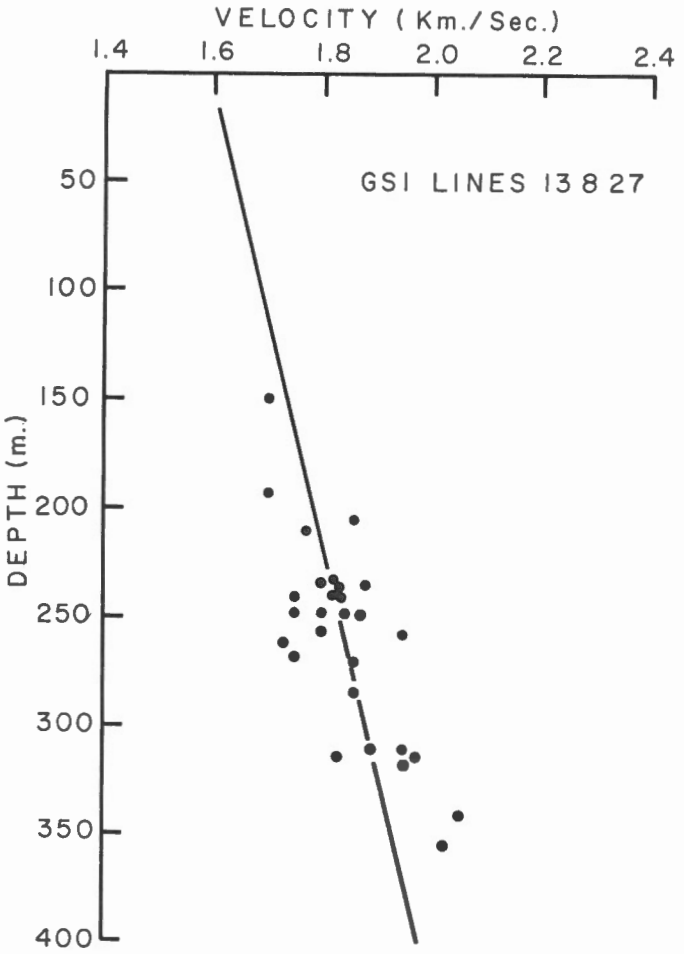


Figure 3.2. Velocity-depth distribution for Mackenzie Bay.

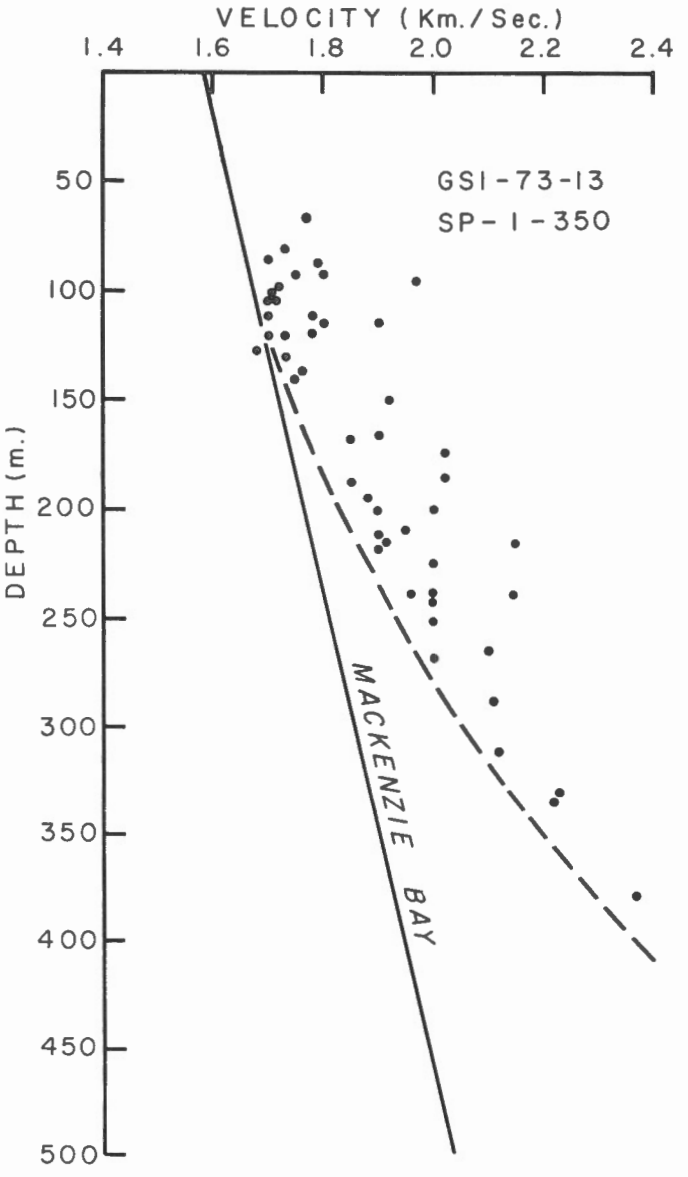


Figure 3.3. Velocity-depth distribution for the Netserk area, north of Garry Island.

divisible into an upper high-velocity group, with a top 60-100 m below sea level, for which the seismic records show an attenuated, intermittent signal, and a lower group (130-200 m below sea level) for which the records show a strong, continuous signal. In Figures 3.6 and 3.7, we have plotted the depth to the top of the two layers. Resolution of depth is ±40 m because of the lack of arrival time information from the shot point to the nearest receiver 300 m away.

A very distinct western boundary for the upper high-velocity layer (Fig. 3.6) strikes northwards from Richards Island along approximately 135°W. Near the western border, this upper layer overlies a deeper layer with an intermediate velocity of the Netserk type whereas, to the east, it overlies a deeper higher velocity layer. From the rapid attenuation of the upper layer signal, the upper layer appears to be thin (10-30 m).

The western boundary of the lower high-velocity layer strikes northeast across the shelf from Garry Island, cutting diagonally across the western boundary of the upper layer. The depth below seabottom of the top of the lower layer is relatively constant (the gentle dip to the north on the map is caused by increasing water depth).

Temperature Studies

The shallow temperature regime at the 135°W velocity boundary was examined in the spring of 1976. Three holes were drilled using a hydraulic drill and the holes instrumented with temperature measuring cables to depths of 30 to 60 m (Judge et al., 1976).

At each of the locations shown in Figure 3.6, subzero temperatures were encountered throughout the holes. During drilling, no hard boundaries were encountered which could be attributed to a frozen-unfrozen interface although ice was encountered in a sand near the base of the westernmost drillhole. Calculated equilibrium temperatures for the central and western sites are shown in Figure 3.8, together with the single set of results obtained for the eastern site prior to cable failure.

The central and westernmost sites exhibited contrasting characteristics of the thermal regime. On the one hand, the central hole showed a negative temperature gradient of 15°/km at a depth of 6 m below the sediment surface and the temperature fell to below -1.9°C at 44 m depth. On the other hand, the western hole exhibited a positive temperature gradient of 57°/km at a depth of 10 m below the sediment surface, and the temperature rose to 0°C at a depth of 35 m

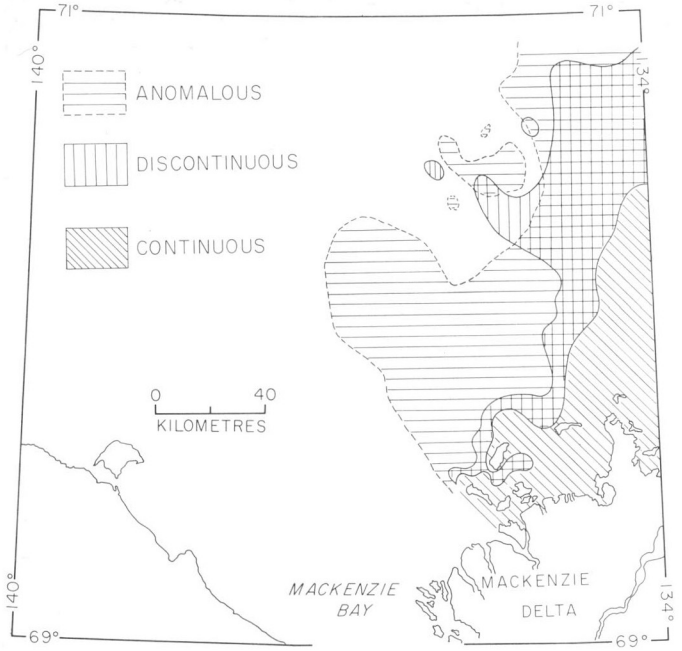


Figure 3.4. Location of the "Netserk" anomaly. This area has anomalous refraction velocities which are less than 2.5 km/s.

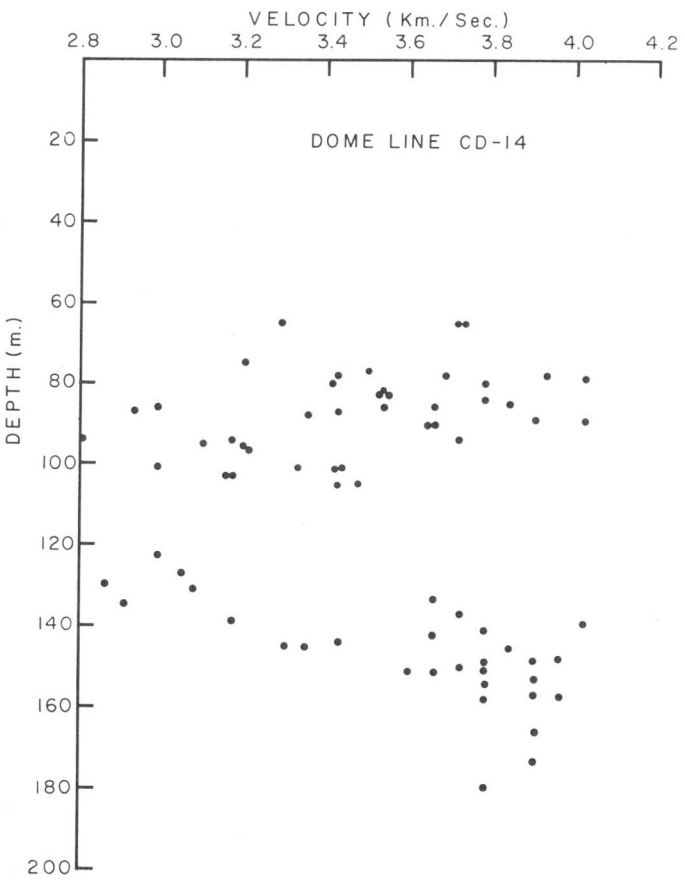


Figure 3.5. Velocity-depth distribution for the high-velocity region north of Tuktoyaktuk.

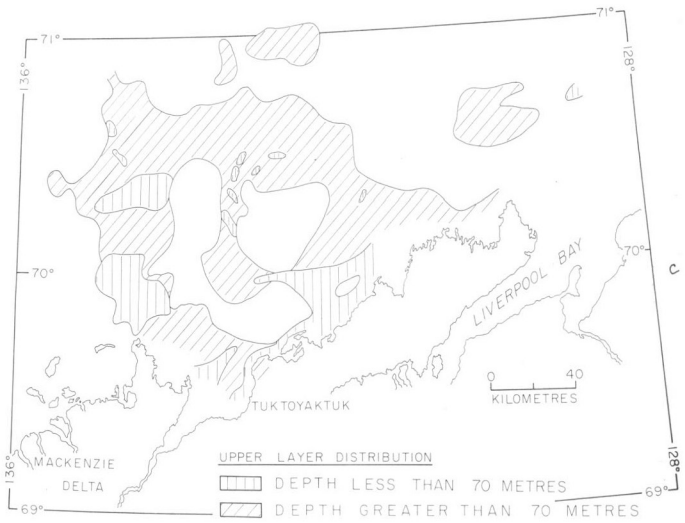


Figure 3.6. Depth to the top of the upper high-velocity layer.

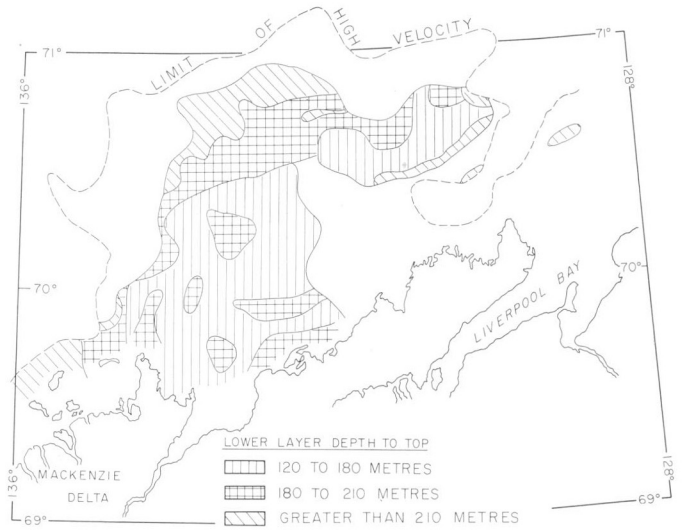


Figure 3.7. Depth to the top of the lower high-velocity layer.

below the sediments. The former profile is typical of thick relict permafrost with ice-bonding probably present where lithology and pore-water salinity are suitable i.e. in fresh-water sands. An alternative explanation of the centre profile, assuming a melting ice-bonded surface at greater depth with high salinity sediments above, seems unlikely in view of the very low temperature determined at bottom hole. The average salinity of seawater in the area would lead to freezing temperatures of -1.7 to -1.9°C. For the latter profile at the westernmost site, the likelihood of a further ice-bonded horizon below the bottom of the hole is small unless the horizon is very close to the melting point.

The one set of results at the easternmost site indicates subzero temperatures. The near-isothermal conditions of the

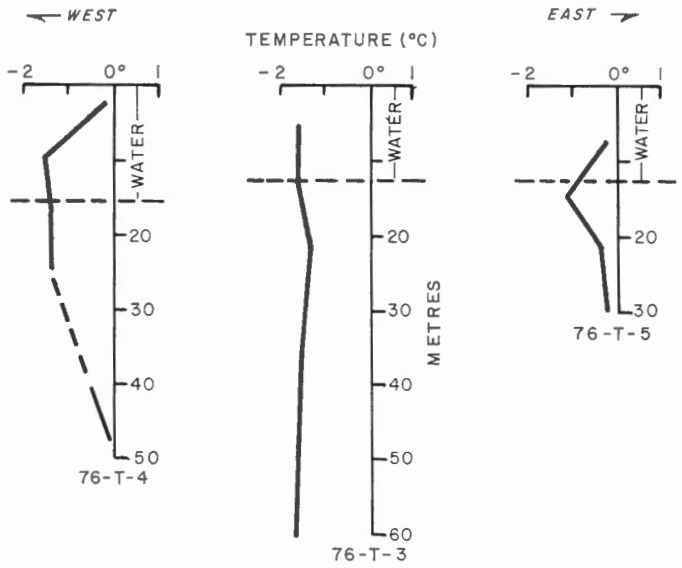


Figure 3.8. Temperature profiles north of Richards Island (from Judge et al., 1976). The locations of the drillholes are shown in Figure 3.6.

bottom two measurements do not clearly indicate the character of the thermal regime, although the low gradient could indicate relict conditions.

The western boundary of the high and intermediate velocity zones near Garry Island were surveyed with 60 m drillholes in the spring of 1977. Cables for temperature observations were installed in nine of the holes, locations of which are shown in Figure 3.10. The tentative equilibrium temperatures are shown as an isothermal cross-section in Figure 3.9. All profiles but the southernmost one indicated temperatures decreasing with depth, although only those north of Netserk B-44 encountered negative temperatures within the depth of observation. A general progression towards lower temperatures was observed from south to north. The cross-section illustrates the complex thermal situation in which the 0°C isotherm is almost vertical, separating warm sediments to the south and cold to the north.

Discussion

No ice-bonding was observed under most of Mackenzie Bay and the area appears free from all but shallow permafrost occurrences in shallow water. This area appears to be restricted to the region of the Mackenzie Canyon (and perhaps the dimensions of the Wisconsin ice lobe) and is sharply bounded on the northeast side. In the Netserk area,

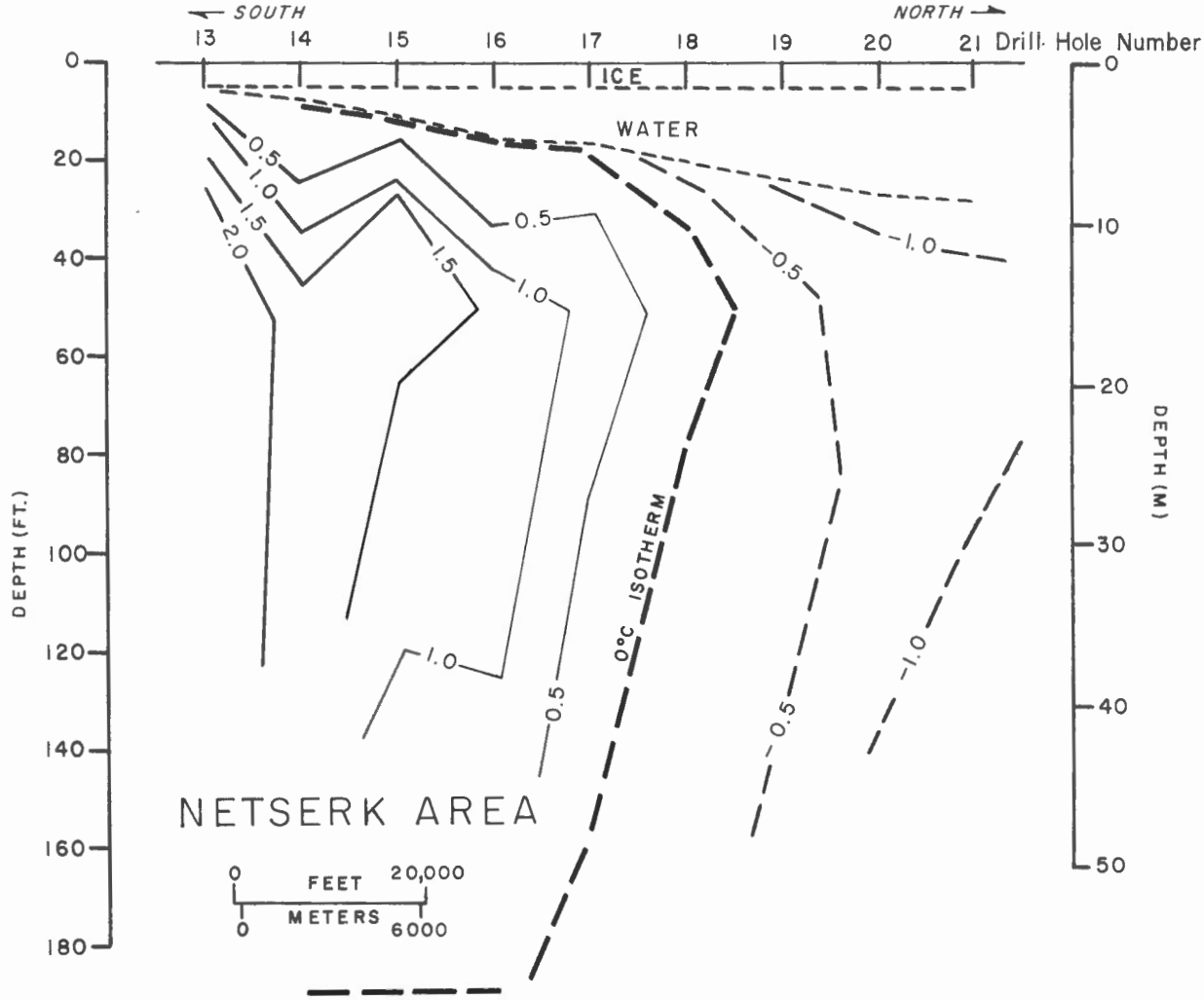


Figure 3.9. Cross-section of the temperature regime north of Garry Island (from MacAulay et al., 1977). The locations of the drillholes are shown in Figure 3.10.

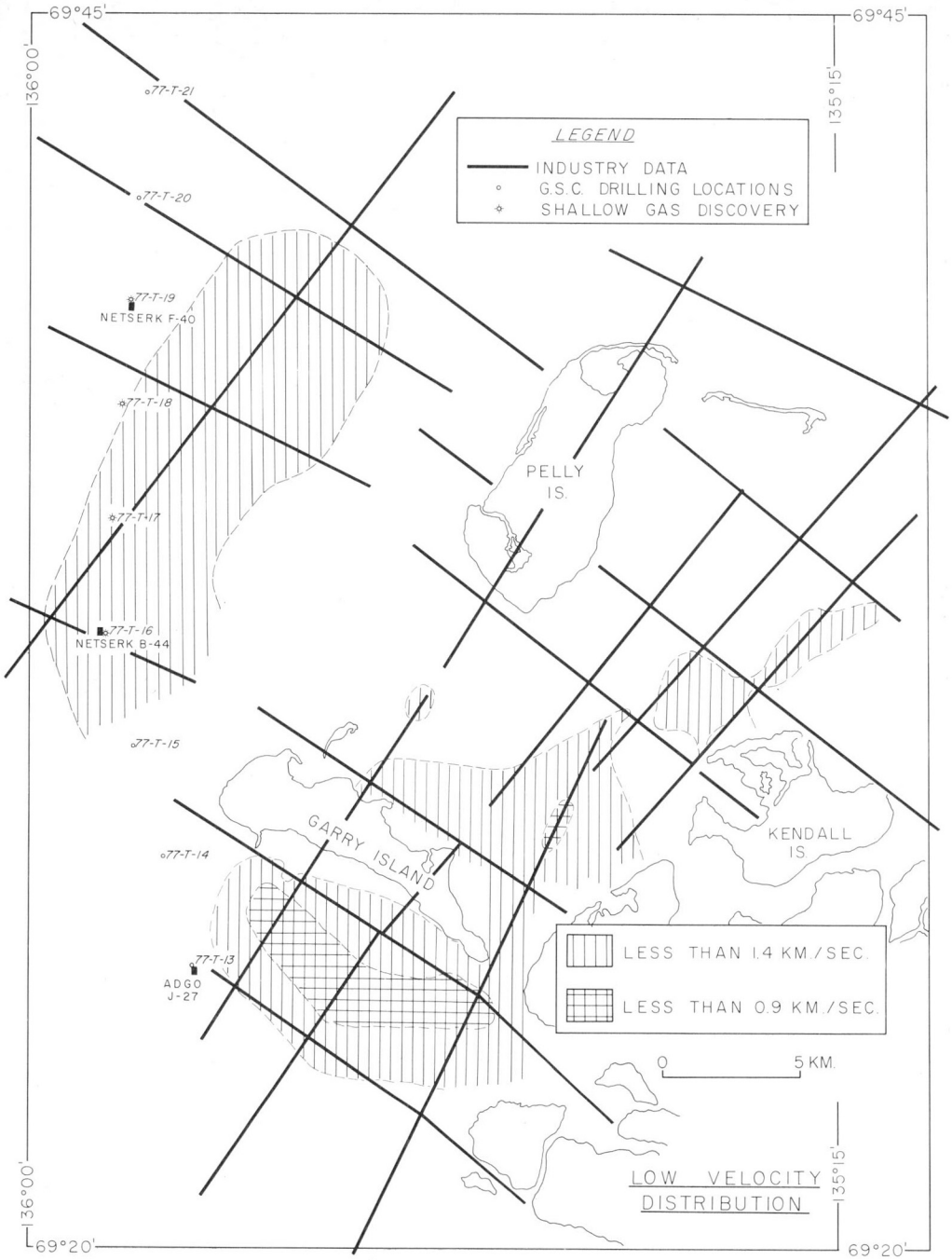


Figure 3.10. Distribution of shallow gas near Garry Island, from drilling observations and from low seismic velocities.

to the north of this boundary, a combination of factors point to gas-hydrate bonding in addition to ice-bonding in the sediments at depths below 150 m (Hunter et al., 1976). Figure 3.9 illustrates the low temperatures encountered and Figure 3.10 shows the holes which encountered gas during drilling. In addition, low seismic velocities in the shallow sediments (lower than the sound velocity in water) were measured in the area shown in Figure 3.10. Low seismic velocities are observed in laboratory measurements when a gas phase is present in the pores of the sediment sample (Gregory, 1976; Domenico, 1976).

These combined factors are good evidence that gas hydrates exist in the Netserk area and the seismic velocity anomaly is consistent with such an interpretation (Stoll et al., 1971).

Shallow gas occurrences of this type may be very common in the vicinity of major permafrost boundaries where the decomposition of degrading hydrates will be most rapid and a permeable path to the surface exists through the unfrozen sediments.

High velocities encountered on the eastern half of the shelf are interpreted as relict ice-bonded permafrost which resulted from a sea level lowering in the past. The upper high velocity layer could result from the presence of intermittent ice-bonding associated with coarse grained lenses embedded in fine grained sediments as observed at the Tingmiark site during engineering drilling (Hunter and Judge, 1975). Possibly the upper layer is composed of segregated ice as observed on land by Rampton and Mackay (1971). Why there are two distinct high-velocity layers is not clear although the explanation could be related to changes of ice content due to changes of temperature, grain size or salinity characteristics. An alternative explanation in terms of a phase change, in which a change from gas-plus-ice to hydrate-plus-ice occurs in the sediment pore spaces below a certain depth, is attractive. The average depth to the top of the lower layer of about 150 m, the depth of stability of hydrates, does not seem entirely fortuitous. Seismic reflections at depths of 150 m in the Alaskan section of the Beaufort Sea have been interpreted as hydrate horizons (Milton, 1977).

Acknowledgments

We acknowledge the assistance and contribution of the oil industry; Gulf Oil Limited, Dome Petroleum Limited, Imperial Oil Limited, Sun Oil Limited, Pan Canadian Petroleum Limited, Geophysical Services Inc., and their partners, who supplied records for this study.

References

Domenico, S.N.
1976: Effect of brine-gas mixture on velocity in an unconsolidated sand reservoir; Geophysics, v. 41 (5), p. 882-894.

Gregory, A.R.
1976: Fluid saturation effects on dynamic elastic properties of sedimentary rocks; Geophysics, v. 41 (5), p. 895-921.

Hofer, H. and Varga, W.
1972: Seismogeologic experience in the Beaufort Sea; Geophysics, v. 37 (4), p. 605-619.

Hunter, J.A. and Judge, A.S.
1975: Geophysical investigations of sub-sea permafrost in the Canadian Beaufort Sea; Proceedings Third International Conference on Port and Ocean Engineering under Arctic Conditions, D.C. Burrell and D.W. Hood, Ed.; Inst. Marine Sci., Univ. Alaska, p. 1025-1057.

Hunter, J.A., Judge, A.S., MacAulay, H.A., Good, R.L., Gagne, R.M., and Burns, R.A.
1976: Permafrost and frozen sub-seabottom materials in the southern Beaufort Sea; Beaufort Sea Project; Tech. Rep. no. 22.

Judge, A.S., MacAulay, H.A., and Hunter, J.A.
1976: An application of hydraulic jet drilling techniques to mapping of sub-seabottom permafrost; in Report of Activities, Part C, Geol. Surv. Can., Paper 76-1C, p. 75-78.

MacAulay, H.A., Judge, A.S., Hunter, J.A., Allen, V.A., Gagne, R.M., Burgess, M., Neave, K.G., and Collyer, J.
1977: A study of sub-seabottom permafrost in the Beaufort Sea by hydraulic drilling methods; Geol. Surv. Can., Open File Report No. 472, Earth Physics Branch Open File No. 77-16.

Milton, D.J.
1977: Methane hydrate in the sea-floor – a significant resource, In The Future Supply of Nature-Made Petroleum and Gas, ed. R.F. Meyer, Pergamon, New York.

Rampton, V. and Mackay, J.R.
1971: Massive ice and icy sediments throughout the Tuktoyaktuk Peninsula, Richards Island and nearby area, District of Mackenzie; Geol. Surv. Can., Paper 71-21, 16 p.

Stoll, R.D., Ewing, J., and Bryan, G.M.
1971: Anomalous wave velocities in sediments containing gas hydrates; J. Geophys. Res., v. 76, p. 2090-2094.

PROBLEMS IN GAMMA-RAY LOGGING: THIN ZONE CORRECTION FACTORS

Project 740085

John G. Conaway
Resource Geophysics and Geochemistry Division

Conaway, John G., Problems in gamma-ray logging: Thin zone correction factors; in Current Research, Part C, Geol. Surv. Can., Paper 78-1C, p. 19-21, 1978.

Abstract

In the case of a gamma-ray log past an isolated zone of radioactive material of effectively infinite thickness and uniform composition the full-width of the anomaly curve at half the maximum count rate is equal to the true zone thickness, regardless of detector length. In the case of thinner isolated zones the full-width half-maximum method gives an erroneously large value for thickness, the degree of error depending in part on detector length. This leads to an underestimation of the concentration of radioactive material, sometimes called 'dilution'. Correction charts given here for a range of detector lengths and probe response functions allow the full-width half-maximum method to be applied to uniform zones of any thickness.

Introduction

The question of how to determine the thickness of a zone of radioactive material is the source of some confusion, and contradictory information regarding this subject is to be found in the literature. It is well known that the full-width of the anomaly curve at half the asymptotic maximum count rate (Fig. 4.1a) is equal to the thickness of a homogeneous zone if the zone is of 'effectively infinite' thickness, that is, if the zone is thick enough so that the gamma-ray count rate nearly achieves the value which would be reached if the zone were truly of infinite thickness. The definition of infinite thickness will be considered in greater detail later in this paper. In the case of a thinner zone however, the full-width half-maximum (FWHM) method gives an erroneously large value for thickness (Fig. 4.1b). Thus, when ore grade G is calculated for the thin zone using the equation

$$G = \frac{KA}{T}$$

(Scott et al., 1961), where A is the area under the anomaly curve, K is the system sensitivity (% U_3O_8 sec/count) as determined in model boreholes and T is the estimated thickness, then the resulting G will be too low; this phenomenon is sometimes called 'dilution' (Dodd and Eschliman, 1972).

The best approach to the general problem of determining the actual distribution of radioactive material along the borehole is some sort of computer processing scheme (see Scott et al., 1961; Conaway and Killeen, in press). If a manual determination of grade and thickness is desired for an isolated thin zone, however, this can be made by using the thin zone correction charts given here. The mathematical development presented here is necessarily brief; a more complete background is given by Conaway and Killeen (in press).

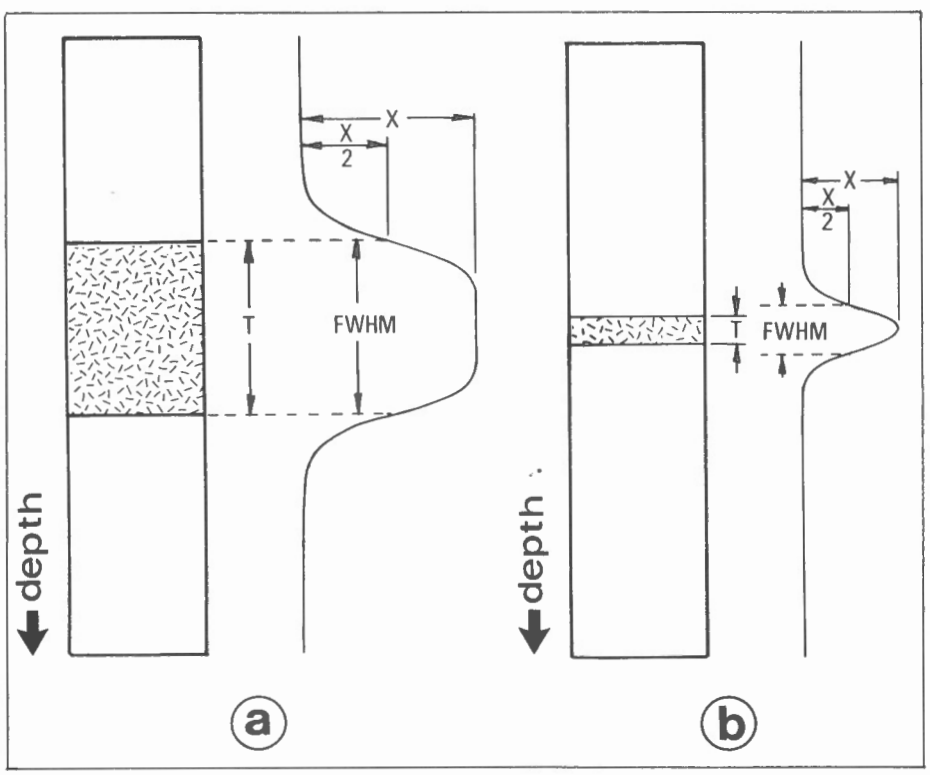


Figure 4.1.

a. Gamma-ray log anomaly due to an isolated uniform zone of radioactive material showing how the full-width half-maximum (FWHM) corresponds to the zone thickness if the zone is of effectively infinite thickness.

b. In the case of a thinner zone the FWHM is greater than the true thickness.

Corrections for Thin Zones

Let the elementary gamma-ray log anomaly due to an infinitesimally thin zone of radioactive material (the 'geologic impulse response') be given by $\phi(z)$, where z is depth. The function q(z) expressing the distribution of ore of grade G for a zone of thickness T is

$$q(z) = G \qquad \text{for } 0 \leq z \leq T$$

$$\text{and } q(z) = 0 \qquad \text{elsewhere} \qquad \ldots(1)$$

The ideal gamma-ray log C(z), using a point detector, will then be given by the convolution of these two functions:

$$C(z) = \int_{-\infty}^{\infty} \phi(\zeta)\, q(z-\zeta)\, d\zeta \qquad \ldots(2)$$

When a detector of length L is used rather than a point detector a detector function f(z) is involved, where

$$f(z) = 1 \qquad \text{for } 0 \leq z \leq L$$

$$\text{and } f(z) = 0 \qquad \text{elsewhere} \qquad \ldots(3)$$

and the gamma-ray log $C_L(z)$ for a detector of finite length is given by

$$C_L(z) = \frac{1}{K} \int_{-\infty}^{\infty} C(\zeta)\, f(z-\zeta)\, d\zeta \qquad \ldots(4)$$

where K is the system sensitivity.

The function $\phi(z)$ will be approximated here as

$$\phi(z) = \frac{\alpha}{2} e^{-\alpha|z|} \qquad \ldots(5)$$

where α is a shape constant determined in model boreholes (see Conaway and Killeen, in press, for more background information).

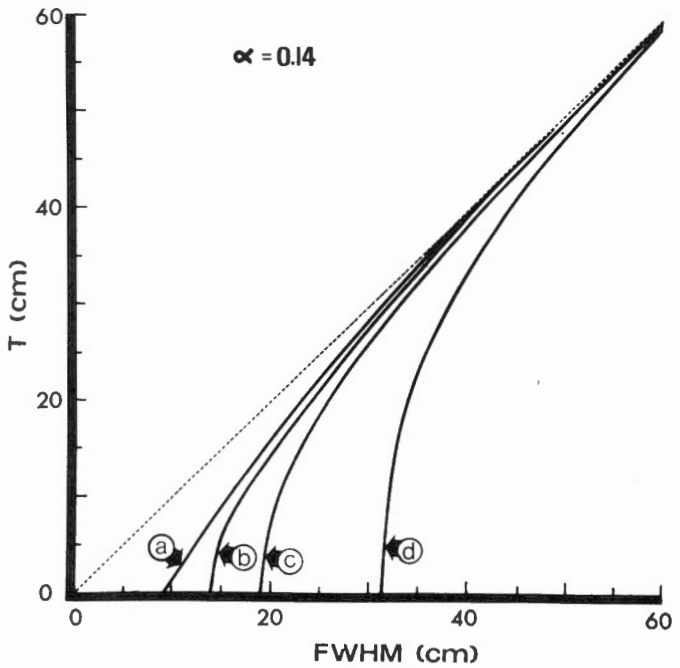


Figure 4.2. Plot of true zone thickness (T) against full-width half-maximum (FWHM) for α = 0.14 and detector lengths of (a) 1 cm, (b) 8 cm, (c) 15 cm, and (d) 30 cm. The dashed line represents the asymptote.

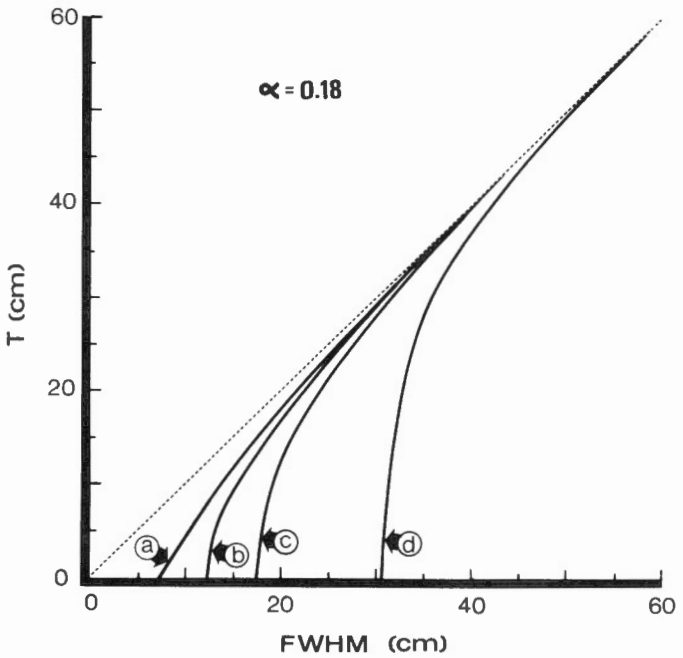


Figure 4.3. Plot of true zone thickness (T) against full-width half-maximum (FWHM) for α = 0.18 and detector lengths of (a) 1 cm, (b) 8 cm, (c) 15 cm and (d) 30 cm. The dashed line represents the asymptote.

Equation (4) was evaluated for various values of T using a digital computer and discrete convolution to yield plots of FWHM apparent zone thickness plotted against true thickness for values of α = 0.14 cm^{-1} and α = 0.18 cm^{-1} (Figs. 4.2, 4.3 respectively). Although α varies with many factors, especially drillhole diameter, fluid content, casing, gamma-ray energy and rock density, it appears that these values of α represent a typical range for Canadian mining boreholes and Geological Survey of Canada logging equipment. Detector lengths chosen for the plots were 1 cm, 8 cm, 15 cm, and 30 cm. Correction factors for other detector lengths can be found from these plots by interpolation.

As an illustration of how to use the correction charts consider once again Figure 4.1b. Let us say that this anomaly is recorded in a borehole under conditions such that α is 0.18 cm^{-1}, and an 8 cm detector was used. The FWHM of the anomaly is measured as 15 cm; from Figure 4.3 the true thickness of the layer (assuming that it is uniform in composition) is about 9.5 cm. In this case the error in ore grade based on the FWHM would be about 37%; this error would be larger for thinner zones, or for smaller values of α.

Zones of Effectively Infinite Thickness

Previously it was stated that the FWHM method gives valid thickness results in the case of isolated uniform zones of effectively infinite thickness. This is true regardless of the detector length. It should be noted, however, that precisely what constitutes effectively infinite thickness depends on the detector length. This relationship is shown in Figure 4.4, determined from numerical calculations based on equations (4) and (5). For practical purposes the effect of detector length on the infinite thickness is quite small for a given value α in the range of detector lengths likely to be used in Canadian mining applications.

Figure 4.4 presents two sets of curves for two different definitions of what constitutes 'effectively infinite' thickness. The solid lines were derived under the assumption that the zone of radioactive material is effectively of infinite

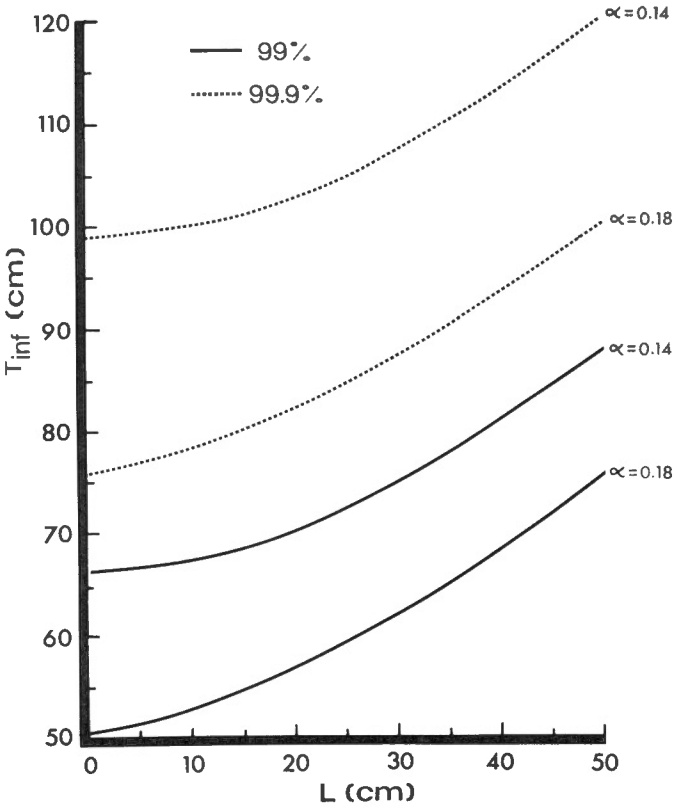


Figure 4.4. Plot of effectively infinite zone thickness (T_{inf}) against detector length (L) for $\alpha = 0.14$ and $\alpha = 0.18$. The solid lines represent the thickness at which the gamma-ray count rate reaches 99 per cent of its asymptotic maximum value, and the dashed lines represent the thickness at which the count rate reaches 99.9 per cent of maximum. For example, for L=8 cm and α=0.18 cm^{-1}, the gamma-ray anomaly will reach 99 per cent of the infinite thickness count rate at approximately T=52 cm, and 99.9 per cent of the infinite thickness count rate at T=78 cm.

thickness when the gamma-ray anomaly achieves 99 per cent of its asymptotic maximum value (i.e. the value which would be achieved if the zone were truly of infinite thickness). In the case shown by the dashed lines that criterion is raised to 99.9 per cent. For most applications the 99 per cent criterion should be adequate.

Conclusions

For isolated thin zones of radioactive material the correction factors given in Figures 4.2 and 4.3 can be used to give an improved estimate of the true thickness over what would be obtained using the full-width half-maximum method. The accuracy of the resulting determinations of thickness and grade can be seriously degraded if poor logging practice is used. In the case of an analog logging system a short ratemeter time constant should be selected in order to minimize distortion. With a digital system it should be obvious that one cannot hope to resolve reliably zones of thickness comparable to, or shorter than, the sampling interval. The sampling interval should be selected with this fact in mind.

Acknowledgment

The author would like to thank P.G. Killeen for helpful discussions regarding the manuscript.

References

Conaway, J.G. and Killeen, P.G.
Quantitative uranium determinations from gamma-ray logs by application of digital time-series analysis; Geophysics (in press).

Dodd, P.H. and Eschliman, D.H.
1972: Borehole logging techniques for uranium exploration and evaluation; in Uranium Prospecting Handbook, S.H.U. Bowie, M. Davis and D. Ostle eds., Inst. Min. Metall. London.

Scott, J.H., Dodd, P.H., Droullard, R.F., and Mudra, P.J.
1961: Quantitative interpretation of gamma-ray logs; Geophysics, v. 26, p. 182-191.

5.

AGE OF CHAMPLAIN SEA AND "LAMPSILIS LAKE" EPISODE IN THE OTTAWA – ST. LAWRENCE LOWLANDS

Project 740068

S.H. Richard
Terrain Sciences Division

Richard, S.H., Age of Champlain Sea and "Lampsilis Lake" episode in the Ottawa – St. Lawrence Lowlands; in Current Research, Part C, Geol. Surv. Can., Paper 78-1C, p. 23-28, 1978.

Abstract

*Radiocarbon dates obtained by the Geological Survey of Canada relating to the late glacial and early postglacial history of the Ottawa-St. Lawrence Lowlands are presented. At the western rim of the Champlain Sea basin near Clayton, Ontario, a radiocarbon date of 12 700 ± 100 years (GSC-2151) was obtained from marine shells, and this indicates a minimum age for deglaciation and marine submergence in that area. Near the top of Rigaud Mountain marine shells from a high level beach of the Champlain Sea yielded a date of 11 200 ± 90 years (GSC-2296) providing a minimum age for deglaciation and marine submergence of the top and southern flank of the mountain. Three dates of 10 600 ± 140 (GSC-2423), 10 300 ± 140 (GSC-2261), and 10 100 ± 130 years (GSC-2189) obtained for marine shells recovered from low level marine beaches near Cazaville, Sainte-Justine-Station, and Deschênes relate to the "**Mya arenaria** phase" and the last stand of the Champlain Sea in the Lowland. A ^{14}C date of 9750 ± 150 years (GSC-2414) was obtained for freshwater shells of the mollusc **Lampsilis siliquoidea** recovered near Saint-Stanislas-de-Kostka from sands of former "**Lampsilis** Lake". The date provides a maximum age for retreat of the Champlain Sea from this part of the St. Lawrence Lowland.*

Introduction

Several radiocarbon dates have been obtained by the Geological Survey of Canada in the last three years relating to the geological history of the western part of the Champlain Sea basin. These dates were obtained for shells collected during field investigations and mapping (1973-1977) of the surficial geology of the Ottawa-St. Lawrence Lowlands.

New dates obtained are listed in Tables 5.1, 5.2, and 5.3, and their geographic locations are shown in Figure 5.1.

Dates Relating to Marine Limit

Clayton Dates

Pelecypod shells (GSC-2151, Table 5.1), identified as **Macoma balthica** by W. Blake, Jr., were collected from an active sand and gravel pit in a beach deposit at an altitude of ca. 168 m, 5.6 km north of Clayton, Lanark County, Ontario (45°14'15"N, 76°19'00"W; Fig. 5.1). A sample dated earlier from this same locality (GSC-1859) provided an age of 12 800 ± 200 years (Richard, 1974, p. 219; 1975, p. 114). The date on the inner fraction of the second run is accepted as being the most reliable age for this site. The age obtained (12 700 ± 100 years) provides a minimum age for deglaciation of the Clayton area and for arrival of marine waters along the western rim of the Champlain Sea basin. The elevation of this collection (ca. 168 m) is believed to represent the marine limit in the area. This date is the oldest for postglacial marine submergence in the entire Champlain Sea basin. A date of 11 500 ± 90 years (GSC-2269) was obtained for the forefin bone of a bowhead whale (Harington, 1977) collected from beach deposits at an elevation of 168 m at White Lake, 35 km northwest of Clayton. It was expected that these two dates would be similar, and the reason for the 1200 year discrepancy is not known.

The date of arrival of marine waters along the western rim of the Champlain Sea basin does not correlate with other published radiocarbon dates relating to the first penetration of marine waters into the basin. The date is virtually identical to that of 12 720 ± 170 years (GSC-102) obtained by Lee in 1963 at Trois-Pistoles, Quebec, east of the study area, for shells of **Portlandia arctica** in clay overlain by deltaic sands; this date (GSC-102) was interpreted as indicating deglaciation of the area and penetration of marine waters at least this far west (Dyck and Fyles, 1963, p. 18). Radiocarbon dates obtained for the area east of Trois-Pistoles show that marine overlap along the south shore of the St. Lawrence River estuary had started around 13 500 years B.P. in the Gulf of St. Lawrence and had progressed up river at least as far as Trois-Pistoles by 12 800 years B.P. (Dionne, 1977, p. 66-67).

West of Trois-Pistoles, however, ^{14}C dates of this general age have not been obtained for marine fossils (Dionne, 1977, p. 68). It has been stated in the past that postglacial marine submergence of the Ottawa-St. Lawrence Lowlands did not start until a narrow corridor had become free of ice on either side of Québec City, so that the waters of the Goldthwait Sea could have access to the Lowlands. The oldest radiocarbon dates obtained for the Québec City region and the area to the south are: 12 400 ± 160 (GSC-1533; Lowdon and Blake, 1973, p. 13) at Charlesbourg, Quebec; 12 230 ± 250 (QU-93; LaSalle, 1974, 13 p.) at Saint-Henri-de-Lévis, Quebec; 12 000 ± 230 (GSC-936; Lowdon and Blake, 1970, p. 58) at L'Avenir, Quebec; and 12 000 ± 200 years (Kirkland and Coates, 1977, p. 501) at Massena, New York, U.S.A.

Although the presence or absence of a marine microfauna at the Clayton site has not been determined, the occurrence of only one molluscan species of macrofossils (**Macoma balthica**), which is quite tolerant to both marine waters of very low salinities and some freshwaters, suggests that the early phase of the Champlain Sea might belong in the "Transitional Phase" of the pre-Burlington Stage of the sea's history (Cronin, 1977, p. 246). This "Transitional Phase" of the Champlain Sea has been identified in Champlain Valley of New York and Quebec by Cronin on the basis of the presence in the faunal assemblage of a "mixed association of fresh water ostracodes with euryhaline marine ostracodes and molluscs", and it is estimated to have lasted in that southern arm of the marine basin from "about 12 500 to 11 600 years B.P."

Table 5.1

Champlain Sea radiocarbon dates relating to marine limit in Ottawa-St. Lawrence Lowlands

Laboratory Dating No.	Date (years B.P.)	Locality	Material	Collector	Reference
GSC-2151	12 800 ± 100 (Outer fraction) 12 700 ± 100 (Inner fraction)	Clayton, Lanark County, Ontario	Marine shells in beach gravels at 168 m a.s.l.	S.H. Richard, W. Blake, Jr.	Unpublished, this paper
GSC-2269	11 500 ± 90	White Lake, Renfrew County, Ontario	Whale bones in beach sands at 168 m a.s.l.	A. Jones, C.C. Kennedy	Harington, 1977, p. 525
GSC-2296	11 200 ± 90	Rigaud, Vaudreuil County, Quebec	Marine shells in beach gravels and sands at 160 m a.s.l.	S.H. Richard	Unpublished, this paper

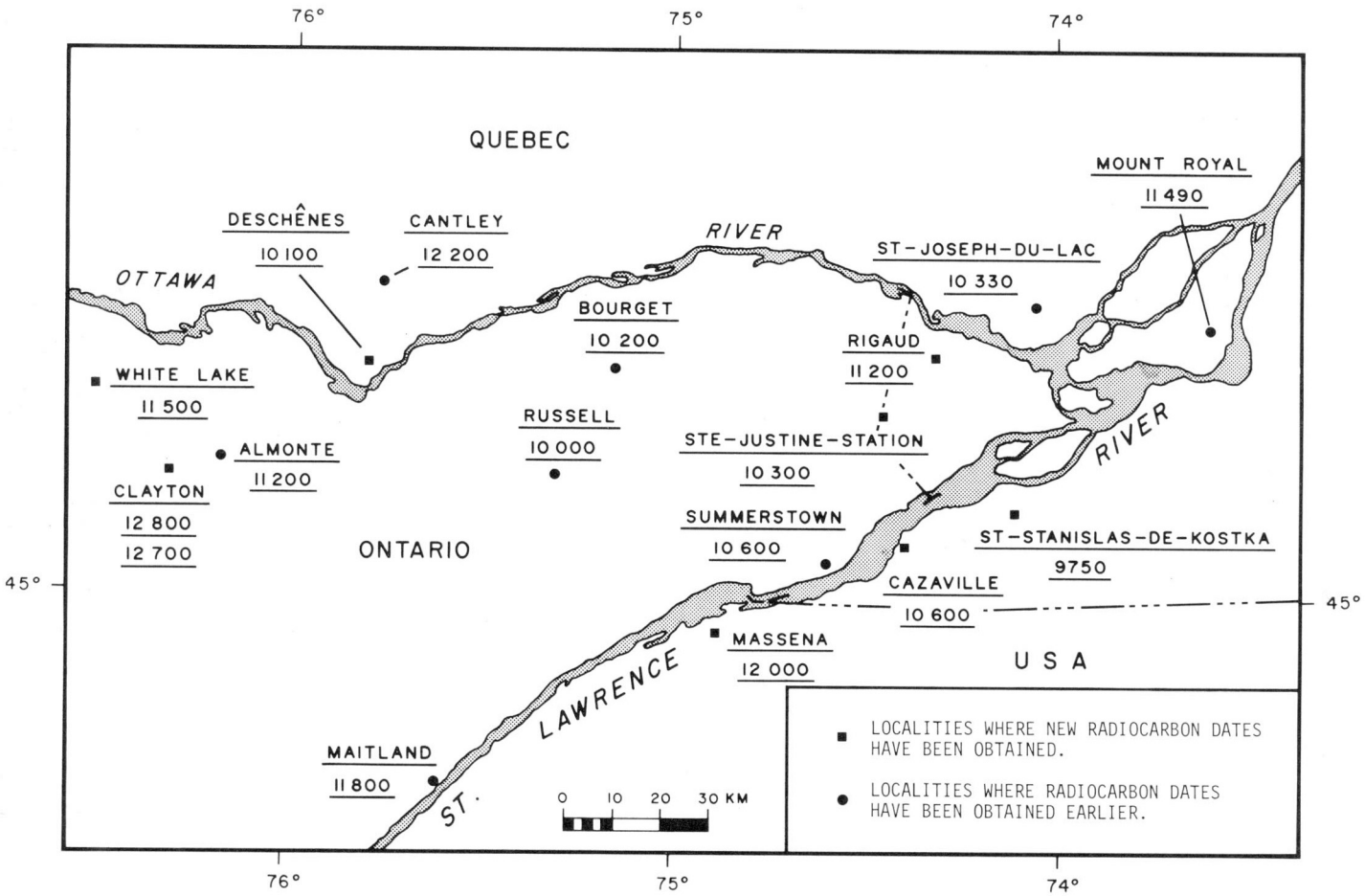


*Figure 5.1. Location map of Ottawa-St. Lawrence Lowlands showing localities where new radiocarbon dates have been obtained for deglaciation, marine limit, "**Mya arenaria** phase" of Champlain Sea and "**Lampsilis** Lake" episode.*

This early "Transitional Phase" of the Champlain Sea in the western part of the basin also has been identified in Gatineau Valley north of Ottawa on the basis of several radiocarbon dates obtained in the last ten years for marine shells of the same species (**Macoma balthica** mainly) collected by various investigators, even if the dates are all younger than the Clayton dates. The oldest ^{14}C dates obtained for the Ottawa region and the area to the south are: 12 200 ± 160 (GSC-1646; Lowdon and Blake, 1973, p. 16-17) at Cantley, Quebec; 11 900 ± 160 (GSC-1772; Lowdon and Blake, 1973, p. 17) at Martindale, Quebec; 11 800 ± 210 (GSC-1013; Lowdon and Blake, 1970, p. 60-61) at Maitland, Ontario; 11 600 ± 150 (GSC-842; Lowdon and Blake, 1970, p. 59) at Meach Lake, Quebec; and 11 500 ± 150 years (GSC-1612; Lowdon and Blake, 1975, p. 12) at Lascelles, Quebec.

An important implication of this 12 700 ± 100 year (GSC-2151) date from Clayton on the deglaciation pattern of southern Quebec and southeastern Ontario already has been shown by Borns and Hughes (1977, p. 204): "A date of 12,800 yrs. B.P. on marine shells reported from the St. Lawrence Lowlands (Prest, pers. comm.) demonstrates that by that time a calving bay had progressed up the Lowlands from the Gulf of St. Lawrence to the vicinity of Ottawa, Ontario. Because of the presence of Laurentide ice in Maine at this time, it is clear that this marine incursion partitioned the Laurentide ice sheet leaving a residual ice cap to the south of the St. Lawrence Lowlands over Quebec, Maine, and New Brunswick after 12,800 yrs. B.P. while at the same time the margin of the main Laurentide ice sheet lay along the northern margin of the sea filling the St. Lawrence Lowlands". Thomas (1977, p. 354-355) used this same assumption.

The interpretation suggested by this new ^{14}C date (GSC-2151) concerning the time of penetration of the Champlain Sea waters in the Ottawa-St. Lawrence Lowland, however, has created a correlation problem with the chronology developed for the deglaciation and proglacial lakes history of the eastern Great Lakes area to the west. Karrow (1975, p. 83) and Dreimanis (1977, p. 45) believed that glacial Lake Iroquois was in existence from 12 600 to 11 900 years ago in the Lake Ontario basin and that it was dammed by ice lying in the upper St. Lawrence Lowlands northeast of the Kingston area before that area was invaded by the marine waters of the Champlain Sea. As already pointed out by LaSalle et al. (1977, p. 37-38), GSC-2151, GSC-1859, and the other early Champlain Sea dates older than ca. 11 800 years mentioned above pose, for the time being, a correlation problem with the late Quaternary chronology developed for the Great Lakes area, and further investigations will be required before it is resolved successfully.

Rigaud Mountain Date

Pelecypod shells (GSC-2296, Table 5.1), identified by W. Blake, Jr. as **Hiatella arctica,** were collected from a sand pit in a beach deposit on Rigaud Mountain at an altitude of ca. 160 m 3.2 km south of Rigaud, Vaudreuil County, Quebec, (45°26'45"N, 74°19'40"W; Fig. 5.1). The date obtained, 11 200 years, provides a minimum age for deglaciation of the top and southern flank of Rigaud Mountain. Gravel and sand near the top of Rigaud Mountain at an elevation of ca. 192 m did not yield marine fossils but the deposit is believed to represent the marine limit in the area. A beach deposit at ca. 180 m a.s.l. and 1 km east of the GSC-2296 sampling site contained fragments of **Hiatella arctica** and **Macoma balthica,** but not enough was recovered for radiocarbon dating (Richard, 1976a, p. 207-208).

This fossiliferous marine beach deposit at ca. 180 m represents the highest well defined Champlain Sea shoreline on the south side of Rigaud Mountain and is believed to be the first and oldest shore feature to have developed in the area (Richard, 1976a, p. 207-208).

The sample date and elevation on Rigaud Mountain may be compared with a date of 11 490 years (GrN-1697) from 172 m "at or near marine limit" on Mont Royal 50 km to the east (Elson, 1969a, p. 367) and another date of 11 370 ± 360 years (Y-233) for marine shells from another site in the same area and at the same elevation (Elson, 1962, p. 61). A date of 11 200 years (GSC-1672; Lowdon and Blake, 1973) was obtained from a Champlain Sea shoreline at 154 m at Almonte, Lanark County, Ontario along the western side of the Champlain Sea basin. This date is from 13 m lower and is 1500 years younger than the local marine limit (see section describing Clayton dates).

Other shells recovered from the Rigaud site include: **Macoma balthica, Mytilus edulis, Balanus hameri,** and **Mya arenaria.** This macrofaunal assemblage seems to suggest a deposition during the late part of the "**Hiatella arctica** phase" of the Champlain Sea just before the transition to the "**Mya arenaria** phase" ca. 11 000 to 10 900 years B.P. (Elson, 1969a, p. 371; Cronin 1977, p. 248) and seems to imply that deposition did not necessarily closely follow deglaciation of the area.

Radiocarbon Dates Relating to "Mya arenaria phase" of the Champlain Sea in Ottawa-St. Lawrence Lowlands

The "**Mya arenaria** phase" is the last phase of the Champlain Sea and lasted from ca. 10 900-10 600 to 10 000-9800 years B.P. in the central part of the basin around Montreal (Elson and Elson, 1959, p. 1596; Elson, 1964, p. 54; 1969a, p. 367-371; Cronin, 1977, p. 245, 248). The faunal assemblage associated with this phase indicates cold-temperate marine conditions.

Sainte-Justine-de-Newton Date

Pelecypod shells (GSC-2261, Table 5.2), identified as **Mya truncata** L. by W. Blake, Jr., were collected from a drainage ditch exposing fossiliferous sand overlying compact, silty to clayey diamicton at an altitude of ca. 75 m, 3.2 km southwest of Sainte-Justine-Station, Quebec (45°20'25"N, 74°27'00"W; Fig. 5.1). This shell sample is from a shallow water or low level beach sand deposit of the Champlain Sea (Richard, 1976a, p. 205). It consisted of paired valves found upright in living position at the base of the sand with the lower part of the specimens anchored in the underlying diamicton. Specimens of other macrofaunal species found in situ in the marine beach deposit include **Mya arenaria, Mytilus edulis,** and **Macoma balthica.** This macrofaunal marine assemblage reflects cold temperate marine water conditions and indicates deposition during the last part of the Champlain Sea episode. This is the farthest west reported occurrence of **Mya truncata** in Champlain Sea sediments (Wagner, 1970, p. 12, 43, 67-72). The date indicates a "**Mya arenaria** phase" age for this deposit (Elson, 1969a) and correlates with a date of 10 330 ± 100 years (GrN-2035) obtained by Elson at Saint-Joseph-du-Lac, Quebec for this same species (**Mya arenaria**) in a similar situation. Shells of **Hiatella arctica** from the underlying diamicton at this locality gave a date of 10 500 ± 100 years (GSC-2391; Richard, 1976a, p. 205).

Deschênes Date

Pelecypod shells (GSC-2189, Table 5.2), identified as **Hiatella arctica** by W. Blake, Jr., were collected from a drainage ditch in pebbly sand at an altitude of ca. 94 m, 3.2 km north of Deschênes, Gatineau County, Quebec, (45°24'40"N, 75°48'00"W; Fig. 5.1).

Table 5.2

Radiocarbon dates relating to "**Mya arenaria** phase" of the Champlain Sea in the Ottawa-St. Lawrence Lowlands

Laboratory Dating No.	Date (years B.P.)	Locality	Material	Collector	Reference
GSC-2261	10 300 ± 140	Sainte-Justine-de-Newton, Vaudreuil County, Quebec	Marine shells in beach sands at 75 m a.s.l.	W. Blake, Jr., E.B. Owen, S.H. Richard	Unpublished, this paper
GSC-2189	10 100 ± 130	Deschênes, Gatineau County, Quebec	Marine shells in beach gravels at 94 m a.s.l.	S.H. Richard	Unpublished, this paper
GSC-2423	10 600 ± 140	Cazaville, Huntingdon County, Quebec	Marine shells in beach sands at 55 m a.s.l.	S.H. Richard	Unpublished, this paper
GSC-1553	10 000 ± 320	Russell, Russell County, Ontario	Marine shells in beach sands at 70 m a.s.l.	S.H. Richard	Lowdon and Blake, 1973, p. 19

These shells were recovered from a shallow water or shoreline pebbly sand that forms the lowest raised beach of the Champlain Sea in the Ottawa-Hull area (Richard, 1974, p. 219; 1976b; Richard et al., 1977). Directly east of the fossiliferous beach deposit the highest post-Champlain Sea river bluff cut into marine clay by the early Ottawa River occurs at an elevation of ca. 90 to 91 m. The presence of the high fluvial terrace associated with this bluff below but near the level of the marine beach suggests that no lacustrine phase, corresponding to "**Lampsilis** Lake" of the upper St. Lawrence valley, followed the Champlain Sea in Ottawa Valley.

This date agrees with GSC-1553 (10 000 ± 320 years) obtained for marine pelecypod shells (**Macoma balthica** and **Macoma calcarea**) recovered from a shallow water or shoreline sand forming the lowest beach of the Champlain Sea at ca. 70 m elevation near Russell, Ontario, 45 km southeast of Deschênes (Lowdon and Blake, 1973, p. 19).

There is, however, a minor discrepancy between this date and GSC-1968 (10 200 ± 90 years) on postmarine submergence **Lampsilis siliquoidea** shells at Bourget, Ontario (Gadd, 1976, p. 2,4,6; Lowdon and Blake, 1976, p. 6).

Cazaville Date

Pelecypod shells (GSC-2423, Table 5.2), identified by S.H. Richard as **Macoma balthica**, were collected from a sand pit in the lowest beach of the Champlain Sea at an altitude of ca. 55 m, 2.3 km northwest of Cazaville, Huntingdon County, Quebec, (45°06'15"N, 74°23'25"W; Fig. 5.1). The shells were collected from the lowest beach of the Champlain Sea in the area south of St. Lawrence River between Valleyfield and Fort Covington and south and west of Montreal Island (Richard, 1977, p. 512). The date compares well with that of 10 600 ± 200 years (L-604C) obtained by Terasmae (1965, p. 36) for shells from the lowest Champlain Sea beach, elevation 61 m, at Summerstown some 14 km west of Cazaville. After the sea fell below 55 m in this area, a change from a marine to a freshwater environment took place and "**Lampsilis** Lake" came into existence.

Radiocarbon Date Relating to the Submergence of Part of the Ottawa-St. Lawrence Lowlands by the Freshwaters of the "Lampsilis Lake".

After the Champlain Sea had fallen to a level at ca. 50 m a.s.l., Ottawa Valley Lowland had emerged, but water remaining in St. Lawrence River Lowland on either side of Montreal between Cornwall and Deschaillons became fresh, forming a water body called "**Lampsilis** Lake" by Elson (Elson and Elson, 1959, p. 1596; Elson, 1962, p. 64-65; 1964, p. 54; 1968, p. 116; 1969a, p. 369; 1969b, p. 254; Prest, 1970, p. 723-724).

Saint-Stanislas-de-Kostka Date

Freshwater bivalve shells (GSC-2414, Table 5.3), identified by A.H. Clark, Jr., National Museum of Natural Sciences, as **Lampsilis siliquoidea**, were collected from a drainage ditch in yellowish sand overlying a marine silty clay at an altitude of ca. 47 m, 3.5 km southeast of Saint-Stanislas-de-Kostka, Beauharnois County, Quebec (45°09'30"N, 74°05'45"W; Fig. 5.1). This sample was collected from 5 to 6 m below the lowest shoreline of the Champlain Sea. The date is the first obtained on the freshwater mollusc **Lampsilis siliquoidea** from estuarine-lacustrine sands overlying Champlain Sea sediments within the "**Lampsilis** Lake" basin as identified and mapped in earlier works (Elson, 1962, p. 65; Prest, 1970, p. 723-724; Richard, 1977, p. 512; Terasmae, 1965, p. 27,37). It agrees well with the estimate of 9500 years made by Terasmae (Terasmae, 1965, p. 37) and the 9300 years estimate by Elson (Elson, 1968, p. 116) to mark the time when the Champlain Sea episode had just come to a close. The date (GSC-2414) seems to correlate with GSC-1976 (9730 ± 140 years) obtained for freshwater shells collected by LaSalle in the Québec City area and identified by A.H. Clark, Jr., National Museum of Natural Sciences, as **Elliptio complanatus** (LaSalle et al., 1977, p. 59). LaSalle's interpretation of this ^{14}C date is that the marine waters of the Champlain Sea already had started to turn fresh in the area west of Québec City more than 9700 years ago and that this freshwater phase probably corresponds to the "**Lampsilis** Lake" episode identified by Elson (1962) in the Montreal area (LaSalle et al., 1977, p. 58-59; Lowdon et al., 1977, p. 6-7).

Table 5.3

Radiocarbon date relating to the post-Champlain Sea submergence of part of the Ottawa-St. Lawrence Lowlands by the freshwaters of "**Lampsilis** Lake"

Laboratory Dating No.	Date (years B.P.)	Locality	Material	Collector	Reference
GSC-2414	9750 ± 150	Saint-Stanislas-de-Kostka, Beauharnois County, Quebec	Freshwater shells in shallow water sands at 47 m a.s.l.	S.H. Richard	Unpublished, this paper

Summary

The dates reported in this paper add more information to the mounting body of data concerning the chronology of the Champlain Sea. The oldest date (12 700 years) was obtained for deposits near Clayton at the western margin of the basin. This date raises problems concerning the route taken by the invading sea because dates this old have not been obtained for marine deposits along the southern margin of the basin. The presence of marine material that is almost as old, in Gatineau River valley, however, seems to indicate that this date is of the correct order of magnitude. There are difficulties reconciling this date with the current deglaciation chronology of the Great Lakes, but this will have to be solved by further research. Dates on the final phase of the Champlain Sea indicate that it was still present in the Ottawa area 10 000 years ago. The freshwater lake that followed the Champlain Sea in the St. Lawrence Lowlands ("**Lampsilis** Lake") was present 9750 years ago.

Acknowledgments

The author is indebted to R.J. Fulton for critical review of and suggested changes to the manuscript. G. Ménard, B. Wilson, and R. Hélie ably assisted the author in the field in the collection of shell samples. Thanks are extended to W. Blake, Jr. who accompanied the author on two occasions and collected shell samples, and who supervised the processing of the samples in the Radiocarbon Dating Laboratory.

References

Borns, H.W., Jr. and Hughes, T.J.
1977: The implications of the Pineo Ridge readvance in Maine; Géogr. phys. Quat., v. XXXI, no. 3-4, p. 203-206.

Cronin, T.M.
1977: Late Wisconsin marine environments of the Champlain Valley (New York, Quebec); Quat. Res., v. 7, no. 2, p. 238-253.

Dionne, J.C.
1977: La mer de Goldthwait au Québec; Géogr. phys. Quat., v. XXXI, no. 1-2, p. 61-80.

Dreimanis, A.
1977: Correlation of Wisconsin glacial events between the Eastern Great Lakes and the St. Lawrence Lowlands; Géogr. phys. Quat., v. XXXI, no. 1-2, p. 37-51.

Dyck, W. and Fyles, J.G.
1963: Geological Survey of Canada radiocarbon dates I and II; Geol. Surv. Can., Paper 63-21, 31 p.

Elson, J.A.
1962: Pleistocene geology between Montreal and Covey Hill; in Intercollegiate Geological Conference Guidebook (ed. T.H. Clark); 54th Ann. Meeting, Montreal, Oct. 5-7, 1962, p. 61-66.

1964: Late Pleistocene water bodies in the St. Lawrence Lowland (abstract); Geol. Soc. Am., Spec. Paper 76, p. 54.

1968: Champlain Sea; in Encyclopedia of Geomorphology (ed. R.W. Fairbridge); Reinhold, New York, p. 116-117.

1969a: Radiocarbon dates, **Mya arenaria** phase of the Champlain Sea; Can. J. Earth Sci., v. 6, no. 3, p. 367-372.

1969b: Late Quaternary marine submergence of Quebec; Rev. Geogr. Montr., v. XXIII, no. 3, p. 247-258.

Elson, J.A. and Elson, J.B.
1959: Phases of the Champlain Sea indicated by littoral mollusks (abstract); Geol. Soc. Am., Bull., v. 70, p. 1956.

Gadd, N.R.
1976: Surficial geology and landslides of Thurso-Russell map-area, Ontario; Geol. Surv. Can., Paper 75-35, 7 p.

Harington, C.R.
1977: Marine mammals in the Champlain Sea and the Great Lakes; in Amerinds and their Paleoenvironments in northeastern North America, ed. W.S. Newman and B. Salwen; N.Y. Acad. Sci., Ann., v. 288, p. 508-537.

Karrow, P.F., Anderson, T.W., Clarke, A.H., Delorme, L.D., and Skreenivasa, M.R.
1975: Stratigraphy, paleontology, and age of Lake Algonquin sediments in southwestern Ontario, Canada; Quat. Res., v. 5, no. 1, p. 49-87.

Kirkland, J.T. and Coates, D.R.
1977: The Champlain Sea and Quaternary deposits in the St. Lawrence Lowland, New York; in Amerinds and their Paleoenvironments in northeastern North America, ed. W.S. Newman and B. Salwen; N.Y. Acad. Sci., Ann., v. 288, p. 498-507.

LaSalle, P.
1974: Géologie des dépôts meubles de la région de Québec, Qué; Min. rich. nat., Dir. Gén. Mines, dossier public no. 249, Rapp., 13 p. et 4 cartes.

LaSalle, P., Martineau, G., and Chauvin, L.
1977: Morphology, stratigraphy and deglaciation in Beauce-Notre-Dame Mountains-Laurentide Park area; Min. rich. nat., Quebec; DPV-516, 74 p.

Lowdon, J.A. and Blake, W., Jr.
1970: Geological Survey of Canada radiocarbon dates IX; Radiocarbon, v. 12, p. 46-86.

1973: Geological Survey of Canada radiocarbon dates XIII; Geol. Surv. Can., Paper 73-7, 61 p.

1975: Geological Survey of Canada radiocarbon dates XV; Geol. Surv. Can., Paper 75-7, 32 p.

1976: Geological Survey of Canada radiocarbon dates XVI; Geol. Surv. Can., Paper 76-7, 20 p.

Lowdon, J.A., Robertson, I.M., and Blake, W., Jr.
1977: Geological Survey of Canada radiocarbon dates XVII; Geol. Surv. Can., Paper 77-7, 25 p.

Prest, V.K.
1970: Quaternary geology of Canada; in Geology and Economic Minerals of Canada, ed. R.J.W. Douglas; Geol. Surv. Can., Econ. Geol. Rep. 1, 5th ed., p. 675-764.

Richard, S.H.
1974: Surficial geology mapping: Ottawa-Hull area (parts of 31 F,G); in Report of Activities, Part B, Geol. Surv. Can., Paper 74-1B, p. 218-219.

1975: Surficial geology mapping: Ottawa Valley Lowlands (parts of 31 G,B,F); in Report of Activities, Part B, Geol. Surv. Can., Paper 75-1B, p. 113-117.

Richard, S.H. (cont'd)
1976a: Surficial geology mapping: Valleyfield-Rigaud area, Quebec (31 G/1, 8,9); in Report of Activities, Part A, Geol. Surv. Can., Paper 76-1A, p. 205-208.

1976b: Surficial geology of Ottawa map-area; Geol. Surv. Can., Open File 366.

1977: Surficial geology mapping: Valleyfield-Huntingdon area, Quebec; in Report of Activities, Part A, Geol. Surv. Can., Paper 77-1A, p. 507-512.

Richard, S.H., Gadd, N.R., and Vincent, J.S.
1977: Surficial materials and terrain features of Ottawa-Hull area; Geol. Surv. Can., Map 1425A.

Terasmae, J.
1965: Surficial geology of the Cornwall and St. Lawrence Seaway Project areas, Ontario; Geol. Surv. Can., Bull. 121, 54 p.

Thomas, R.H.
1977: Calving bay dynamics and ice sheet retreat up the St. Lawrence Valley system; Géogr. phys. Quat., v. XXXI, no. 3-4, p. 347-356.

Wagner, F.J.E.
1970: Faunas of the Pleistocene Champlain Sea; Geol. Surv. Can., Bull. 181, 104 p.

6.

INTERPRETATION OF A MARINE DEEP SEISMIC SOUNDING SURVEY IN WINONA BASIN OFF THE WEST COAST OF CANADA

E.M.R. Research Agreements 1135-D13-4-92/76, 2239-4-87/77, 2239-4-167/78

R.M. Clowes[1], A.J. Thorleifson[1,2], and S. Lynch[1,2]
Regional and Economic Geology Division

Clowes, R.M., Thorleifson, A.J., and Lynch, S., Interpretation of a marine deep seismic sounding survey in Winona Basin off the West Coast of Canada; in Current Research, Part C, Geol. Surv. Can., Paper 78-1C, p. 29-34, 1978.

Abstract

During 1975, three reversed deep seismic sounding profiles and additional subcritical incidence reflection profiles were recorded in Winona Basin, a deep water sedimentary basin west of northern Vancouver Island. Analyses of the reflection data indicate an upper sedimentary structure of three or four prominent horizons with interval velocities ranging from 1.6 to 3.8 km/s, and having a total depth extent of about 2 km in the central basin. This is underlain by a lower sedimentary structure with velocity of approximately 4.3 km/s and thickness of about 2 km. From the analysis of the refraction data, the average velocity of the subsediment crustal section is approximately 6.0 km/s and its thickness is about 10 km along the central basin. Significant lateral variations in crustal structure occur across the basin. The seismic results are consistent with a proposal of oblique subduction between the Explorer and American plates.

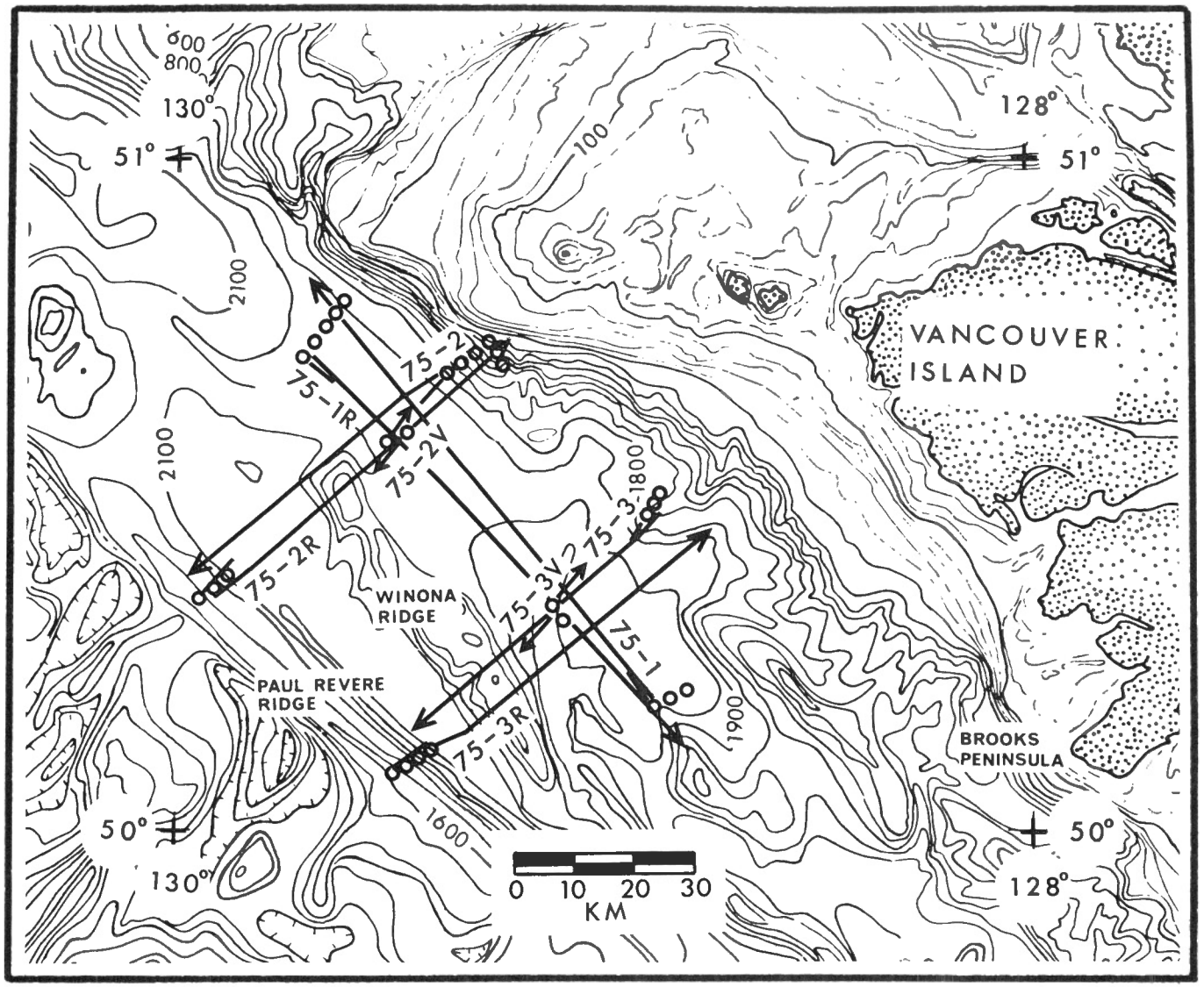


Figure 6.1. Location of 1975 marine deep seismic sounding profiles in Winona Basin. Open circles show the drift track of the receiving ship during the profile runs.

[1]Department of Geophysics and Astronomy, University of British Columbia, Vancouver, B.C. V6T 1W5.

[2]Present address: Gulf Oil Canada Limited, P.O. Box 130, Calgary, Alberta T2P 2H7.

Introduction

During 1975, three reversed deep seismic sounding (DSS) profiles and additional subcritical incidence reflection profiles were recorded in Winona Basin, a deep water sedimentary basin west of northern Vancouver Island (Fig. 6.1). Signals from six individual hydrophones suspended at 45 m depth from a 600 m cable trailed behind the receiving ship were recorded digitally while the shooting ship detonated explosive charges ranging in size from 2.2 kg to 200 kg at distances from less than 1 to 95 km. Clowes (1977) has described the marine DSS system in detail. To acquire complementary data, three vertical incidence continuous seismic profiles (CSP's) using a 300 $in.^3$ air gun and a single channel streamer were recorded along three of the DSS profiles (75-1R, 75-2R and 75-3, Fig. 6.1).

The explosion seismograms are statics – and amplitude – corrected, filtered and, if necessary, stacked before compilation into record sections. To obtain velocity-depth information from the subcritical reflection data, the T^2-X^2 and ray parameter methods are used. For the refraction data, traveltime of first and secondary arrivals and the relative amplitude characteristics of the seismic sections are used in conjunction with synthetic seismograms to provide an interpreted velocity/depth model. The latter approach requires an assumption of lateral homogeneity. However,the data recorded along the two reversed profiles across the basin (profiles 75-2 and 75-2R; 75-3 and 75-3R) indicated that such an assumption was not justified. As a result, a computer program for ray tracing through a laterally inhomogeneous medium was developed. Traveltime-distance curves are determined from reflected and refracted P-wave ray paths through the medium and compared with observed traveltime characteristics.

Reflection Data

The CSP data show a number of features as the basin is crossed. Starting from the west at Paul Revere Ridge, the eastern face of the ridge dips eastward at about 10° beneath flat lying turbidite sediments. In the region between Paul Revere and Winona ridges, the young sediments are arched as if they were being compressed. Winona Ridge is an outstanding topographical feature with virtually no evidence for layering such as that seen in the young sediments to either side of it. The turbidite sedimentary sequence east of Winona Ridge thickens toward the continental slope. None of the CSP data show sufficient penetration to identify acoustic

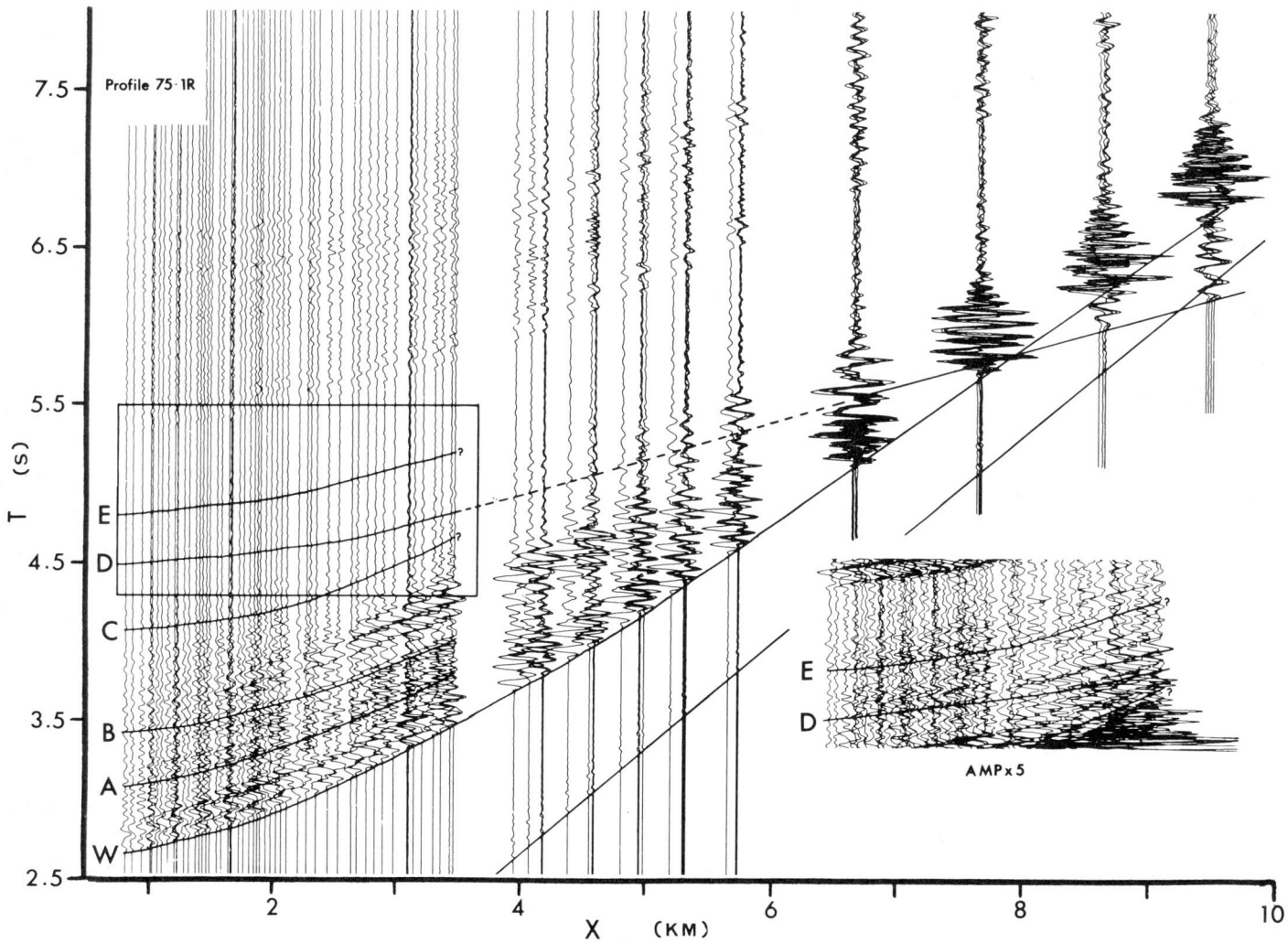
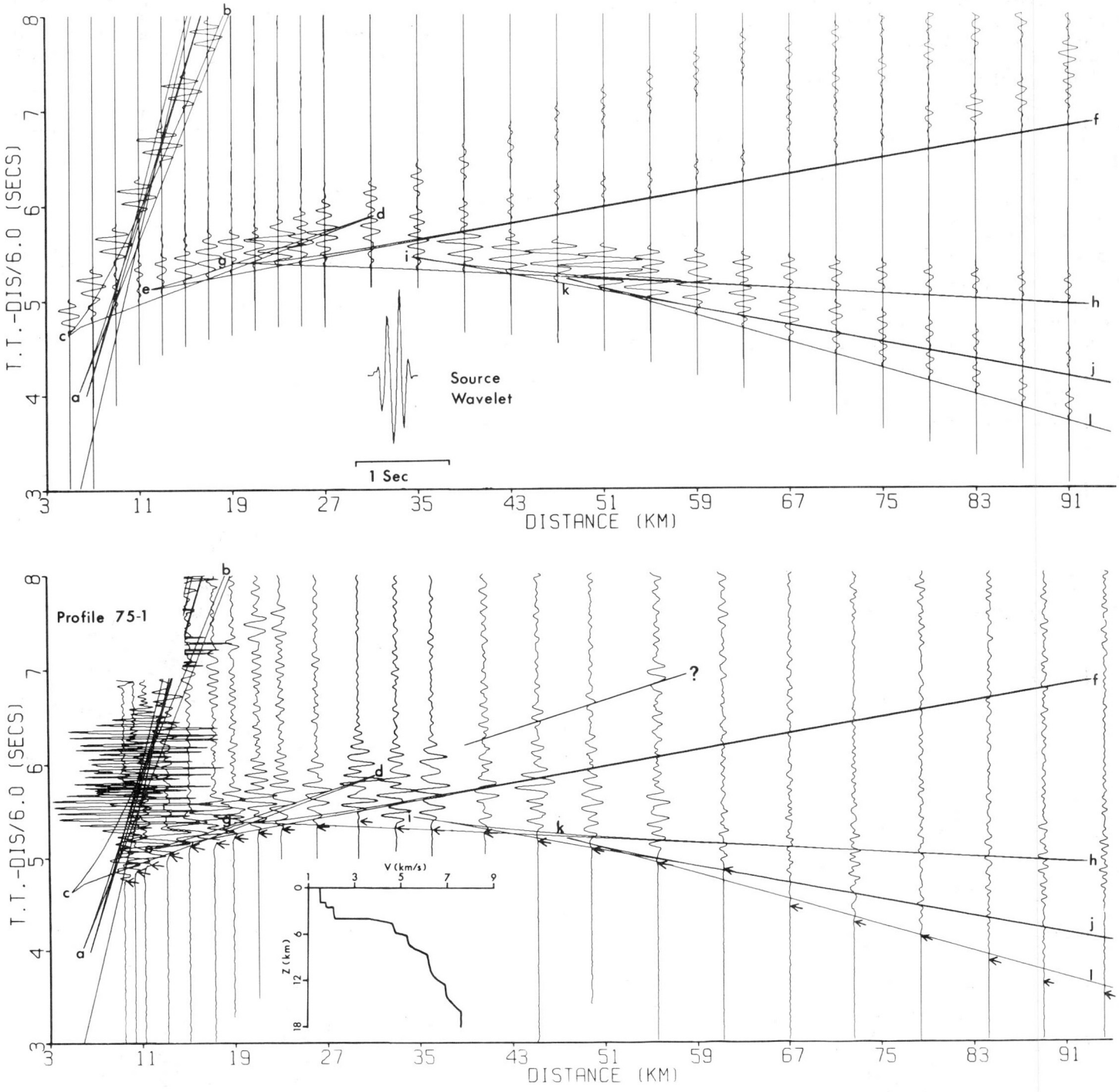


Figure 6.2. Record section of reflection profile 75-1R. Amplitude corrections have been applied and the data are filtered from 5 to 30 Hz. The part of the section within the rectangle is shown on the right side with a five-fold increase in amplitude. The DWW arrival lies along the steeper straight line. Curved lines show the six reflection phase correlations which were timed. W is the bottom reflection. C and E were not used in the computations. The dashed line shows the transition from a deep reflector to the first refraction arrival.



Top: *Synthetic seismograms and travel times computed to fit the stacked traces of profile 75-1. The insert shows the source wavelet which was convolved with the results of the synthetic calculation.*

Bottom: *Data from profile 75-1 with synthetic travel times superposed. Lower case letters have been added to identify the various travel time branches. The arrows show the first arrival picks made from the raw data. The insert shows the velocity-depth model.*

Figure 6.3

basement beneath the thick turbidite deposits. However, they are very useful for near-surface control of the DSS profiles.

In total, eight subcritical incidence reflection profiles were recorded – one at the receiver end of each of the individual refraction profiles plus 75-2V and 75-3V located at the intersections of these profiles (Fig. 6.1). Reflections from shallow sedimentary layers could be phase correlated on all profiles but substantial penetration was achieved only on three of them. On at least one of these, we believe seismic energy returning from the oceanic basement (top of layer 2) can be identified but the data quality is not adequate to phase correlate reliably for determination of velocities.

Figure 6.2 shows the reflection record section for profile 75-1R at the northwestern end of the basin. The first arrival seen on the profile is the direct water wave. Both the bottom reflection and its multiple can be identified, the first starting about 2.7 s and the second about 5.4 s. All of the reflections timed for analysis are shown on the sections, although horizons C and E were too poorly defined to allow proper analysis and so were not used in the final computations. Correlations and time picks were not made from the record section shown, but were determined from enlarged segments of it. The curved lines on Figure 6.2 show the general trend of the correlations.

Both T^2-X^2 analyses and ray parameter methods (Keen, 1976) were applied to these and similar data. The results of the two different approaches were completely consistent. Table 6.1 gives the velocities and thicknesses determined from analysis of the data shown in Figure 6.2. Other profiles give similar results.

Table 6.1

Layer	Velocity (km/s)	Thickness (km)	*Subbottom depth (km)
water	1.50±.02	2.00±.01	0.00
W to A	1.79±.08	0.33±.01	0.33
A to B	2.02±.06	0.32±.01	0.65
B to D	2.14±.03	1.17±.02	1.82

*Datum level for water bottom is 2.00 km.

Refraction Data

Profiles 75-1 and 75-1R form a 95 km reversed pair along the length of the basin (Fig. 6.1). The two profiles were similar in both their traveltime and amplitude characteristics. Thus interpretation with the aid of synthetic seismograms, the theory for which assumes lateral homogeneity, is justified.

The lower part of Figure 6.3 shows the refraction data for profile 75-1 after the six traces recorded for each shot have been stacked. Small arrows indicate first arrival picks. One of the most notable features is the lack of correlative secondary arrivals. From an interpretive viewpoint, this indicates that the velocity-depth curve cannot be composed of simple homogeneous layers; some form of velocity gradients is required. The velocity-depth model interpreted for 75-1 also is shown on Figure 6.3.

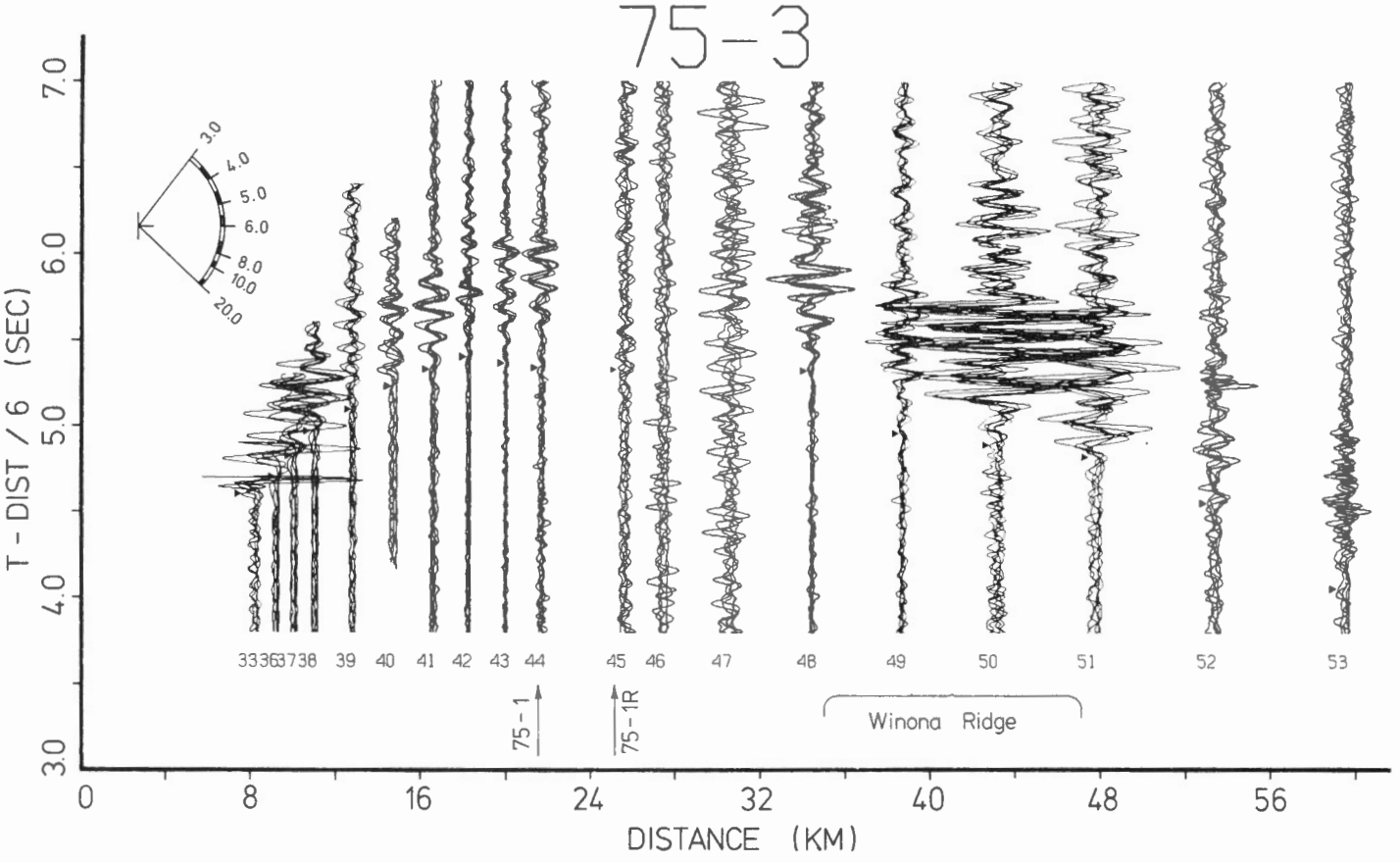
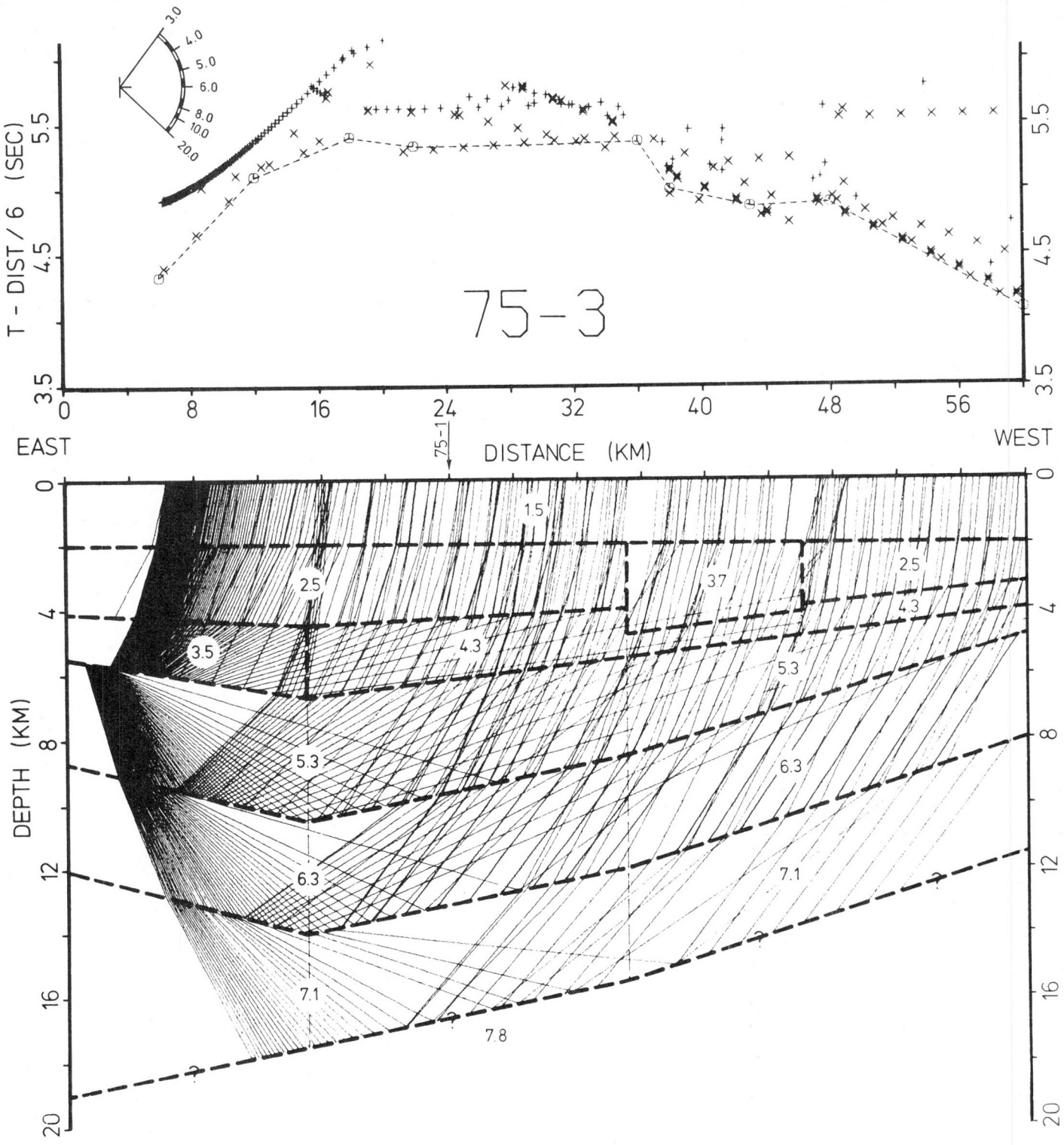


Figure 6.4. Reduced record section for refraction profile 75-3. The solid triangles indicate first arrival picks: the smaller ones correspond to more emergent arrivals. All traces have been filtered from 5 to 20 Hz. Each set of six traces is labelled with its corresponding shot number. Amplitude correction with distance is r^2.



Top: Traveltime curves for profile 75-3. The dashed line represents the first arrival picks taken from the record section of Figure 6.4. Plus signs correspond to reflected ray paths and crosses correspond to refracted ray paths in the model shown below.

Bottom: Crustal model for profile 75-3. Ray paths are superposed. Numbers within blocks outlined by heavy dashed lines are velocities in kilometres per second. The question marks on the bottom interface indicate that the first arrival traveltimes could be satisfied without arrivals from this boundary; therefore its position is not well defined. Vertical exaggeration is 2X.

Figure 6.5

The synthetic seismograms (computed by the recently developed disc ray theory of Wiggins, 1976), which correspond to the model, are shown in the upper part of Figure 6.3. There is good agreement with both traveltimes and amplitudes. Traveltime curves derived for the model are superposed on both the synthetic and observed record sections.

Profiles 75-2 and 2R and 75-3 and 3R, which were recorded across Winona Basin, had an entirely different character than those along the basin. A preliminary examination indicated that an assumption of lateral homogeneity was not justified. In order to interpret the data, we developed a ray tracing computer program for laterally inhomogeneous media. The constraints of (i) data from reversed profiles, (ii) the velocity-depth models derived for the central basin, and (iii) the general geological and tectonic regime of the area, enabled a realistic cross-basin crustal structure to be determined.

Figure 6.4 shows the refraction data for profile 75-3. Solid triangles give first arrival picks. A traveltime advance of about 0.25 s over Winona Ridge and significant amplitude changes with distance are clearly observed.

The interpreted crustal model which satisfies these data is shown in Figure 6.5. Ray paths are superposed on the model. To keep the model as simple as possible, constant velocity blocks, rather than ones with gradients, were used. On the traveltime curves above the model, the first arrival picks from Figure 6.4 are represented by the dashed line. Plus signs and crosses identify traveltimes for reflected and refracted rays respectively. The traveltime fit between the model data and the observations is excellent. And the same crustal model gives just as good a fit for the reversed profile.

Discussion

The principal features derived from analyses of the subcritical incidence reflection data are low velocity (1.6 to 2.0 km/s) sediments at subbottom depths of less than 1 km and higher velocity (2.1 to 3.8 km/s) sediments at subbottom depths ranging from less than 1 km to about 2 km. At depths greater than 2 km below the seabottom, there is a marked increase in velocity, although the value is not determined by reflection data. The first arrival on seismograms at distances near 8.6 and 9.5 km is a refraction phase. When the straight line through these arrivals (and ones at greater distances) is extrapolated to lesser distances, it is tangent to reflecting horizon D. The velocity determined from the inverse slope of the line is about 4.3 km/s. This indicates that the velocity of the material directly below horizon D has this value, although the velocity increases rapidly with depth as shown by the refraction data.

The velocity-depth curve (Fig. 6.3) shows that the subsediment crustal section in the central part of the basin extends from a depth of 6 km to about 16 km. Three layers are distinguished by rapid changes in velocity with depth. Pronounced velocity gradients exist within the 'layers'. Average velocities are consistent with the normal seismic structure of the oceanic crust (Christensen and Salisbury, 1975) but the thicknesses of the 'layers' are greater than average, giving a relatively thick crust beneath the sediments. The 10 km thickness is about the same as that determined by Malecek and Clowes (in press) from DSS profiles recorded east of Explorer Ridge on Explorer plate.

The crustal structure across the basin is shown by the model of Figure 6.5 for profile 75-3. A similar, but not identical, model was derived from the reversed profiles, 75-2 and 75-2R. In order to generate the observed traveltime advances, Winona Ridge has a higher velocity than the sediments on either side. This could be the effect of compression forcing up older, more consolidated sediments prior to the deposition of the layered low velocity sediments.

The most striking features of the models are the eastward dipping layers on the west side of the basin and the westward dipping layers on the east side. The former is consistent with a plate being subducted beneath the continent. The latter is close to, or part of, the region of transition between oceanic and continental crust. Perhaps the westward dipping layers represent a buckling of the crust in response to a recent initiation of subduction or increase in subduction rate in this area.

The results of this study, combined with other geological and geophysical information off the west coast of Canada (Riddihough and Hyndman, 1976; Riddihough, 1977; Murray and Tiffin, 1974; Chase et al., 1975) are best explained by oblique subduction between the Explorer and American plates.

Acknowledgments

We would like to express our appreciation to the officers and crew of **CFAV Endeavour** and **CFAV Laymore** as well as the explosives experts from the Fleet Diving Unit, Pacific Maritime Command, Esquimalt, British Columbia, for their assistance during the cruise.

Funding for this project was provided through a research contract and research agreements with the Geological Survey of Canada, Department of Energy, Mines and Resources and through operating grant A7707 of the National Research Council of Canada. Additional funds were supplied by Mobil Oil Canada Ltd., Shell Canada Resources Ltd. and Chevron Standard Ltd.

References

Chase, R.L., Tiffin, D.L., and Murray, J.W.
1975: The western Canadian continental margin; Can. Soc. Petrol. Geol., Mem. 4, p. 701-721.

Christensen, N.I. and Salisbury, M.H.
1975: Structure and constitution of the lower oceanic crust; Rev. Geophys. Space Phys., v. 13, p. 57-86.

Clowes, R.M.
1977: A marine deep seismic sounding system; Can. J. Earth Sci., v. 14, p. 1276-1285.

Keen, M.J.
1976: The ray parameter method for the reduction of wide-angle reflection data; Unpublished report, Dalhousie University, Halifax.

Malecek, S.J. and Clowes, R.M.
Crustal structure near Explorer ridge from a marine deep seismic sounding survey; J. Geophys. Res. (in press)

Murray, J.W. and Tiffin, D.L.
1974: Patterns of deformation, sedimentation and tectonism, southwestern Canadian continental margin; Ann. Soc. Geol. Belgique, v. 97, p. 169-183.

Riddihough, R.P.
1977: A model for recent plate interactions off Canada's west coast; Can. J. Earth Sci., v. 14, p. 384-396.

Riddihough, R.P. and Hyndman, R.D.
1976: Canada's active western margin — the case for subduction; Geosci. Can., v. 3, p. 269-278.

Wiggins, R.A.
1976: Body wave amplitude calculations II; Geophys. J. Roy. Astr. Soc., v. 46, p. 1-10.

7.

K/AR AGES AND SIGNIFICANCE OF MAFIC ROCKS, SABINE PENINSULA, MELVILLE ISLAND, DISTRICT OF FRANKLIN

Projects 750024 and 760019

H.R. Balkwill and N.E. Haimila
Institute of Sedimentary and Petroleum Geology, Calgary, Alberta

Balkwill, H.R. and Haimila, N.E., K/Ar ages and significance of mafic rocks, Sabine Peninsula, Melville Island, District of Franklin; in Current Research, Part C, Geol. Surv. Can., Paper 78-1C, p. 35-38, 1978.

Abstract

A gabbro dyke, cutting Carboniferous rocks at southern Sabine Peninsula, Melville Island, yielded a K/Ar age of about 123 Ma. Samples of gabbro sills, cutting Permian rocks deep in the Panarctic et al. Drake Point D-68 well, yielded K/Ar ages of about 131 Ma and 152 Ma.

The age of the dyke is broadly contemporaneous with an important unconformity at the margin of Sverdrup Basin, between Cretaceous and Jurassic rocks. The sills may be broadly contemporaneous with phases of crustal subsidence and marine transgression in Sverdrup Basin.

Introduction

Three samples of mafic igneous rocks from Sabine Peninsula, Melville Island, were dated by the K/Ar method (whole rock analysis) by Geochron Laboratories Division (Krueger Enterprises, Cambridge, Massachusetts). One sample was collected from a dyke that cuts surface rocks at Tingmisut Lake; the other two samples are from deep levels in the Panarctic et al. Drake Point D-68 well (Fig. 7.1).

Tozer and Thorsteinsson (1964) mapped the surface rocks of Sabine Peninsula. Upper Paleozoic, Mesozoic, and lower Tertiary rocks of Sverdrup Basin rest unconformably on folded Devonian and older rocks (Fig. 7.1). The Sverdrup Basin succession dips regionally northward, and is interrupted on northern Sabine Peninsula by circular diapirs composed of Carboniferous evaporites. Across the southern part of the peninsula, Lower Cretaceous sandstones (Isachsen Formation) lie on progressively older Jurassic strata eastward, above a low-angle unconformity.

Basalt flows, and dykes and sills ranging in composition from olivine-bearing gabbro to quartz diorite are important constituents of Carboniferous to Upper Cretaceous rocks in Sverdrup Basin, Queen Elizabeth Islands (Blackadar, 1964; Thorsteinsson and Tozer, 1970; Balkwill, 1978). The flows and intrusive bodies are intercalated with and transect Sverdrup Basin sedimentary rocks systematically: the mafic rocks are stratigraphically highest in the succession in the axial part of the basin, where the sedimentary succession is thickest, and are at progressively lower stratigraphic levels toward the basin margins, where the succession is much thinner. The oldest mafic rocks are Carboniferous basalts at northern Axel Heiberg Island (Thorsteinsson, 1974); the youngest are Upper Cretaceous (probably Turonian) basalts at western Axel Heiberg Island (Souther, 1963). Between those lowest and highest levels there are abundant basalt flows and sills and dykes. The isotopic ages of mafic intrusive rocks are known to range from about 190 Ma to about 86 Ma (Balkwill, 1978). From this, it is evident that mafic activity played a long lasting, regionally significant role in the crustal mechanics of basin evolution. Furthermore, levels of organic metamorphism were raised locally in country rocks adjacent to mafic intrusive bodies, affecting generation of hydrocarbons (Powell, 1978).

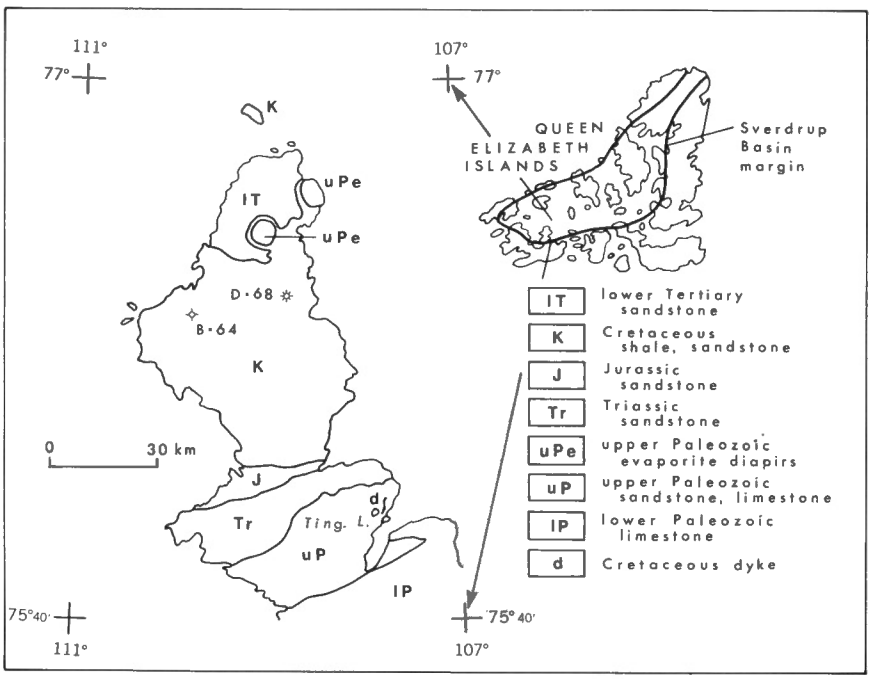


Figure 7.1

Geological setting, Sabine Peninsula, Melville Island. Details of geology are provided by Tozer and Thorsteinsson (1964).

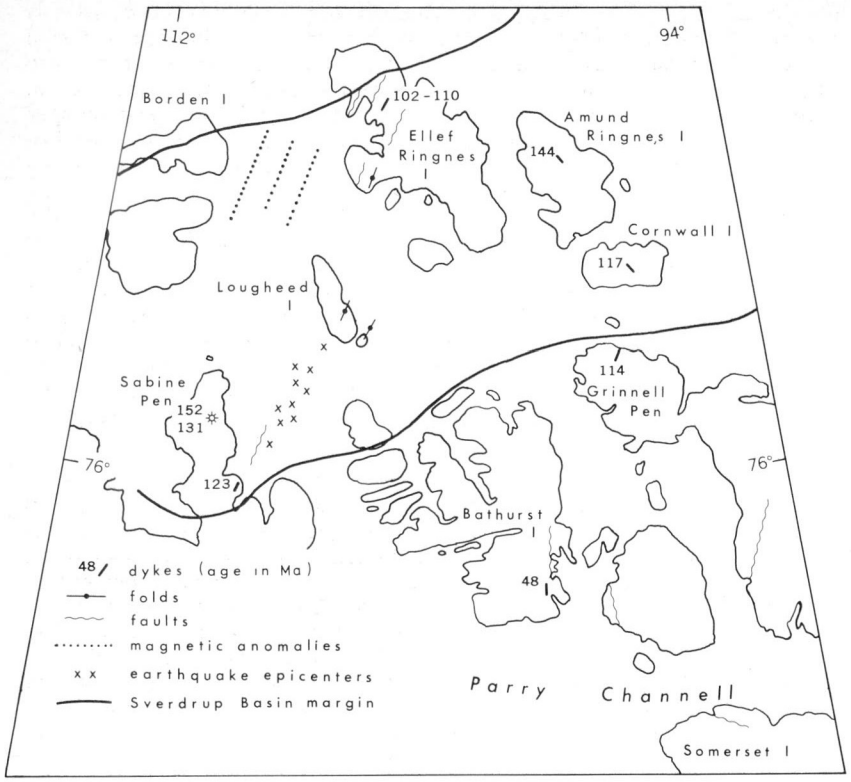


Figure 7.2

West-central Queen Elizabeth Islands, showing northeast-striking structures of Sverdrup Basin, structures of Eurekan Rifting Episode (after Kerr, 1977), and approximate age of mafic intrusions.

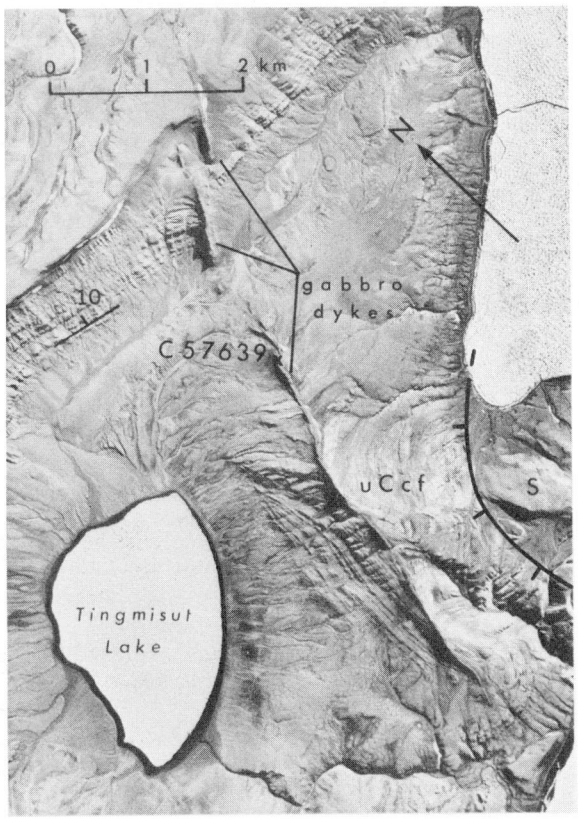


Figure 7.3. Vertical air photo of Tingmisut Lake mafic dykes (part of N.A.P.L. photo A16763-54). uPcf: Canyon Fiord Formation; S: Silurian dolomite; C-57639: sample location.

Not far south of the Sverdrup Basin margin, on eastern Bathurst Island (Fig. 7.2), there is a Maastrichtian basalt flow and some mafic dykes that have been dated isotopically at 48 Ma and 60 Ma (Eocene and Paleocene) (Kerr, 1974). No mafic rocks as young have been proven to be present in Sverdrup Basin, but the dyke at Tingmisut Lake was undated until now, so it has been uncertain whether it is related to the Sverdrup Basin assemblage of intrusions, or to the younger mafic rocks at Bathurst Island.

Mafic Igneous Rocks at Sabine Peninsula

Mafic igneous rocks outcrop at three localities on Sabine Peninsula (Tozer and Thorsteinsson, 1964). There are masses of gabbro – some of which may be ring dykes – in each of the two large circular evaporite piercement domes near the northern coast of the peninsula, and a northeast-striking system of dykes that cut slightly tilted, Carboniferous sedimentary rocks near Tingmisut Lake (Fig. 7.1).

Slightly sinuous dykes at Tingmisut Lake strike N20°E (Fig. 7.3). The largest dyke is about 50 m wide and 4 km long. Two small dykes lie northeastward of the large dyke and strike parallel to it. The dyke rocks are moderately jointed, lying partly as resistant felsenmeer piles at the surface. The rocks are dark green-grey and coarsely crystalline. Blackadar (in Tozer and Thorsteinsson, 1964, p. 173) determined that the large Tingmisut dyke has a subophitic texture, and on the basis of plagioclase composition is a gabbro. The rocks contain as much as 10 per cent titaniferous magnetite. The dykes cut red, orange, and buff quartz sandstones of the Canyon Fiord Formation, which at Sabine Peninsula contain Late Carboniferous fossils. In an irregular zone, a few metres wide, the sandstones are bleached light grey-buff and are cemented by quartz. Canyon Fiord sandstones are part of a northward-dipping homocline, interrupted east of Tingmisut Lake by a normal fault across which Silurian dolomite is juxtaposed against the Carboniferous rocks.

The two sills in the Drake Point D-68 well are similar in gross composition. Both are composed of feldspar, quartz, amphibole, chlorite, titaniferous magnetite and biotite. Their average compositions are more similar than the internal variations with either of the sills. The sills are unusual in that quartz constitutes a relatively high proportion of the total rock. The quartz content varies from 8 to 25 per cent with the greater abundance occurring in the upper half of the sills. The feldspar content is fairly constant throughout the sills with the original feldspar content varying between 40 and 50 per cent. This proportion is now reduced due to intense sericitization throughout all the feldspars. Determinations by X-ray indicate that the mafic minerals in the sills are predominantly amphibole and chlorite with illite reflecting the sericitization of the feldspar. The amphibole content varies inversely with the quartz content and ranges between 10 and 20 per cent. The amphibole content is greater in the lower half of both sills. The chlorite content is relatively uniform: between 10 and 12 per cent, possibly increasing to 15 per cent near the margins of the sills. Biotite occurs in places within the thin-sectioned chip samples and may constitute 3 to 5 per cent of individual chips. An opaque mineral, probably titaniferous magnetite, constitutes the remaining 5 to 12 per cent of the rock.

From their present composition the sills are classified as diorite to quartz diorite. Because of the extensive alteration of the sills, the isotopic ages would have to be considered as minimum ages even though most of the alteration appears to have occurred during the emplacement and crystallization of the sills.

K/Ar Ages

Sample C-57639, collected at the north end of large Tingmisut Lake dyke (Fig. 7.3), yielded an isotopic age of 123 ± 6 Ma.

Panarctic et al. Drake Point D-68 is the deepest well drilled at Sabine Peninsula (T.D. 5415 m, 17 766 ft). Two mafic sills were penetrated in the Lower Permian succession of strata in the D-68 well: between 4682 and 4767 m (15 360-15 640 ft), and between 4883 and 4945 m (16 020-16 225 ft).

A sample from the upper sill, collected from a cored interval at 4685 m (15 369.5 ft), yielded an age of 152 ± 6 Ma and sample from the lower sill, collected from drill cuttings between 4929 and 4947 m (16 170-16 230 ft), an age of 131 ± 6 Ma.

The only other mafic intrusive body in Sabine Peninsula wells is present in Lower Permian rocks, between 3397 and 3452 m (11 145-11 325 ft), in the Panarctic Chads Creek B-64 well. That sill has not been dated.

Discussion

Along the southern margin of Sverdrup Basin, Permian and older rocks at Grinnell Peninsula (Fig. 7.2) are cut by a gabbro dyke that yielded a K/Ar age of about 114 Ma (Kerr, 1976), and Triassic rocks at Cornwall Island have abundant dykes and sills from which a 117 Ma K/Ar age was obtained (Balkwill, in press). K/Ar ages of 112 to 110 m.y. (Larochelle et al., 1975) and 144 Ma (Balkwill, in press) have been obtained from other mafic intrusions in the Ringnes Islands. The radiometric ages of the intrusive rocks at Sabine Peninsula indicate that they are part of the widespread, long-lasting Sverdrup Basin assemblage of Mesozoic intrusions and volcanic flows, and are not part of the latest Cretaceous-early Tertiary family of mafic rocks represented at Bathurst Island. The latter seem to be related genetically to a phase of latest Cretaceous-Tertiary graben formation within and adjacent to Parry Channel, which Kerr (1977) called the Eurekan Rifting Episode.

The stratigraphic age of the Tingmisut Lake dyke is approximately Hauterivian. A thick succession of nonmarine sandstones (Isachsen Formation) represents the late Valanginian-Hauterivian-Barremian-early Aptian interval in Sverdrup Basin. Isachsen Formation sandstones (and younger Cretaceous deposits) broadly overstep the basin margins, giving evidence of fundamental re-ordering of tectonic-depositional regimes in mid-Cretaceous (Balkwill, 1978). Basal Isachsen beds beyond Sverdrup Basin margins are locally as young as Barremian. The basal Isachsen beds above the Jurassic rocks at southern Sabine Peninsula are undated, but, from the foregoing regional considerations, they must lie in the interval late Valanginian-Barremian. The time-stratigraphic age of the dyke at Tingmisut Lake (Hauterivian) is therefore broadly contemporaneous with the phase of tilting, differential uplift, and erosion that produced the unconformity beneath the Isachsen Formation at southern Sabine Peninsula.

A narrow array of north-northeastward-striking structural elements is present in western Sverdrup Basin (Fig. 7.2) (Balkwill et al., in press). The array includes the dykes at Tingmisut Lake, some faults cutting Mesozoic and older rocks east of Drake Point, a swarm of recent earthquake epicentres between Sabine Peninsula and Lougheed Island, folds in Cretaceous rocks on Lougheed Island and western Ellef Ringnes Island, and large, linear magnetic anomalies of undetermined origin between Borden Island and Ellef Ringnes Island. If the Tingmisut Lake dyke is as old as its isotopic age suggests, then crustal instability has prevailed since Early Cretaceous (or earlier) time in a zone that strikes across western Sverdrup Basin in a northeastward direction.

The upper and lower sills in Drake Point D-68 have respective stratigraphic ages of approximately Oxfordian, and late Berriasian or early Valanginian. The Oxfordian was a time of widespread marine transgression and deposition of dark shales in Sverdrup Basin, as was the early Valanginian; late Berriasian was a time of marine regression at the basin margins. For some other time-stratigraphic intervals, transgressive marine dark shales in the Sverdrup Basin succession are matched, approximately, by phases of mafic intrusion or basaltic volcanism; those relationships suggest that transgression was prompted partly by crustal foundering and enlargement of basin space (Balkwill, 1978).

References

Balkwill, H.R.
1978: Evolution of Sverdrup Basin, Arctic Canada; Am. Assoc. Pet. Geol. Bull., v. 62, p. 1004-1028.

Geology of Amund Ringnes, Cornwall, and Haig-Thomas Islands, District of Franklin; Geol. Surv. Can., Mem. 390. (in press)

Balkwill, H.R., Hopkins, W.S., and Wall, J.H.
Geology of Lougheed Island and nearby small islands, District of Franklin; Geol. Surv. Can., Mem. 395. (in press)

Blackadar, R.G.
1964: Basic intrusions of the Queen Elizabeth Islands, District of Franklin; Geol. Surv. Can., Bull. 97.

Kerr, J.W.
1974: Geology of Bathurst Island Group and Byam Martin Island, Arctic Canada; Geol. Surv. Can., Mem. 378.

1976: Geology of outstanding Arctic aerial photographs, 3. Margin of Sverdrup Basin, Lyall River, Devon Island; Bull. Can. Pet. Geol., v. 24, p. 139-153.

Kerr, J.W. (cont'd.)
1977: Cornwallis Fold Belt and the mechanism of basement uplift; Can. J. Earth Sci., v. 14, p. 1374-1401.

Larochelle, A., Black, R.F., and Wanless, R.K.
1965: Paleomagnetism of the Isachsen diabasic rocks; Nature, v. 208, no. 5006, p. 179.

Powell, T.G.
1978: An assessment of the hydrocarbon source rock potential of the Canadian Arctic Islands; Geol. Surv. Can., Paper 78-12.

Souther, J.G.
1963: Geological traverse across Axel Heiberg Island from Buchanan Lake to Strand Fiord in Geology of the north-central part of the Arctic Archipelago, Northwest Territories (Operation Franklin); Geol. Surv. Can., Mem. 320, p. 426-448.

Thorsteinsson, R.
1974: Carboniferous and Permian stratigraphy of Axel Heiberg Island and western Ellesmere Island, Canadian Arctic Archipelago; Geol. Surv. Can., Bull. 224.

Thorsteinsson, R. and Tozer, E.T.
1970: Geology of the Arctic Archipelago in Geology and economic minerals of Canada, R.J.W. Douglas, ed.; Geol. Surv. Can., Econ. Geol. Rep. No. 1, 5th ed., p. 548-590.

Tozer, E.T. and Thorsteinsson, R.
1964: Western Queen Elizabeth Islands, Arctic Archipelago; Geol. Surv. Can., Mem. 332.

8.

CORRELATION OF THE JURASSIC BUG CREEK FORMATION IN THE SUBSURFACE OF THE MACKENZIE DELTA, DISTRICT OF MACKENZIE

Project 750067

T.P. Poulton
Institute of Sedimentary and Petroleum Geology,
Calgary, Alberta

Poulton, T.P., Correlation of the Jurassic Bug Creek Formation in the subsurface of the Mackenzie Delta, District of Mackenzie; in Current Research, Part C, Geol. Surv. Can., Paper 78-1C, p. 39-42, 1978.

Abstract

The Jurassic Bug Creek Formation in the subsurface of Mackenzie Delta between 68°N and 68°30'N exhibits the same northwestward-thickening trend observed in the northern Richardson Mountains immediately to the west. The same members are present, the same southeastward loss of section below an unconformity within the formation and the same increased amount of sandstone relative to argillaceous rocks. Correlation of lower parts of the formation north of 68°30'N is tenuous. This is due in part to an apparent change of facies of a glauconitic sandstone unit that serves as an important marker in the southern wells. Subsurface thinning of the entire formation approaching 69°N does not have equivalent expression at the surface because exposures do not extend that far north.

The writer has spent two field seasons studying the Bug Creek Formation of northern Richardson Mountains. This report was written to show that the major results of the field work apply equally well to the subsurface of the Mackenzie Delta immediately to the east (Figs. 8.1 to 8.3). Also, an attempt has been made to correlate some of the units northward as far as Reindeer Channel (Fig. 8.1). Although the present interpretations are based on independent study of the logs and samples of the wells by the writer and are primarily lithological in character, they nevertheless have been influenced by the previous interpretations and micropaleontological data available.

The Bug Creek Formation was originally described by Jeletzky (1967), with its type section at Bug Creek (Fig. 8.1). This description and subdivision of the formation is applicable regionally, although additional members are present farther basinward (west and north) and an unconformity that was recognized within the formation by Jeletzky (1967) has been relocated higher in the succession. These major results of fieldwork were summarized in brief preliminary reports (Poulton and Callomon, 1976; Poulton, 1978). Detailed documentation of the stratigraphic and biostratigraphic data is in preparation.

The Bug Creek Formation and its western argillaceous equivalent, the Kingak Formation, considered together, form a clastic package in the northern Richardson Mountains that becomes thicker, proportionally richer in argillaceous rocks, and more complete, to the north and west (Fig. 8.2). Two major sandstone units within this package form the basis of correlation with the subsurface units of the Mackenzie Delta. These are the upper sandstone member, and the lower part of what Jeletzky (1967) called the intermediate sandstone member. The lithological correlation of these units over the entire northern Richardson Mountains and adjacent Mackenzie Delta area should not be taken as evidence of synchroneity, or of physical continuity from one outcrop or well to another as a single depositional unit.

The upper sandstone member is nearly everywhere a fine- to medium-grained quartz-rich sandstone, distinguished from sandstone units above and below by its characteristic light brown colour. It is most commonly very well sorted and tightly cemented with silica. Finely dispersed "limonite" gives the rock its colour, at least in large part. The grain size decreases to silt-grade in the northernmost interpreted occurrence of the unit near Reindeer Channel (Kugpik O-13).

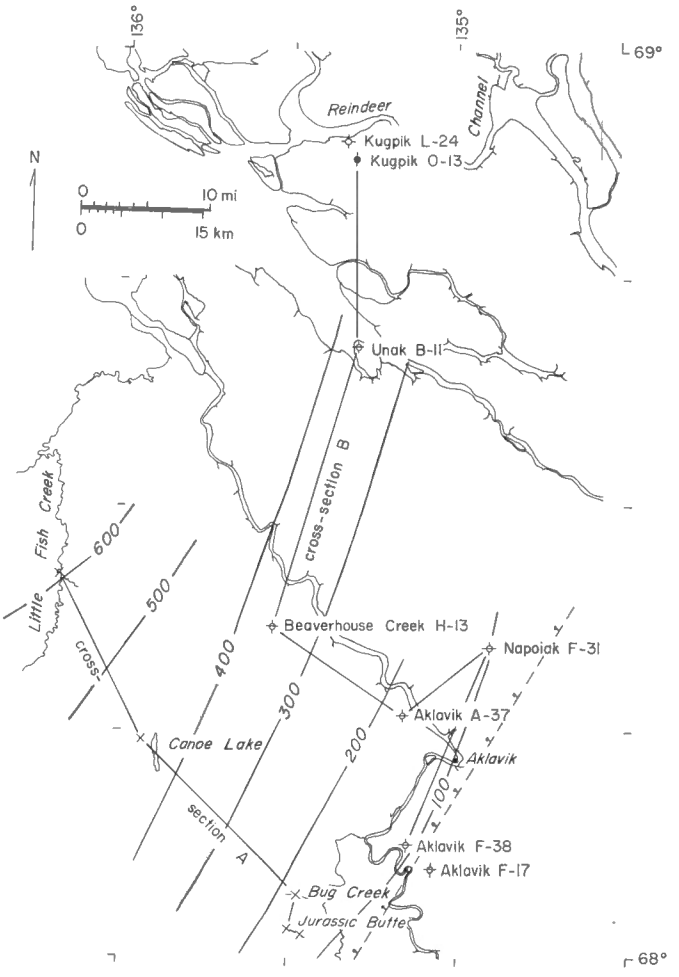


Figure 8.1. Index map, northeastern Richardson Mountains and adjacent Mackenzie Delta area, showing isopachs (in metres) of Bug Creek Formation, and locations of stratigraphic sections, wells, and cross-sections A and B (Figs. 8.2, 8.3).

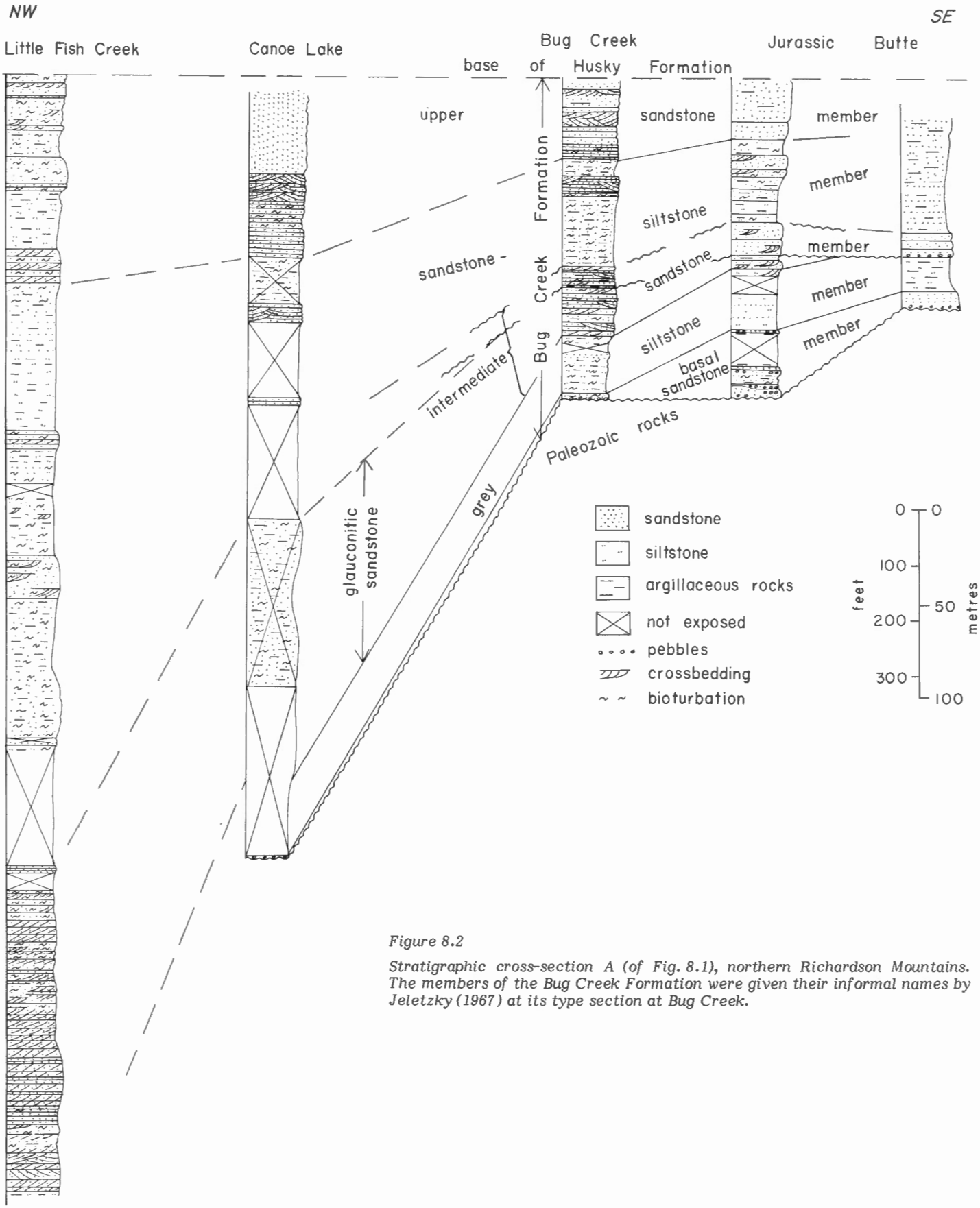


Figure 8.2

Stratigraphic cross-section A (of Fig. 8.1), northern Richardson Mountains. The members of the Bug Creek Formation were given their informal names by Jeletzky (1967) at its type section at Bug Creek.

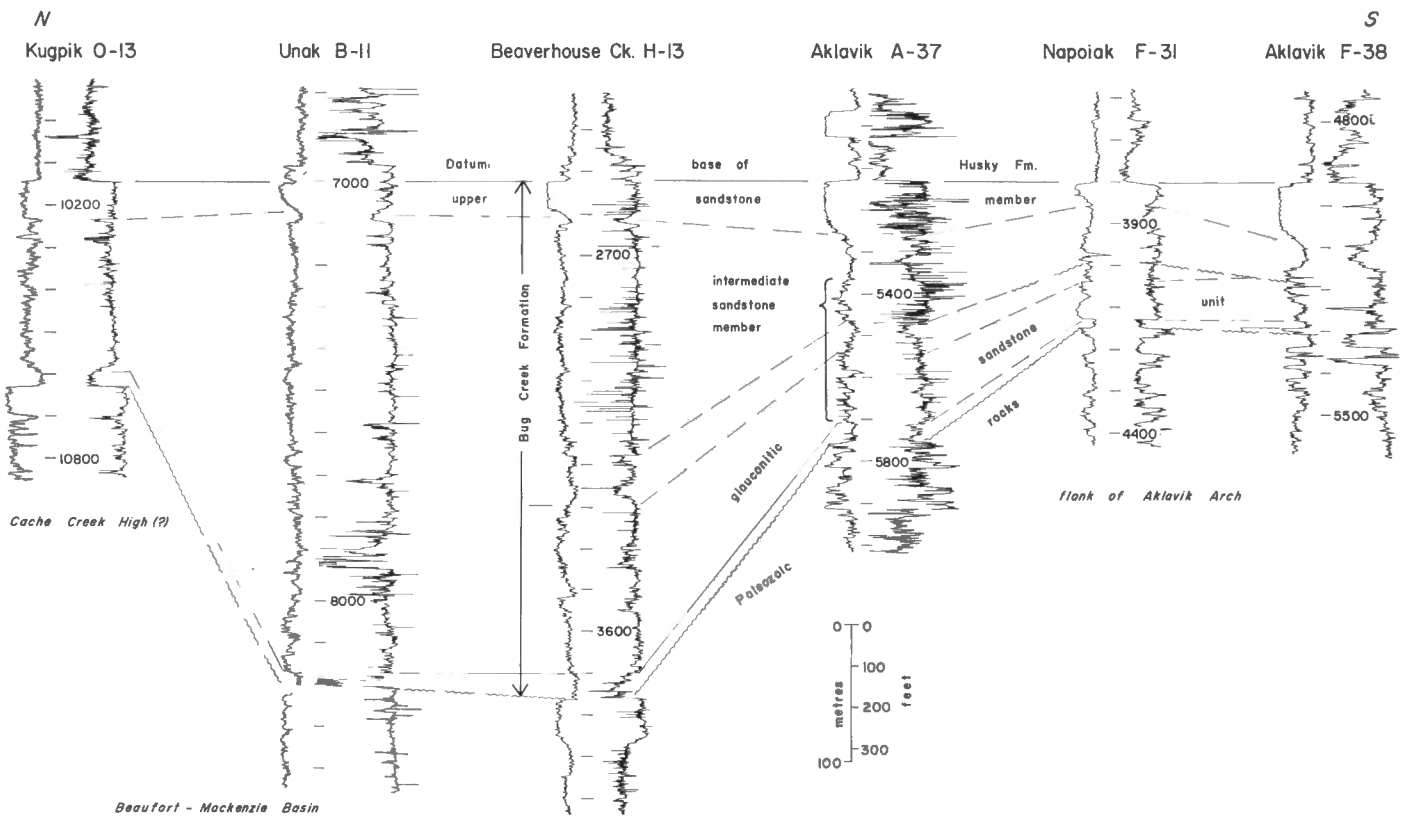


Figure 8.3. Stratigraphic cross-section B (of Fig. 8.1), western Mackenzie Delta (gamma ray-sonic logs).

The second sandstone that serves as a recognizable marker unit comprises the lower, strongly glauconitic part of a sequence which, together with disconformably overlying Upper Bajocian sandstones in the type section of the Bug Creek Formation, Jeletzky (1967) called the intermediate sandstone member. This sandstone unit is distinguished from other units throughout most of the northern Richardson Mountains by its high glauconite content and the abundance of red-brown ferruginous beds and patches. It is recognizable by these criteria in those wells (Aklavik F-58, A-37; Napoiak F-31; Beaverhouse Creek H-13) immediately east of the outcrop area. Farther north, the correlation of this unit in the subsurface is tenuous because glauconite is not present in large quantities. Here, recognition of this unit is based on the presence of abundant fine grained (to silt-grade) quartz-rich sandstones of white to light grey colour that dominate the interval below what appears to be the upper sandstone member and above, at least in places (e.g. Kugpik L-13, L-24), Paleozoic limestones. This sandstone is not readily distinguishable from similar upper Paleozoic(?) sandstone in some subsurface localities (e.g. Unak B-11) and this is also true in outcrop localities in the northern Richardson Mountains.

Other units of the Bug Creek Formation that occur between these two sandstone units in the outcrop area are undoubtedly present in the subsurface also but they are less distinctive and, hence, less important as tools for correlation.

The Paleozoic strata lying immediately below the Bug Creek Formation are different from place to place, comprising limestone, sandstone, and shale. This is also the case in the northern Richardson Mountains where a regional unconformity separates the two sequences.

In the wells illustrated (Fig. 8.3), the Bug Creek Formation is overlain everywhere by the Husky Formation. It is mainly black shale, but contains significant interbeds of sandstone and siltstone which vary greatly in their proportion and stratigraphic position from place to place. For the most part, these are strongly bioturbated argillaceous sandstones. Well-sorted sandstones occur low in the Husky Formation here and there, and in places (e.g. Unak B-11; Beaverhouse Creek H-13; Aklavik A-37, F-38) form thin coarsening-upward units near the base of the Husky that may represent reworking of sands of the upper sandstone member of the Bug Creek Formation.

The southward thinning of the Bug Creek Formation from Beaverhouse Creek H-13 to Aklavik area shown in Figure 8.3 allows eastward extension of the facies and thickness trends indicated by surface sections (Fig. 8.2) immediately along strike to the southwest. The absence of glauconite as a correlation criterion and the thinning to the north from Beaverhouse Creek H-13 to Kugpik O-13 do not have expression on the surface, as these phenomena occur north of the northernmost Bug Creek outcrops. Together with the fining to silt grade of the upper sandstone member, they may indicate basinward changes of facies and the presence of tectonostratigraphic elements that preclude extension of the Bug Creek Formation as such northward beyond the latitude of Reindeer Channel. The thin section of the Bug Creek Formation in Kugpik O-13 and nearby wells corresponds in location with the Cache Creek High, and may indicate deposition on, or erosion from it (F.G. Young, pers. comm.). Equivalent rocks exposed along strike to the southwest do not, however, appear to have been significantly influenced by the Cache Creek High, which had its main effect on younger strata. An analogous thin succession over a syn-Jurassic high has been recognized in the White Mountains area 50 km (approx.) west of Jurassic Butte (Poulton and Callomon, 1976; Poulton, 1978). There is no reason to think that the Bug Creek Formation is thin in Reindeer Channel area due to shaling out, nor due to subsequent erosion as is the case west of Shallow Bay, if the writer's correlation of the sandstone units (Fig. 8.3) is correct.

South of Aklavik F-38, on the upthrown side of a major north-northeast-south-southwest trending fault (Young et al., 1976), the Bug Creek Formation is apparently entirely absent (e.g. Aklavik F-17 well). Therefore Poulton's (1978, Fig. 2) extrapolation into this area of a transgression of Upper Bajocian or Bathonian rocks over Paleozoic rocks beyond the limits of lower Jurassic rocks is not valid.

Acknowledgments

F.G. Young and A.F. Embry helped the writer with geophysical and lithological log interpretations. They and D. Long critically read the manuscript.

References

Jeletzky, J.A.
1967: Jurassic and (?)Triassic rocks of the eastern slope of Richardson Mountains, northwestern District of Mackenzie, 106M and 107B (parts of); Geol. Surv. Can., Paper 66-50.

Poulton, T.P.
1978: Internal correlations and thickness trends, Jurassic Bug Creek Formation, northeastern Yukon and adjacent Northwest Territories; Geol. Surv. Can., Paper 78-1B, p. 27-30.

Poulton, T.P. and Callomon, J.H.
1976: Major features of the Lower and Middle Jurassic stratigraphy of northern Richardson Mountains, northeastern Yukon Territories, and northwestern District of Mackenzie; Geol. Surv. Can., Paper 76-1B, p. 345-352.

Young, F.G., Myhr, D.W., and Yorath, C.J.
1976: Geology of the Beaufort-Mackenzie Basin; Geol. Surv. Can., Paper 76-11.

9. THE WINDSOR GROUP IN ATLANTIC CANADA – AN UPDATE

Project 740110

H.H.J. Geldsetzer
Regional and Economic Geology Division

Geldsetzer, H.H.J., The Windsor Group in Atlantic Canada – An update; in Current Research, Part C, Geol. Surv. Can., Paper 78-1C, p. 43-48, 1978.

Abstract

The lower Carboniferous Windsor Group sediments were deposited in a wide embayment with a probable connection to an oceanic seaway to the east of the continental shelf of Nova Scotia. The stratigraphic successions of the lower Carboniferous in Atlantic Canada and in the central Appalachians of the United States are similar, and show a hiatus from the middle Tournaisian to the middle Viséan (post-Horton/Pocono and pre-Windsor/Greenbrier).

The "Windsor Sea" flooded a wide basin which may have been below sea level base during the preceding hiatal episode. A subtidal, hypersaline origin for the cryptalgal laminite at the base of the Windsor is suggested by its widespread distribution, by the absence of desiccation features, by the laterally persistent lamination and by its association with a subtidal and possibly euryhaline fossil assemblage. Stagnation of the "Windsor Sea" led to extensive precipitation of gypsum, followed by halite in areas of accelerated subsidence and potash salts in distal embayments.

Upper Windsor sedimentation was controlled by differences in the rate of subsidence and the rate of fine grained, clastic supply. An equilibrium of the two variables produced detrital mudflat deposits and thin evaporites, whereas periods of increased subsidence resulted in widespread, normal marine carbonate deposition.

Introduction

Field work on the Lower Carboniferous Windsor Group in the Atlantic Provinces continued in 1977. The stratigraphic framework of the Windsor Group in Cape Breton Island (Geldsetzer, 1977) can generally be applied in northern Nova Scotia, southwestern Newfoundland and southern New Brunswick. Local modifications due to nearshore facies changes are necessary in some areas.

Distribution

A compilation of onshore and offshore data (Fig. 9.1) illustrates the wide distribution of Windsor Group sediments occupying a large portion of the Grand Banks, the southern half of the Gulf of St. Lawrence and part of the continental shelf northeast of Newfoundland. The dominantly marine aspect of these sediments necessitates an oceanic connection during Windsor time. A new interpretation of paleomagnetic data by Irving (1977) positions eastern North America adjacent to northwestern South America during the Carboniferous, with paleolatitudes ranging from the equator to 20 degrees south. A seaway probably separated eastern North America from northwestern South America and may have extended into western Europe. The "Windsor Sea" probably formed a wide embayment on the north side of such a seaway extending about 1400 km in an east-west direction at a paleolatitude of 5 degrees south and varying in width from 150 to 400 km. Seawater might have entered this embayment from the south, between the Grand Banks and the Scotian Shelf, or from the northeast, through a basement low on the Grand Banks (Fig. 9.1) which is believed to have served as a marine connection during Jurassic time (Jansa and Wade, 1975) and may well have done so during Windsor time. An oceanic connection to the west, through the Bay of Fundy, is unlikely. In southern New Brunswick the basal carbonates of the Windsor Group have a high terrigenous component and are separated from the overlying evaporites by an eastward thinning wedge of red, fine to coarse clastics. The evaporites contain a substantial amount of potash and the upper Windsor grades westward into coarse, red, nonmarine conglomerates. These facies changes suggest that southern New Brunswick occupied a distal part of the "Windsor Sea".

The continental aspect of the upper Devonian rock recorded in the northeastern United States and eastern Canada indicates that the New England region remained a source area throughout late Devonian and early Carboniferous time (Geldsetzer, 1971) contributing the detritus of intermontane deposits (Perry Formation; Horton Group) and of several clastic wedges along the central Appalachians in New York and Pennsylvania (Catskill Group, Pocono Group and Mauch Chunk Group).

The distribution of Windsor Group sediments shows that outcrop data come from the southwestern margin of the "Windsor Sea" in northern Nova Scotia and southeastern New Brunswick, and from a small section of the north-central margin, in southwestern Newfoundland. This would suggest that outcrop data may reflect relatively nearshore environments of deposition assuming that the present distribution coincides approximately with the original extent of the Windsor sediments. This assumption is only partially valid because the lower Windsor Group is abruptly truncated due to erosion and/or faulting in southwestern Newfoundland and north-central Nova Scotia. The original extent of the upper Windsor strata is conjectural because they are known to have overlapped the lower Windsor strata. Erosion of the Windsor Group sediments had already begun during the hiatal episodes preceding the Riversdalian and Pictouan depositional intervals of Westphalian A and C age respectively, and there are indications that Windsor sediments were partly removed as early as early Namurian, preceding the deposition of Canso sediments.

Correlation

A comparison of the lower Carboniferous stratigraphic successions to the east (Atlantic Canada) and west (New York and Pennsylvania) of the paleo-Appalachian upland area shows that their sedimentological and tectonic development is similar. Even though the two regions are different in their paleogeographical setting (the sediments on the east having been deposited in a land-locked, trough-like embayment, whereas those on the west spread onto a wide craton) they were affected by the same tectonic pulses. The much less

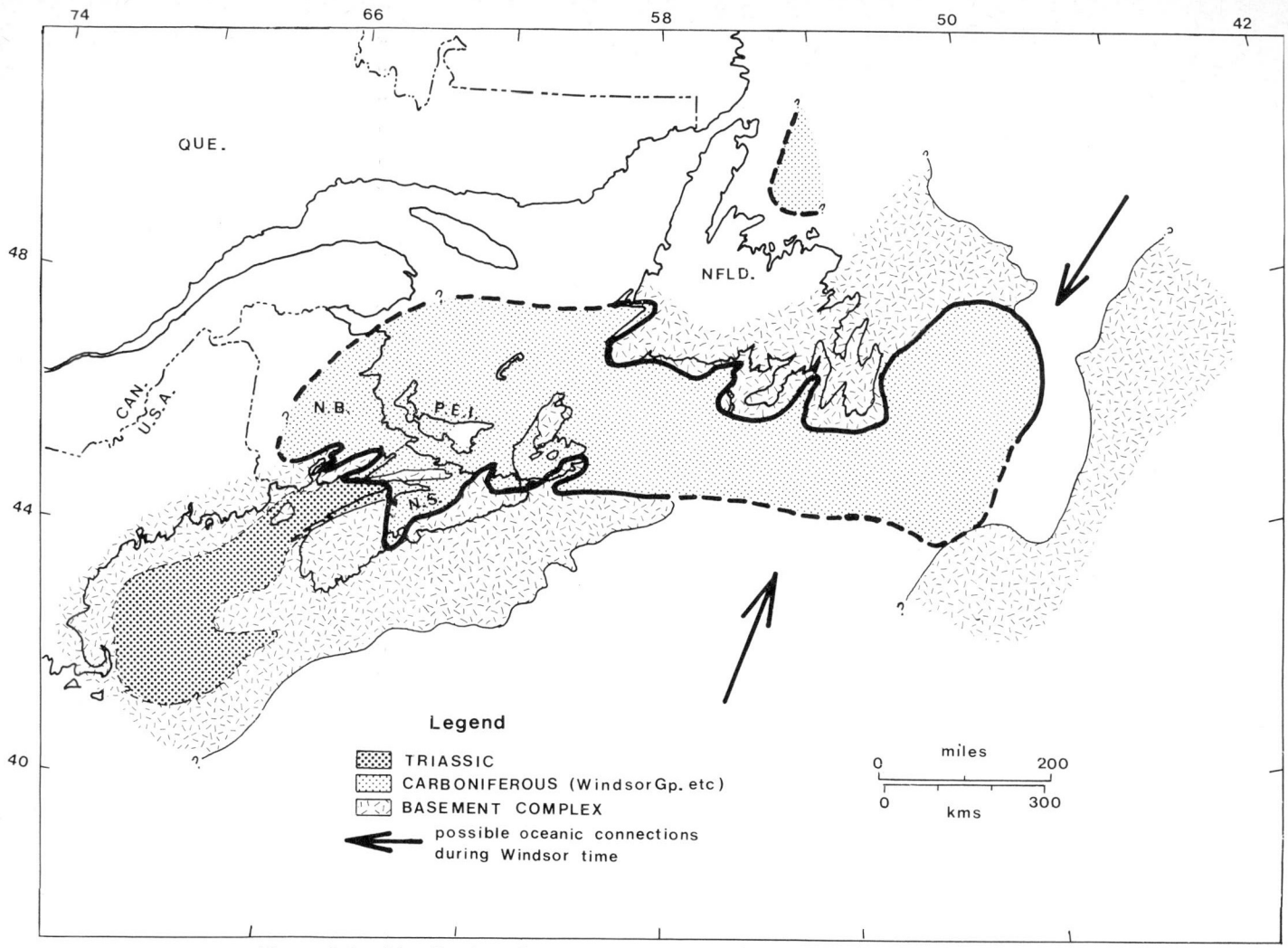


Figure 9.1. Distribution of Windsor sediments (after Jansa and Wade, 1975).

deformed, better preserved and hence better documented lower Carboniferous of the eastern United States is used to place the corresponding strata in eastern Canada into the international time-scale and to draw attention to the probable existence of a significant hiatus within the early Carboniferous (Table 9.1).

The detrital basin deposits of the Horton Group correlate with the clastic wedge of the Pocono Group, and the Windsor carbonates and fine clastics are similar in age and lithologic character to the Greenbrier Group (Loyalhanna Limestone) and Mauch Chunk fine clastics respectively.

The Horton-Pocono correlation is based on floral data by Bell (1960) who confirmed earlier work by White (1913). The Pocono Group grades to the west into marine clastics and carbonates which have been shown to be older than the Osagean, or middle and upper Tournaisian (Caster, 1934). The Horton-Pocono interval is therefore probably of early Tournaisian age. This has recently been confirmed by Higgs (1975) who compared spores from the Horton Group with Irish sections and implied an age corresponding to the NV spore zone of Neves et al. (1972).

The absence of middle Tournaisian to middle Viséan (Osagean to middle Meramecian) rocks above the Horton and Pocono clastics appears to indicate an episode of widespread epeirogenic uplift centring along the paleo-Appalachians and causing the adjacent regions of previous clastic deposition to rise above base level. Farther west, in the Midcontinent area, fine clastics and carbonates continued to accumulate during the Osagean, but changed to carbonate deposition during the Meramecian. A similar pattern of continued deposition has so far not been observed in Atlantic Canada.

Rocks of the Windsor Group correlate well with the uppermost Meramecian and lower Chesterian rocks of the Midcontinent area (St. Genevieve Limestone to Homberg Group) based on both macrofaunal (Bell, 1929) and microfaunal (Mamet, 1970) data. Renewed subsidence in Atlantic Canada (Windsor Group) affected as well the western flank of the Appalachian upland area, where uppermost Meramecian and Chesterian rocks (Greenbrier and Mauch Chunk Groups) rest on Pocono clastics. Both the upper Windsor and the Mauch Chunk are characterized by fine red clastics, implying that the Appalachian upland area had reached a relatively advanced stage of denudation.

Windsor Stratigraphy

Data on the Windsor Group were almost entirely derived from outcrops and onshore borehole cores along the western periphery of the "Windsor Sea". The outcrop belt is, nevertheless, almost 600 km long and up to 150 km wide. The stratigraphic succession is remarkably consistent for the lower Windsor throughout this region, whereas the upper Windsor shows subtle regional facies changes.

Table 9.1

Lower Carboniferous Correlation Chart

	STAGES (Internat.)		ROCK UNITS: ATLANTIC CANADA	ROCK UNITS: CENTRAL APPALACHIANS (Penns., USA)	ROCK UNITS: MID-CONTINENT (USA)	STAGES (USA)	MIOSPORE ZONATION (British Isles)	FORAMINIFERA ZONATION (North America)
CARBONIFEROUS	NAMURIAN		CANSO	MAUCH CHUNK	ELVIR	CHESTERIAN	NC	17
	VISEAN	u	WINDSOR	GREENBRIER	HOMBERG		VF	16s
					GASPER			16i
					ST.GENEVIEVE	MERAMECIAN	NM	15
							TC	14
		m			ST.LOUIS		PU	13
					SALEM			12
		l			WARSAW			11
	TOURNAISIAN	u			KEOKUK	OSAGEAN		10
								9
		m			BURLINGTON			8
							CM	7
		l	HORTON	POCONO	CHOUTEAU HANNIBAL	KINDERHOOKIAN	NV	6
DEVONIAN	FAMENNIAN		UTTING, 1978; HIGGS, 1975 / MAMET, 1970	CATSKILL / ADAMS, 1970	LOUISIANA / PRIOR & SABLE, 1974		PL / NEVES et al., 1972	5 / MAMET & SKIPP, 1970

The lower Windsor Group consists of thin basal carbonates overlain by generally massive evaporites, which in turn grade upsection into interbedded evaporites and thin, highly fossiliferous carbonates. The upper Windsor is a thick succession of mostly fine grained, red clastics which are periodically interrupted by evaporites of thin fossiliferous carbonates (Fig. 9.2).

The lithologic character of the basal carbonates changes with the underlying rock type. Cryptalgal laminite (Macumber Formation, A-1 Limestone, Ship Cove Limestone) overlies redbeds (Horton Group, Moncton Group, Grantmire Formation, Anguille Group), whereas biohermal accumulations, generally dominated by brachiopods, gastropods, bryozoa and algae, overlie pre-Carboniferous basement highs (Fig. 9.3-i).

The cryptalgal laminite is generally up to 15 m thick and displays a distinct vertical sequence throughout the Windsor outcrop belt. The basal one to two metres are characterized by widely spaced algal laminae (5-10 mm) separated by pellets which are often inversely graded. However, the bulk of the cryptalgal laminite (up to 14 m thick) consists of thin laminae, generally less than 1 mm thick, with windblown, silt-size quartz grains or algal-coated intraclasts between the laminae (Schenk, 1967). This upper, thinly laminated portion appears to consist of filamentous blue-green algae of the oscillatoriacean type, whereas the lower, pelletal section appears to have been formed by a combination of oscillatoriacean and coccoid blue-green algae. The latter are known to form pellets in situ by the calcification of colonies of unicells (Monty, 1976).

There is considerable evidence to suggest a subtidal origin for the cryptalgal laminite:

a) The laminite is extremely widespread, at least 300 km along and up to 60 km across the sedimentary strike. Both dimensions are limited by a lack of additional outcrops rather than by facies changes. Relatively cohesive algal mats that could potentially be preserved and lithified into a cryptalgal laminite occur today only in the narrow, high intertidal and supratidal zones of hot and/or arid environments. The width of the basal Windsor laminite surpasses the narrow belts of modern intertidal zones by at least an order of magnitude.

However, the laminite could be the result of a regressing or transgressing intertidal facies. This would require that the rate of subsidence or emergence was maintained over a long period of time in order to

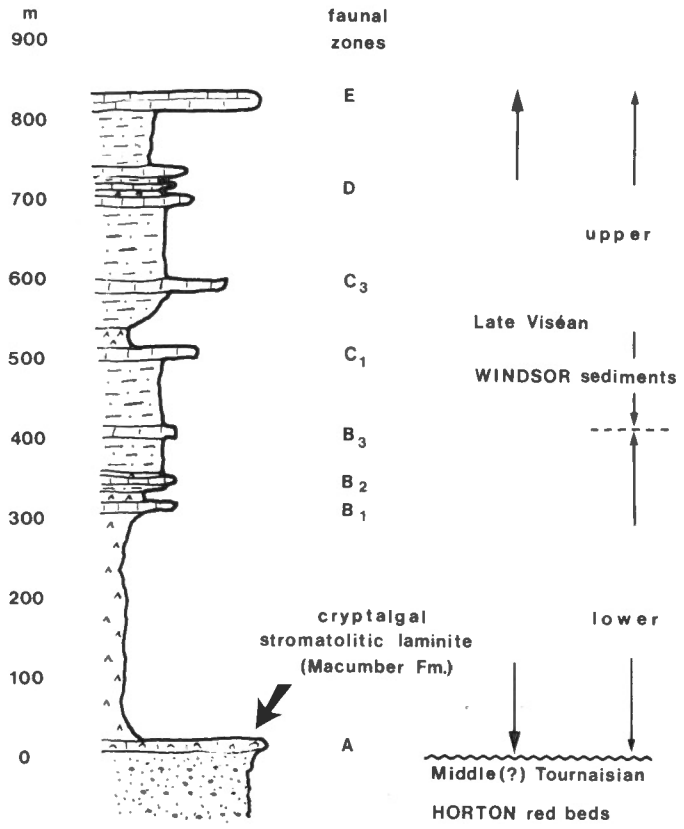


Figure 9.2. Windsor section (generalized).

prevent the development of other carbonate facies. In the case of regression the laminite should have overstepped basinward a subtidal facies, deposited prior to the onset of regression. However, the laminite rests everywhere on Horton clastics or, rarely, on basement rocks. The case of transgression is discussed under (d) below, where the association of cryptalgal laminite and subtidal fossil assemblages is evaluated.

b) The basal laminite is devoid of desiccation cracks which are common features in modern intertidal and supratidal algal mats.

c) The laminite is evenly laminated whereas modern algal mats generally display a variety of mound-like growth forms in response to chemical or physical variations which are particularly abundant in the intertidal zone. The lack of various growth forms suggests uniform physico-chemical conditions in a low stress, subtidal environment during early Windsor time.

d) The laminite is associated with brachiopod-gastropod-bryozoa-algal assemblages which accumulated in situ on basement highs which projected through the Horton clastics. These assemblages were of subtidal origin implying that the topographically lower laminite was subtidal as well.

If the cryptalgal laminite were attributed to the intertidal-supratidal zone of a slowly transgressing sea, it is hard to explain why the algal mats did not simply grow up the flanks and on top of the basement highs, but left these habitats to faunal communities. This anomalous pattern could be overcome by quickly submerging the basement highs after the intertidal phase and, thus, creating a favourable environment for a subtidal faunal community. This solution is theoretically possible, but is thought unlikely in light of the evidence listed above, particularly the absence of desiccation features.

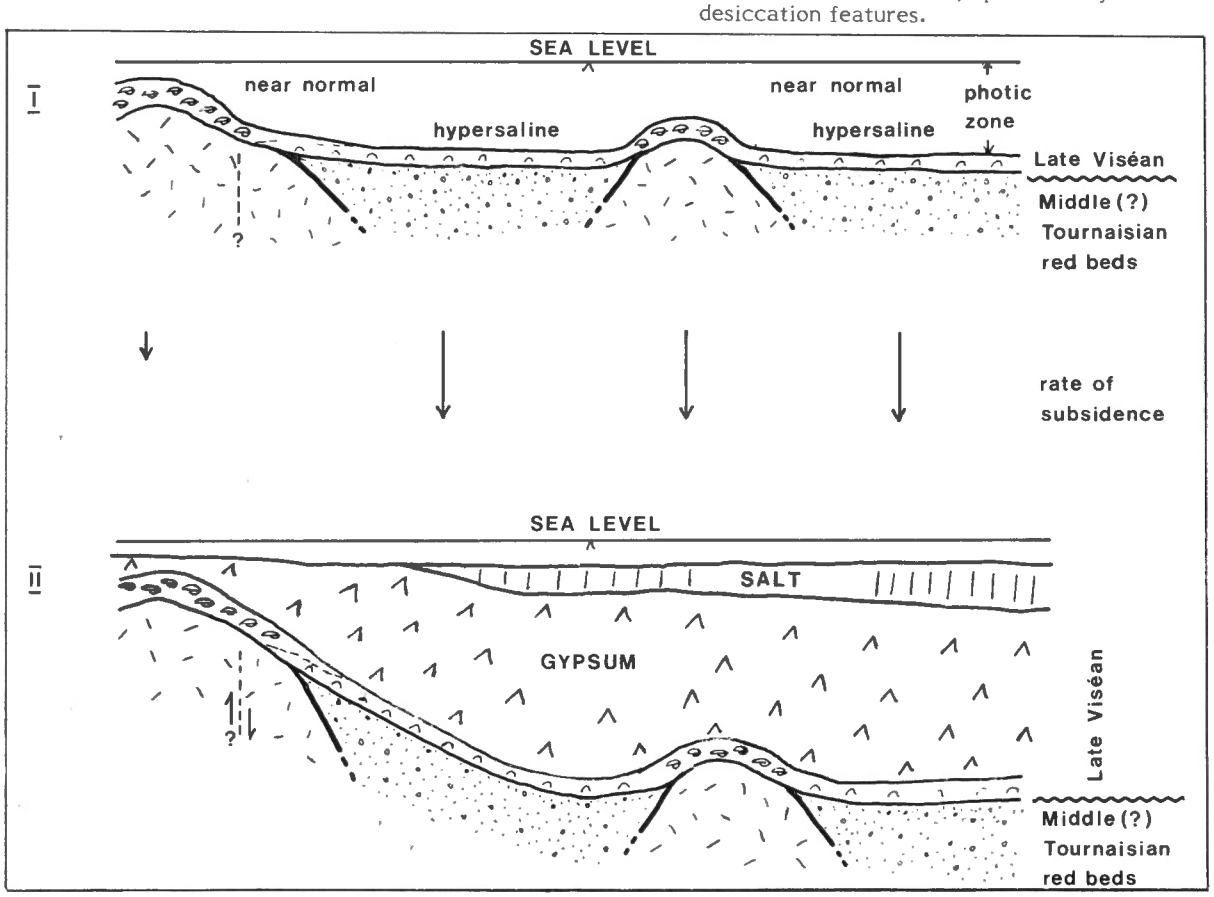


Figure 9.3. Depositional sequence during early Windsor time.

The widespread preservation of blue-green algal mats or other growth forms during the Phanerozoic is mainly due to the presence of hypersaline conditions hostile to grazing metazoa. This is the reason why blue-green algal mats are preserved in some modern intertidal environments. Referring back to the basal Windsor carbonates, it must be assumed that the gastropods were confined to the basement highs due to an intolerable salinity at deeper water levels. In fact, the salinity of the seawater at higher levels was probably also above normal because the invertebrate communities lack salinity-sensitive forms such as crinoids and solitary corals. The abrupt disappearance of pellets one to two metres above the base of the laminite may also be related to a dynamic parameter such as increasing salinity.

The argument for hypersalinity receives its ultimate confirmation near the top of the laminite where molds of gypsum crystals appear between the thin laminae. In many instances the laminae pinch and swell around the molds indicating that the gypsum formed diagenetically during or shortly after the growth of the laminae. In some borehole cores and a few favourable outcrops (Fischells River, Newfoundland; Edgetts Landing, southeastern New Brunswick) the cryptalgal laminite grades upsection through laminite with gypsum molds, into laminite with gypsum nodules, into finely nodular gypsum and finally into bedded gypsum or anhydrite. These vertical facies changes appear to be related to a gradual increase in salinity, causing gradually increasing growth of diagenetic gypsum, which at a later stage replaced and displaced the laminae. The tolerance level of blue-green algae was passed, and the last stage was precipitation of gypsum out of solution. The nodular texture in the transition zone from laminite to bedded gypsum has been interpreted as evidence for intertidal-supratidal, Sabkha-type conditions (Schenk, 1969). However, Dean et al. (1975) showed that nodular gypsum can equally well form under a standing body of water. Other associated parameters, such as the presence or absence of desiccation cracks, must be considered before an environmental interpretation is deduced from a nodular texture in gypsum. Therefore, during early Windsor time subtidal conditions appear to have existed from the time of deposition of the laminite to the time of gypsum precipitation.

Considerable brecciation within the upper laminite has been considered as evidence for a period of emergence which preceded the deposition of evaporites (Geldsetzer, 1977). Additional field work suggests, however, that these breccias are the result of post-Windsor dissolution of diagenetic and bedded evaporites. Calcite veins in unbrecciated cryptalgal laminite end abruptly at an interbedded breccia horizon or cavity, but continue in unbrecciated laminite above. Laminite fragments with calcite veins are randomly oriented in the solution breccia. Locally the entire evaporite and part or all of the basal carbonate are brecciated as for example south of Ingonish and near Mabou Mines, Nova Scotia. Elsewhere the solution breccia occurs only along the laminite-evaporite contact zone as for example, at Crystal Cliffs north of Antigonish. A post-Windsor origin was also suggested for the Pembroke Breccia in the Windsor-Truro area of Nova Scotia (Clifton, 1967).

Evaporite deposition reached its climax during early Windsor time with the precipitation of halite and potash salts. Halite has been found in the peripheral areas of the "Windsor Sea" as well as in the basin proper. The more soluble potash salts appear to be largely restricted to the distal, western portions of the basin, in southeastern New Brunswick.

Further exploration for potash will hopefully more clearly define the physical and chemical parameters that led to the formation of potash horizons. Is it possible that these last salts precipitated in distal embayments blocked off from the basin proper by "anhydrite walls" which had formed earlier in front of such minor embayments and became physical barriers during the advanced stage of evaporative draw-down of the "Windsor" sea level? Such anhydrite walls have been identified by numerous boreholes through the Permian Zechstein of Central Europe, where these walls became effective barriers behind which salts were precipitated (Richter-Bernburg, 1955).

Thin, highly fossiliferous carbonates appear in the uppermost part of the lower Windsor evaporites indicating that normal marine conditions prevailed occasionally within the "Windsor Sea". A second drastic lithological change was the influx of fine red clastics, the dominant lithology of the upper Windsor Group. The red clastics are extensively rippled, locally contain gypsum and salt casts or molds, and are rarely mudcracked. Occasional fossiliferous carbonate horizons have been used to subdivide the upper Windsor into faunal zones (Bell, 1929). In southwestern Newfoundland, the clastic component is characterized by a large number of massive sandstones, while in southeastern New Brunswick the entire upper Windsor appears to grade to the west into a coarse grained, red conglomerate.

Discussion

The available evidence suggests that the deposition of the basal Windsor carbonates took place in a subtidal environment. The carbonates rest on a subaerial erosion surface which may have been below sea level prior to the time of marine transgression. Data on the transport direction of the underlying Horton clastics are not yet available, but the presence of nonmarine evaporites in the middle Horton Group (the Albert Formation of New Brunswick) suggests the existence of a large basinal area with an interior drainage (Kirkham, 1978). Tectonic movements or a eustatic rise of sea level may have resulted in the abrupt flooding of the sub-sea level area and the establishment of the "Windsor Sea".

The presence of algal beds at the base of the Windsor Group requires that the water depth in the peripheral areas of this sea remained within the photic zone, which may extend down to a depth of 1000 m for some algal groups, but for blue-green algae of the oscillatoriacean type the maximum depth observed so far is 25 m (Monty, 1977). However, an accurate determination of the depth range of these algae in a normal marine environment is probably severely limited by the grazing activities of metazoa. It is unlikely that the marginal areas of the "Windsor Sea" were not deeper than 25 m over distances of several hundred kilometres. Water depth probably exceeded 25 m by perhaps as much as an order of magnitude in some areas. No data are known from the central portions of the "Windsor Sea". Therefore, estimates of the water depth during early Windsor time for an area such as the Grand Banks are a matter of speculation.

Asuming the depth range of the algal forms at the base of the Windsor was 250 m this depth would still not have been sufficient to accommodate the thickest evaporite sections which exceed 350 m in areas such as southwestern Newfoundland, western Cape Breton Island and in the Shubenacadie region of Nova Scotia. These areas must have subsided at an accelerated rate and may well have been topographic depressions on the sea floor ideally suited for the collection of high-density brines and the precipitation of halite (Fig. 9.3-II).

During late Windsor time the availability of clastics was sufficient to keep pace with the rate of subsidence. Occasional evaporite horizons probably formed in local depressions where the rate of subsidence temporarily exceeded the rate of clastic supply. Periodic increases in the rate of subsidence over the entire region led to widespread marine transgressions over the shallow-water to subaerial mud flats. These events temporarily reduced the dispersal

range of detrital material and led to the deposition of the fossiliferous marine carbonates which serve to subdivide the upper Windsor. A return to "normal" subsidence rates caused a total or partial regression of the sea, and mudflats once again became dominant. The source area for the fine clastics was probably to the west because in southeastern New Brunswick the upper Windsor grades laterally into massive red conglomerates which appear to be alluvial fanglomerates.

Acknowledgments

Geologists of the Provincial Surveys, mining companies and universities of the Atlantic Provinces provided valuable information on field localities and on stratigraphic aspects. The author benefitted from many discussions with colleagues of the Geological Survey, particularly with R.D. Howie, R.V. Kirkham and J. Lydon, H.E. Dunsmore, W.H. Poole and B.V. Sanford reviewed and improved the manuscript.

References

Adams, R.W.
1970: Loyalhanna Limestone – crossbedding and provenance; Chapter 5, p. 83-100, in Studies of Appalachian geology, central and southern, eds. G.W. Fisher, F.J. Pettijohn, J.C. Reed and K.N. Weaver, Interscience Publishers.

Bell, W.A.
1929: Horton-Windsor district, Nova Scotia; Geol. Surv. Can., Mem. 155, 268 p.

1960: Mississippian Horton Group of type Windsor-Horton District, Nova Scotia; Geol. Surv. Can., Mem. 314.

Caster, K.E.
1934: The stratigraphy and paleontology of northwestern Pennsylvania; Part 1: Stratigraphy; Bull. Am. Paleontol., v. 21, p. 1-185.

Clifton, H.E.
1967: Solution – collapse and cavity filling in the Windsor Group, Nova Scotia, Canada; Geol. Soc. Am. Bull., v. 78, p. 819-832.

Dean, W.E., Davies, G.R., and Anderson, R.Y.
1975: Sedimentological significance of nodular and laminated anhydrite; Geology, v. 3, p. 367-372.

Geldsetzer, H.H.J.
1971: Tectonically controlled sedimentation during the Middle Paleozoic of northeastern North America; unpublished Ph.D. thesis, Queen's Univ., Kingston, 273 p.

1977: The Windsor Group of Cape Breton Island, Nova Scotia; in Report of Activities, Part A, Geol. Surv. Can., Paper 77-1A, p. 425-428.

Higgs, K.
1975: Upper Devonian and Lower Carboniferous miospore assemblages from Hook Head, County Wexford, Ireland; Micropalaeontology, v. 21, p. 393-419.

Irving, E.
1977: Drift of the major continental blocks since the Devonian; Nature, v. 270, p. 304-309.

Jansa, L.F. and Wade, J.A.
1975: Geology of the continental margin off Nova Scotia and Newfoundland; p. 51-105, in Offshore geology of eastern Canada, Vol. 2 – Regional geology, eds. W.J.M. Van der Linden and J.A. Wade, Geol. Surv. Can., Paper 74-30.

Kirkham, R.V.
1978: Base metal and uranium distribution along the Windsor-Horton contact, Central Cape Breton Island, Nova Scotia; in Current Research, Part B, Geol. Surv. Can., Paper 78-1B, p. 121-135.

Mamet, B.L.
1970: Carbonate microfacies of the Windsor Group (Carboniferous), Nova Scotia and New Brunswick; Geol. Surv. Can., Paper 70-21, 121 p.

Mamet, B.L. and Skipp, B.
1970: Lower Carboniferous calcareous foraminifera: preliminary zonation and stratigraphic implications for the Mississippian of North America; in C.R. 6eme Cong. Int. Strat. Geol. Carb., Sheffield, 1967, p. 1129-1146.

Monty, C.L.V.
1976: The origin and development of cryptalgal fabrics; in Stromatolites, ed. M.R. Walter, Developments in Sedimentology 20, p. 193-249.

1977: Evolving concepts on the nature and the ecological significance of stromatolites: a review; in Fossil algae, recent results and developments, ed. E. Fluegel, Springer-Verlag, p. 15-35.

Neves, R., Gueinn, K.J., Clayton, G., Ioannides, N., and Neville, R.S.W.
1972: A scheme of miospore zones for the British Dinantian; in C.R. 7eme Cong. Int. Strat. Geol. Carb., Krefeld, 1971, p. 347-353.

Prior, W.A. and Sable, E.G.
1974: Carboniferous of the eastern Interior Basin; in Carboniferous of the southeastern United States, ed. G. Briggs, Geol. Soc. Am., Special Paper 148, p. 281-313.

Richter-Bernburg, G.
1955: Ueber salinare Sedimentation; Z. Deutsch. Geol. Gesellschaft, v. 105, p. 593-645.

Schenk, P.E.
1967: The Macumber Formation of the Maritime Provinces – a Mississippian analogue to Recent strand-line carbonates of the Persian Gulf; J. Sed. Petrol., v. 37, p. 365-376.

1969: Carbonate-sulfate-red bed facies and cyclic sedimentation of the Windsorian State (Middle Carboniferous), Maritime Provinces; Can. J. Earth Sci., v. 6, p. 1037-1066.

Utting, J.
1978: Palynological investigation of the Windsor Group (Mississippian) of Port Hood Island and other localities on Cape Breton Island, Nova Scotia; in Current Research, Part A, Geol. Surv. Can., Paper 78-1A, p. 205-207.

White, D.
1913: The Horton Flora; Geol. Surv. Can., 13th Int. Geol. Cong. 1913, Guide Book No. 1, p. 144-146.

10.

MINERALOGICAL STUDY OF AN UNNAMED BARIUM CALCIUM CARBONATE FROM THE CAVE-IN-ROCK DISTRICT, ILLINOIS

Project 680023

A.C. Roberts
Central Laboratories and Administrative Services Division

Roberts, A.C., Mineralogical study of an unnamed barium calcium carbonate from the Cave-in-Rock District, Illinois; in Current Research, Part C, Geol. Surv. Can., Paper 78-1C, p. 49-52, 1978.

Abstract

A new mineral, nearly identical to alstonite, was discovered by X-ray powder diffraction methods in three samples which originated from the Cave-in-Rock district, Illinois, U!S!A! It occurs as colourless euhedral crystals about 1 mm long which display {221} pyramidal habit and a vitreous lustre. The hardness is between 4 and 4 1/2. It fluoresces pale to bright orange, and effervesces in dilute HCl. The symmetry is hexagonal, space group choices are P312, P321, P3ml, P3lm, $P\bar{3}ml$ or $P\bar{3}ml$; refined unit cell parameters are a=8.692 (3) Å, c=6.148 (4) Å, V=402.24 Å^3. The strongest lines (Å) of the X-ray powder diffraction pattern are 3.550 (100)(111), 2.510 (67)(300), 2.048 (21)(221), 6.15 (18)(001), 1.943 (18)(302), and 1.853 (15)(113). Microprobe analysis (averaged) gave BaO 45.6, CaO 18.8, SrO 5.2, CO_2 (calc.) 30.0 wt.%, corresponding to $Ba_{0.8722}$, $Ca_{0.9832}$, $Sr_{0.1473}$ $(CO_3)_2$ or ideally Ba Ca $(CO_3)_2$. The number of formula weights per unit cell (Z) is 3 and the calculated density (Dx.) is 3.62. Optically, it is uniaxial negative with n_ε=1.527 (3) and n_ω=1.672 (3). Pertinent data on alstonite are also reported, particularly those data useful in distinguishing between the two minerals. The crystallographic relationship suggests that they belong to a family of OD (order-disorder) structures of general composition Ba Ca $(CO_3)_2$.

Introduction

During an extensive study of alstonite (Roberts, 1976), a mineral was found that could not be identified by its X-ray powder diffraction pattern. The data reported here are results from a mineralogical study of the mineral and are compared to alstonite.

Locality and Specimen Description

The unnamed mineral, referred to as BA-1 in this report and in Roberts (1976), has been encountered in three samples, all labelled "Cave-in-Rock district, Illinois, U.S.A.". The specific locality is uncertain, but the specimens probably originated from the Minerva #1 Mine.

The largest specimen, measuring 11 by 10 by 5 cm, consists of centimetre-sized scalenohedra of yellow calcite protruding from a matrix of massive to globular barite. BA-1 coats the globular barite as thin layers of colourless, hexagonal pyramids. Associated phases include drusy aggregates of grey alstonite, traces of purple fluorite and dark brown sphalerite. The other two specimens consist entirely of numerous crystal fragments of BA-1 without matrix.

Morphological, Physical and Optical Properties

BA-1 occurs as euhedral crystals, not exceeding 1 mm in length, with an approximate length to width ratio of 2:1. The crystals are hexagonal and display {221} pyramidal habit. Hexagonal dipyramids have been observed but are rare. The faces are heavily striated normal to the axis of elongation (c-axis) and are divided parallel to the c-axis by a medial, irregular, slightly reentrant "suture".

The crystals are colourless to smoky white, grading to grey-white in masses, and have a vitreous lustre. The streak is white; the hardness is between 4 and 4 1/2; the fluorescence varies from pale to bright orange under long wave ultraviolet light; and the effervescence is quite vigorous in dilute HCl.

The optical characterization of BA-1 is as follows: colourless in transmitted light, uniaxial negative with n_ε=1.527 (3) and n_ω=1.672 (3).

Crystallography

Pyramids of BA-1 were crushed, and selected fragments checked for multiple reflections using the precession camera. Untwinned chips were subsequently run on precession and Weissenberg cameras by utilizing both Zr-filtered Mo radiation ($\lambda MoK\alpha$=0.7107Å) and Ni-filtered Cu radiation ($\lambda CuK\alpha$ =1.5418Å).

Single crystal photographs indicate that the symmetry of BA-1 is hexagonal with measured cell parameters a=8.68 Å and c=6.14 Å. The hkO level photographs display 6 mm symmetry, whereas hk1 and hk2 level photographs show three fold symmetry with a mirror plane coincident with a*. This implies that six space group choices are possible: P312 (149), P321 (150), P3ml (156), P3lm (157), $P\bar{3}lm$ (162), and $P\bar{3}ml$ (164). Least squares refinement of the approximate cell parameters yielded a=8.692 (3) Å and c=6.148 (4) Å, with a computed cell volume of 402.24 Å^3. A fully indexed powder diffraction pattern is presented in Table 10.1.

Twinning

Complete pyramids of BA-1 are twinned, as shown on single crystal films. The "a" cell parameter is doubled to approximately 17.40 Å by the presence of medium to weak supercell reflections and the hexagonal 6 mm symmetry is retained throughout the zero and upper levels. These diffraction phenomena due to twinning are not unexpected since the twin condition for hexagonal crystals states that a^2: c^2 must approach a rational number and the calculated ratio for BA-1, 1.997:1.000 fulfills this requirement perfectly.

Chemical Composition

Colourless pyramidal aggregates of BA-1 were hand-picked under a 50X binocular microscope, mounted in a polished section and submitted for electron microprobe analysis. Because preliminary energy dispersive spectra indicated the presence of major amounts of Ba and Ca and minor amounts of Sr, quantitative determinations for these elements were carried out with a MAC electron microprobe, using benitoite (Ba), calcite (Ca) and strontianite (Sr) as standards. Sample degradation was minimized by operating

Table 10.1

Powder diffraction data for unnamed $BaCa(CO_3)_2$*

I/Io	2θmeas.	dÅ meas.	dÅ calc.	hkl
2	11.79	7.51	7.53	100
18	14.39	6.15	6.15	001
3	18.64	4.76	4.76	101
11	20.41	4.35	4.35	110
100	25.08	3.550	3.549	111
2	27.83	3.206	3.210	201
3	29.03	3.076	3.074	002
11	31.38	2.851	2.846	102
5	34.75	2.581	2.582	211
67	35.71	2.510	2.509	300
1	37.97	2.370	2.381	202
6	38.77	2.323	2.323	301
9	41.52	2.175	2.173	220
8	43.39	2.085	2.088	310
21	44.22	2.048	2.049	221
3	45.96	1.975	1.977	311
18	46.74	1.943	1.944	302
15	49.16	1.853	1.853	113
1	50.76	1.799	1.799	401
3	51.56	1.773	1.774	222
2	53.01	1.727	1.727	320
2	55.23	1.663	1.663	321
2	55.98	1.643	1.643	410
2	57.43	1.605	1.605	402
11	58.13	1.587	1.587	411
1	60.25	1.536	1.537	004
1	61.60	1.506	1.506	104
6	62.30	1.490	1.491	223
2	63.60	1.463	1.463	501
9	64.35	1.448	1.449	330
2	65.65	1.422	1.422	420
2	66.30	1.410	1.410	331
1	67.62	1.385	1.386	403
1	69.55	1.352	1.352	510
2	71.37	1.321	1.321	323
			1.320	511
8	72.04	1.311	1.311	304
			1.310	332
1	73.22	1.293	1.291	422
6	73.94	1.282	1.282	413
11	75.77	1.255	1.255	600
3	76.96	1.239	1.238	512
			1.238	430
2	77.64	1.230	1.230	005
2	78.79	1.215	1.213	503
			1.213	431

*—114.6 mm Debye-Scherrer camera; Ni filtered Cu Kα radiation;
—line intensities calculated from diffractometer trace;
—indexed with a=8.692 Å, c=6.148 Å;
—film No. 48934 corrected for film shrinkage.

Table 10.2

Comparison of unnamed $BaCa(CO_3)_2$ and alstonite powder patterns

Unnamed $BaCa(CO_3)_2$ Cave-in-Rock, Ill. (This Study)		Alstonite (ROM-M4872) Northumberland, England (Roberts, 1976)	
I/Io	dA meas.	I/Io	dA meas.
2	7.51		
18	6.15	1	6.12
		7	5.65
		1	4.99
3	4.76		
11	4.35	4	4.35
		1	4.17
		1	3.88
100	3.550	100	3.549
		5	3.461
2	3.206		
3	3.076	6	3.057
11	2.851	8	2.835
		3	2.687
5	2.581	3	2.583
67	2.510	46	2.509
		10	2.499
1	2.370	1	2.375
6	2.323		
		3	2.290
9	2.175	7	2.178
		4	2.155
8	2.085		
21	2.048	26	2.052
		1	2.024
3	1.975	1	1.975
18	1.943	25	1.943
		1	1.900
15	1.853	19	1.846
1	1.799		
3	1.773	2	1.772
2	1.727		
2	1.663	1	1.665
2	1.643	2	1.643
2	1.605		
11	1.587	8	1.590
1	1.536	2	1.530
1	1.506		
6	1.490	3	1.489
2	1.463		
9	1.448	5	1.450
2	1.422		
2	1.410		
1	1.385		
1	1.352		
2	1.321		
8	1.311	6	1.311
1	1.293		
6	1.282	4	1.283
11	1.255	3	1.259
3	1.239		
2	1.230		
2	1.215		
		2	1.188

Table 10.3

Chemical composition of unnamed $BaCa(CO_3)_2$ and alstonite

Unnamed $BaCa(CO_3)_2$ Cave-in-Rock, Illinois (This Study)				Alstonite (ROM-M4872) Northumberland, England (Roberts, 1976)			
	wt.%	molecular ratio			wt.%	molecular ratio	
BaO	45.6	0.2985	0.6854	BaO	47.0	0.3093	0.6902
CaO	18.8	0.3365		CaO	20.2	0.3634	
SrO	5.2	0.0504		SrO	1.8	0.0175	
CO_2	30.0	0.6844		CO_2	30.1	0.6901	
Total	99.6			Total	99.1		
Specific Composition*: $Ba_{0.872}Ca_{0.983}Sr_{0.147}(CO_3)_2$				Specific Composition*: $Ba_{0.896}Ca_{1.053}Sr_{0.031}(CO_3)_2$			
Molecular Weight: 292.14				Molecular Weight: 289.90			
Z: 3				Z: 12			
Dx: 3.62 g/cc				Dx: 3.60 g/cc			

*Calculated assuming 6 oxygen atoms per formula unit cell.

Table 10.4

Crystallographic parameters for unnamed $Baa(CO_3)_2$ and alstonite

	Unnamed $BaCa(CO_3)_2$ (This Study)	Alstonite (ROM-M4872) (Roberts, 1976)	Alstonite (Sartori, 1975)
SYMMETRY	Hexagonal	Triclinic	Triclinic
SPACE GROUP	P312, P321, P3m1, P31m, $P\bar{3}1m$ or $P\bar{3}m1$	P1 or $P\bar{1}$	C1 or $C\bar{1}$
CELL PARAMETERS	a = 8.692 (3) Å c = 6.148 (4) Å V = 402.24 Å^3	a = 17.38 Å b = 17.40 Å c = 6.123 Å $\alpha \simeq 90°$ $\beta \simeq 90°$ $\gamma \simeq 120°$ V ≃ 1603.55 Å^3	a = 30.14 Å b = 17.40 Å c = 6.12 Å $\alpha = 90°$ $\beta = 90°$ $\gamma = 90°$ V = 3209.55 Å^3
NUMBER OF FORMULA WEIGHTS PER UNIT CELL	Z = 3	Z = 12	Z = 24

at 20 KV with a sample current of 0.03 micro-amps and using a beam of 20 microns diameter. Data were recorded at 20 spots within two areas, then averaged and corrected for matrix effects using an updated and modified version of a computer program written by Rucklidge and Gasparrini (1969).

This particular sample was apparently homogeneous and contained traces of Fe, Mn and Mg, but all were less than 0.05 per cent. A chemical analysis by the Penfield method indicated the complete absence of water, thus CO_2 was calculated to satisfy the values for stoichiometric $BaCO_3$, $CaCO_3$ and $SrCO_3$.

The averaged analysis was as follows: BaO 45.6, CaO 18.8, SrO 5.2, CO_2 30.0 wt.%. Calculated on the basis of 6 oxygen atoms this yields the following formula: $Ba_{0.8722}$, $Ca_{0.9832}$, $Sr_{0.1473}(CO_3)_2$ or ideally $BaCa(CO_3)_2$. The Sr substitutes for both Ba and Ca, and apparently is non-essential to the stability of the structure.

The computed molecular weight (292.14) and volume (402.24 Å), coupled with the measured specific gravity (Dm=3.75 g/cc) dictated that there be 3 formula weights per unit cell. The calculated density (Dx) with Z=3 is 3.62 g/cc.

This discrepancy between calculated and measured densities is unsatisfactory and must be attributed to barite impurities present in the hand-picked samples submitted to Berman balance density measurements. There are two reasons for this contention:

1) Quantitative energy dispersive analysis of the pyramidal clusters submitted for microprobe analysis clearly indicated several zones adjacent to the unnamed carbonate for which only Ba and S spectra were observed.

2) Debye-Scherrer powder diffraction patterns of several optically homogeneous pyramids revealed several medium to weak lines with d-spacings corresponding to the stronger reflections of barite.

Comparison with Alstonite

Alstonite is an anhydrous barium, calcium carbonate which has recently been independently re-examined by Sartori (1975) and by Roberts (1976). Both studies clearly established the true symmetry as triclinic, even though the single crystal patterns displayed special types of non-space group absences as well as several pseudo-symmetrical crystallographic cells. To account for these peculiarities, Sartori (1975) suggested that alstonite belongs to a family of OD (order-disorder) structures of which it is an ordered member. Roberts (1976) noted the crystallographic and chemical similarities that exist between alstonite and BA-1, and proposed that they be considered as polymorphs of $BaCa(CO_3)_2$.

The chemical results summarized in Table 10.3 indicate that the specific compositions, molecular weights, and calculated densities are very nearly identical. Whether the excess strontium in BA-1 is characteristic is unknown, owing to the limited number of specimens available for study. Nevertheless, the chemical identity of the two phases is clearly evident.

Because alstonite and BA-1 are morphologically and physically indistinguishable (Roberts, 1976) as well as being chemically analogous, sophisticated methods such as optical microscopy, X-ray powder diffraction and X-ray single crystal are necessary to reliably distinguish one from the other. Optically, alstonite is biaxial negative with a 2V of 7°, whereas BA-1 is uniaxial negative; hence they are distinguishable if a favourable orientation is available. Routine identification by X-ray powder diffraction may be accomplished by using two simple criteria:

1) intensity variation of the 001 reflection at or near 6.12 Å (strong for BA-1, weak to absent for alstonite);

2) identification of a diffraction line at 5.6 Å (medium to medium weak for alstonite, completely absent for BA-1).

A comparative listing of all front reflection d-spacings are given in Table 10.2. Note that many of the stronger reflections are common to both patterns, suggesting a structural resemblance, especially for the heavier atoms. Nevertheless, structural uniqueness is obvious when all the d-spacings are taken into account.

This structural affinity is similarly pronounced in selected single crystal photographs. The most intense diffraction nodes on hkO photographs, related to the barium and calcium atoms, are identical in distribution and intensity for both phases. Only when the weaker nodes, representative of the carbonate groups, are taken into account does the structural divergence become readily apparent. The unit cell parameters, summarized in Table 10.4, may be correlated as follows:

a Å BA-1 ≈ 1/2 a Å alstonite (Roberts, 1976)

b Å BA-1 ≈ 1/2 b Å alstonite

c Å BA-1 ≈ c Å alstonite

V Å BA-1 ≈ 1/4 V Å alstonite

Sartori (1975) proposed that alstonite, which displays triclinic symmetry, is an ordered member of a family of OD structures with general composition $BaCa(CO_3)_2$. From the foregoing discussion, it seems reasonable to include BA-1, which displays hexagonal symmetry, within the same group as a disordered member. Confirmation of this hypothesis must await detailed crystal structure determinations of both minerals.

Acknowledgments

The data presented in this paper are based in part on a M.Sc. thesis submitted by the author in 1976. I wish to thank my supervisor, Dr. L.G. Berry, for his helpful assistance and guidance, as well as constructive criticism, throughout the course of this study. I also wish to acknowledge the following: Dr. A.G. Plant, for electron microprobe analysis, and Mr. L. Moyd, for furnishing specimens used in this study.

Bibliography

Roberts, A.C.
1976: A mineralogical investigation of alstonite $BaCa(CO_3)_2$; unpubl. M.Sc. thesis, Queen's University, Kingston, Ontario, Canada.

Rucklidge, J.C. and Gasparrini, E.L.
1969: Electron microprobe analytical data reduction; EMPARDR VII; Dep. Geol., Univ. Toronto.

Sartori, F.
1975: New data on alstonite; Lithos, v. 8, p. 199-207.

11. LIMITS OF ICE ADVANCE, GLACIAL LAKES, AND MARINE TRANSGRESSIONS ON BANKS ISLAND, DISTRICT OF FRANKLIN: A PRELIMINARY INTERPRETATION

Project 740065

Jean-Serge Vincent
Terrain Sciences Division

Vincent, Jean-Serge, Limits of ice advance, glacial lakes and marine transgressions on Banks Island, District of Franklin: A preliminary interpretation; in Current Research, Part C, Geol. Surv. Can., Paper 78-1C, p. 53-62, 1978.

Abstract

Three glaciations with associated marine and glaciolacustrine phases on Banks Island are recognized for the first time. The oldest (Banks Glaciation) affected all but the northwest part of the island; glacial lakes Egina and Storkerson were formed during deglaciation. Ice of the Thomsen Glaciation of pre-Sangamonian age covered the south and east and flowed down Thomsen River valley. Associated with it are glacial lakes Parker and Dissection in the northeast and a marine transgression, the Big Sea, which followed the ice during deglaciation and inundated much of western, central, and eastern Banks Island. The youngest, or Amundsen Glaciation, of probable Early or Middle Wisconsinan age involved two icelobes that impinged on the east and southwest coasts creating glacial lakes Raddi, Masik, Rufus, De Salis, Cardwell, and Sarfarssuk at their limit. Ice of the Viscount Melville Glaciation, possibly equivalent to the Amundsen Glaciation and probably also of Wisconsinan age, impinged on the north coast and created glacial lakes Ballast and Ivitaruk. The East Coast Submergence, which inundated the east coast up to 120 m, may be equivalent to the Meek Point Sea that covered the west up to 20 m; both possibly relate to Early or Middle Wisconsinan deglaciation. The Schuyter Point Sea of Late Wisconsinan – Holocene age drowned the east coast up to 25 m and is possibly a transgression that occurred in an icefree area. Sand Hills Readvance in Thesiger Bay and Russell Readvance on the northeast coast are possibly late readvances of Amundsen and Viscount Melville ice, respectively.

Introduction

Reconnaissance mapping of surficial deposits (Vincent, 1978a) and stratigraphic investigations (Vincent, 1978b) gave new insight into the sequence of Quaternary events. The extents of several ice advances are recognized and delineated for the first time along with inundations by glacial lakes and by the sea. For easier description the different glacial, glaciolacustrine, and marine events are named. The study area is shown in Figure 11.1.

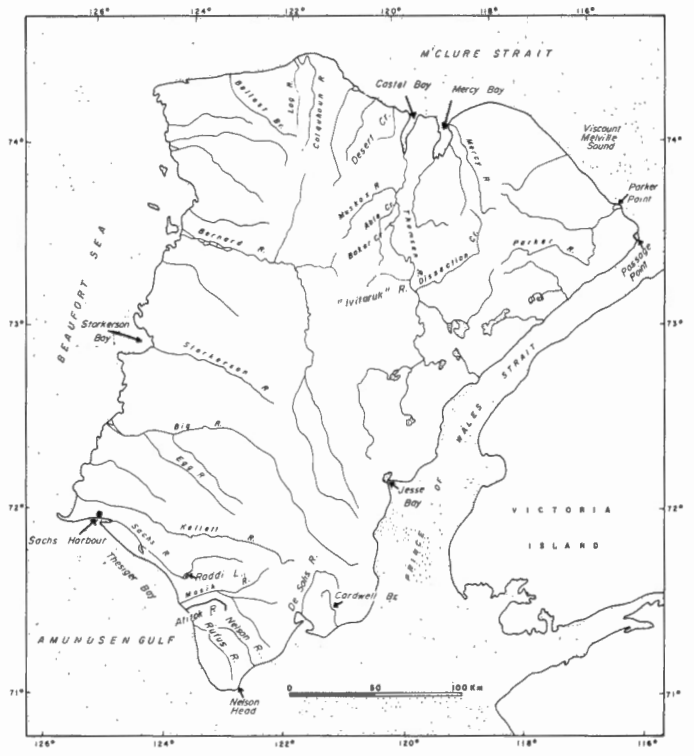


Figure 11.1. Map showing study area.

Previous Work

The glaciation of Banks Island has been investigated by few authors, and they have attempted only to delineate the extent of the latest ice advance. Hobbs (1945) showed a boundary for "Wisconsin" ice crossing the island northeastward from Thesiger Bay to Parker Point as marked by chains of lakes on the island. Jenness (1952) drew a similar line but indicated that it marked the limit of "continental" ice. He also surmised that northern Banks Island was untouched by continental ice but possibly was subjected to local glaciation and that the glacial history of the western portion was uncertain. Following the work of Fyles (1962), an ice limit for the "last" or "classical Wisconsin" was drawn on the Glacial Map of Canada (Prest et al., 1968), showing that southern and eastern Banks Island as well as the extreme north of the island along M'Clure Strait was glaciated during the latest Wisconsinan stade. The remainder of the island is shown as having been glaciated entirely in pre-"Wisconsin" time.

Glacial Limits

Major textural differences in tills, stratigraphic relationships, and well defined ice-marginal features permit the delineation of a boundary for three main glaciations and two readvances (Fig. 11.2). The tills of each glaciation contain Precambrian erratics from the mainland, probably from the District of Keewatin. While this does not rule out the possibility of local ice caps on the island, no evidence for such glaciation has been found. The glacial limits depict areas that show clear evidence of glaciation and generally are thought to represent the maximum extent of an ice sheet. In some cases, the ice may well have extended farther than these limits leaving little evidence.

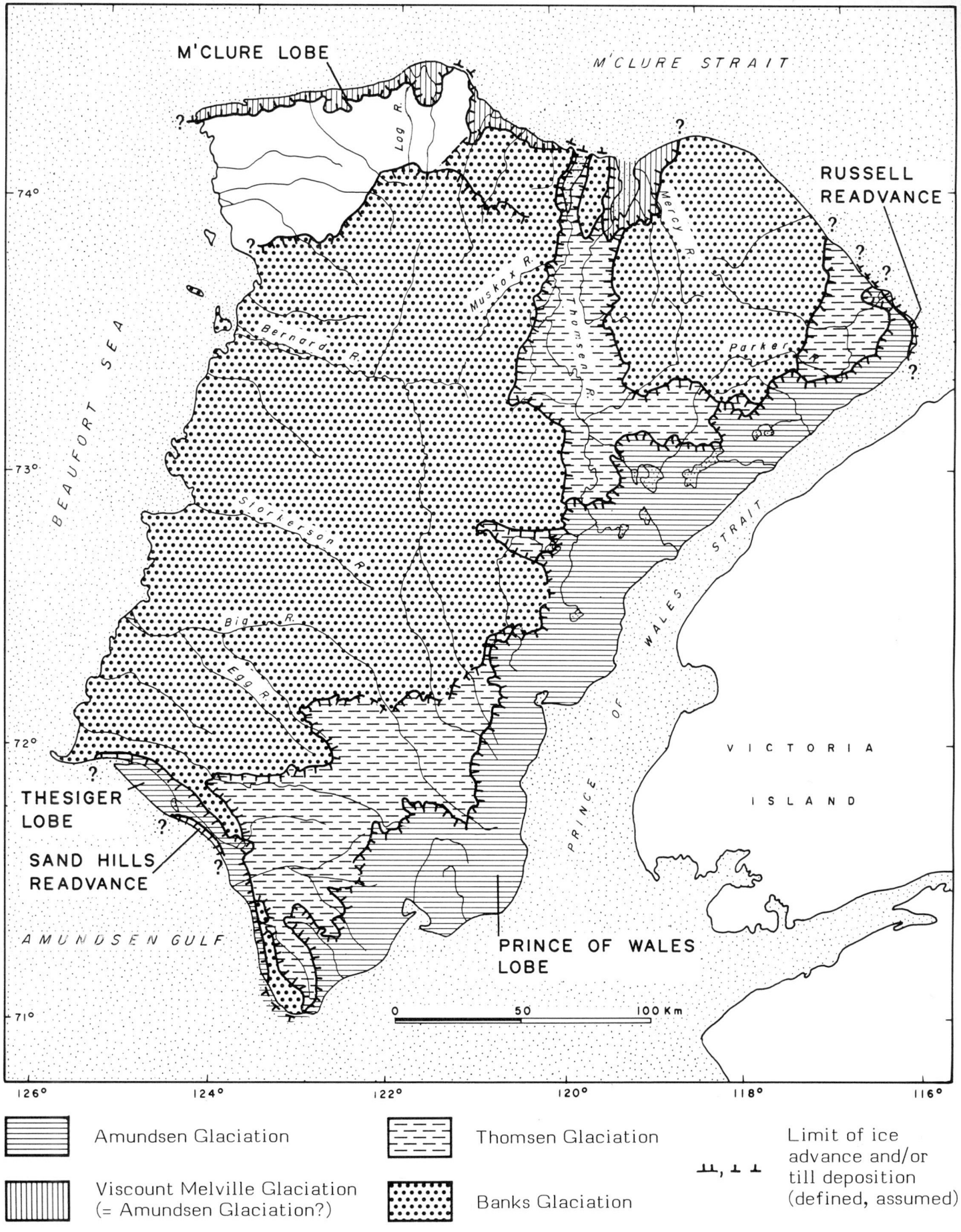


Figure 11.2. Map showing glacial limits on Banks Island.

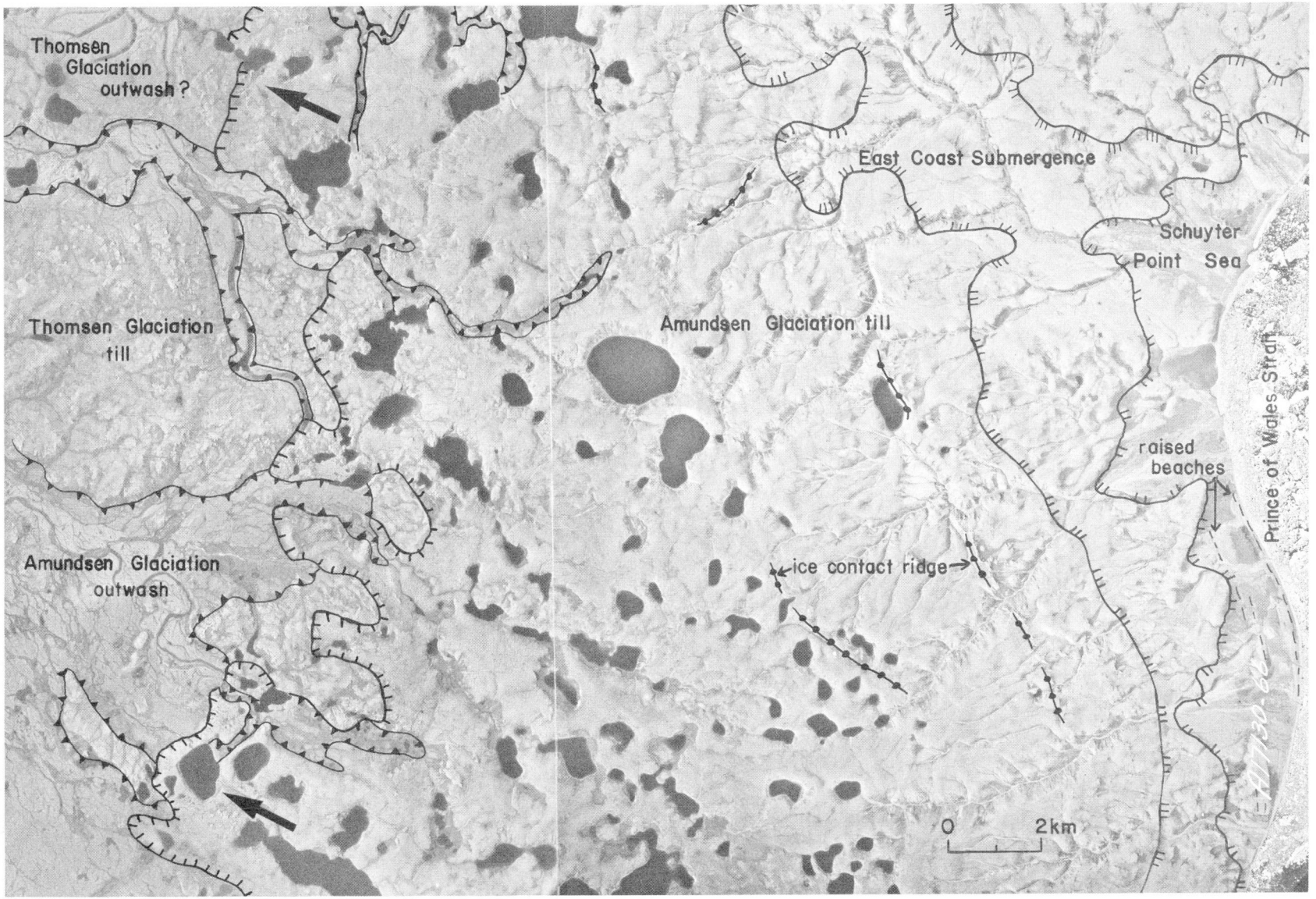


Figure 11.3. An area on the east coast of Banks Island just south of Jesse Bay showing: the limit of the Amundsen Glaciation (⊣⊣⊣); the limit of meltwater channels (◂▲▲▲); the upper trimline of the East Coast Submergence (⊣⊣⊣); the upper trimline of the Schuyter Point Sea (⊣⊣⊣); raised beaches of the Schuyter Point Sea (- - -); ice-contact ridges (●●●); and ice flow direction (arrow). Note the contrast between the till surface above and below the upper submergence limit as well as the contrast between the till surfaces associated with the Amundsen and Thomsen glaciations. Part of photographs A17057-93 and A17130-66, National Air Photographic Library, Department of Energy, Mines and Resources, Ottawa.

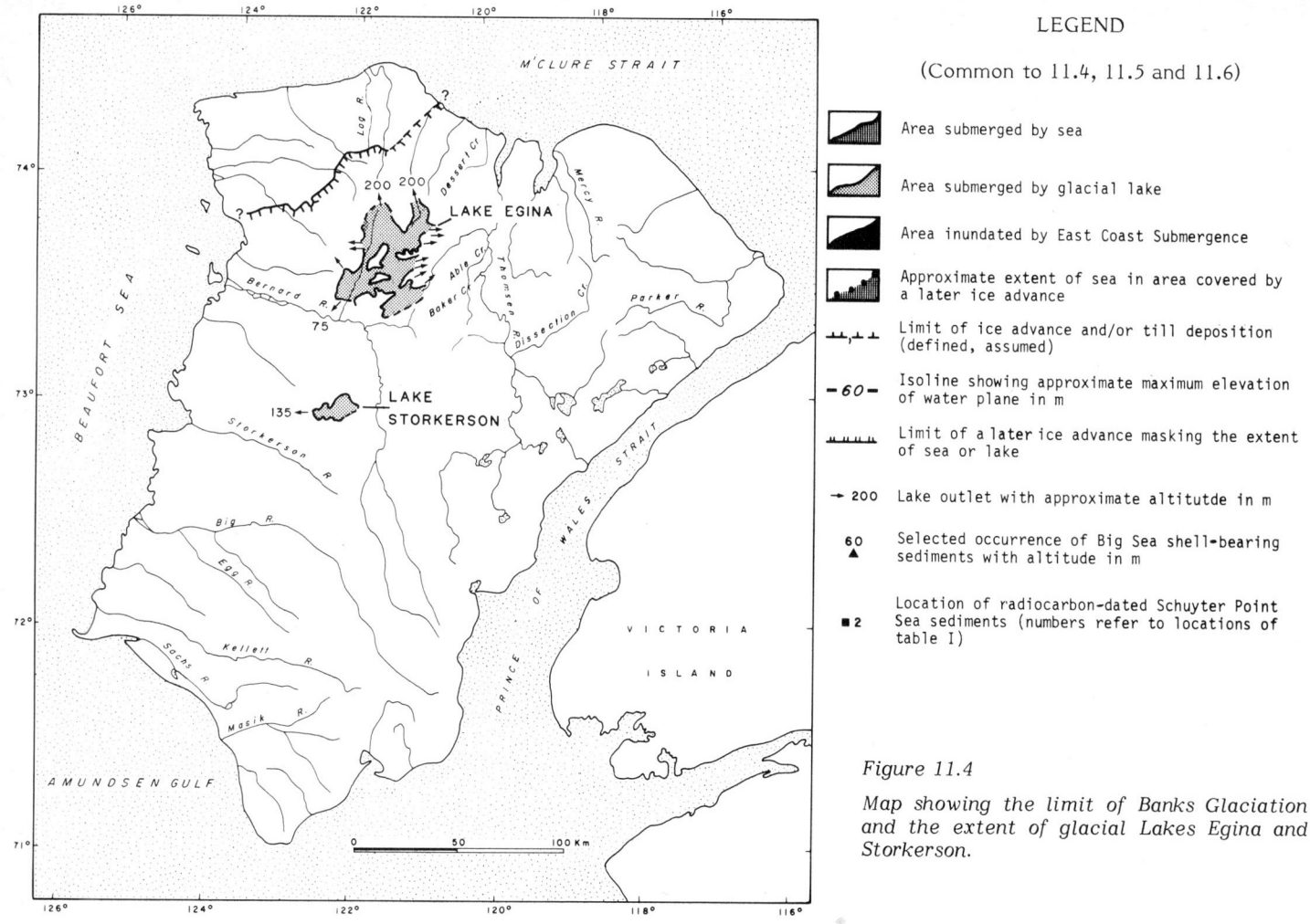


Figure 11.4

Map showing the limit of Banks Glaciation and the extent of glacial Lakes Egina and Storkerson.

Banks Glaciation

The oldest glacial event, herein named the Banks Glaciation (Fig. 11.2), is the most widespread glaciation of known extent recognized on Banks Island. It deposited a clayey till, derived mainly from the fine textured underlying unlithified or poorly lithified Cretaceous and Tertiary formations. The till, which is not very stony but contains mainland erratics, is found over most of Banks Island either at the surface in interfluve areas in the west or in sections below younger glacial and nonglacial sediments in the east.

The defined limit in northwestern Banks Island corresponds to the limit of the clayey till, whereas the assumed limit approximately marks the edge of a dissected area west of Desert Creek where sparse evidence of glaciation exists. The till that is widespread over the southern portion of northeastern Banks, as well as the till on high ground north of Nelson Head in the south, is believed to have been deposited during this glaciation. The high and dissected area east and northeast of Mercy Bay shows little evidence of glaciation except for sparse erratics, but it may have been covered by nonerosive ice or the erratics may be evidence of an earlier glacial episode.

The northwest part shows no evidence of glaciation apart from rare erratics and channels which may be glacial in origin. Hence, it is uncertain whether that area was ever covered by actively moving ice or if it was overridden by the Banks Glaciation or an older unrecognized glaciation of which little evidence remains. There is no information regarding the age of the Banks Glaciation except that its sediments are thought to be overlain by deposits of at least two full interglaciations.

Thomsen Glaciation

The Thomsen Glaciation (named here) overrode large areas of southern and eastern Banks Island with a lobe channelled along Thomsen River valley (Fig. 11.2). At its northern extremity it separated into two smaller lobes, flowing down into Mercy and Castel bays on each side of an upland. Sandy till containing mainland erratics was deposited during this glaciation, which apparently was influenced by marine and glaciolacustrine bodies of water discussed below.

At the northeastern tip of the island the glacial limit corresponds to the limit of sandy till. Ice may have occupied M'Clure Strait, but there is no clear evidence for this. In the southern portion of the Devonian plateau which extends throughout northeastern Banks, the limit is marked by several well defined ice-contact features. East of Thomsen River the ice was confined by bedrock scarps, and the boundary is set at the approximate limit of glacial erosion and deposition. West of Thomsen River the limit is defined by the extent of the sandy till and by moraines, kames, and channels. In the southern part of the island the extent of Thomsen Glaciation

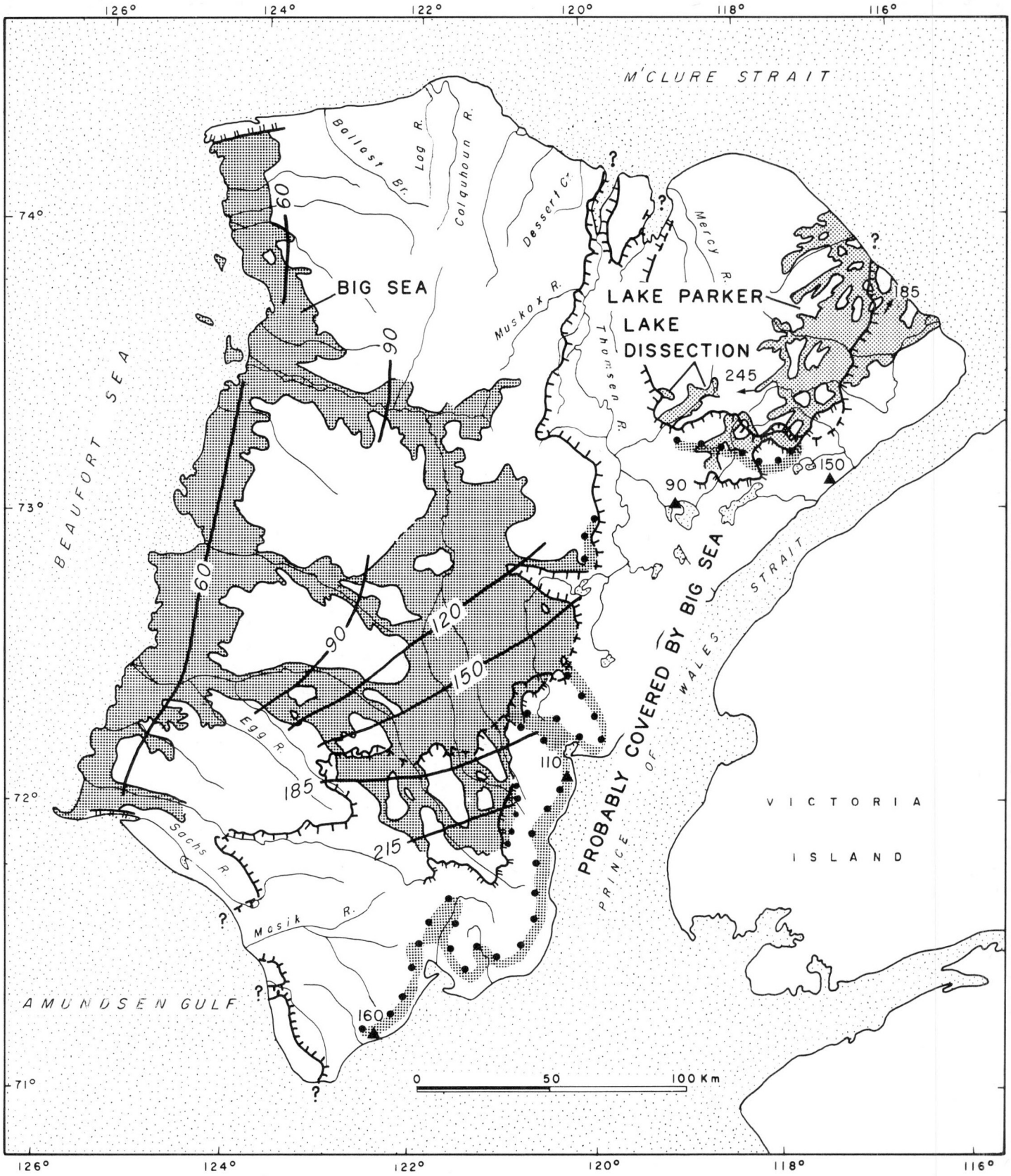


Figure 11.5. Map showing the limit of Thomsen Glaciation and the extent of glacial Lake Parker and Lake Dissection as well as the Big Sea. See Figure 11.4 for legend.

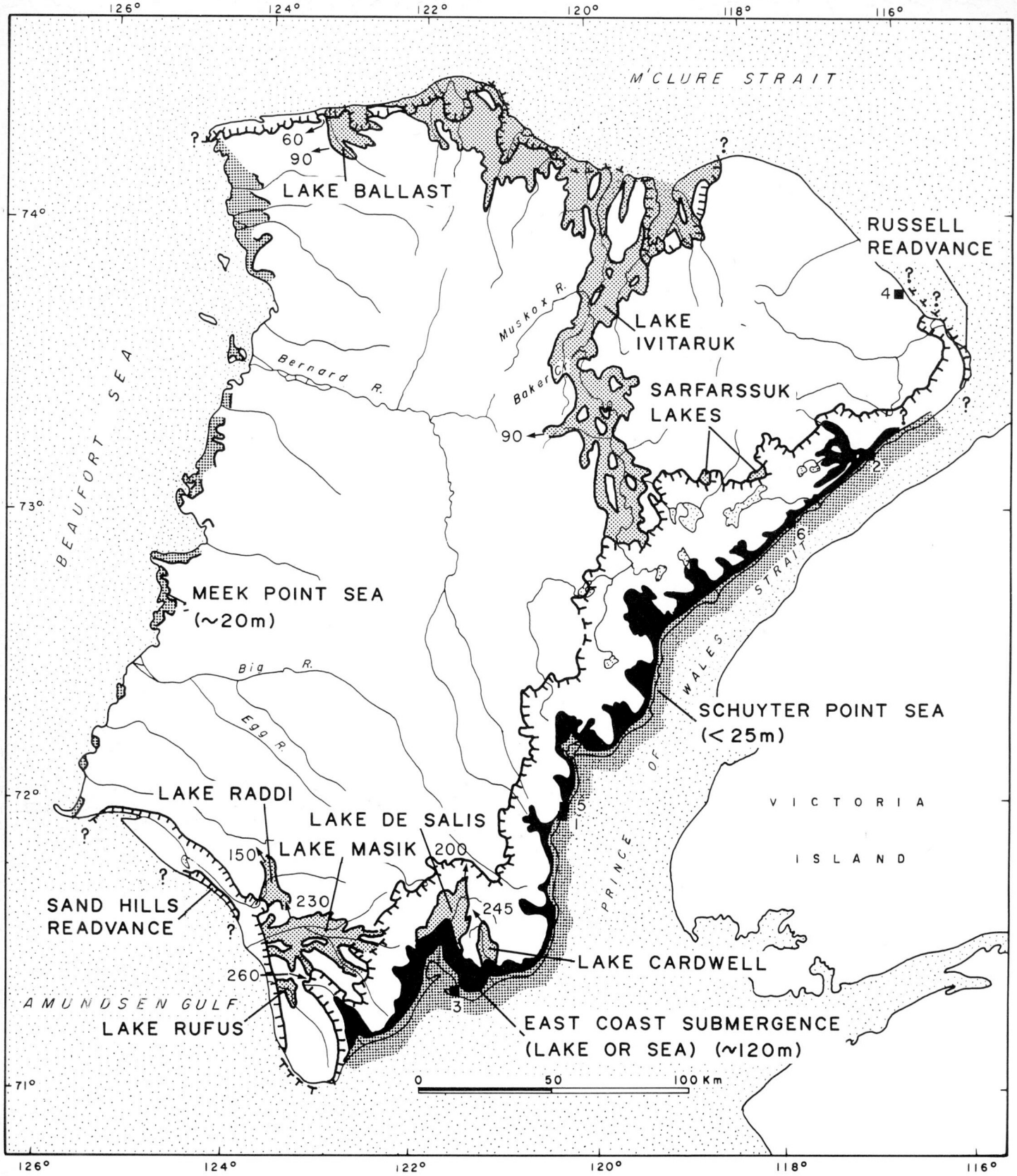


Figure 11.6. Map showing the limit of the Amundsen and Viscount Melville (=Amundsen Glaciation?) glaciations and the Russell and Sand Hills readvances. The map also shows the extent of glacial lakes Raddi, Masik, Rufus, Cardwell, De Salis, Sarfarssuk, Ballast, and Ivitaruk as well as the limit of the East Coast Submergence, the Schuyter Point Sea, and the Meek Point Sea. See Figure 11.4 for legend.

is taken to be that of the sandy till. In the upper reaches of Big River the ice may well have extended farther north, but a marine submergence has washed and reworked the till surfaces, and dissection of large areas by meltwater makes it difficult to define the limit.

On the basis of available stratigraphic and chronologic (amino acid dating) data, the Thomsen Glaciation is believed to be younger than the Banks Glaciation and older than the presumably Wisconsinan Amundsen Glaciation.

Amundsen Glaciation

The Amundsen Glaciation (named here) is defined as the result of two lobes emanating from Amundsen Gulf (Fig. 11.2). The Prince of Wales Lobe, flowed along Prince of Wales Strait impinging on the east coast of Banks Island and the west coast of Victoria Island; the Thesiger Lobe extended into Thesiger Bay and lapped onto the southwest coast of the island. The limit of these lobes is similar to that shown on the Glacial Map of Canada (Prest et al., 1968) except that the extent of Wisconsinan ice in the south as shown in Figure 11.2 is restricted to a more southerly position.

The Amundsen Glaciation resulted in the deposition of a moderately stony, generally thin (<1.5 m), very calcareous, pinkish grey silty till containing mainland erratics. The silty nature is due to thick sequences of fine marine sediments over which the ice moved. The glacial limit corresponds to the extent of the till which is characterized by high-centred polygons (Fig. 11.3).

On the basis of amino acid ratios of shells from marine deltas, this glaciation occurred during Wisconsinan time. Evidence pertaining to marine inundation (discussed below) indicates that Amundsen ice may not have been present on Banks Island in Late Wisconsinan time. It may well be of Early or Middle Wisconsinan age.

Viscount Melville Glaciation (=Amundsen Glaciation?)

The Viscount Melville Glaciation (Fig. 11.2) is herein defined on the basis of a sandy till and ice-contact ridges that were deposited on the north coast by ice (M'Clure Lobe) that flowed westward in M'Clure Strait from Viscount Melville Sound (and Victoria Island?). The former existence of this body of ice in M'Clure Strait is shown on the Glacial Map of Canada (Prest et al., 1968) and was reported by Fyles (1969). This earlier work suggests correlation of Viscount Melville and Amundsen glaciations; however data available from the present study neither confirm nor deny this interpretation.

Sand Hills and Russell Readvances

Southeast of Sachs Harbour, well developed, "young looking", morainic topography extends along the coast of Thesiger Bay for a distance of about 25 km (Fig. 11.2). The terrain is underlain by ice-contact gravelly deposits as well as a bouldery sand till containing blocks of sedimentary and basic rocks of the Proterozoic Glenelg Formation which outcrops to the south. This system is believed to have been constructed by a local readvance (Sand Hills Readvance) of ice in Thesiger Bay at an undeterminate time following the initial retreat of the Thesiger Lobe during the Amundsen Glaciation.

At the northeastern extremity of the island (Fig. 11.2), between Passage Point and Parker Point, is a ridge composed of deformed, fine grained marine(?) sediment that has been deeply dissected since deposition. A readvance (Russell Readvance) of Viscount Melville ice over marine mud could account for this feature.

Glacial Lakes and Marine Transgressions

Several distinct bodies of marine or fresh water were associated with the various glaciations of Banks Island. Except for Lake Ballast and the Meek Point Sea, all were recognized as a result of current surficial geology mapping, and all are depicted here for the first time.

Water Bodies Associated with Banks Glaciation

A large area of northwestern Banks (Fig. 11.4) was inundated by glacial Lake Egina which was impounded between a southeastward-retreating ice front and high ground to the north. The history of the lake is complex due to the shifting ice front configuration, the dissected nature of the terrain, and the large number of outlets. Initial lake phases correspond to outlets at about 200 m that permitted drainage towards M'Clure Strait. As the ice retreated, new, lower outlets were uncovered to permit drainage either towards M'Clure Strait via Thomsen River drainage or towards the Beaufort Sea via small streams on the western side of the lake. Eventually Lake Egina drained when ice retreat permitted free drainage into Bernard River.

Glacial Lake Storkerson is a small body of water (Fig. 11.4) which was dammed between high ground to the north and the ice front. The outlet was at about 135 m elevation, and water flowed towards the Beaufort Sea via Storkerson River and one of its northern tributaries. The lake drained when the ice reached a position where flow into Bernard River system was possible.

Water Bodies Associated with Thomsen Glaciation

Marine waters submerged western, central, and eastern Banks Island up to 215 m elevation during Thomsen Glaciation. As this inundation was most extensive in the valley of Big River, among others, it is herein named the Big Sea (Fig. 11.5, 11.7).

The sea extended inland as the Thomsen ice retreated southeastward and inundated large areas of eastern Banks Island. Mainly in this eastern part, thick sequences of widespread stratified, deep water marine sediments were laid down. During final stages of regression shell-bearing deltaic sediments were deposited. Figure 11.5 shows the known and approximate extent of the Big Sea, and with the aid of isolines, gives an idea of the maximum elevation of the sea. Also indicated are a few locations of sediments containing shells that give amino acid ratios suggesting a pre-Sangamonian age. These determinations are crucial because they suggest that Thomsen Glaciation predates the Wisconsinan and further that the only glacial events that could be Wisconsinan are the Amundsen and Viscount Melville glaciations and the Sand Hills and Russel readvances.

The Big Sea was the most extensive marine inundation and it accordingly reflects the presence of a large ice load. Consequently it should be possible to correlate this well documented, high level sea with other high level seas in the arctic islands.

Glacial Lake Parker (Fig. 11.5) in the northeast was dammed between the ice front to the east and southeast and high ground to the west. The lake inundated extensive areas of the southern and eastern portion of the Devonian plateau. Bedrock surfaces were washed bare and fine grained glaciolacustrine sediments, first noted by Fyles (1962, p. 8), were laid down and still are preserved locally in most valleys that dissect the plateau. The initial outlet, a well defined, deeply incised channel in fine grained Cretaceous sediments, was at an altitude of about 245 m on the divide between Thomsen River and Parker River basins. What happened to the water

on the western side of the divide is not clear because ice probably occupied Thomsen valley; perhaps water drained into glacial Lake Dissection and then found a way to the sea along the ice margin.

The ice likely retreated, in an eastward direction, glacial Lake Parker followed the ice, draining through successively lower outlets and eventually emptied into Viscount Melville Sound.

Glacial Lake Dissection (Fig. 11.5) was a small lake dammed in a tributary by the Thomsen Valley ice lobe. Its outlet is not evident and may have been along the ice margin.

Water Bodies Associated with Amundsen Glaciation

The Sarfarssuk Lakes (Fig. 11.6) were small glacial lakes dammed between the Prince of Wales Lobe to the south and high ground to the north. These small, short-lived lakes drained eastward via tributaries of Thomsen River, possibly into Lake Ivitaruk discussed below. Other glacial lakes may have existed along the margin of the ice lobe in northeastern Banks Island, but they are not recognized easily since they would have inundated areas in most part previously occupied by glacial Lake Parker. For example, a glacial lake must have existed in the lower Parker River drainage basin when ice from the Prince of Wales Lobe stood in Viscount Melville Sound.

Glacial Lakes Masik, Rufus, and Raddi were dammed in Masik, Rufus, and Sachs River basins (Fig. 11.6) when the Thesiger Lobe of the Amundsen Glaciation stood in Thesiger Bay. Glacial Lake Rufus inundated the lower Rufus River basin up to about 260 m and probably drained eastward into Nelson River. Glacial Lake Masik inundated large parts of the Masik River and Atitok River basins up to about 230 m. Lake Masik drained northwards via a channel across the divide between Masik River and Sachs River basins, probably into a shallow glacial lake dammed in the Sachs River basin east of modern Raddi Lake. This shallow lake, glacial Lake Raddi, drained into the Kellett River system and thence into the Beaufort Sea.

Glaciolacustrine deltas were built into the southern portions of Lakes Rufus and Masik at the mouths of glacial meltwater channels of the Prince of Wales Lobe. The presence of these deltas is extremely important because they indicate without doubt that ice was present both in Thesiger Bay and over eastern Banks Island at the same time.

East Coast Submergence. Along the eastern coast of Banks Island (Fig. 11.6), from Nelson Head to near the northeastern tip of the island, a well defined continuous trimline cuts into the till deposited by the Prince of Wales Lobe. This trimline varies a few metres above and below 120 m, except in the upper Cardwell Brook and De Salis River basins where it is distinctly higher. The higher trimlines are thought to have been formed by glacial lakes dammed between the margin of the retreating Prince of Wales Lobe and higher ground to the north. Glacial Lake Cardwell (Fig. 11.6) in the upper Cardwell Brook drained westward at an elevation of about 245 m into Glacial Lake De Salis (Fig. 11.6) in the upper De Salis River. This glacial lake, standing at about 200 m, in turn drained north into the Big River drainage system.

Apart from the glaciolacustrine trimlines noted above, it is uncertain whether the 120 m trimline found elsewhere along eastern Banks Island (Fig. 11.6) is glaciolacustrine or marine. Along the east coast the till surface below 120 m has been wave washed (Fig. 11.3), but no distinct shore features such as raised beaches or deltas resulted. No shells have been found in the course of numerous foot traverses across the area. This problematic water body inundating the east coast to 120 m is named the East Coast Submergence, and its marine or glaciolacustrine origin is not specified.

A glacial lake could have been impounded by the ice as it retreated downslope, but it is difficult to explain the regularity of the trimline in such a situation because altitudinal variations in levels related to the ice front configuration would be expected. Alternatively the inundation could have been marine and could represent rapid uplift at the time of deglaciation. If this were the case, the

Table 11.1

Radiocarbon dates – Schuyter Point Sea

Site No. (see Fig. 11.6)	Laboratory Dating No.	Uncorrected Age (years B.P.)	$\delta^{13}C$	Corrected Age (years B.P.)	Dated Material	Location	Approximate Elevation[1] (m)	Geological Environment	Collector and Year of Collection	References
1	GSC-2545	11 100±100	+1.4	11 200±100	**Hiatella arctica**	72°02'15"N 120°15'45"W	21	Sublittoral fine sands	J-S. Vincent 1977	
2	GSC-2413	11 000±400	+1.5	11 000±400	**Hiatella arctica**	73°13'30"N 116°37'00"W	16	Poorly defined strandline developed on old (pre-Wisconsinan) marine silts	J-S. Vincent 1975	
3	GSC-49	10 920±100			**Hiatella arctica**	71°24'N 121°26'W	15-18	Surface of gullied clay	J.G. Fyles 1960	Dyck and Fyles (1963)
4	GSC-1437	10 600±270			**Hiatella arctica**	73°46'N 116°02'W	85-88	Surface of possibly icethrust fine marine sediments	D.M. Barnett 1970	Lowdon and Blake (1973)
5	GSC-2633	10 500±110			**Hiatella arctica**	72°02'50"N 120°14'15"W	10	Sublittoral fine sands	J-S. Vincent 1977	
6	GSC-2099	10 200±170	-0.4	10 200±170	**Hiatella arctica**	73°00'50"N 117°33'00"W	8	Poorly stratified sublittoral silts and sands	J-S. Vincent 1974	

[1]Elevations measured by aneroid barometer.

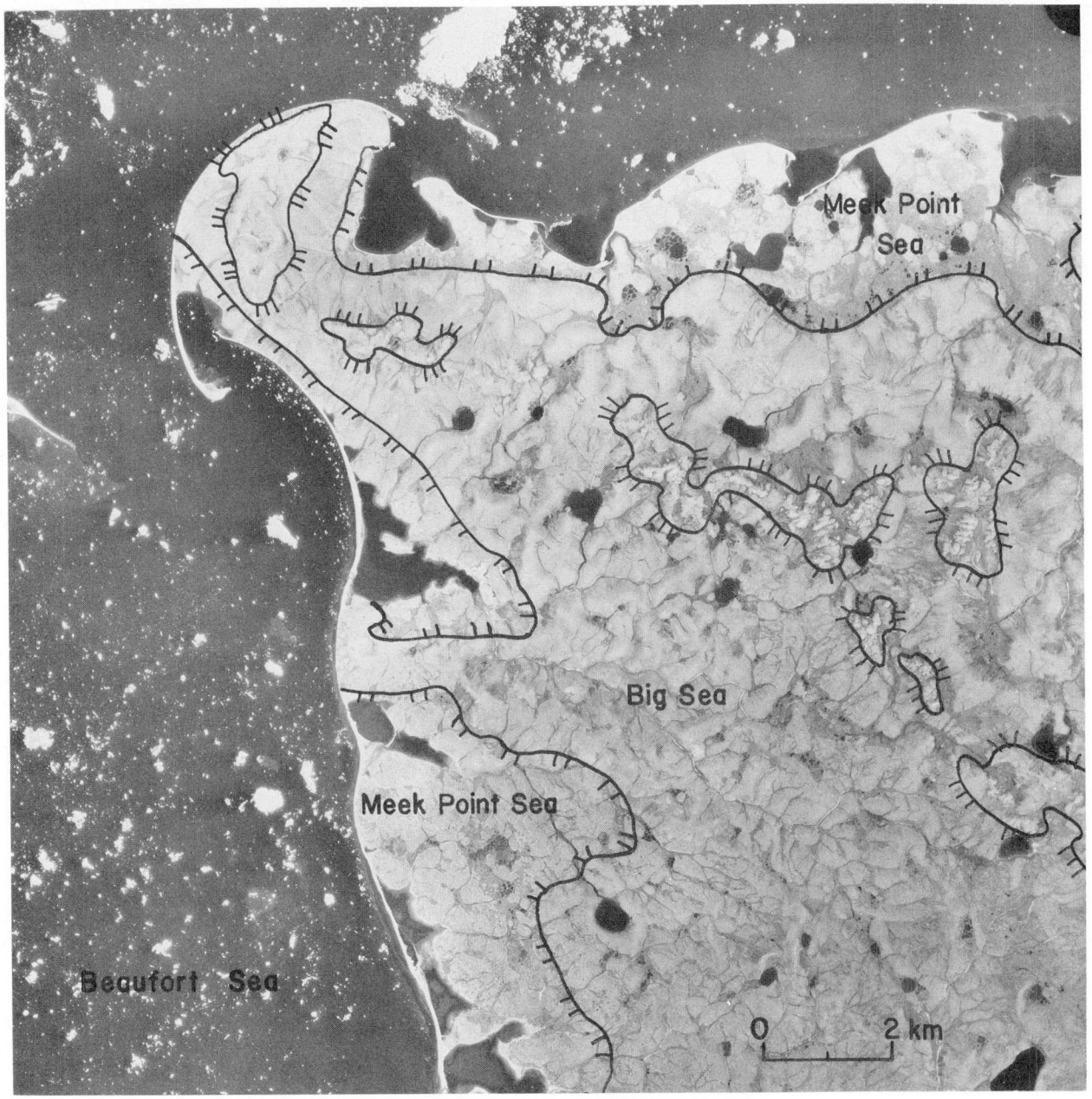


Figure 11.7. Air photograph of an area on the west coast just south of Storkerson Bay showing the upper trimline of the Big Sea (⩚⩛) and of the Meek Point Sea (⩚⩚). The area is underlain by Beaufort Formation sands and gravels and by a veneer of deposits from the Banks Glaciation. Apart from small islands that protruded out of the Big Sea, the whole area has been extensively washed and reworked by the seas. Part of photograph A17053-15, National Air Photographic Library, Department of Energy, Mines and Resources, Ottawa.

East Coast Submergence either could represent a higher Schuyter Point Sea (discussed below) or could be a separate marine event associated with the Amundsen deglaciation. Of the three hypotheses, the last is favoured.

Schuyter Point Sea. Along the east coast (Fig. 11.6), below approximately 25 m, prelittoral sediments, locally shell-bearing, and poorly developed raised beaches occur (Fig. 11.3). The body of water responsible for the deposition of these sediments is called the Schuyter Point Sea; a list of the sites where samples were collected and dated by the radiocarbon method is given in Table 11.1. The dates generally indicate a progressive lowering of relative sea level between 11 200 and 10 200 years ago. Site 4 is problematic because of its high altitude; the shells may have been emplaced here by ice thrusting related to the Russell Readvance.

The Schuyter Point Sea, whose sediments overlie till developed by the Prince of Wales Lobe of the Amundsen Glaciation, likely did not abut an ice margin on Banks Island. As suggested previously, it may represent a later phase of the East Coast Submergence or it may be a totally separate event resulting from glacio-isostatic depression by Late Wisconsinan ice that did not reach Banks Island.

Water Bodies Associated with Viscount Melville Glaciation (=Amundsen Glaciation?)

Glacial Lake Ballast. As the M'Clure Lobe stood against the northern coast of Banks Island, lakes were dammed in valleys to the south. Glacial Lake Ballast (Fig. 11.6) drowned a portion of Ballast Brook valley to over 90 m elevation. The presence of a lake in this area was first established by Fyles (1969, p. 195) and was discussed in more detail by French (1972). The initial drainage of the lake was probably towards Beaufort Sea via a channel on the west side of Ballast Brook valley. As the ice retreated northward a lower outlet, at approximately 60 m, initially cut as a meltwater channel, came into operation. Glacial Lake Ballast drained into M'Clure Strait when ice had retreated to a more northerly position.

Glacial Lake Ivitaruk. To the east of Lake Ballast, glacial Lake Ivitaruk (Fig. 11.6) also was created by the M'Clure Lobe. This lake inundated, to an elevation of about 90 m, extensive areas of the north coast as well as a major portion of Thomsen River drainage basin. Lakes Ballast and Ivitaruk were not initially in contact with each other, since the portion of the ice margin east of Ballast Brook prevented contiguity. The lowest point where the water could have been evacuated is situated on the divide between Thomsen and Bernard rivers at an altitude of about 90 m along a stream informally named "Ivitaruk" River. At the head of the "Ivitaruk" a well defined channel, used as a meltwater channel during the Banks and/or Thomsen glaciations, exists and is assumed to have served as the outlet for the glacial lake. As the M'Clure Lobe receded, the contiguity of glacial Lake Ballast and Lake Ivitaruk was made possible. At this time the level of Lake Ivitaruk dropped about 30 m since it was by now able to use the outlet of Lake Ballast at 60 m elevation. Final drainage to M'Clure Strait occurred as the ice retreated to a sufficiently northerly position.

Meek Point Sea

Craig and Fyles (1960, p. 10) noted that a low marine shoreline occurred locally on the west coast of Banks Island. This shoreline (Fig. 11.6) now has been mapped, and the body of water responsible for it has been termed the Meek Point Sea. The shoreline, usually marked by a well developed scarp (Fig. 11.7) and locally by poorly developed beach ridges, stands around 15 to 20 m. Patches of fine grained sediments also were found seaward of the shoreline, but no shells were observed in them.

The Meek Point Sea has been correlated tentatively with the Amundsen Glaciation (Fig. 11.6), but its age is not known precisely. The Meek Point Sea is obviously younger than the Big Sea associated with the Thomsen Glaciation and its trimline appears to cut glacial deposits of the M'Clure Lobe. This same shoreline also may truncate glacial sediments of the Thesiger Lobe west of Sachs Harbour. These relationships make the age of the submergence equal to or younger than that of the Amundsen Glaciation. Moreover, the morphology of its landforms suggests a longer period of mass wasting compared to that on the area submerged by the Schuyter Point Sea. It is hypothesized, therefore, that the Meek Point Sea correlates with the East Coast Submergence and that both bodies of water existed during the retreat of Amundsen ice, possibly in Early or Middle? Wisconsinan time. The Schuyter Point Sea then would be a separate transgression of Late Wisconsinan age that occurred in an ice-free area. Incidentally, this situation would duplicate that on southern Somerset Island described by Dyke (1978).

Conclusion

An attempt has been made to identify a sequence of Quaternary glaciations and inundations from the complex morphostratigraphy of Banks Island. Correlations are tentative and are likely to be altered as new data become available.

Banks Island appears to record more major episodes spanning a longer time period than other areas in the Canadian Arctic, hence the implications on the regional Quaternary history are numerous. It should be possible to define reference stratigraphic units which could be used to correlate events controlled by the mainland ice sheets with those occurring elsewhere in the Arctic.

Acknowledgments

The Polar Continental Shelf Project provided logistical support during 1974, 1975, and 1977. Stimulating discussions were held on problems relating to the Quaternary geology of Banks Island with various colleagues, particularly J.G. Fyles, D.R. Grant, and A.S. Dyke. Thanks are extended to D.R. Grant and R.J. Fulton for their helpful comments on the manuscript. G.H. Miller (University of Colorado) supplied amino acid analyses on marine shells.

References

Craig, B.G. and Fyles, J.G.
1960: Pleistocene geology of Arctic Canada; Geol. Surv. Can., Paper 60-10, 21 p.

Dyck, W. and Fyles, J.G.
1963: Geological Survey of Canada radiocarbon dates I and II; Geol. Surv. Can., Paper 63-21, 31 p.

Dyke, A.S.
1978: Glacial history of and marine limits on southern Somerset Island, District of Franklin; in Current Research, Part B, Geol. Surv. Can., Paper 78-1B, p. 218-223.

French, H.M.
1972: The proglacial drainage of northwest Banks Island; The Musk-Ox, Publ. no. 10, p. 26-31.

Fyles, J.G.
1962: Physiography; in Banks, Victoria and Stefansson Islands, Arctic Archipelago; Geol. Surv. Can., Mem. 330, p. 8-17.

1969: Northwestern Banks Island, District of Franklin; in Report of Activities, Part A, Geol. Surv. Can., Paper 69-1A, p. 194-195.

Hobbs, W.H.
1945: The boundary of the latest glaciation in Arctic Canada; Science, v. 101, no. 2631, p. 549-551.

Jenness, J.C.
1952: Problem of glaciation in the western islands of Arctic Canada; Geol. Soc. Am., Bull., v. 63, p. 939-952.

Lowdon, J.A. and Blake, W., Jr.
1973: Geological Survey of Canada radiocarbon dates XIII; Geol. Surv. Can., Paper 73-7, 61 p.

Prest, V.K., Grant, D.R., and Rampton, V.N.
1968: Glacial Map of Canada; Geol. Surv. Can., Map 1253A.

Vincent, J-S.
1978a: Lithostratigraphy of the Quaternary sediments east of Jesse Bay, Banks Island, District of Franklin; in Current Research, Part A, Geol. Surv. Can., Paper 78-1A, p. 189-193.

1978b: Surficial geology of Banks Island, District of Franklin, N.W.T.; Geol. Surv. Can., Open File 577 (NTS map areas 88F, 97G,H, 98A-F, pts. 88B-D).

12.

OXFORDIAN-KIMMERIDGIAN DINOFLAGELLATE ASSEMBLAGE, RINGNES FORMATION, ARCTIC CANADA

Project 500029

J.T. Tan and L.V. Hills[1]
Institute of Sedimentary and Petroleum Geology, Calgary

Tan, J.T. and Hills, L.V., Oxfordian-Kimmeridgian dinoflagellate assemblage, Ringnes Formation, Arctic Canada; in Current Research, Part C, Geol. Surv. Can., Paper 78-1C, p. 63-73, 1978.

Abstract

Dinoflagellates can be utilized to distinguish the Ringnes Formation from underlying and overlying formations in the Sverdrup Basin and to correlate it with its equivalents in the subsurface. ***Psaligonyaulax dualis, Horologinella spinosigibberosa, Pareodinia borealis, Sirmiodinium grossii, Lanterna saturnalis*** *and* ***Pareodinia capillosa*** *are characteristic of the Ringnes Formation and are indicative of a late Oxfordian to Kimmeridgian age. The latter two species occur only in the upper part of the formation and extend into the overlying formation.*

Introduction

Balkwill et al. (1977) erected the Ringnes Formation for a widespread concretionary shale which outcrops in the Sverdrup Basin. The formation is distinguishable from the underlying Savik and overlying Deer Bay formations by the presence of large calcitic and sideritic mudstone concretions (1.5 – 2 m in diameter) and a lighter toned aspect in outcrop. The basal beds are defined as the lowest occurrence of large yellow buff concretions which lie conformably on the Savik Formation. The formation top is placed at the uppermost limit of the concretionary shale which may be gradational over a few metres into the Deer Bay Formation. The formation is underlain by the Wilkie Point Formation and overlain by the Mould Bay Formation on Prince Patrick Island. Marine macrofossils (mainly **Buchia**) and foraminifers indicate a late Oxfordian to Kimmeridgian age for the formation.

Because of the wide areal extent of this unit in the surface sections, its identification is of major importance for correlations in the subsurface. Correlation by lithologic criteria and macrofossils in the subsurface is hampered because both are destroyed by drilling. Furthermore, the unit is not distinct on electric logs. Therefore, a detailed dinoflagellate study was undertaken in order to characterize it palynologically and to ascertain if it could be distinguished from underlying and overlying units by this technique.

Upper Jurassic palynology of the Sverdrup Basin has been discussed by Johnson and Hills (1973), who described Toarcian to Volgian dinoflagellate assemblages from the eastern Sverdrup Basin. Brideaux and Fisher (1976) described the taxonomy, biostratigraphy, and geographic distribution of the Upper Jurassic to lowermost Cretaceous dinoflagellate assemblages of northern Canada and the Sverdrup Basin. Pocock (1976) presented a preliminary dinoflagellate zonation of the uppermost Jurassic to lowermost Cretaceous (Tithonian to Albian) applicable in part to the area. Van Helden (1977) correlated Toarcian-Bajocian dinoflagellate assemblages with ammonite faunas from the Wilkie Point Formation on Prince Patrick Island.

These papers provided an overview of the taxonomy and biostratigraphy of dinoflagellates within the area. However, at the time of their publication the Ringnes Formation had not been defined and therefore no attempts have been made previously to identify dinoflagellates which may be useful in its identification in the subsurface.

To ascertain the dinoflagellate biostratigraphy of the Ringnes Formation, four sections were measured and sampled (Fig. 12.1, 12.2). These included one section on Mackenzie King Island (77°48'N, 112°20'W), two on Prince Patrick (76°29'N, 117°45'W; 77°34'N, 118°30'W) and one on Melville Island (76°22'N, 115°30'W). On Mackenzie King Island 13 samples were taken from the Ringnes Formation which is 45 m thick (Fig. 12.2, 12.3). Four samples were taken from the Melville Island section where the formation is approximately 35 m thick. Eleven samples were taken on the eastern side of Intrepid Inlet where the formation (65 m thick) is underlain by white sand of the Wilkie Point Formation and overlain by the Mould Bay Formation. In addition, samples were taken from the underlying Savik and Wilkie Point formations and the overlying Deer Bay and Mould Bay formations in order to characterize biostratigraphic changes if they occurred.

Macrofossils collected during this study included **Buchia concentrica** (Sowerby), **Cardioceras** sp., **Rasenia** sp. aff. **R. orbignyi** (Tornquist), gastropods, belemnites and bivalves. According to H. Frebold and J.A. Jeletzky (unpublished GSC reports) these fossils are indicative of an Oxfordian to Kimmeridgian age. Their stratigraphic occurrence is indicated on Figures 12.3 to 12.6.

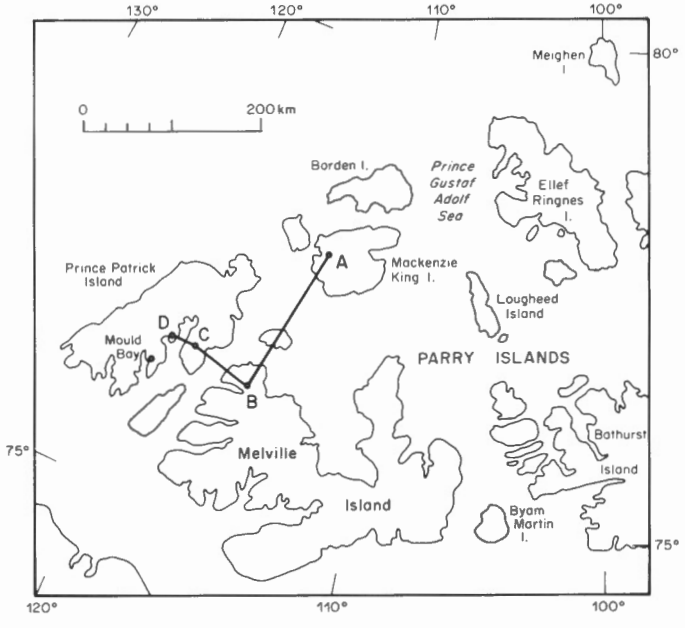


Figure 12.1. Index map of the western Arctic Islands showing the location of measured and sampled sections.

[1] Department of Geology, The University of Calgary, Calgary, Alberta, T2N 1N4.

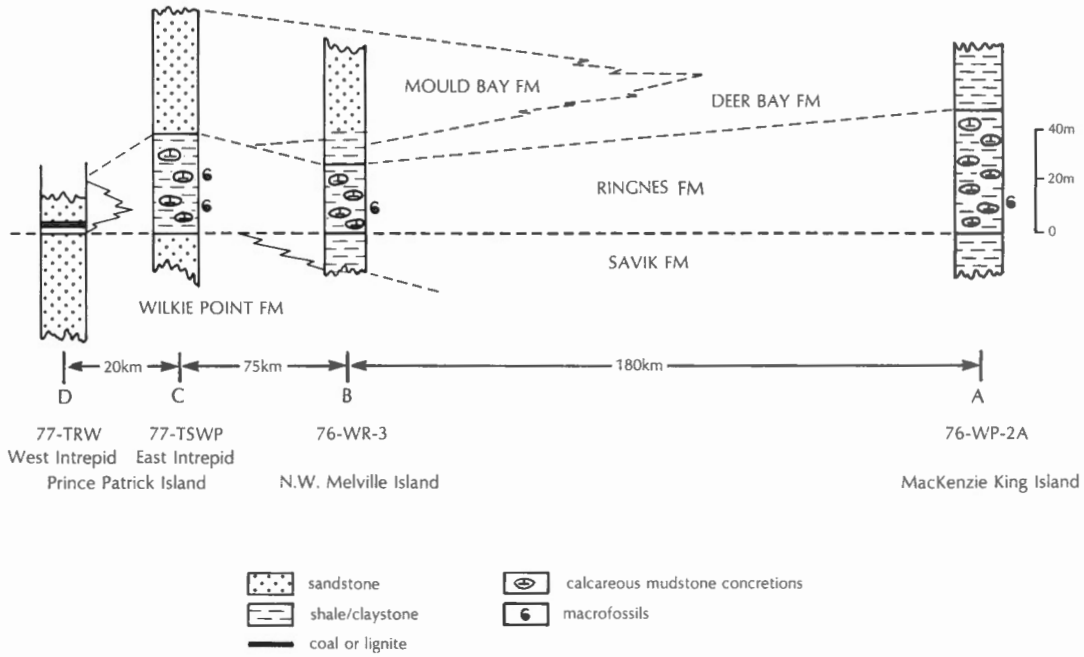


Figure 12.2. Correlation of Ringnes Formation, western Arctic Islands. Note the upper part of the Wilkie Point Formation, west Intrepid Inlet section is correlated with the Ringnes Formation on the basis of dinoflagellates.

Dinoflagellate Biostratigraphy

The distributions of dinoflagellates encountered in this study are summarized on Figures 12.3 to 12.6. Each formation is characterized by its own assemblage.

The Savik Formation is characterized by the following taxa: **Gonyaulacysta jurassica** (Deflandre, 1938) Norris and Sarjeant, 1965; **Gonyaulacysta jurassica** subsp. **longicornis** (Deflandre, 1938) Lentin and Williams, 1973; **Gonyaulacysta cladophora** (Deflandre, 1938) Dodekova, 1967; **Acanthaulax** sp.; **Meiourogonyaulax** sp.; and **Tenua pilosa** (Ehrenberg, 1843) Sarjeant, 1968. Most of these disappear at the base of the Ringnes Formation.

The important taxa for identification of the Ringnes Formation are: **Psaligonyaulax dualis** Brideaux and Fisher, 1976; **Pareodinia borealis** Brideaux and Fisher, 1976; **Sirmiodinium grossii** Alberti, 1961, emend, Warren, 1973; **Pareodinia ceratophora** Deflandre, 1947, emend, Gocht, 1970; **Horologinella spinosigibberosa** Brideaux and Fisher, 1976; **Pareodinia capillosa** Brideaux and Fisher, 1976; and **Lanterna saturnalis** Brideaux and Fisher, 1976.

The Deer Bay (= Mould Bay) Formation is characterized by: **Glabridinium apatelum** (Cookson and Eisenack) Brideaux, 1977; **Sirmiodinium grossii; Gonyaulacysta longicornis; Prolixosphaeridium** sp.; and the continued occurrence of: **Lanterna saturnalis, Pareodinia borealis,** and **Pareodinia capillosa.**

Age and Correlation

The macrofossil evidence for the age of the Ringnes Formation has already been stated and therefore the following discussion is restricted to dinoflagellate evidence. According to Brideaux and Fisher (1976, p. 29, Fig. 13) the lowest occurrence of the **borealis** assemblage, characterized by the presence of **Psaligonyaulax dualis, Pareodinia borealis** and **Horologinella spinosigibberosa,** is of late Oxfordian age. The presence of **Lanterna saturnalis, Pareodinia capillosa,** and **Gonyaulacysta longicornis** at the top of the Ringnes Formation is indicative of middle to late Kimmeridgian age. Therefore, the evidence indicates that the Ringnes Formation is of late Oxfordian to early Kimmeridgian age on Mackenzie King and Melville islands, and late Oxfordian to late Kimmeridgian age on east Intrepid Inlet, Prince Patrick Island.

Strata from the upper part of a unit mapped as Wilkie Point on west Intrepid Inlet, Prince Patrick Island by Tozer and Thorsteinsson (1964) contain **Psaligonyaulax dualis, Sirmiodinium grossii, Horologinella spinosigibberosa, Pareodinia borealis, P. ceratophora,** and **P. ceratophora** subsp. **scopaeus** (Sarjeant) Lentin and Williams, indicating it can be correlated on the basis of these dinoflagellates to the Ringnes Formation (Fig. 12.2, 12.6).

Figure 12.7 (modified from Brideaux and Fisher, 1976) illustrates that the characteristic dinoflagellates of the Ringnes Formation are recognizable in the subsurface as the **borealis** assemblage and can be used for subsurface correlation in the Sverdrup Basin.

Species List and Comments

The taxonomy of the dinoflagellates listed will be published at a later date.

1. **Acanthaulax** sp.

   Proximate cyst with a covering of spines on the periphragm. It occurs only in the Savik Formation, Mackenzie King Island.

2. **Chytroeisphaeridia chytroeides** (Sarjeant, 1962) Davey, 1977

   The type species **C. chytroeides** was re-examined by Davey (1977) and the archeopyle was found to be precingular in position instead of apical. **Chytroeisphaeridia chytroeides** encountered in this study appears to have an archeopyle formed by the loss of a single precingular paraplate. The archeopyle appears to be apical in some specimens because they are broken during preservation.

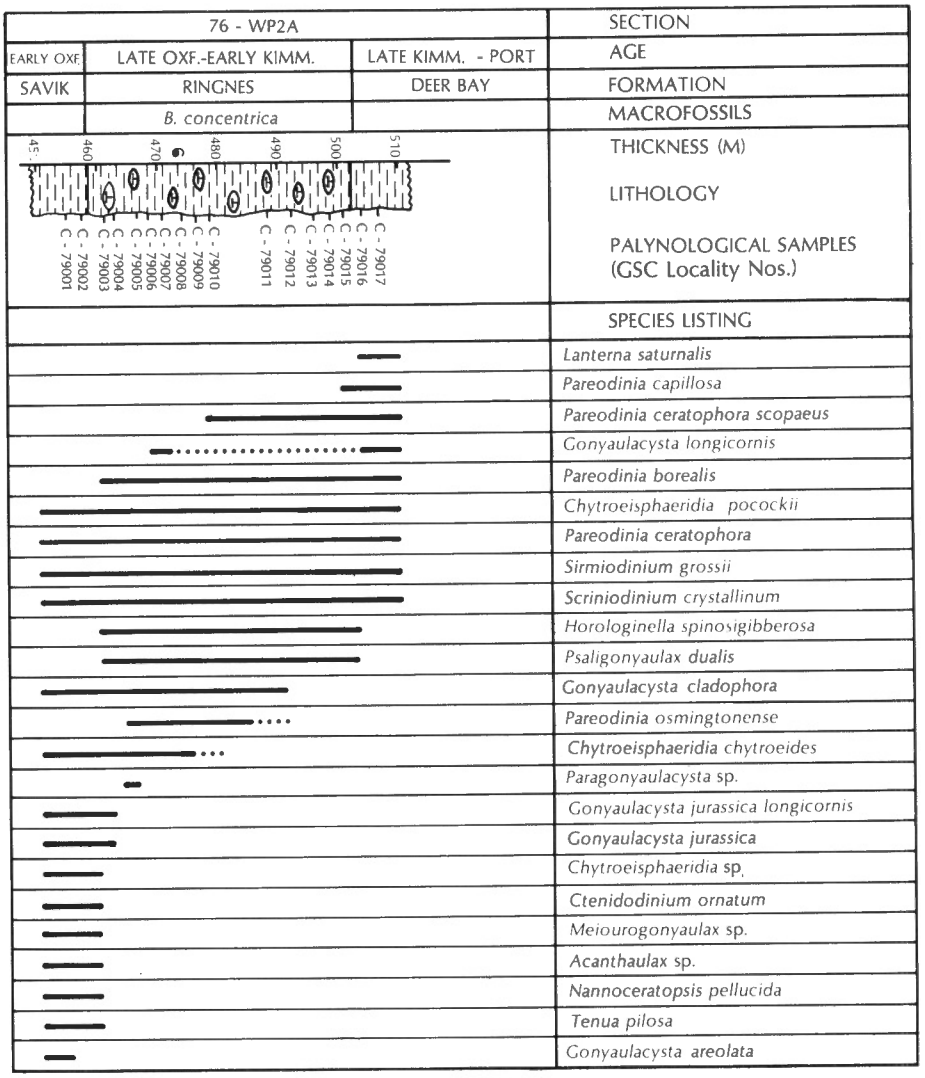


Figure 12.3

Lithology and stratigraphic distribution of dinoflagellates in the Mackenzie King Island section.

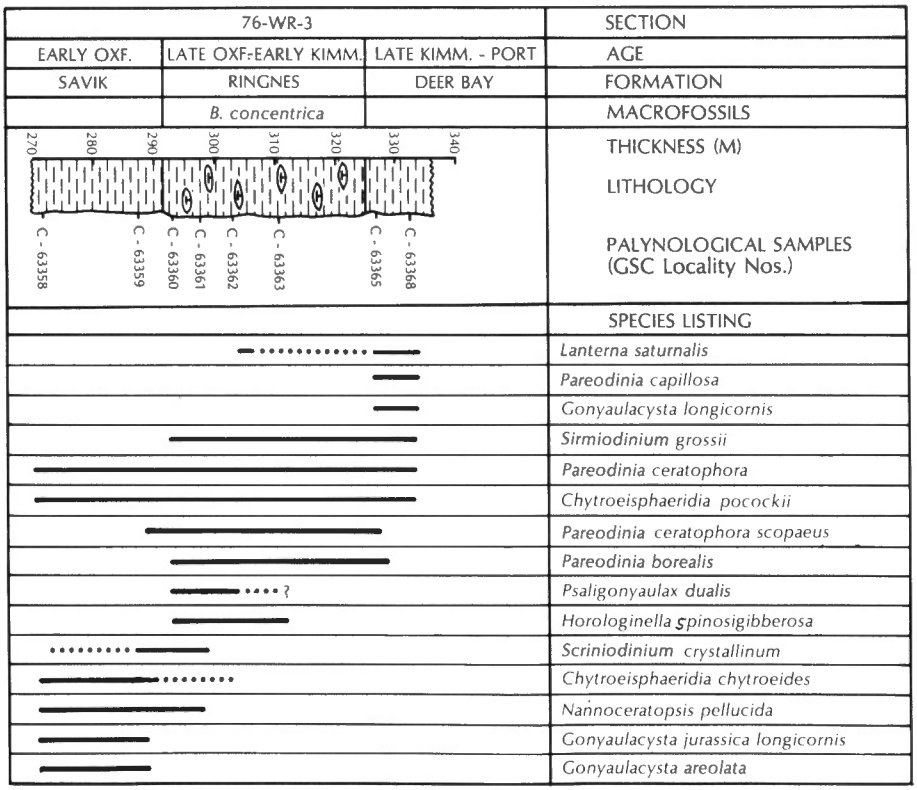


Figure 12.4

Lithology and stratigraphic distribution of dinoflagellates in the Melville Island section.

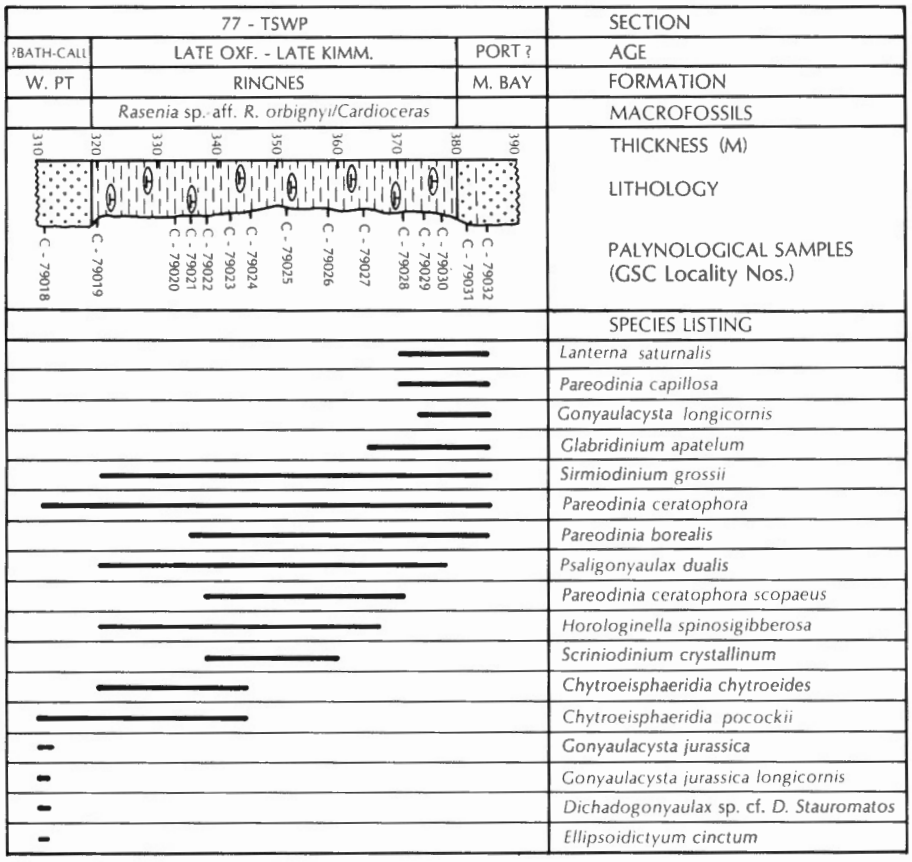


Figure 12.5

Lithology and stratigraphic distribution of dinoflagellates in the east Intrepid Inlet section, Prince Patrick Island.

3. **Chytroeisphaeridia pocockii** Sarjeant, 1968

4. **Chytroeisphaeridia** sp. (Plate 12.1, fig. 1, 2, 3)

   This proximate cyst is ovoidal to egg-shaped in outline, with a slight apical prominence. The antapex is broadly rounded and smooth. The periphragm is smooth, without any indication of paratabulation. Archeopyle precingular, with a distinct notch in some specimens, operculum free.

5. **Ctenidodinium ornatum** (Eisenack, 1935) Deflandre, 1938

   A common species occurring in the Savik Formation shale on Mackenzie King Island.

6. **Dichadogonyaulax** sp. cf. **D. stauromatos** Sarjeant, 1976

   Two specimens were observed with an epicystal archeopyle, and the parasutures marked by low ridges consisting of spines. **Dichadogonyaulax** Sarjeant is probably a junior synonym of **Ctenidodinium** Deflandre. The presence of paracingular crest in **Ctenidodinium** is not a sufficient character for generic differentiation.

7. **Ellipsoidictyum cinctum** Klement, 1960

8. **Glabridinium apatelum** (Cookson and Eisenack, 1960) Brideaux, 1977

9. **Gonyaulacysta areolata** Sarjeant, 1961

10. **Gonyaulacysta cladophora** (Deflandre, 1938) Dodekova, 1967 (Plate 12.1, fig. 4)

11. **Gonyaulacysta jurassica** (Deflandre, 1938) Norris and Sarjeant, 1965 (Plate 12.1, fig. 5)

    The upper limit of the range of **G. jurassica** in this area is early Oxfordian, being succeeded by **Psaligonyaulax dualis** which ranges from late Oxfordian to Kimmeridgian. An apical pericoel can be observed in most specimens of **G. jurassica.**

12. **Gonyaulacysta jurassica** subsp. **longicornis** (Deflandre, 1938) Lentin and Williams, 1973 (Plate 12.1, fig. 6)

    The subspecific character appears to be the longer apical horn, longer than 1/3 the cyst length. Apparently, this subspecies has a stratigraphic range similar to **G. jurassica.**

13. **Gonyaulacysta longicornis** (Downie, 1957) Sarjeant, 1969 (Plate 12.1, fig. 7)

14. **Horologinella spinosigibberosa** Brideaux and Fisher, 1976 (Plate 12.1, fig. 8)

    Specimens range in length from 30 µm to 58 µm and bear spiny to coarsely granulate ornamentation. An angular apical archeopyle can be seen in some specimens.

15. **Lanterna saturnalis** Brideaux and Fisher, 1976 (Plate 12.1, fig. 9, 12)

16. **Meiourogonyaulax** sp. (Plate 12.1, fig. 11)

    Proximate cyst, ovoidal in outline, with distinct paratabulation, 4', 0a, 6", 6c, 6‴, ?1p, 1⁗, outlined by low parasutural ridges. Paracingulum is helicoid, laevorotatory. Periphragm smooth to finely granulate. Apical archeopyle with operculum often attached. Dimensions: Maximum diameter; 76 to 92 µm (15 specimens).

17. **Nannoceratopsis pellucida** Deflandre, 1938, emend. Evitt, 1961 (Plate 12.1, fig. 10)

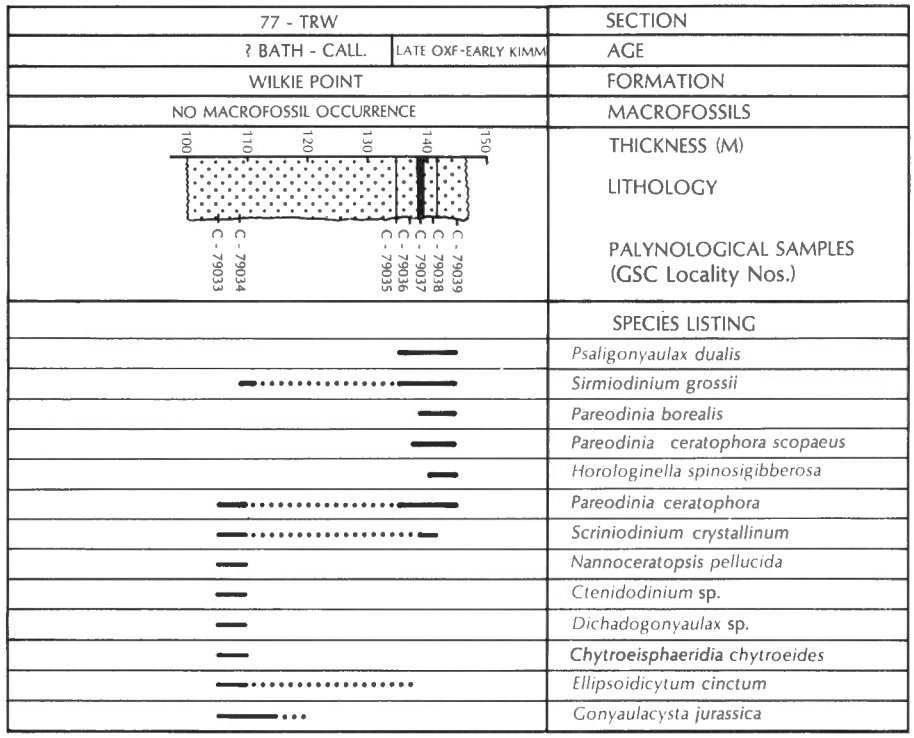


Figure 12.6

Lithology and stratigraphic distribution of dinoflagellates in the west Intrepid Inlet section, Prince Patrick Island.

18. **Paragonyaulacysta** sp. (Plate 12.2, fig. 1, 2)

    This species is similar to **P. calloviense** Johnson and Hills, in shape, size, and the possession of low parasutural ridges. The most obvious difference is in the character of their surface ornamentation. **P. calloviense** has a smooth periphragm, whereas **Paragonyaulacysta** sp. has granulate to very finely reticulate ornamentation. **Paragonyaulacysta** sp. has a third apical and a third anterior intercalary plate, with paratabulation formula of 3', 3a, 6", 6c, 6‴, 1p, 1⁗. The difference in the ornamentation may have specific significance or be the result of preservation, or due to environmental variations. According to Johnson and Hills (1973), **P. calloviense** occurs in lower Callovian sediments, but the presence of **Paragonaulacysta** sp. in the Ringnes Formation (late Oxfordian – early Kimmeridgian age) may indicate two possibilities:

    a) the specimens were reworked from eroded Callovian strata; or

    b) **Paragonyaulacysta** ranges into the Kimmeridgian. Because only three specimens were encountered, the writers suspect the former is probably true.

19. **Pareodinia borealis** Brideaux and Fisher, 1976 (Plate 12.2, fig. 5)

20. **Pareodinia capillosa** Brideaux and Fisher, 1976 (Plate 12.2, fig. 6)

    The hair like processes on the periphragm, characteristic of the species, are not present on some specimens. This may be due to preservation factors. However, Wiggins (1975, pl. 4, fig. 6-9) showed that other species of **Pareodinia** may also have hair like processes on the periphragm. One of the diagnostic features of **P. capillosa** in this study, is the prominent antapical prominence.

21. **Pareodinia ceratophora** Deflandre, 1947, emend. Gocht, 1970 (Plate 12.2, fig. 3)

22. **Pareodinia ceratophora** subsp. **scopaeus** (Sarjeant, 1972) Lentin and William, 1973 (Plate 12.2, fig. 4)

23. **Pareodinia** sp. cf. **P. osmingtonensis** (Sarjeant, 1962) Wiggins, 1975

24. **Psaligonyaulax dualis** Brideaux and Fisher, 1976 (Plate 12.2, fig. 7, 8)

    The stratigraphic succession of this species over **G. jurassica** is very important for correlation in early/late Oxfordian. Most specimens of **P. dualis** show distinct apical and antapical pericoels.

25. **Scriniodinium crystallinum** (Deflandre, 1938) Klement, 1960

26. **Sirmiodinium grossii** Alberti, 1961, emend. Warren, 1973 (Plate 12.2, fig. 9)

    The occurrence of **S. grossii** in the Savik Formation extends its range into the early Oxfordian or older. Previously, it was reported only from the Kimmeridgian (Brideaux and Fisher, 1976, p. 29, fig. 13). In these Jurassic specimens, the outline of the cyst is ovoidal to slightly pentagonal. Trilobate forms were not encountered. There may be an important correlation between variation in shape and stratigraphic distribution. Warren (1973) made a morphological distribution study from the uppermost Jurassic (Tithonian) to lower Cretaceous (Valanginian) forms and interpreted the oscillatory trends as being due to iterative evolution. From the observations in this study, we can make a generalization for the Sverdrup Basin that in the Oxfordian, most of the specimens are ovoidal and in the Portlandian, the dominant shape is pentagonal, with the trilobate forms characteristic of the lower Cretaceous.

27. **Tenua pilosa** (Ehrenberg, 1843) Sarjeant, 1968

PLATES

In the explanation of figures illustrated, the species name is followed by the GSC (ISPG) locality number, section number (e.g. 76-WP2A), slide number (e.g. T86-1/5), stage co-ordinates for Wild microscope No. M20-68036 at the Department of Geology, University of Calgary (e.g. 942/385), the GSC figured specimen number and magnification. P.C. refers to Phase Contrast illumination. Distance between vertical bars is 50 µm. The figured specimens are stored at the Institute of Sedimentary and Petroleum Geology, Calgary, Canada.

Plate 12.1

Figure 1. **Chytroeisphaeridia** sp. C-79001, 76-WP2A, T86-2/5, 812/465, GSC-58341, X400.

Figure 2. **Chytroeisphaeridia** sp. C-79001, 76-WP2A, T86-2/5, 664/342, GSC-58342, X400, P.C.

Figure 3. **Chytroeisphaeridia** sp. C-79001, 76-WP2A, T86-3/5, 818/354, GSC-58343, X700, P.C.

Figure 4. **Gonyaulacysta cladophora** (Deflandre) Dodekova, C-79001, 76-WP2A, T86-2/5, 734/289, GSC-58344, X400.

Figure 5. **Gonyaulacysta jurassica** (Deflandre) Norris and Sarjeant, C-79001, 76-WP2A, T86-2/5, 664/458, GSC-58345, X400.

Figure 6. **Gonyaulacysta jurassica** subsp. **longicornis** (Deflandre) Lentin and Williams, C-79001, 76-WP2A, T86-4/5, 910/319, GSC-58346, X400.

Figure 7. **Gonyaulacysta longicornis** (Downie) Sarjeant, C-79016, 76-WP2A, T93-3/5, 855/449, GSC-58347, X400.

Figure 8. **Horologinella spinosigibberosa** Brideaux and Fisher, C-79013, 76-WP2A, T91-4/5, 943/344, GSC-58348, X400.

Figure 9. **Lanterna saturnalis** Brideaux and Fisher, C-79017, 76-WP2A, T95-2/5, 816/357, GSC-58349, X400, P.C.

Figure 10. **Nannoceratopsis pellucida** Deflandre emend. Evitt, C-79001, 76-WP2A, T86-3/5, 920/364, GSC-58350, X400.

Figure 11. **Meiourogonyaulax** sp. C-79001, 76-WP2A, T86-2/5, 756/469, GSC-58351, X400.

Figure 12. **Lanterna saturnalis** Brideaux and Fisher, C-79017, 76-WP2A, T95-3/5, 800/368, GSC-58352, X400, P.C.

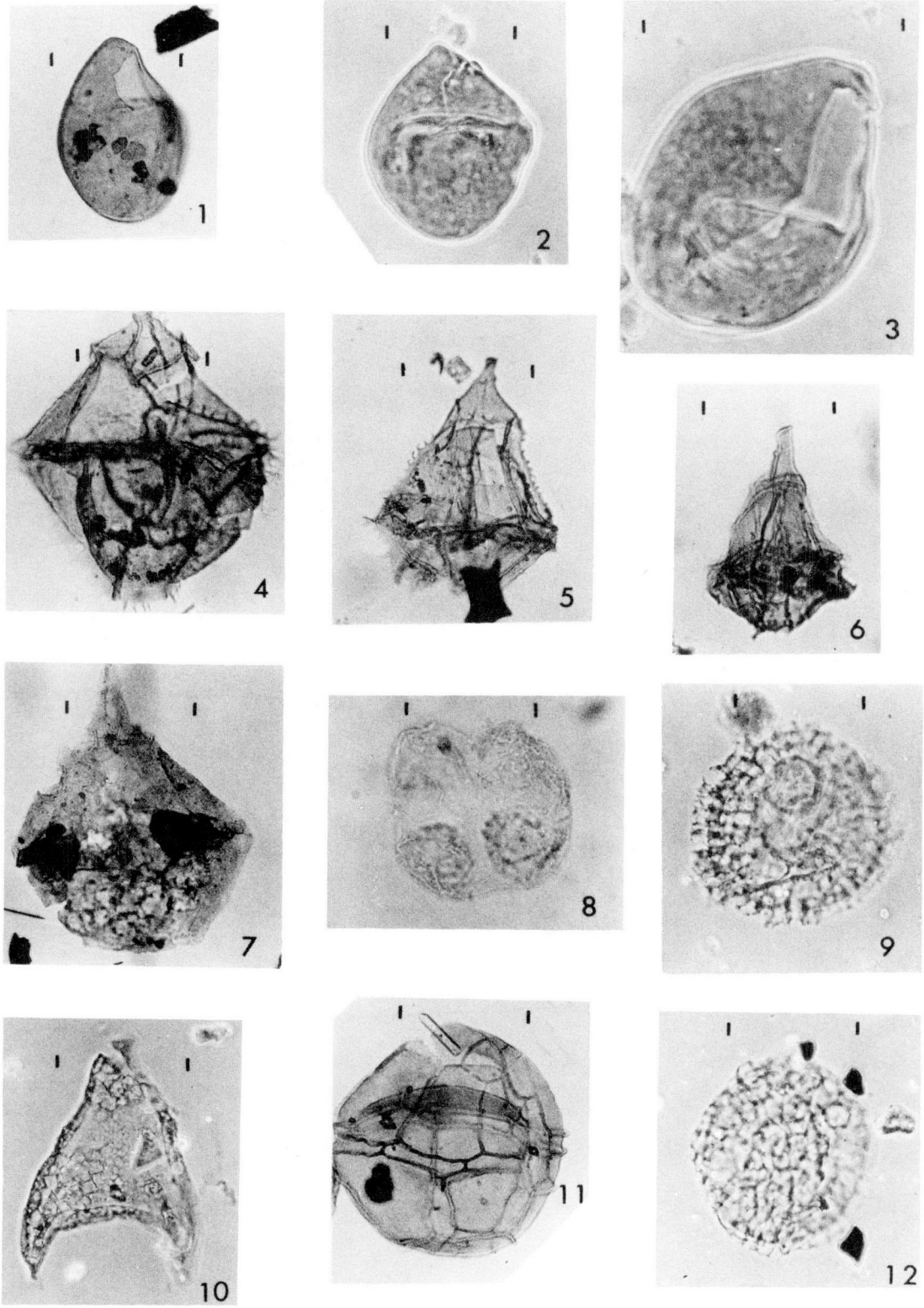

1
2
3
4
5
6
7
8
9
10
11
12

Plate 12.2

Figure 1,2. **Paragonyaulacysta** sp. C-79004, 76-WP2A, T26-1/5, 894/380, GSC-58353, X400 (Fig. 2 – P.C.).

Figure 3. **Pareodinia ceratophora** Deflandre emend. Gocht, C-79001, 76-WP2A, T86-2/5, 947/358, GSC-58354, X700.

Figure 4. **Pareodinia ceratophora** subsp. **scopaeus** (Sarjeant) Lentin and Williams, C-79002, 76-WP2A, T87-3/5, 756/345, GSC-58355, X700.

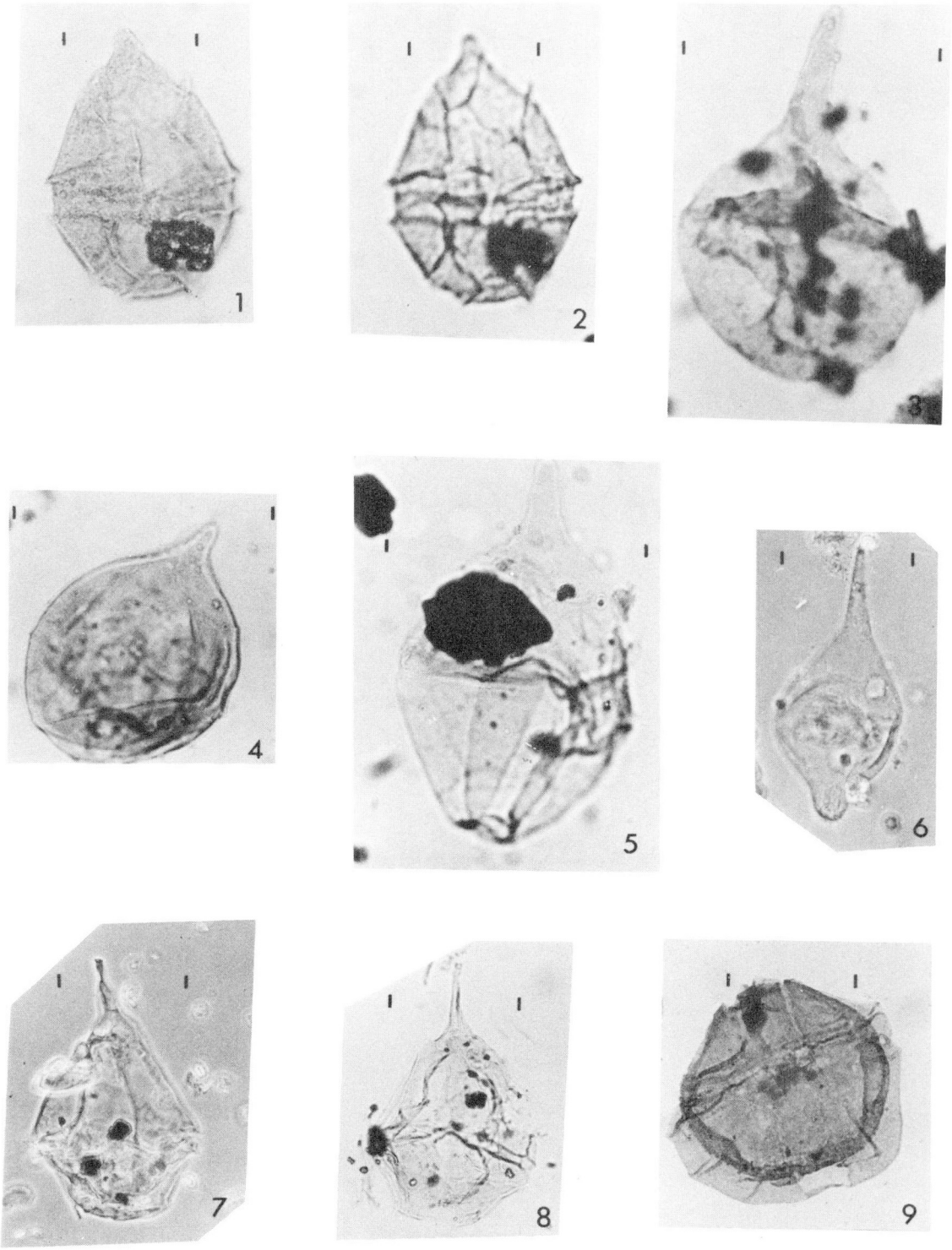
Figure 5. **Pareodinia borealis** Brideaux and Fisher, C-79013, 76-WP2A, T91-2/5, 732/447, GSC-58356, X700.

Figure 6. **Pareodinia capillosa** Brideaux and Fisher, C-79015, 76-WP2A, T92-4/5, 762/459, GSC-58357, X400, P.C.

Figure 7. **Psaligonyaulax dualis** Brideaux and Fisher, C-79013, 76-WP2A, T91-1/5, 782/352, GSC-58358, X400, P.C.

Figure 8. **Psaligonyaulax dualis** Brideaux and Fisher, C-79013, 76-WP2A, T91-1/5, 687/444, GSC-58359, X400.

Figure 9. **Sirmiodinium grossii** Alberti emend. Warren, C-79001, 76-WP2A, T86-5/5, 890/398, GSC-58360, X400.


1
2
3
4
5
6
7
8
9

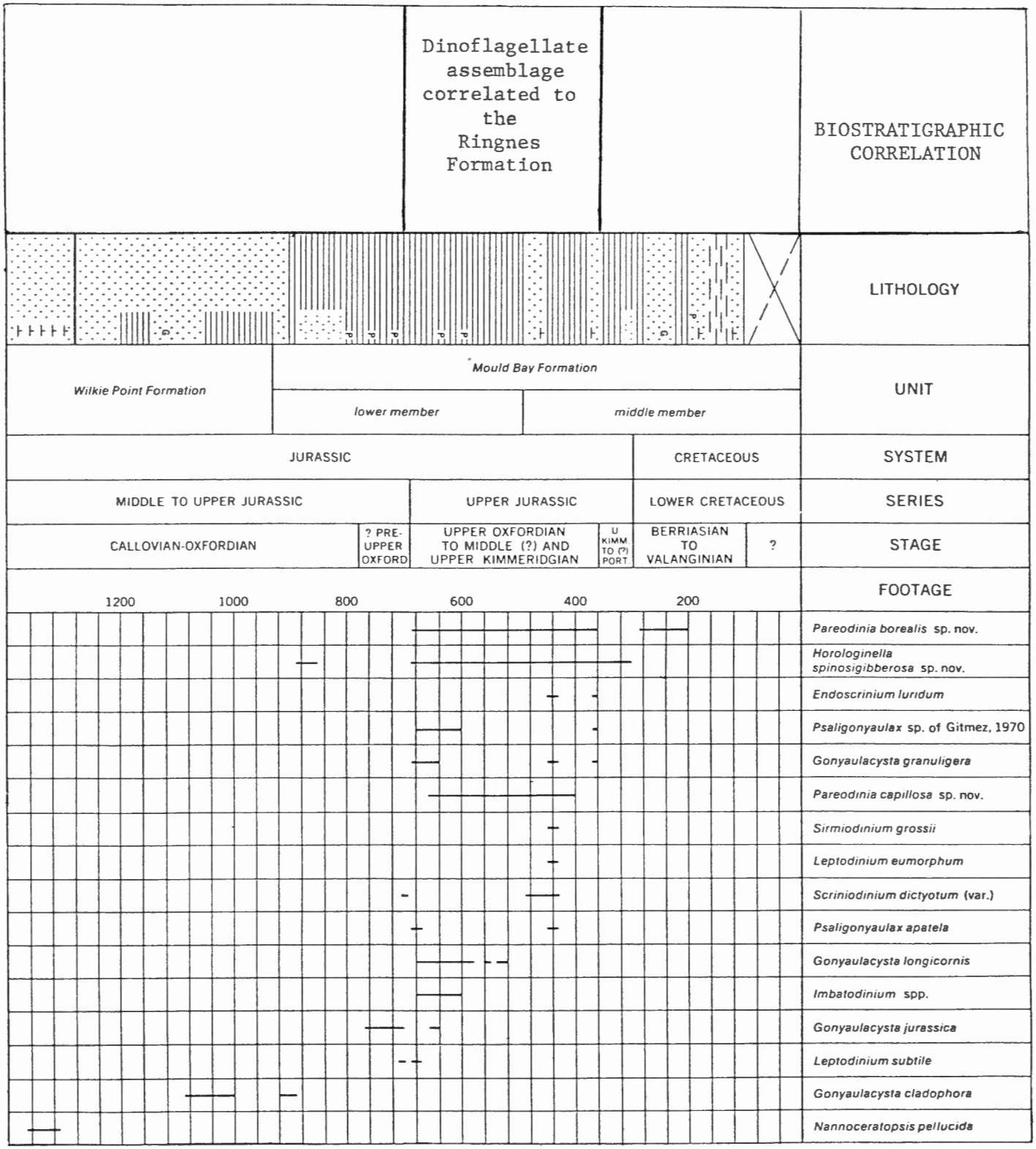


Figure 12.7. Dinoflagellate distribution in the Elf Jameson C-31 well with the dinoflagellate assemblage characteristic of the Ringnes Formation delineated (modified from Brideaux and Fisher, 1976).

Acknowledgments

The authors acknowledge the field assistance of H. Balkwill, T. Poulton, D. Braman and D. Wilson. D. Wilson collected the samples from Melville Island. H. Balkwill discussed the stratigraphy with the authors. E. Sangster and J. Keith prepared the palynological slides. Receipt of an Alberta Provincial Government Scholarship, the Ian N. McKinnon Memorial Fellowship, a Special Gulf Oil Scholarship and the Dean's Special Scholarship is gratefully acknowledged by the senior author. National Research Council Grant in Aid of Research and a Petroleum Aid to Education Grant to L.V.H. provided field and laboratory expenses for which the authors are grateful. W.W. Brideaux and N. Ioannides critically reviewed the manuscript.

References

Balkwill, H.R., Wilson, D.G., and Wall, J.H.
1977: Ringnes Formation (Upper Jurassic), Sverdrup Basin, Canadian Arctic Archipelago; Bull. Can. Pet. Geol., v. 25, no. 6, p. 1115-1144.

Brideaux, W.W. and Fisher, M.J.
1976: Upper Jurassic – Lower Cretaceous dinoflagellate assemblages from Arctic Canada; Geol. Surv. Can., Bull. 259, 53 p.

Davey, R.J.
1977: A re-appraisal of the genus **Chytroeisphaeridia** Sarjeant, 1962; Tenth Annual meeting, Am. Assoc. Stratigr. Palynol., (Abstract p. 9), Tulsa, Oklahoma.

Johnson, C.D. and Hills, L.V.
1973: Microplankton zones of the Savik Formation (Jurassic), Axel Heiberg, and Ellesmere Islands, District of Franklin; Bull. Can. Pet. Geol., v. 21, no. 2, p. 178-218.

Pocock, S.A.J.
1976: A preliminary dinoflagellate zonation of the uppermost Jurassic and lower part of the Cretaceous, Canadian Arctic, and possible correlation in the western Canada Basin; Geoscience and Man, v. XV, p. 101-114.

Tozer, E.T. and Thorsteinsson, R.
1964: Western Queen Elizabeth Islands, Arctic Archipelago; Geol. Surv. Can., Mem. 332, 242 p.

Van Helden, B.G.T.
1977: Correlation of microplankton assemblages with ammonite faunas from the Jurassic Wilkie Point Formation, Prince Patrick Island, District of Franklin; in Report of Activities, Part B, Geol. Surv. Can., Paper 77-1B, p. 163-171.

Warren, J.S.
1973: Form and variation of the dinoflagellate **Sirmiodinium grossi** Alberti, from the Upper Jurassic and Lower Cretaceous of California; J. Paleontol., v. 47, no. 1, p. 101-114.

Wiggins, V.D.
1975: The dinoflagellate family Pareodiniaceae: A discussion; Geoscience and Man, v. 11, p. 95-115.

13.

EARLY MIDDLE ORDOVICIAN CONODONTS OF NORTH ATLANTIC PROVINCE FROM NORTHEASTERN ELLESMERE ISLAND, ARCTIC CANADA

Project 500029

R.S. Tipnis
Institute of Sedimentary and Petroleum Geology, Calgary

Tipnis, R.S., Early Middle Ordovician conodonts of North Atlantic Province from northeastern Ellesmere Island, Arctic Canada; in Current Research, Part C, Geol. Surv. Can., Paper 78-1C, p. 75-78, 1978.

Abstract

An early Middle Ordovician North Atlantic conodont fauna from the Franklinian Miogeocline includes the first record of ***Pygodus*** *from Arctic Canada. The finding is consistent with the previously noted restriction of conodonts of the North Atlantic faunal Province to strata marginal to the North American craton.*

Introduction

Barnes (1974) pointed out the close similarity of the Ordovician conodont faunas of the Franklinian miogeocline to those of the Midcontinent. Nowlan (1976) supported this conclusion but recognized two incursions of North Atlantic conodonts; the first in the late Canadian to earliest Middle Ordovician when elements of **Oepikodus communis** (Ethington and Clark), became abundant, and the second in the Late Ordovician when elements of **Amorphognathus** and **Periodon** flourished.

This note provides evidence for the presence of North Atlantic forms in lower Middle Ordovician beds of the Franklinian miogeocline, and for the first time records the occurrence of **Pygodus** in the Canadian Arctic region.

Occurrence of Conodonts

The conodont fauna under consideration was recovered from samples collected from Judge Daly Promontory (Fig. 13.1), about 10 km east of the head of Ella Bay at 81°05.7'N, 69°24.3'W (UTM Zone 19 X; 9903800 N, 493200 E) by H.P. Trettin who reports as follows:

"The conodonts occur 16 to 32 m above the base of a 40 m thick unit that is composed mainly of massive lime wackestone with minor amounts of slaty, silty and argillaceous lime mudstone. The wackestone contains abundant echinoderm fragments and lesser amounts of micritized or recrystallized ostracodes and bryozoans; coated grains and peloids are also common.

"The limestone overlies the Hazen and underlies the Imina, two formations that normally succeeded each other in this region without intervening carbonates. The Hazen Formation is composed of resedimented carbonate deposits ranging in grade from lime mudstone to boulder conglomerate and dark grey mudrocks and radiolarian chert beds both containing a sparse graptolitic fauna. The formation was deposited in progressively deeper slope and bottom environments of the Hazen Trough. The fossil locality lies close to the southeastern facies boundary of the formation where it grades into shelf carbonate deposits of the miogeocline. The Imina Formation consists of clastic sediments with flysch-like primary structures and was deposited by sediment gravity flows in submarine fan and bottom environments of the Hazen Trough.

"Fossil collections from nearby other localities indicate that the base of the Imina Formation is close to the Ordovician-Silurian boundary in this general area. Graptolites of the late Ashgillian **Dicellograptus ornatus complanatus** Zone were found in uppermost parts of the Hazen Formation in the vicinity of Ella Bay and St. Patrick Bay, Archer Fiord, 11 km to the west and 118 km to the northeast respectively (unpub. identifications by B.S. Norford and J. Riva, 1977). About 8 km to the southeast (vicinity of section 1 of Kerr, 1968), where the Imina Formation oversteps the miogeoclinal carbonate succession, the index coral **Bioghornia** sp. of Ashgillian age occurs in the upper part of the latter. The oldest graptolites from the Imina Formation, which is very poor in autochthonous fossils, generally are not older Llandoverian (e.g. **Cyrtograptus canadensis** Jackson and Etherington and **Stomatograptus** sp. cf. **S. grandis** (Suess) from Caledonian Bay, Cañon Fiord, etc.; Trettin, in press). The lowermost part of the Hazen Formation at Ella Bay is dated as late Early Cambrian on the basis of **Olenellus** sp. (unpub. identif. by W.H. Fritz, 1977).

"The occurrence of a shelf-type limestone unit with echinoderms, bryozoans and Middle Ordovician conodonts between these two formations is anomalous with respect to age, lithology, and depositional environment. A fault relationship can probably be ruled out but field and laboratory observations are compatible with the hypothesis that the limestone originally was deposited in an outer shelf environment of the miogeocline and transported into the Hazen Trough as part of an extensive submarine slide in a northwestward direction. Age and lithology are compatible with derivation from the Eleanor River Formation (cf. Kerr, 1968, Section 1). Although it appears that the slide was emplaced just prior to the onset of flysch deposition in the latest Ordovician or Early Silurian, the underlying strata are not necessarily of that age because they probably were structurally disturbed by the slide.

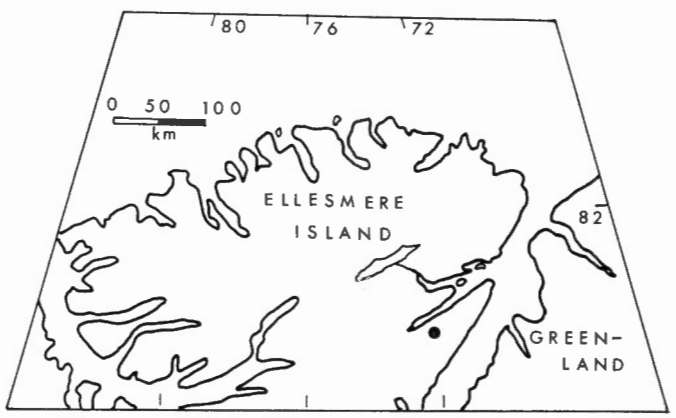
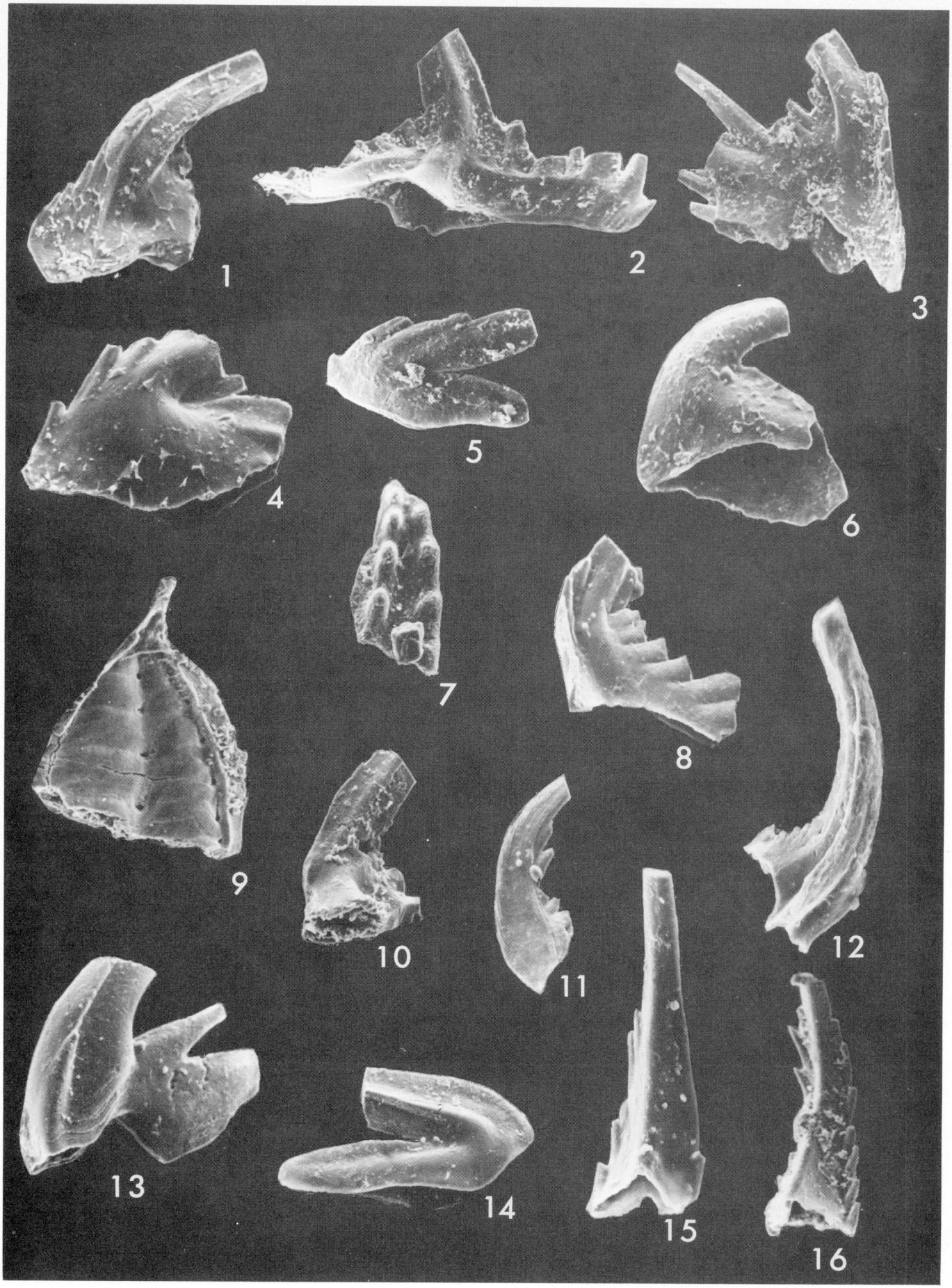


Figure 13.1. Map of northern Ellesmere Island, Arctic Canada, with the black dot indicating the location of samples.


1
2
3
4
5
6
7
8
9
10
11
12
13
14
15
16

"A problem with this interpretation is that most submarine slides known from the Franklinian Geosyncline are of about the same age as the enclosing strata, but there are exceptions. The Lower Devonian Svartevaeg Formation of northern Axel Heiberg Island, for example, a deep-water deposit composed mostly of proximal mass flow deposits and volcanics, includes a large limestone block with a shelf fauna of Early or Middle Silurian age (Trettin, 1969, p. 25). The field investigation of the postulated slide has not yet been completed".

Conodont Fauna

Plate 13.1 illustrates some of the North Atlantic Province conodonts in the collection studied. Only the more significant taxa are included here, namely the multielement taxa **Pygodus** sp. (7), **Periodon aculeatus** Hadding (15) and **Phragmodus** sp. (3) and the form taxa **"Tetraprioniodus"** cf. **"T." lindstroemi** Sweet and Bergström (1), **"Roundya" pyramidalis** Sweet and Bergström (3), **"Belodina" monitorensis monitorensis** Ethington and Schumacher (2), **"Oistodus" venustus** Stauffer (5) and **"O."** sp. aff. **"O." nevadensis** Ethington and Schumacher (1). (The figures in brackets indicate the number of specimens recovered.)

Plate 13.1

(All magnifications are approximately X 200 unless otherwise stated)

All illustrated material comes from GSC collection C-74618 unless otherwise noted separately. Locality of the samples is NTS-120 C, UTM-19X, 900300 mN; 493200 mE. Specimens stored in the GSC Invertebrate Type Collection, Ottawa.

Figures 1-5. **Periodon aculeatus** Hadding. 1. Lateral view, cladognathiform element, GSC 58226. 2. Lateral view, prioniodiniform element, GSC 58227. 3. Lateral view, ligonodiniform element, GSC 58228. 4 and 5. Lateral views, falodiform elements, GSC 58229 and GSC 58230 respectively.

Figure 6. **"Oistodus"** sp. aff. **"O." nevadensis** Ethington and Schumacher. Lateral View, GSC 58231.

Figures 7-9. **Pygodus** sp. 7, 9. Inner and upper views of pygodiform elements, GSC 58232 and GSC 58233 respectively. 8. Lateral view, haddingodiform element, GSC 58234.

Figures 10, 13. **Phragmodus** sp. 10. Lateral view, dichognathiform element, GSC 58235, x 80. 13. Lateral view, phragmodiform element, GSC 58236.

Figure 11. **"Belodina" monitorensis monitorensis** Ethington and Schumacher. Lateral view, GSC 58237; collection C-74617.

Figure 12. **"Tetraprioniodus"** cf. **"T." lindstroemi** Sweet and Bergström. Lateral view, GSC 58238, x 80.

Figure 14. **"Oistodus" venustus** Stauffer. Lateral view, GSC 58239.

Figures 15, 16. **"Roundya" pyramidalis** Sweet and Bergström, GSC 58240 and GSC 58241 respectively, x 80 and x 200 respectively.

Sweet and Bergström (1974) have noted that only four Middle Ordovician genera, namely **Eoplacognathus, Periodon, Prioniodus** and **Pygodus** may be regarded as truly North Atlantic. All of the elements of the multielement taxa **Pygodus** and **Periodon** appear to be present in the collections, and probably there was little destruction of elements or winnowing during the taphonomy of these samples. Bergström (1971) remarked that elements similar to the form taxa **"Tetraprioniodus"** cf. **"T." lindstroemi** and **"Roundya" pyramidalis,** which frequently occur with **Pygodus** spp., could be tetraprioniodiform and roundyaform elements of the **Pygodus** apparatus but decided that the evidence was insufficient. This association was based on the criteria of frequent co-occurrence as well as matching morphology with the haddingodiform element of the **Pygodus** apparatus.

In most cases, excepting those described by Bergström et al. (1974), **"Roundya" pyramidalis** and **"Tetraprioniodus" lindstroemi,** either together or singly, have been associated with **Pygodus anserinus** (Hamar, 1964; Sweet and Bergström, 1962; Bergström et al., 1974; and Viira, 1974). Tipnis et al. (in press) reported the occurrence of over 100 elements of **Pygodus serrus,** but failed to find a single specimen of either the roundyaform element or the tetraprioniodiform element noted above. Therefore it is possible that **P. serrus** and **P. anserinus** differed in elemental composition, with **P. serrus** lacking roundyaform and tetraprioniodiform elements for at least part of its stratigraphic range.

The three taxa **"Belodina" monitorensis monitorensis, "Oistodus" venustus** Stauffer and **Phragmodus** sp. are all known to occur in the Road River Formation, Llanvirnian in age, from the southwestern Mackenzie Mountains (Tipnis et al., in press), which also contains conodonts of the North Atlantic Province (Tipnis et al., 1975). **"Oistodus"** sp. aff. **"O." nevadensis** has been reported from **Pygodus** bearing strata in the Copenhagen Formation (Ethington and Schumacher, 1969).

Discussion

The occurrence of North Atlantic Province conodonts in marginal deposits of the North American continent is well established from such widely separated areas as Texas-Oklahoma (Bradshaw, 1969), the eastern Appalachians (Bergström, 1971), Newfoundland (Fåhraeus and Nowlan, 1978), the southern Mackenzie Mountains (Tipnis et al., 1975), and the Great Basin of Utah and Nevada (Bergström, 1971). In all these regions the North Atlantic Province conodonts occur in outer shelf or slope settings, and the Midcontinent faunas in adjacent shallower environments (Barnes et al., 1973). The present occurrences fits quite well into this pattern.

Following the discussion above, the age of the collection that includes **Pygodus** sp. is suggested to be Late Llanvirnian to Llandeilian (the complete range of **Pygodus** however includes also an early Llanvirnian age).

Acknowledgments

I am indebted to H.P. Trettin, ISPG, Calgary, for providing the samples which yielded these conodonts and for supplying much stratigraphic and sedimentologic data. H.P. Trettin and T.T. Uyeno read an early version of this manuscript and offered advice and comments. B.D.E. Chatterton, University of Alberta, also read and commented on the manuscript.

References

Barnes, C.R.
1974: Ordovician conodont biostratigraphy of the Canadian Arctic; in J.D. Aitken and D.J. Glass (ed.), Geol. Assoc. Can. - Can. Soc. Petrol. Geol., Spec. vol., p. 221-240.

Barnes, C.R., Rexroad, C.B., and Miller, J.F.
1973: Lower Paleozoic conodont provincialism; in F.H.T. Rhodes (ed.), Conodont Paleozoology, Geol. Soc. Am., Spec. Paper 141, p. 157-196.

Bergström, S.M.
1971: Conodont biostratigraphy of the Middle and Upper Ordovician of Europe and eastern North America; Geol. Soc. Am., Mem. 127, p. 83-157.

Bergström, S.M., Riva, J., and Kay, M.
1974: Significance of conodonts, graptolites, and shelly faunas from the Ordovician of western and north-central Newfoundland; Can. J. Earth Sci., v. 11:12, p. 1625-1660.

Bradshaw, L.E.
1969: Conodont from the Fort Péna Formation (Middle Ordovician), Marathon Basin, Texas; J. Paleontol., v. 43, p. 1137-1169.

Ethington, R.L. and Schumacher, D.
1969: Conodonts of the Copenhagen Formation (Middle Ordovician) in central Nevada; J. Paleontol., v. 43, p. 440-484.

Fåhraeus, L.E. and Nowlan, G.S.
1978: Franconian (Late Cambrian) to Early Champlainian (Middle Ordovician) conodonts from the Cow Head Group, western Newfoundland; J. Paleontol., v. 52, p. 444-471.

Hamar, G.
1964: The Middle Ordovician of the Oslo region, Norway, 17: Conodonts from the lower Middle Ordovician of Ringerike; Norsk Geol. Tidsskrift., v. 44, p. 243-292.

Kerr, J.Wm.
1968: Stratigraphy of central and eastern Ellesmere Island, Arctic Canada, Part II Ordovician; Geol. Surv. Can., Paper 67-27.

Nowlan, G.S.
1976: Lake Cambrian to Late Ordovician conodont evolution and biostratigraphy of the Franklinian Miogeosyncline, eastern Canadian Arctic Islands; unpubl. Ph.D. dissertation, Dept. Biology, Univ. Waterloo, Ontario.

Sweet, W.C. and Bergström, S.M.
1962: Conodonts from the Pratt Ferry Formation (Middle Ordovician) of Alabama; J. Paleontol., v. 35, p. 1214-1252.

1974: Provincialism exhibited by Ordovician conodont faunas; in Paleogeographic Provinces and Provinciality, C.A. Ross, ed., Soc. Econ. Paleontol. Mineral. Tulsa, Spec. Publ. 21, p. 189-202.

Tipnis, R.S., Chatterton, B.D.E., and Ludvigsen, R.
1975: The paleoecological and paleobiogeographic significance of some Early and Middle Ordovician conodont faunas from the southern Northwest Territories, Canada; Geol. Soc. Am., Abstr. Prog., North-Central section, Waterloo, p. 872.

Biostratigraphy of Ordovician conodonts from the southern Mackenzie Mountains; in C.R. Stelck and B.D.E. Chatterton, ed., P.S. Warren Biostratigraphy Symposium, Geol. Assoc. Can., Special Paper 18. (in press)

Trettin, H.P.
1969: Pre-Mississippian geology of northern Axel Heiberg and northwestern Ellesmere Islands, Arctic Archipelago; Geol. Surv. Can., Bull. 171.

1971: Geology of Lower Paleozoic Formations, Hazen Plateau and Southern Grant Land Mountains, Ellesmere Island, Arctic Archipelago; Geol. Surv. Can., Bull. 203.

Middle Ordovician to Lower Devonian deep-water succession at southeastern margin of Hazen Trough, Cañon Fiord, Ellesmere Island; Geol. Surv. Can., Bull. 272. (in press)

Viira, V.
1974: Ordovician conodonts of the east Baltic (in Russia); Eesti NSV Tead. Akad. Geol. Inst., 140 p.

14.

THE STRUCTURAL HISTORY OF THE AMER MYLONITE ZONE, CHURCHILL STRUCTURAL PROVINCE, DISTRICT OF KEEWATIN

Project 760025

Subhas Tella and W.W. Heywood
Regional and Economic Geology Division

Tella, Subhas and Heywood, W.W., The structural history of the Amer Mylonite Zone, Churchill Structural Province, District of Keewatin; in Current Research, Part C, Geol. Surv. Can., Paper 78-1C, p. 79-88, 1978.

Abstract

The Amer mylonite zone is an approximately 10 km wide northeast trending belt of cataclastic to mylonitic rocks. The polydeformed and polymetamorphosed granitoid and sedimentary rocks of the zone exhibit a variety of cataclastic textures which have been classified as blastomylonites, mylonite gneisses, protomylonites, mylonites, cataclasites and microbreccias, following the 1971 classification scheme of Higgins. A comparative study of quartz microstructures from this zone and those described from other mylonite zones, indicates that they were developed under conditions of ductile deformation, by a combination of processes such as intragranular movements, recovery, and recrystallization.

Field relations, textural aspects, and K-Ar mineral dates reveal that movement took place along the zone during at least two periods. The earlier event was one of ductile deformation and was responsible for the development of the mylonite zone, possibly during Late Aphebian or early Helikian times. The second event overprinted the rocks of the region with textures characteristic of brittle deformation, and produced dextral strike slip displacements of undetermined magnitude along the Amer Fault. Porphyritic granite and related rocks were emplaced in the interval between these two events. Later displacements on the Amer Fault predate regionally pervasive northwest trending faults and may have continued sporadically into Paleozoic time.

Introduction

Recent field work in the northern half of the Amer Lake map area (NTS 66H) has established the presence of a northeasterly trending cataclastic to mylonitic zone (Heywood, 1977). This zone, the Amer mylonite zone, represents a relatively short segment of the spectacular regional McDonald-Amer-Meadowbank Fault System; the system that subdivides the northern Churchill Structural Province into three structural blocks – the Queen Maud, the Committee Bay, and the Armit Lake Blocks (Heywood and Schau, 1978). In the Amer Lake map area the mylonite zone is coincident with a pronounced aeromagnetic lineament (Geophysical Series Map 7869G).

Geology, Structure and Metamorphism

The regional geology of the northern half of the Amer Lake map area (NTS 66H N1/2) was briefly described by Heywood (1977). The distribution of rock units is shown in Figure 14.1, and the structural and metamorphic history is summarized in Table 14.1.

Medium- to coarse-grained granulite, biotite paragneiss, mafic schist, and associated minor amphibolite of undetermined origin appear to be the oldest rocks (Unit 1) in the Amer Lake area. Unit 2, structurally above Unit 1, is composed of medium- to coarse-grained grey paragneiss and orthogneiss of granodioritic to quartz dioritic composition and minor layered amphibolite (Unit 2a). Plutonic rocks of Unit 3 intrude Units 1 and 2, and comprise at least three separate phases. The two earlier phases are characteristically medium- to coarse-grained and porphyritic, and have compositions ranging from granodiorite to granite. In general these rocks show a weak to well developed foliation. The third phase of Unit 3 is commonly aplitic to pegmatitic. In some localities the early granitoid phase of Unit 3 forms the basement to the Amer group* (Tippett and Heywood, 1978), but elsewhere a pink aplitic to pegmatitic phase of a similar unit has intruded the basal Amer group quartzites. A K-Ar age of 1729 ± 41 Ma (Table 14.2) on muscovite from this pegmatite may date the time of emplacement of the pegmatite. The above relationships indicate that the plutonic rocks of Unit 3 in part predate and in part postdate the lower Amer group. It has not been possible to separate the individual intrusive phases into mappable units.

Fine- to medium-grained, well foliated and mylonitized quartzite, quartz mica-schist, minor dolomite, slate and hornfelsed metasediments of Unit 4 outcrop as discontinuous lenses along the Amer Fault (Fig. 14.1), and in isolated areas to the west and northwest of the fault. These rocks appear to be mylonitized equivalents of the Amer group (Unit 4a). Unfoliated, medium- to coarse-grained, massive, pink mafic syenite (Unit 5) outcrops in the east-central part of the Amer Lake map area south of the Meadowbank fault. A K-Ar date of 1833 ± 32 Ma (Table 14.2) on hornblende from this body probably dates the time of its emplacement. Although the intrusive relationships with the country rocks have not been established, the massive, unfoliated and unmetamorphosed character of the unit indicates that it postdates the rocks described above, with the possible exception of the pegmatite. A similar, and probably related mafic syenite body exposed in the northeastern corner of the map area (Fig. 14.1), shows well developed mylonitic textures.

White to pink, porphyritic granitoid rocks of Unit 6 are exposed in the northwestern part of the area (Fig. 14.1). They are commonly coarse grained, massive to weakly foliated, and contain abundant hornfelsed inclusions of Unit 4. Amphibolite inclusions and xenoliths of older para- and orthogneisses are also common. Unit 7 is a massive, pink porphyritic granite (sphene- and fluorite-bearing) exposed in the southwestern corner of the area. Although the contact relationships between Units 6 and 7 are not known, the massive character of Unit 7 suggests that its emplacement may have postdated that of Unit 6.

The tentative sequence of events, listed in Table 14.1, is based on field relations, structural data and petrography. Metamorphic isograds could not be defined because diagnostic mineral assemblages are generally absent. Moreover, the establishment of time relations between metamorphism and tectonism (Table 14.1) is further complicated by a paucity of crucial metamorphic textures.

*Amer group is an informal term.

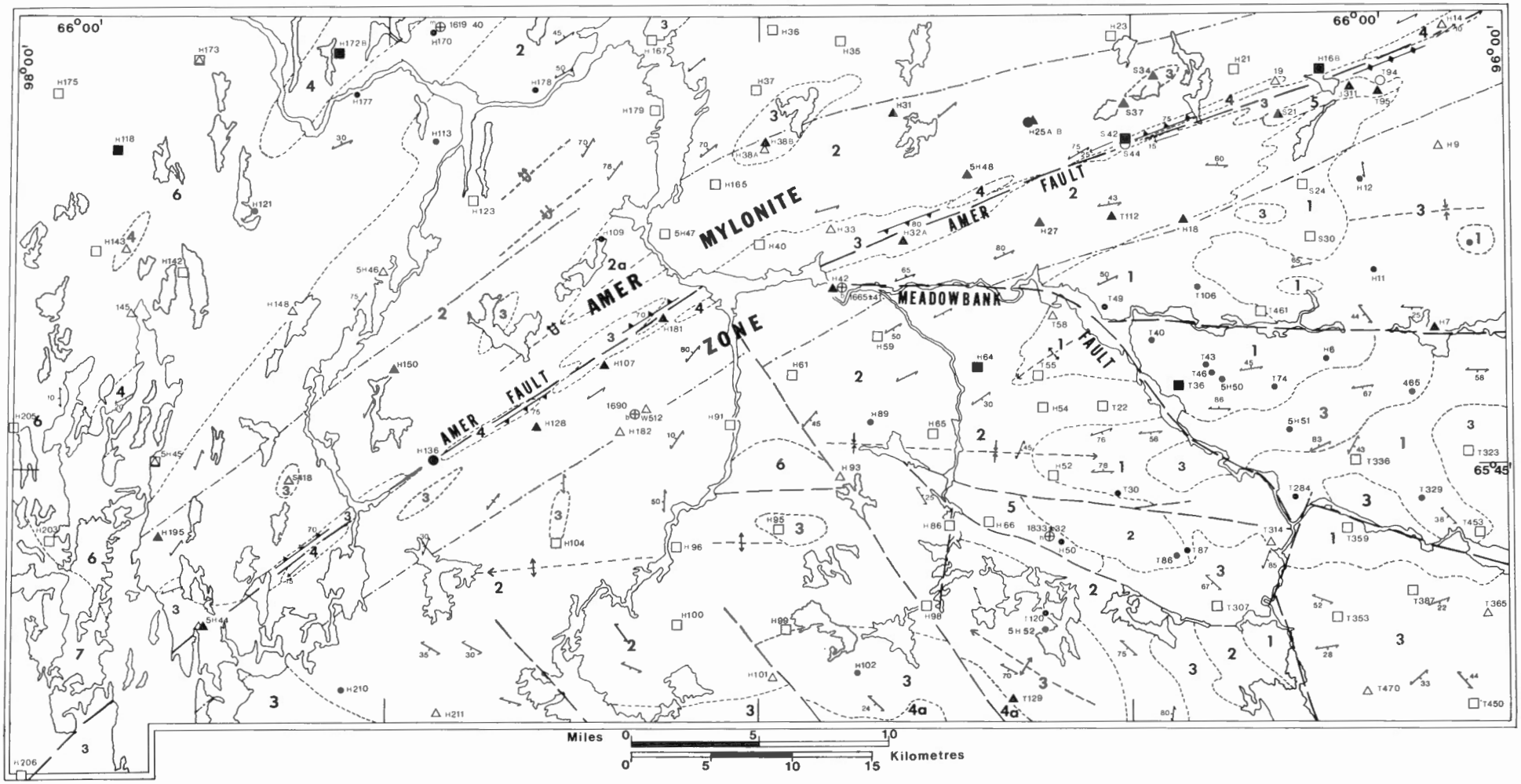
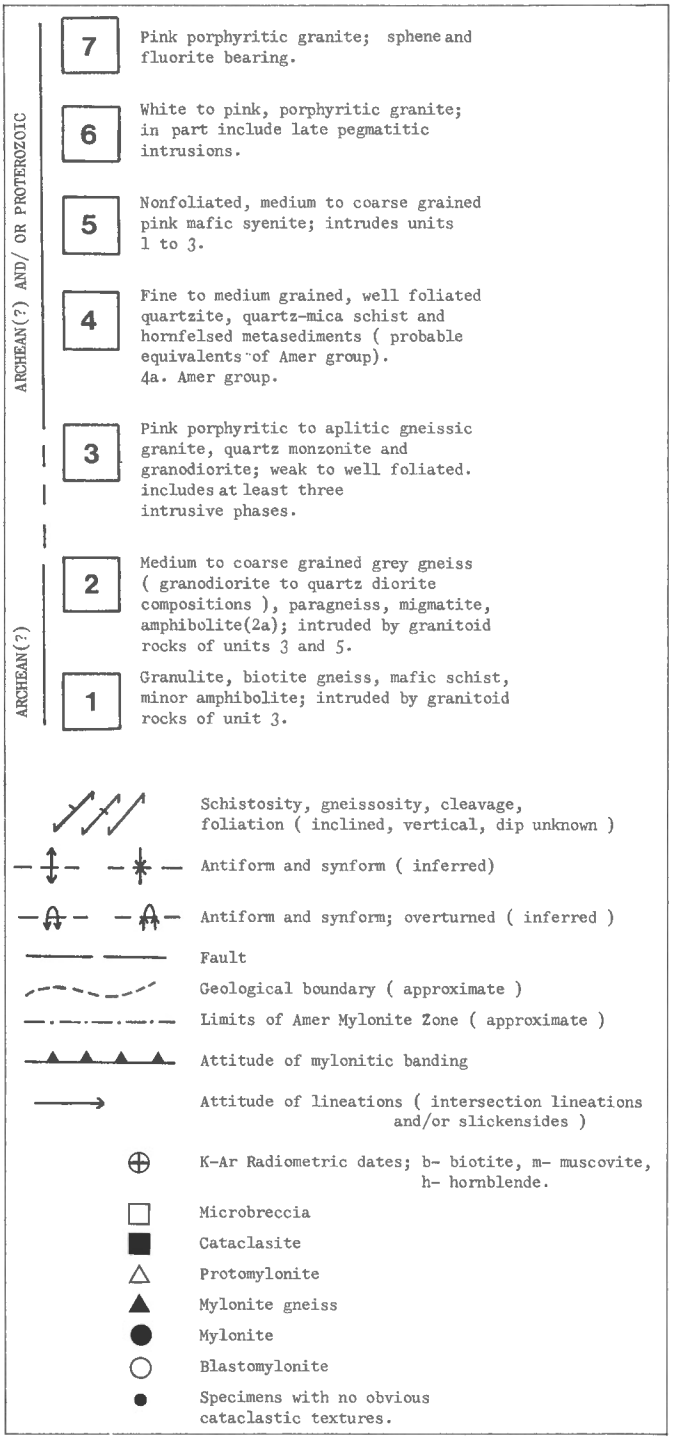


Figure 14.1. Geology of northern parts of the Amer Lake map area.

Legend to Figure 14.1.



To define and document the tectonic history of the Amer mylonite zone and of the spatially associated Amer Fault, numerous microstructures were examined within and outside the mylonite zone in rocks of Units 1 to 7 inclusive. Northwest and north-northeast trending faults, some of which appear to displace the Amer Fault and the Amer mylonite zone with an apparent dextral slip displacement, will not be considered further.

Microstructures and Textures

More than 80 thin sections[1] were examined to describe the variations in microstructures and textures across the mylonite zone. The observed textures have been classified into several types, shown in Table 14.3, following the scheme outlined by Higgins (1971). Although there are several classification schemes for cataclastic rocks (Christie, 1960; Higgins, 1971; Sibson, 1977; Spry, 1969; Zeck, 1974), the classification proposed by Higgins is adopted here because the observed textures can be adequately described within the scheme with a minimum of modification. All textures are gradational even on thin section scale, hence the most appropriate term has been applied to classify the rock textures. The gross features of these microstructures and textures are summarized in Table 14.4.

Metamorphic recrystallization textures in Units 1 and 2 commonly mimic mylonite gneisses from which they are difficult to separate. The mylonite gneisses are generally characterized by recrystallization and neomineralization, processes believed to be concurrent with the development of the mylonite. The textures developed in Units 3, 4 and 5 are easier to interpret.

A comprehensive study of these microstructures and textures (Table 14.4) demonstrates the following relationships in the Amer mylonite zone:

i) The distribution of blastomylonite, mylonite gneiss, mylonite and protomylonite in the Amer Lake area (Fig. 14.1) define the approximately 10 km wide Amer mylonite zone. Blastomylonite and mylonite (Fig. 14.2A) are, however, restricted to a narrow zone along the trace of the Amer Fault. These textures are exclusively developed in Units 1 to 5, and are absent from Units 6 and 7.

ii) Within the Amer mylonite zone, recrystallization and neomineralization predominate over cataclasis in Units 1 to 5. Plastic strain features such as deformation lamellae and extinction bands, are however locally common both in the larger nonrecrystallized grains as well as in the finer recrystallized grains of quartz.

iii) Cataclasite and microbreccia are common both within and outside the mylonite zone. Quartz and feldspar show abundant plastic strain, microfracturing and microfaulting that increase in intensity towards the Amer Fault. These textural types appear to have developed in response to more than one event of deformation.

Discussion and Conclusions

Microstructural and textural studies of quartz have received the most attention in recent years in the interpretations of various mylonite zones (Bell and Etheridge, 1973, 1976; Christie, 1960; Sinha Roy, 1977; Wilson, 1975). This is because of increased understanding of their origin and development through the works of Carter et al. (1964), Green et al. (1970), Hobbs (1968), Hobbs et al. (1972), Tella (in prep.), and White (1973, 1976) on both experimentally and naturally deformed quartzites, which also involved the application of advanced X-ray, and scanning and transmission electron-microscope techniques (Baeta and Ashbee, 1973; Baker et al., 1969; McLaren and Hobbs, 1972; McLaren and Retchford, 1969). In addition, experimental studies by Baeta and Ashbee (1969) have identified numerous slip systems in quartz. In most of these studies the microstructures and fabrics of quartz were interpreted as being developed by the following combination of mechanisms (see also Hobbs et al., 1976):

i) intergranular movements which involve external rotation, cataclastic flow, and development of preferred dimensional orientation of grains.

[1] A detailed list of quartz microstructures and textures, and a list of mineral assemblages noted in these sections are available as appendices and may be obtained by writing to the authors.

Table 14.1

Suggested sequence of tectonic and metamorphic events in the northern part of Amer Lake map area (NTS 66H)

Rock Unit(s) involved	Types of structures developed	Penetrative fabric elements	Attitude of fabric elements	Deformation event	Metamorphism	Plutonism	Temporal relations between deformation metamorphism and plutonism
1,2,3,4, and 5	Faults	None; except local development of planes of shearing	Northwest and northeast	Faulting	None		Post Aphebian Postdate emplacement of units 6&7
1 to 7	Amer fault and possibly Meadowbank fault; dextral strike slip displacement on unit 7	Shearing along fault planes; non-penetrative slickensides	Northeast-Southwest; subhorizontal slickensides	Faulting	Late alteration along shearplanes		
6 and 7						Intrusion of granite, pegmatite and related rocks	Post mylonite intrusion (? 1619 ± 40 m.y.)
1 to 5	Cataclastic to mylonitic textures (Amer Mylonite Zone)	Mylonitic foliation	Northeast-southwest; steep to vertical	Mylonitization	Retrogression; lower greenschist facies assemblages		Post Aphebian mylonitization; but predate the intrusive rocks of units 6 and 7. The mylonite zone may have been active prior to the deposition of Amer group but cannot be substantiated.
3c*						Intrusion of aplite to pegmatite granite into basal Amer group	Post Aphebian (Hudsonian?) (1729 ± 41 Ma)
5						Intrusion of mafic syenite	(1833 ± 32 Ma)
4 and 4a	Mesoscopic to macroscopic upright to overturned tight isoclines; open upright folds and thrust faults	Axial plane foliations, crenulation surfaces, intersection lineations ($S_1/S_2/S_0$); fold axes	Commonly coaxial coplanar D_1 and D_2 fabric elements; east-west to southwesterly trends with shallow to steep dips; west to southwest plunging(shallow) linear elements with local reversal to the east	+D_{1A},D_{2A},D_{3A}	Syn D_{1A} metamorphism; greenschist to amphibolite		Late Aphebian or post Aphebian
1,2, and 3a,b	Mesoscopic to macroscopic open upright folds (F_1&F_2)(general warping of earlier structures)	Axial planes and fold axes.	Variable attitudes, but generally northwest and north trending axial surfaces; fold axes plunge steeply either to the north or to the south.	D_3 and D_4	None		
1,2, and 3a,b*	Mesoscopic to macroscopic open to tight upright folds(F_2) coaxial to F1.	S_2 foliations, fold axes, mineral lineations(?), S_1/S_2 intersection lineations; crenulation surfaces	Northeast to east trending foliations and axial planes with moderate to steep dips; fold axes plunge moderately to the southwest and west	D_2	Greenschist to amphibolite facies		Late Archean ? or Aphebian; predate the deposition of Amer group. Considered to be a stable structural block during and subsequent deformation of the Amer group
3a&b						Granite, granodiorite, and quartz monzonite intrusions	
1 and 2	Mesoscopic, upright to overturned tight isoclinal folds(F_1) of rare occurrence	Foliations(S_1), mineral lineations (?), and fold axes	Northeast to east trending foliations with steep dips: fold axes and lineations with shallow to moderate plunge to the southwest	D_1	Amphibolite to granulite facies		Origin of units 1 and 2 ??

* Units 3a & b refer to the two earlier phases of granitoid rocks and 3c refers to the latest phase.

\+ D_{1A}, D_{2A}, & D_{3A} refer to deformational events in the Amer group.

Table 14.2

K-Ar radiometric data

Rock Unit	Sample	Mineral Dated	Age	Remarks
2	W 512	biotite	1690 Ma	rock units within the mylonite zone
2	WN 228 (=H42)	biotite	1665 ± 41 Ma	
3	HF 76-T 649	muscovite	1729 ± 41 Ma	
5	WN 227 (=H50)	hornblende	1833 ± 32 Ma	
6	HF 170	muscovite	1619 ± 40 Ma	5 to 10% feldspar contamination

Table 14.3

Classification of cataclastic rocks (after Higgins, 1971)

Approximate volume per cent porphyroclasts in rocks with fluxion structure. or Approximate volume per cent fragments in rocks without fluxion structure	Rocks without primary cohesion	Rocks with primary cohesion			Approximate size of most porphyroclasts in rocks with fluxion structure. or Approximate size of most fragments in rocks without fluxion structure.
		Cataclasis dominant over neomineralization recrystallization		Neomineralization recrystallization dominant over cataclasis	visible to naked eye.
		Rocks without fluxion structure	Rocks with fluxion structure	Rocks with fluxion structure	
>50 <50 30	Fault breccia	Microbreccia*	Protomylonite	Mylonite gneiss (mylonite schist)	
>10 <10	Fault gouge	Cataclasite	Mylonite / Ultramylonite	Phyllonite (variety) / Blastomylonite	>0.2 <0.2

All rocks are gradational

*In the present study this term has been used to include all rocks which show microfractures and microfaults without accompanying fine grained crushed matrix.

Table 14.4

Summary of microstructures and textures

Rock Units	Plastic strain in quartz	Recrystallization textures in quartz	Other textures	Textural type(s)
1,2,3,4 and 5 (figures: 2,3 and 4A)	undulatory extinctions, extinction bands; some are related to pre-recrystallization strain and few are related to post recrystallization strain	incipient polygonal subgrain mosaic development; granoblastic polygonal in some; strain-free neomineralized grains around strained hosts; ribbons of quartz with internally recrystallized subgrain polygonal mosaics	weak to well defined dimensional orientation of grains; larger feldspars with well developed mortar textures; microkinks and microfaults within plagioclase twins	Blastomylonite Mylonite gneiss Protomylonite Mylonite Cataclasite Microbreccia
6 and 7 (figures: 4B and C)	abundant microfractures, deformation lamellae, inclusion trails, undulatory extinctions and extinction bands	absent	microfaults in plagioclase twins; shearing and fracturing within and across grain boundaries	Microbreccia

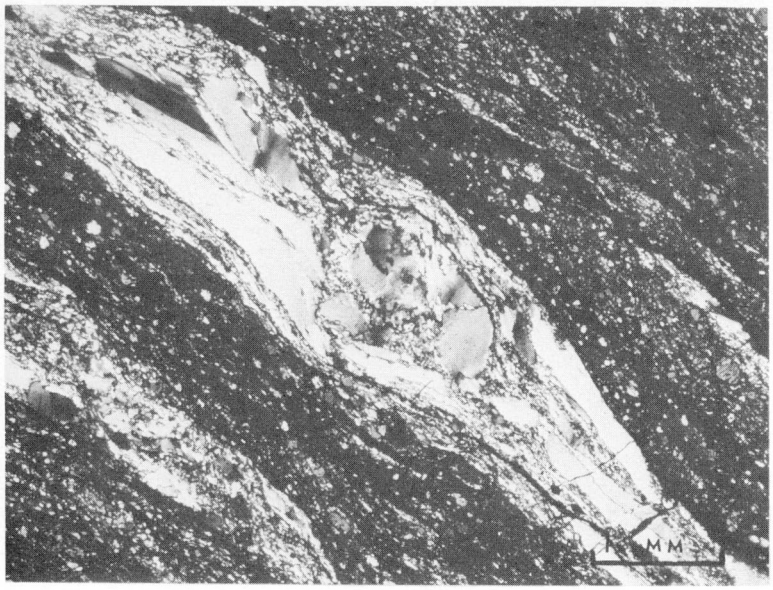


Figure 14.2A

Blastomylonite (S44B); Ribbons of quartz show extensive recrystallization with the development of subgrain polygonal mosaics. Larger clasts show conjugate microfractures and plastic strain. Neomineralization along fractures. (GSC 203308-L)

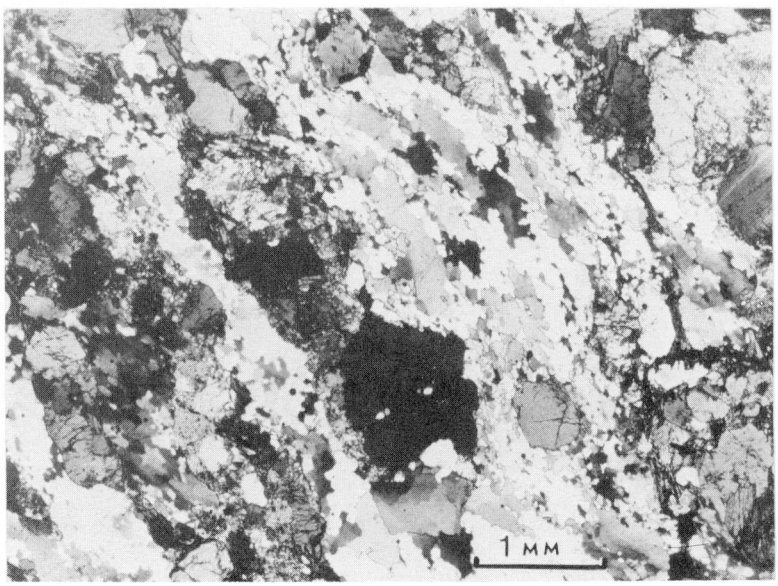


Figure 14.2B

Mylonite gneiss (H27B); Subgrain polygonal mosaics in elongate quartz grains. Feldspars show shearing and microfracturing. (GSC 203308-N)



Figure 14.2C

Protomylonite (H38A); Dimensional orientation of quartz, sutured to embayed grain boundaries; minor recrystallization with the development of finer polygonal quartz grains. (GSC 203308-Q)

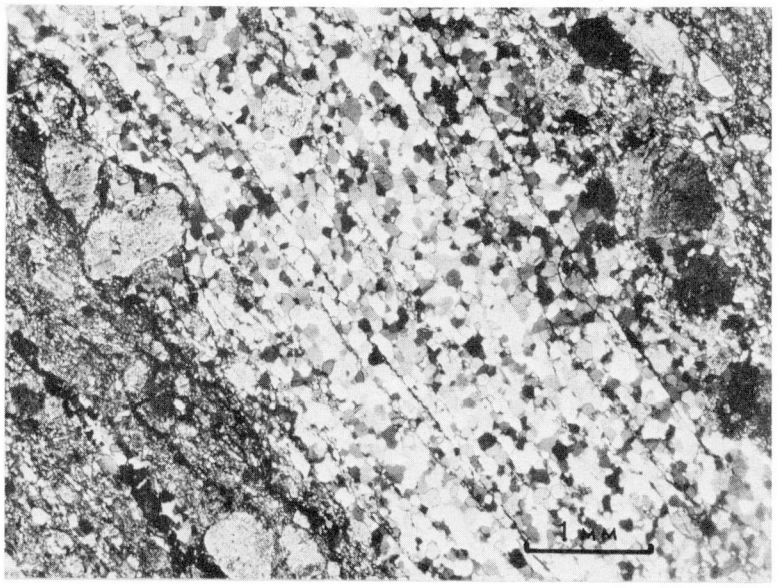


Figure 14.3A

Mylonite gneiss (H107A); Granoblastic polygonal quartz in quartz-rich layers; adjacent matrix show cataclasis (cataclasite). Recrystallization dominates over cataclasis. (GSC 203308-K)

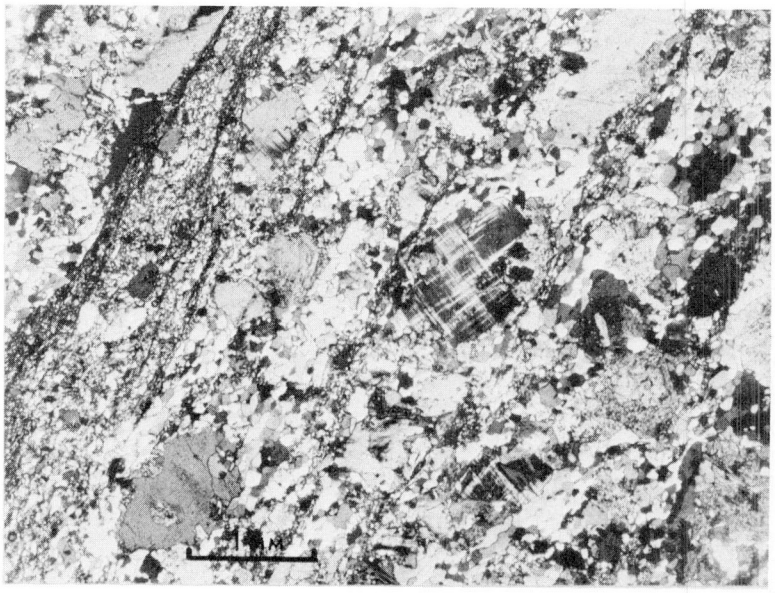


Figure 14.3B

Mylonite gneiss (H7); Recrystallized quartz show weak dimensional orientation; feldspars with granulated and corroded grain boundaries show microfractures. (GSC 203308-M)

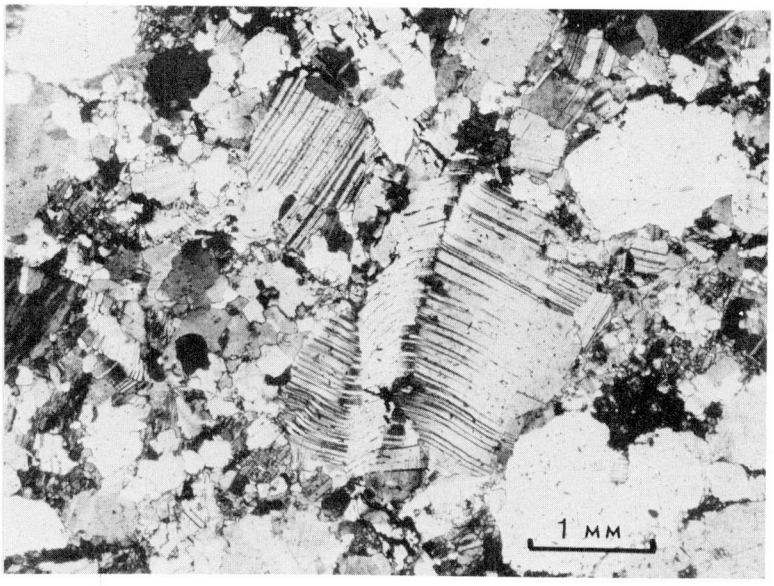


Figure 14.3C

Microkinks and microfaults within plagioclase (T323). (GSC 203308-H)

ii) intragranular movements involving gliding flow and plastic deformation within the crystals, accompanied by external grain rotations to develop preferred crystallographic orientations.

iii) recovery processes in which the plastic strain undergone by the crystal is released by a dissipation of stored strain energy whereby the crystal tends to return to its undeformed state without the formation and migration of high angle grain boundaries, and result in a polygonal texture with the development of strain-free grains.

iv) static and/or dynamic (syntectonic) recrystallization process involving a complete or progressive dissipation of stored strain energy, remaining after recovery, with the development of strain-free grains within strained hosts.

The microstructures and textures which have an important bearing on the origin and development of the Amer mylonite zone are as follows (see also Table 14.4):

1. Larger feldspar grains show well developed mortar textures, whereas both quartz and feldspar show marginal granulation and conjugate microfractures. Cataclastic fabric usually wraps around the feldspar clasts, and the pressure fringes are filled by recrystallized quartz grains (Fig. 14.3B, 14.4A).

2. Quartz clasts, where they are demonstrably coarser (Fig. 14.2A), show abundant plastic strain and conjugate shear fractures. Normals to the planes of fabric bisect the acute angle of these fractures and suggest that they were probably developed during the initial stages of flattening. Finer neomineralized quartz grains with triple junctions occupy the interstices of the fracture planes. Mylonitic fabric which wraps the plastically strained quartz clasts show well developed ribbons. These ribbons commonly show polygonal subgrain mosaics (Figs. 14.2A, 14.2B).

3. In some mylonite gneisses quartz-rich layers (Fig. 14.3A) show granoblastic polygonal texture with perfect triple junctions, whereas adjacent finer grained matrix show cataclasis and granulation. Feldspar clasts have corroded grain boundaries and a weak to well developed mortar texture.

4. Recrystallization and neomineralization predominates over cataclasis in most parts of the zone. Most specimens show variable degrees of cataclasis, recrystallization and neomineralization.

These textural aspects of quartz from the mylonite zone suggest at least two stages of development. An initial stage of cataclasis and granulation which developed undulatory extinctions, extinction bands, deformation lamellae and microfractures, was followed by a more pronounced second stage of recrystallization. This later stage is characterized by a common development of granoblastic polygonal subgrain mosaics, neomineralized and recrystallized quartz around larger host grains, and strain-free polygonal quartz. An overall examination of these textures suggests that the two stages are probably synchronous and are the result of a progressive deformation. The presence of abundant chlorite along the mylonitic planes, together with a single occurrence of garnet in mylonitized granite, may indicate that some metamorphism had occurred during deformation.

A comparison of the above microstructures and textures to those developed in experimentally deformed synthetic and natural quartzites suggests that a combination of intragranular movement, recovery and recrystallization processes were the most influential mechanisms for their development in the Amer mylonite zone. These textures are typical of rocks which fall in the quasi-plastic regime of Sibson (1977).

Although the development of these microstructures can be explained satisfactorily, the problem of determining the type of strain, which was responsible for the development of the Amer mylonite zone remains. Two contrasting opinions are commonly being expressed on the subject of mylonite formation – shear strain versus flattening strain (Ramsay and Graham, 1970; Schwerdtner and Bauer, 1975; Johnson, 1967; Tullis et al., 1973; Ross, 1973; Eisbacher, 1970), it is not uncommon, however, to find that the planes of maximum shear may also represent planes of flattening on their progressive rotation during deformation (Ramsay and Graham, 1970; Sinha Roy, 1977). A majority of the microtextures within the Amer mylonite zone indicate an overall flattening strain, but it is conceivable that the total strain may have had a shearing 'history' in the early stages of the mylonite development.

The presence of abundant deformation lamellae, microfractures and microfaults in rocks of Units 6 and 7, on the other hand, suggests that intergranular and intragranular movements have influenced their development. These textures are typical of rocks which fall in the elastico-brittle regime of Sibson (1977) and hence indicate a different mode of deformation for the Amer Fault.

An analysis of the textures so far described suggests that the Amer mylonite zone was developed prior to the emplacement of the plutonic rocks of Units 6 and 7. As the rocks of Unit 5 show evidence of mylonitization, this event must postdate the emplacement of Unit 5 and must predate the emplacement of Unit 6. Although it is not possible to date the event in an absolute sense, relatively younger K-Ar dates of 1690 and 1665 ± 41 Ma (W512 and WN228, Table 14.2) on obviously older grey gneiss, together with the fact that these represent the rocks within the mylonite zone, suggest that these dates may reflect the time of mylonitization. A complete or partial loss of radiogenic argon from these rocks during intense mylonitization may result in obtaining relatively younger ages for the minerals dated.

Intense microfracturing and microfaulting in Units 6 and 7, together with an abrupt truncation of Unit 7 near the Amer Fault in the southwestern portion of the map (Fig. 14.1), suggest an active displacement along the Amer Fault after intrusion of Units 6 and 7; and hence, a second movement within the Amer mylonite zone. The movement on the Amer Fault obviously postdates the emplacement of Units 6 and 7 and predates the northwest trending faults. Some of these northwest trending faults elsewhere in the northern Churchill Province displace Silurian sediments (Heywood, 1967); and the easterly extension of the Meadowbank Fault displaces Silurian rocks on Southampton Island (Heywood and Sanford, 1976; Heywood and Schau, 1978). These relationships indicate that the last displacements on these faults are post-Silurian.

Stratigraphic studies (Hoffman et al., 1977) to the southwest along the Amer Fault, suggested a 75 km dextral slip movement on the McDonald portion of the McDonald-Amer-Meadowbank Fault System (Heywood and Schau, 1978). Although no marker horizons are present to determine the nature and cumulative displacements along the Amer Fault within the present study area, microfaulting with consistent dextral offsets, together with the presence of horizontal to subhorizontal slickensides indicate that the last movement on the fault was of dextral strike slip. A distinctive high magnetic anomaly pattern displayed by Unit 7 shows dextral offsets along the trace of the fault on aeromagnetic maps (Geophysical Series Maps 7870G, NTS 66G; 7869G, NTS 66H) and suggests a similar movement.

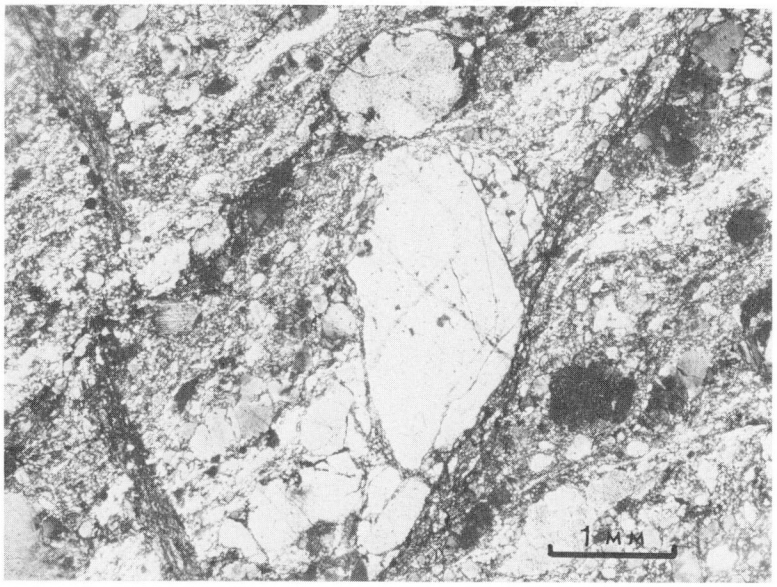


Figure 14.4A

Mylonite (H136); Large angular to subrounded quartz clasts in a fine grained matrix composed of feldspar and quartz. Microfractures and deformation lamellae common. (GSC 203308-J)

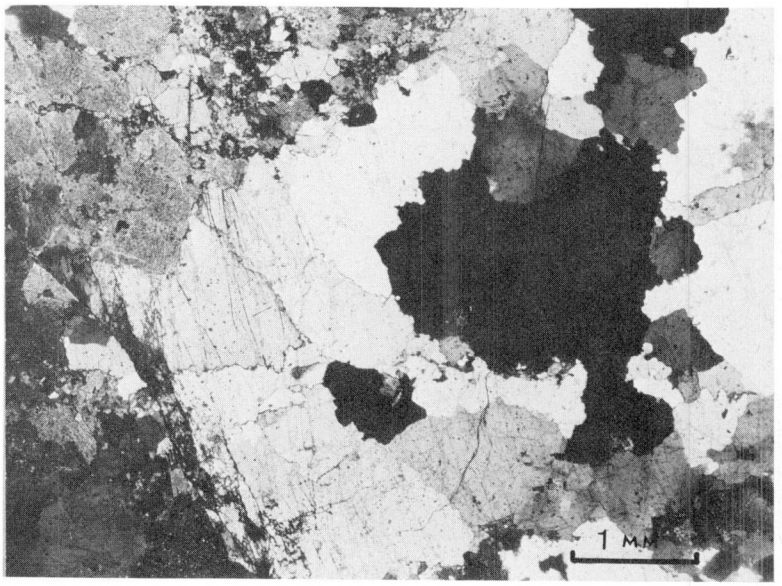


Figure 14.4B

Microbreccia (H203); Quartz with strongly sutured grain boundaries, microfractures and inclusion trails within and across grain boundaries. (GSC 203308-G)

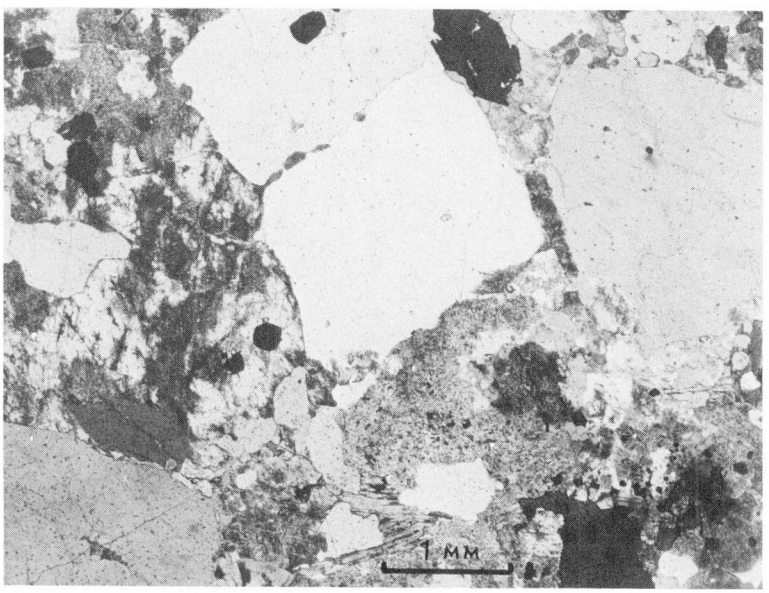


Figure 14.4C

Angular to subrounded quartz with abundant inclusion trails, microfractures and deformation lamellae (H206). Lacks penetrative mylonitic fabric observed in Figures 14.2, 14.3A and 14.3B. (GSC 203308-S)

References

Baeta, R.D. and Ashbee, K.H.G.
1969: Slip systems in quartz. I. Experiments; Am. Mineral., Vol. 54, p. 1551-1573.

1973: Transmission electronmicroscopy studies of plastically deformed quartz; Phys. Status Solidi A, Vol. 18, p. 155-170.

Baker, D.W., Wenk, H.R., and Christie, J.M.
1969: X-ray analysis of preferred orientation in fine-grained quartz aggregates; Jour. Geol., Vol. 77, p. 144-177.

Bell, T.H. and Etheridge, M.A.
1973: Microstructures of mylonites and their descriptive terminology; Lithos, 6, p. 337-348.

1976: The deformation and recrystallization of quartz in a mylonite zone, central Australia; Tectonophysics, Vol. 32, p. 235-267.

Carter, N.L., Christie, J.M., and Griggs, D.T.
1964: Experimental deformation and recrystallization of quartz; J. Geol., 72, p. 687-733.

Christie, J.M.
1960: Mylonitic rocks of the Moine thrust-zone in the Assynt Region, NW Scotland; Trans. Geol. Soc. Edinb. 18, p. 79-93.

Eisbacher, G.H.
1970: Deformation mechanics of mylonitic rocks and fractured granites in Cobequid Mountains, Nova Scotia, Canada; Bull. Geol. Soc. Am., 81, p. 2009-2020.

Geological Survey of Canada
1974: Amer Lake; Geophysical Series (Aeromagnetic) Map 7869G.

1974: Deep Rose Lake; Geophysical Series (Aeromagnetic) Map 7870G.

Green, H.W., Griggs, D.T., and Christie, J.M.
1970: Syntectonic and annealing recrystallization of fine-grained quartz aggregates; in Paulisch (ed.), Experimental and natural rock deformation; Springer-Verlag, N.Y., p. 272-335.

Heywood, W.W.
1967: Geological notes, northeastern District of Keewatin and southern Melville Peninsula, District of Franklin, Northwest Territories (Parts of 46, 47, 56, 57); Geol. Surv. Can., Paper 64-40.

1977: Geology of the Amer Lake map area, District of Keewatin; in Report of Activities, Part A, Geol. Surv. Can., Paper 77-1A, p. 409-410.

Heywood, W.W. and Sanford, B.V.
1976: Geology of Southampton, Coats and Mansel Islands, District of Keewatin, Northwest Territories; Geol. Surv. Can., Mem. 382.

Heywood, W.W. and Schau, Mikkel
1978: A subdivision of the northern Churchill Structural Province; in Current Research, Part A, Geol. Surv. Can., Paper 78-1A, p. 139-142.

Higgins, M.W.
1971: Cataclastic Rocks; Prof. Pap. U.S. Geol. Surv., 687, 97 p.

Hobbs, B.E.
1968: Recrystallization of single crystals of quartz; Tectonophysics, 6, p. 353-401.

Hobbs, B.E., McLaren, A.C., and Paterson, H.S.
1972: Plasticity of single crystals of synthetic quartz; Geophys. Monogr. Ser., 16, p. 29-53.

Hobbs, B.E., Means, W.D., and Williams, P.
1976: An outline of Structural Geology; New York: John Wiley.

Hoffman, P.F., Bell, I.R., Hildebrand, R.S., and Thorstad, L.
1977: Geology of the Athapuscow Aulacogen, East Arm of Great Slave Lake, District of Mackenzie; in Report of Activities, Part A, Geol. Surv. Can., Paper 77-1A, p. 117-129.

Johnson, M.R.W.
1967: Mylonite zones and mylonite banding; Nature, 213, p. 246-247.

McLaren, A.C. and Hobbs, B.E.
1972: Transmission electron microscope investigation of some naturally deformed quartzites; Geophys. Monograph, 16, p. 55-66.

McLaren, A.C. and Retchford, J.A.
1969: Transmission electron microscope study of the dislocations in plastically deformed synthetic quartz; Phys. Status Solidi, 33, p. 657-668.

Ramsay, J.G. and Graham, R.H.
1970: Strain variation in shear belts; Can. J. Earth Sci., 7, p. 786-813.

Ross, J.V.
1973: Mylonitic rocks and flattened garnets in the Southern Octanagon of British Columbia; Can. J. Earth Sci., 10, p. 1-17.

Schwerdtner, W.M. and Bauer, G.
1975: Tectonic significance of mylonite zones; N. Jb. Mineral. Mh. 11, p. 500-509.

Sibson, R.H.
1977: Fault rocks and fault mechanisms; Geol. Soc. Lond., J.V. 133, p. 191-213.

Sinha Roy, S.
1977: Mylonitic microstructures and their bearing on the development of mylonites – an example from deformed trondhjemites of the Bergen Arc region, SW Norway; Geol. Mag. 114 (6), p. 445-458.

Spry, Alan
1969: Metamorphic textures; Pergamon Press, 350 p.

Tella, S.
Microstructures and preferred orientations of quartz in tectonites of different metamorphic grade; Ph.D. thesis in progress, McGill University, Montreal. (in prep.)

Tippett, C. and Heywood, W.W.
1978: Stratigraphy and structure of the northern Amer group (Aphebian), Churchill Structural Province, District of Keewatin, N.W.T.; in Current Research, Part B, Geol. Surv. Can., Paper 78-1B.

Tullis, J., Christie, J.M., and Griggs, D.T.
1973: Microstructures and preferred orientations of experimentally deformed quartzites; Bull. Geol. Soc. Am. 84, p. 297-314.

White, S.
1973: Syntectonic recrystallization and texture development in quartz; Nature, Lond. 244, p. 276-278.

1976: The effects of strain on the microstructure, fabrics and deformation mechanisms in quartzites; Phil. Trans. Roy. Soc. Lond., A. 283, p. 69-86.

Wilson, C.J.L.
1975: Preferred orientations in quartz ribbon mylonites; Bull. Geol. Soc. Am. 86, p. 968-974.

Zeck, H.P.
1974: Cataclasites, hemiclastites, homoclastites, blastoditto, and myloblastites – cataclastic rocks; Am. J. Sc. 274, p. 1064-1073.

15. STRATIGRAPHY OF THE YELLOWKNIFE SUPERGROUP IN THE MARA-BACK RIVERS AREA, DISTRICT OF MACKENZIE

Project 750008

R.A. Frith and J.A. Percival[1]
Regional and Economic Geology Division

Frith, R.A. and Percival, J.A., Stratigraphy of the Yellowknife Supergroup in the Mara-Back rivers area, District of Mackenzie; in Current Research, Part C, Geol. Surv. Can., Paper 78-1C, p. 89-98, 1978.

Abstract

The supracrustal rocks of the Archean Yellowknife Supergroup in the Mara-Back rivers area are divisible into three groups. The lowermost Hackett River Group consists of the Siorak, the Nauna and the Ignerit formations. These represent respectively the basal gneisses and schists, a metavolcanic unit, and the upper volcanic and chemical metasedimentary rocks of the Hackett River volcanic belt. The Hackett River Group is overlain by the Beechey Lake Group, consisting of mudstone-greywacke, and this is overlain by and interfingered with the Back Group, comprising lavas, pyroclastics and associated sediments. A granitoid terrane, parts of which may be older than the Hackett River Group, is informally named the Hanimor granitoid complex.

Introduction

Reconnaissance helicopter mapping at a scale of eight miles to one inch was carried out by Wright (1957) and Fraser (1964). More detailed mapping at a scale of two inches to one mile began in 1974 with the mapping of the Department of Indian and Northern Affairs (Padgham et al., 1975a, 1975b; Jefferson et al., 1976a, 1976b). The Geological Survey mapped the remaining parts of the region at scales of 1:50 000 and 1:25 000 as part of a regional compilation of the Nose-Beechey lakes map-area and topical study of the volcanic rocks in the Back River region (Frith and Hill, 1975; Frith et al., 1977; Lambert, 1976, 1978). In addition to government surveys, mining interests, in particular those at 'Camp' and 'Aitch' lakes (Fig. 15.1) carried out detailed mapping and drilling of selected parts of the Hackett River volcanic belt. Topical studies on economic geology (Frith and Roscoe, in prep.; Sangster, 1972; Franklin, 1976; Casselman, 1977), on sedimentology (Henderson, 1975), on stratigraphy (Percival, 1978), on volcanology (Ewing, 1977) and on geochemistry (Cameron and Durham, 1974) have been carried out and others are still in progress.

The Yellowknife Supergroup

J.M. Bell (1929) referred to the rocks at Yellowknife as the Yellowknife Series. These were renamed the Yellowknife Group by J.F. Henderson (1938). J.B. Henderson (1970) raised the Yellowknife Group to Supergroup rank with the intention that it include all supracrustal rocks of Archean age within the Slave Structural Province. He subdivided and named the rocks of the Supergroup in the Yellowknife Bay-Prosperous Lake area down to formational level. This area is generally considered as a "reference area" for the Yellowknife Supergroup.

Early work in the Slave Province divided the Yellowknife Supergroup into two units either dominantly volcanic or sedimentary. Formations have been named in some areas (Bostock, in press), but in general Yellowknife rock units have not been named (e.g. Tremblay, 1971, 1976).

Recent mapping in the Nose-Beechey lakes map area has shown that the Yellowknife consists of a volcanic and overlying sedimentary group, as in the Yellowknife-Prosperous Bay area, but a third stratigraphically younger group of volcanic rocks is present and this has been informally referred to as the Back River greenstone belt (Frith and Hill, 1975) or as the Back River volcanic complex (Lambert, 1976).

The volcanic rocks of the Nose-Beechey lakes map area differ from those of the "reference area" at Yellowknife. The Hackett River Group volcanics are distinctly more felsic and the published analytical work (Cameron and Durham, 1974) suggests that the volcanics are dominantly calc-alkaline rather than dominantly tholeiitic, as at Yellowknife (Baragar, 1966). The Back Group is unique in the Slave in its higher stratigraphic position and in its apparently emergent to shallow depositional environment (Lambert, 1976). It too appears to follow a calc-alkaline geochemical trend. On the other hand, the mudstone-greywacke sequence of the Beechey Lake Group appears similar to sedimentary rocks of the Yellowknife-Prosperous reference area (Henderson, 1975).

Contacts between the groups are generally conformable. The base of the Hackett River Group is obscured, but if a prevolcanic granitoid basement is present it would presuppose an unconformable surface. However, poor exposure, metamorphic and tectonic effects and crosscutting late granitoid and basic intrusions, make this supposition difficult to establish. Local angular discordance is present within the group and in places the basal Back Group consists of conglomerate lying with slight angular discordance on strata of the Beechey Lake Group.

Rocks of the Yellowknife Supergroup underlie about two thirds of the Nose-Beechey lakes map area (Fig. 15.2). The total thickness of the supergroup is unknown. The Hackett River Group appears to thicken and thin along a homoclinal belt about 200 km in length (Fig. 15.2) with thicknesses of up to 8000 m. The Beechey Lake Group is commonly tightly folded, making its true thickness difficult to estimate. The Back Group is essentially flat lying. However, its upper members have probably been removed by erosion and estimates of thickness are further hindered by multiple caldron collapse structures (Lambert, 1978).

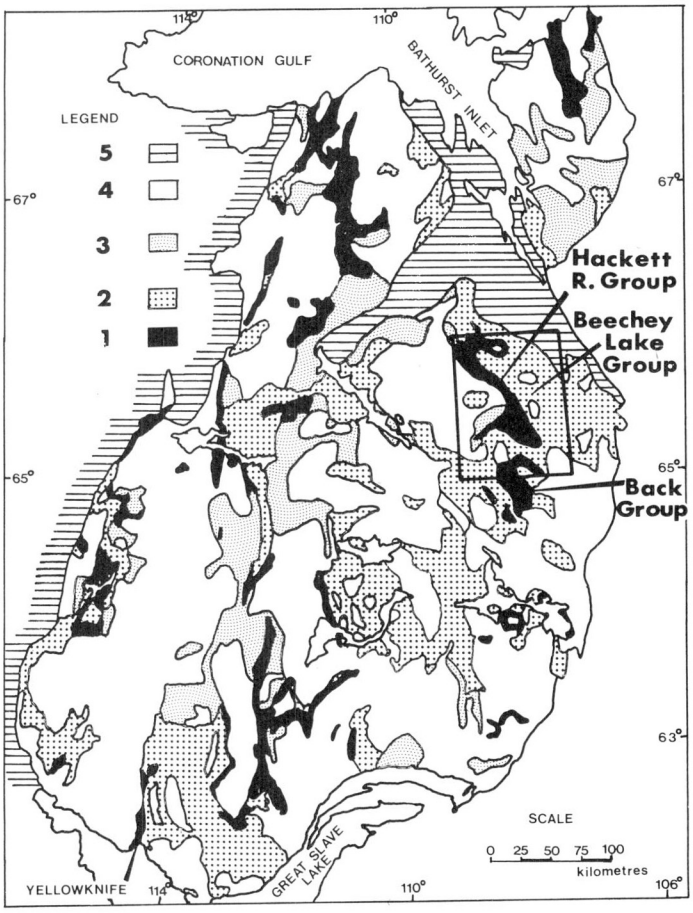
The ages of rocks in the Yellowknife Supergroup have been determined by various methods. Galenas from the sulphides near 'Camp' Lake and near 'Aitch' Lake, that are in the upper part of the Hackett River Group, formed about 2800 Ma ago (using $\mu = 8.0$, Thorpe, pers. comm., 1978). Zircons extracted from rhyolite from the Back Group give a preliminary age of 2670 Ma (Lambert, 1976).

Several cross-sections are given in Figures 15.3 and 15.4. One of the principal characteristics of the belt is the lateral discontinuity of the individual beds, which commonly pinch out or interfinger with other beds along strike. In addition, where detailed work has been carried out, steep, possibly synvolcanic faults have been noted cutting across strike, further disrupting stratigraphic continuity.

[1]Queen's University, Kingston, Ontario. K7L 3N6

TABLE OF FORMATIONS

TIME			SUPERGROUP, GROUP FORMATION, MEMBER	LITHOLOGY
Cenozoic				Glacial gravel, sand, silt, clay
Profound Unconformity				
PRECAMBRIAN	PROTEROZOIC	HELIKIAN	Mackenzie diabase	Gabbro, diabase dykes and sills
			Intrusive Contact	
			Gabbro Sill	
			Intrusive Contact	
		APHEBIAN	Goulburn Group	
			Burnside River Formation	Pink quartzite, conglomerate, sandstone
			Western River Formation	
			Upper argillite member	including greywacke, grey argillite, siltstone, quartzite
			Quartzite member	including sandstone, dolomitic sandstone
			Red siltstone member	including white quartzite, carbonate rocks, sandstone
			Local argillite member	
			Unconformity	
			Malley diabase	Gabbro, diabase dykes
	?		Intrusive Contact	
			Regan intrusive suite	
			Pegmatite	composed of muscovite, quartz and K-feldspar
			Granite	muscovite, biotite granite
			Granodiorite	biotite and/or hornblende granodiorite
			Tonalite	biotite and/or hornblende tonalite
			Diorite	hornblende diorite
			Intrusive Contact	
	ARCHEAN		Yellowknife Supergroup	
			Back Group	Flows, pyroclastics, chemical sediments
			Beechey Lake Group	Greywacke, sandstone, siltstone, argillite
			Hackett River Group	Dominantly volcanic rocks
			Ignerit Formation	Felsic to basic volcanics with chemical sediments
			Nauna Formation	Basic to felsic volcanics, flows and pyroclastics
			Siorak Formation	Quartzofeldspathic and mafic gneiss and schist
			Unconformity(?)	
			Hanimor granitoid complex	Tonalite, diorite, granodiorite, gabbro and migmatite



1 = Yellowknife Supergroup volcanic rocks

2 = Yellowknife Supergroup sedimentary rocks

3 = migmatite derived from Yellowknife Supergroup rocks

4 = granitoid rock

5 = Proterozoic cover rocks

Figure 15.1

Geologic sketch map of the Slave Province with the location of the supracrustal rocks of this report and the principal geographic locations of the region as a whole.

Hacket River Group

The Hackett River Group includes all of the supracrustal rocks that make up the informally termed Hackett River greenstone belt (Frith and Hill, 1975; Frith et al., 1977; Padgham et al., 1975b). The group is divided into three formations, which include: the Siorak, a lower gneissic and schistose formation that overlies a granitoid complex; the Nauna, an intermediate, dominantly metavolcanic formation; and the Ignerit, an upper mixed metavolcanic and metasedimentary formation which overlies most parts of Siorak and Nauna formations.

Siorak Formation The type section for the Siorak Formation is in the Hackett River area (Fig. 15.2). The formation derives its name from the Bathurst Innuit word for 'sand'. Five stratigraphic sections were studied and one type section selected (A-A', Fig. 15.4).

The Siorak Formation comprises schists and gneisses exposed on the flanks of the Hackett River gneiss dome. Although the original thickness of the formation is unknown, its present thickness is between 500 and 1000 m. Intraformational folds are locally present; however, the stratigraphic order of the members as shown in Figure 15.4 is constant.

The base of the Siorak Formation is in contact with the Hanimor granitoid complex. Contact relations are, for the most part, obscured by pegmatitic intrusions and intense deformation. Where the contact is visible, it is sharp, but the nature of the contact is unknown. The contact of the Siorak with the overlying Ignerit Formation is gradational and contacts of members within the Siorak Formation are also gradational.

The Siorak Formation consists of four members. The lowest is an interlaminated quartzofeldspathic gneiss and biotitic schist, approximately 250-350 m thick. The gneiss is a medium grained foliated rock consisting mainly of quartz, plagioclase and biotite, with minor cordierite, chlorite, sillimanite, kyanite, garnet, gedrite, cummingtonite and apatite. The biotitic schist is medium- to coarse-grained, and made up primarily of biotite, chlorite, quartz and plagioclase, with some cordierite, apatite and ilmenite. Elliptical to round quartz bodies 1-30 cm in diameter are common in the upper two thirds of the member.

The second member is a coarse grained, mafic gneiss or schist consisting mainly of amphibole (anthophyllite-gedrite, cummingtonite), as well as cordierite, garnet, biotite, chlorite, staurolite, quartz, plagioclase, ilmenite, magnetite and chalcopyrite. It is up to 20 m thick and occurs 310-475 m above the base of the formation. Rounded to irregular quartz bodies of uncertain origin are present, as are quartzofeldspathic layers.

The third member, interlaminated quartzofeldspathic gneiss and biotite schist, is 100-500 m thick and resembles the lowermost member of the formation.

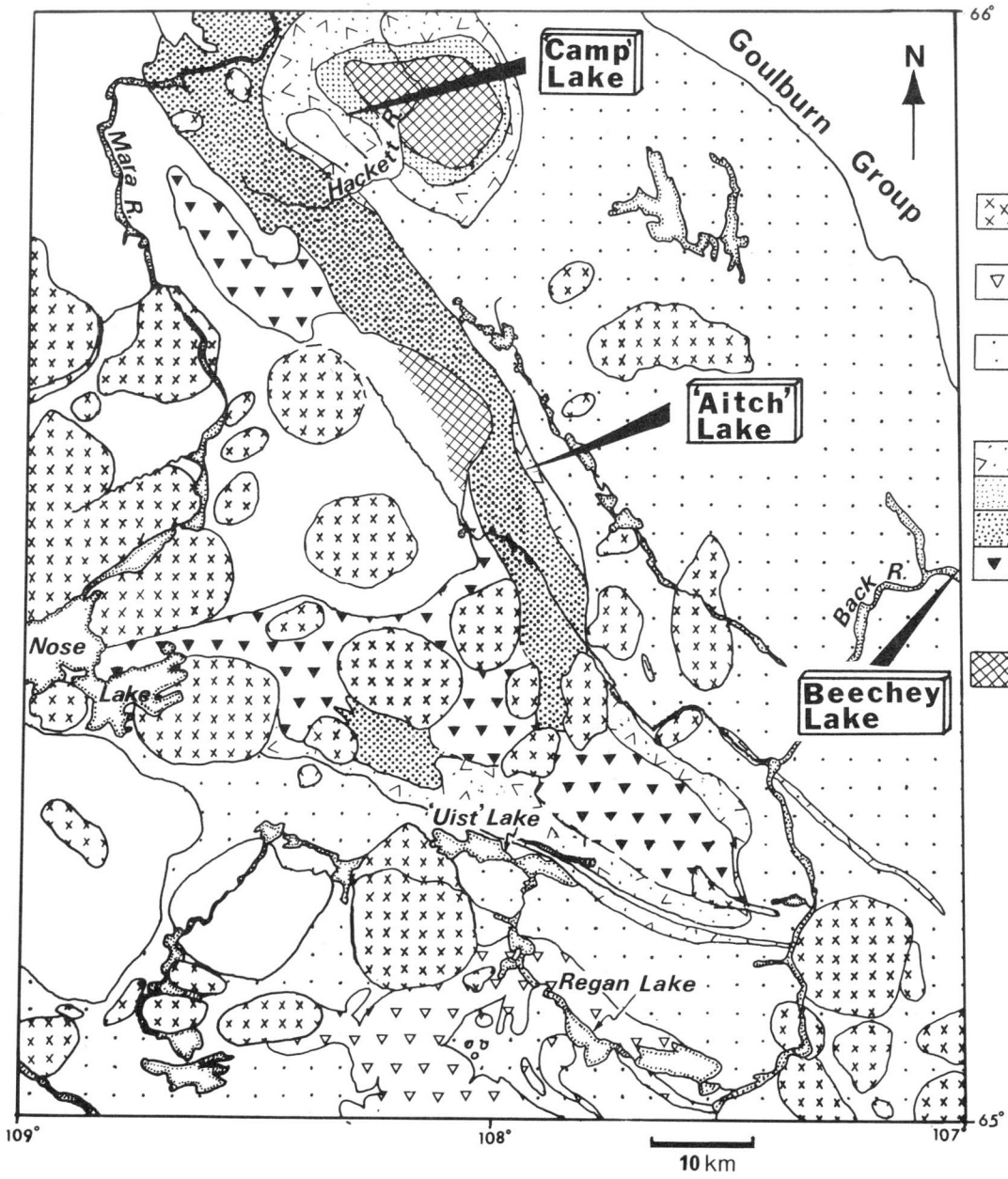
The fourth member is a sericitic schist 35-50 m thick. It is medium grained and consists of muscovite, quartz, plagioclase, biotite and some sillimanite.

In general, throughout the more mafic rocks, basic pods may occur, 1-50 m thick, of foliated hornblende-plagioclase-cummingtonite rocks.

Nauna Formation The Nauna Formation is named after the Bathurst Inlet Innuit word for 'unknown'. The formation extends the length of the Hackett River volcanic belt and its thickness ranges from 2000 m near the centre of the belt to more than 8000 m southwest of Hackett River.

The formation is made up dominantly of volcanic flows, pyroclastics and intrusive sills of felsic and mafic composition. The northern sector of the belt is more felsic than the central and southern sectors. Individual units that make up the formation are characteristically discontinuous along strike.

A type section (C-C', Fig. 15.3) was chosen where metamorphic grade is lowest, near the centre of the belt, and where detailed 1:6000 scale mapping (unpublished) was



LEGEND

- Regan intrusive suite
- Back Group
- Beechey Lake Group
- Hackett River Group
  - Ignerit Formation
  - Siorak Formation
  - Nauna Formation
    - Highly deformed and metamorphosed volcanic rocks, probably Nauna
- Hanimor granitoid complex, in part younger than Hackett River Group
- Granitoid rocks, gneisses of uncertain stratigraphic age

Figure 15.2

Geological sketch-map of the Nose-Beechey lakes map areas, showing the locations of geographic names mentioned in the text.

carried out by S.M. Roscoe and others. An additional reference section is included to represent lithologies from another depositional environment. In the type section, textures developed in a submarine environment are common, whereas in section D-D', volcanic textures of both submarine and subaerial origin are present. The description of the type section follows.

The type section (C-C', Fig. 15.3) contact of the Nauna with the basal Hanimor granitoid complex is sharp and steeply dipping. The basal member is a fine grained pyritiferous amphibolite gneiss that is locally mylonitized. The rocks are fine grained, veined, and contain hornblende phenocrysts. This member is 80 m thick and vertical bedding, possibly with pillow structures, is present. It is overlain by an aphanitic, massive quartz-eye rhyolite with some apparent primary flow banding. Mylonite zones are present in some outcrops. Fine sericite is the only secondary mineral evident. The rhyolite, which is 340 m thick, is intruded midway by an elliptical plug of fine, even grained gabbro that is about 160 m thick. A 50 m thick quartz-eye rhyolite unit overlies the massive rhyolite body and is distinguished from it by the presence of streaky mafic layers intercalated with flinty massive light-green rock. The upper rhyolite is overlain by a 160 m thick unit of pillowed, amygdaloidal andesite and basalt. The pillowed sequence is overlain by a 10 m thick layer of aphanitic, grey, quartz-eye rhyolite. This sequence of volcanic rocks, although of mixed lithology, is predominantly felsic.

This is overlain by a 600 m thick sequence that consists mainly of pillowed andesite and basalt with 5-10 m interlayers of rhyolitic tuff. Thin pyritiferous zones a few centimetres thick occur at the tops of some flow units, along with thin pyritiferous basaltic tuff beds that show excellent graded bedding. Three distinct rusty flow-top horizons can be observed within this sequence. The top of the Nauna is marked by the contact between the mafic volcanics and the overlying calcareous volcanic breccia of the Ignerit Formation that in this locality is only 60 m thick.

Contrasting with rocks of the type section are rocks of the 'Aitch' Lake caldron structure (D-D', Fig. 15.3), the centre of which contains the Yava layered sulphide deposit. Parts of the section and environs have been diamond drilled and the region has been mapped at a 1:6000 scale.

In this section the contact with the Hanimor granitoid complex is covered by drift, but isolated outcrops of the lowest unit are basic gneisses. These consist of either coarse andesite-basalt flows or intrusive diorite-gabbro. The granitoid gneisses of the Hanimor granitoid complex are cut by dykelets of aplite and granite that strike consistently in an east-west direction. The lower basic gneisses are intruded by, and exhibit sharp contacts with, a thick sill of massive hornblende tonalite that is about 3000 m thick. Smaller but more extensive sills of similar composition intrude part of the overlying Ignerit Formation. These are late-volcanic sills presumably associated with calderon subsidence (Frith and Roscoe, in prep.). The sills are fresh-looking and undeformed, except along upper contacts, which are locally altered and biotitized.

The volcanic rocks overlying the tonalite sill are vertically foliated and consist of a 7200 m thick sequence of basaltic flows with minor pyroclastics and thin beds of rhyolitic tuff and quartz-eye rhyolite. Along the base, a brecciated rhyolite zone is present. Irregular, 300 m thick bodies, mapped as gabbro or flows, occur within the sequence. No textures diagnostic of submarine conditions were recognized along this part of the section. However, 4-5 km along strike to the south some pillow structures are present, indicating the base of the sequence may have been deposited under submarine conditions. The depositional environment in the upper part of the member remains uncertain.

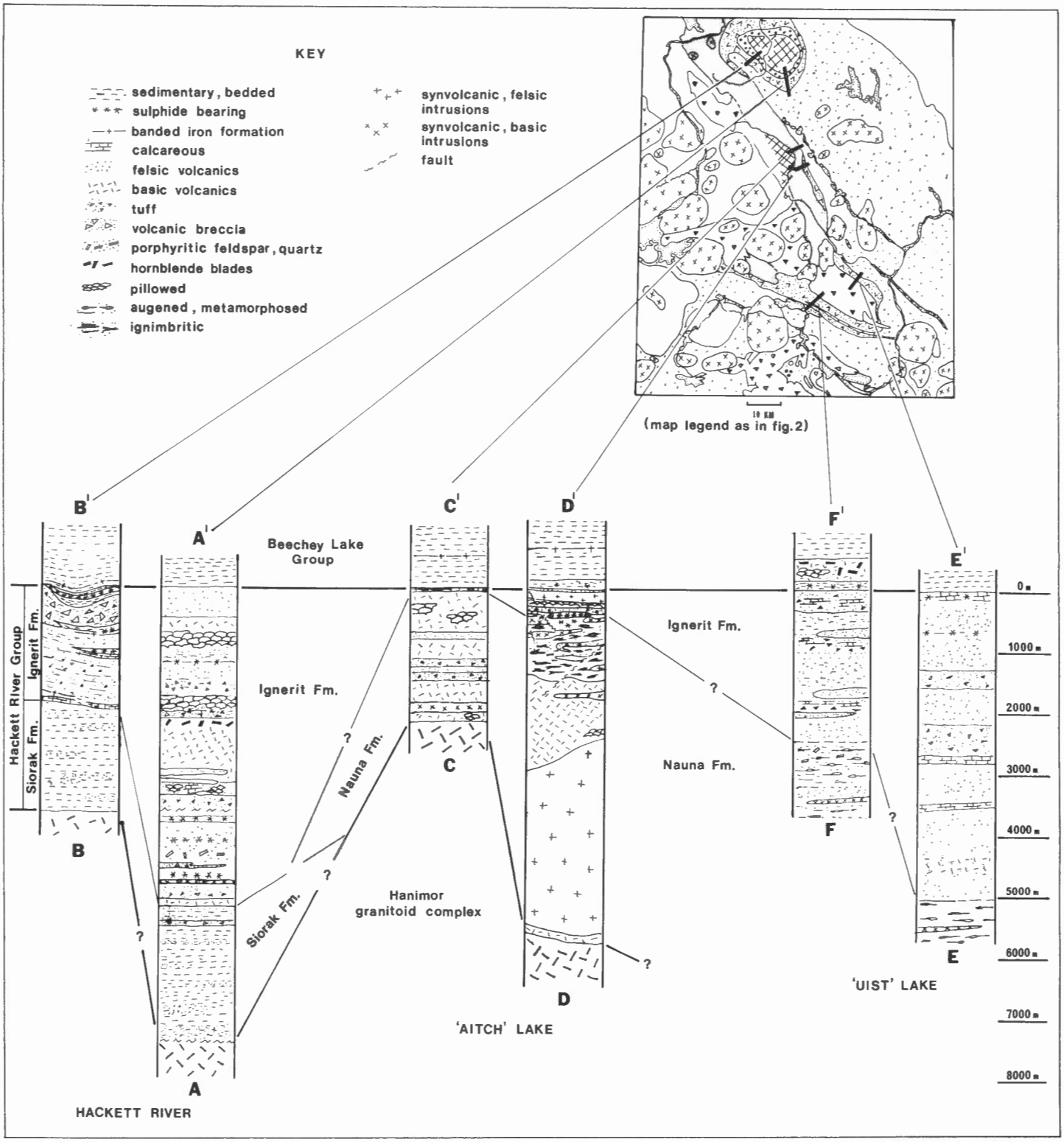
Overlying the basaltic flows is a sequence characterized by welded tuff textures, indicating subaerial deposition. The rocks are relatively homogeneous and their bulk composition is andesitic (Cameron and Durham, 1974). In detail, they are made up of small irregular fragments, many of which are dark, wispy, frayed and biotite-bearing. These fragments are commonly flattened into irregular discoid shapes, and have been interpreted as squashed pumice fragments (Lambert, pers. comm.; Frith et al., 1977). Other fragments are rhyolitic and basaltic, indicating two sources. Parts of the sequence are dacitic in bulk composition and occur in 60-120 m thick laterally discontinuous beds.

The upper part of the ignimbritic sequence is complex. The upper part contains flows or intrusions up to 150 m thick of basalt or gabbro, some of which show crosscutting relationships. These bodies commonly terminate abruptly. The overlying rocks are tuffs with fine graded bedding which forms part of the overlying Ignerit Formation. Along strike these contain the layered sulphides of the Yava deposit, along with other chemical and volcanic sediments, flows and pyroclastics.

Ignerit Formation The Ignerit Formation derives its name from the Innuit name for 'pyrite'. It contains all the potentially important mineral deposits of the Hackett River volcanic belt. The unit is mainly volcanic, but is distinguished from the Nauna volcanics by the greater abundance of dolomite, calcium carbonate, silicate iron formation, chert, oxide iron formation and sulphide deposits. In addition, the rocks are locally argillaceous and more micaceous where metamorphosed. Laterally extensive zones of sulphide mineralization, banded iron formation and graphitic shale, are common.

The principal rock types of the Ignerit Formation are thinly bedded, felsic and basic flows and pyroclastics that are separated and intercalated with chemical sediments, principally sulphides. In the type section (A-A', Fig. 15.3) the proportion of felsic to basic volcanics is about equal. The formation can be divided into four members, each capped by a zone of sulphide-rich, commonly bleached volcanic rock. The lower contact of the Siorak grades from a sericitic tuff to a tuff with no sericite. The tuff is about 100 m thick, and is overlain by thin andesitic flows with hornblende phenocrysts, and by rhyolite pyroclastic rocks. The second member is mostly rhyolite, with layers of breccia containing felsic clasts in a mafic matrix and one locally pyritiferous zone. The third member is a thin rusty andesite overlain by rhyolite tuff and pillowed to massive andesite, with some layers of rhyolite. The top consists of mafic hornblende porphyry overlain by a calc-silicate-bearing rhyolite-carbonate bed with an upper rusty zone. The upper member consists of pillowed and massive andesite with pyroclastic andesite and rhyolite, and is 2000 m thick.

In the reference section through 'Camp' Lake (B-B', Fig. 15.3, 15.5) the Ignerit Formation overlies the Siorak. The lower member of the formation is felsic, as in A-A' and it thickens to 1000 m. Other differences include the presence of an extensive carbonate and banded iron formation at the base of the formation. In section A-A' there are four or possibly five zones of chemical sediments. These are also present in section B-B' and may be correlative. The uppermost zone forms the layered sulphide deposits of the 'Camp' Lake region. The stratigraphy contrasts with A-A' in the upper third of the stratigraphic pile, which forms the footwall rocks of the 'Camp' Lake deposit in B-B'. A laharic breccia unit, concave upward and lensoid in shape in section, underlies a finely bedded member of volcanic and sedimentary rocks that contain abundant sillimanite porphyroblasts. Alteration stockworks within this member are highly silicified and contain varied amounts of sulphide minerals, including chalcopyrite,



A-A' *Type-section for the Ignerit Formation and the Siorak Formation. See also section A-A' (Fig. 15.4).*

C-C' *Type-section for the Nauna Formation.*

Figure 15.3. Reference and type-sections for formations of the Hackett River Group.

Figure 15.4. Reference sections and type-section (A-A') for the Siorak Formation near Hackett River.

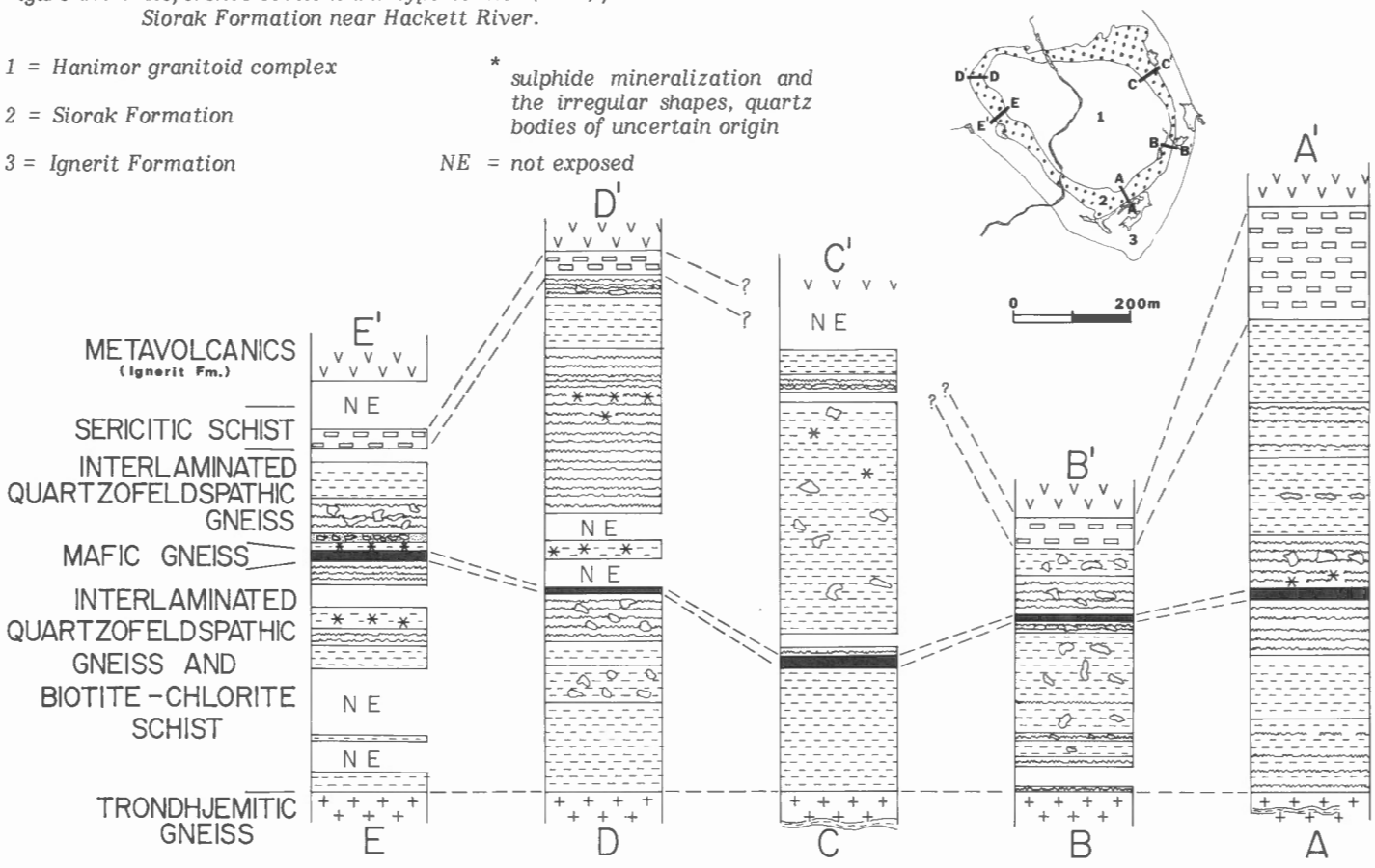
1 = Hanimor granitoid complex

2 = Siorak Formation

3 = Ignerit Formation

* *sulphide mineralization and the irregular shapes, quartz bodies of uncertain origin*

NE = not exposed



sphalerite and galena. The altered member is overlain by an interlayered sedimentary and volcanic member which includes the main sulphide deposits, along with chert, cherty tuff, calc-silicate rock, and argillaceous tuff. The sulphides occur as disseminated and massive layered units.

Parts of the Hackett River Group are highly deformed, metamorphosed or migmatized and division into formations was not practical. These rocks have been grouped with those of the Hackett River Group because of their bulk compositional similarity, remnant volcanic textures and structures, and their obvious structure and stratigraphic relationship to the group as a whole. Most are thought to be reworked Nauna volcanics.

Beechey Lake Group

The Beechey Lake Group is named after Beechey Lake, a large lake that forms part of the Back River, where it changes course from north to east. The group was informally referred to as the "Index Lake" group by Jefferson et al. (1976b). The present terminology includes all metasedimentary rocks and some minor metavolcanic rocks which overlie the Hackett River Group, but excludes the Back Group (see below) in the Nose and Beechey lakes map areas.

The Beechey Lake Group within the map area consists primarily of greywacke-mudstones that are thin to thickly bedded and vary in metamorphic grade from greenschist to upper amphibolite. The low-grade rocks are usually made up of quartz, plagioclase, chlorite, biotite and muscovite. The rocks are tightly folded and the thickest sections are exposed only on the limbs of the larger folds. No complete stratigraphic section is known in the map area. Three areas are described: one near the Back River; one overlying the main limb of the Hackett River belt; and the third in the southern part of the map area near the Back Group.

The rocks of the group are steeply dipping and generally overturned. Northeast of the Hackett River Group, along the Back River, the bedding is overturned to the southwest for 5 km and then to the northeast almost to the contact with the Goulburn Group. Thrust faulting to the northeast has probably caused repetition of beds as the apparent thickness in some areas would be in excess of 40 km. Some isoclinal fold closures are present near these possible dislocations, but bedding is reversed only locally. The sequence near the volcanic-sedimentary interface is made up of argillaceous mudstones, whereas farther away from the interface, argillaceous to sandy greywackes and coarse sandy greywackes are prevalent. The best exposures parallel the mostly navigable Back River.

The lowermost rocks of the Beechey Lake Group in the 'Aitch' Lake area (Section D-D', Fig. 15.3) have been described by Henderson (1975). The basal member is a carbonaceous and pyritic shale about 200 m thick that lies conformably on the Hackett River Group volcanic rocks. This extends about 10 km along the volcanic-sedimentary contact, gradually thinning to the margins of a basin centred over the 'Aitch' Lake caldron structure. This is overlain along a relatively sharp contact by thin bedded volcanogenic siltstones which become progressively coarser toward the east, where they become more typical of the Yellowknife Supergroup.

A thin discontinuous bed of silicate-chert-magnetite iron formation, followed within a few metres by a 50 m thick sequence of oxide iron formation containing argillite and chert, occurs 500 metres east of the shale-siltstone contact within the greywacke turbidites. The aeromagnetic expression of the iron formation can be traced, with some nebulous intervals, for 55 km.

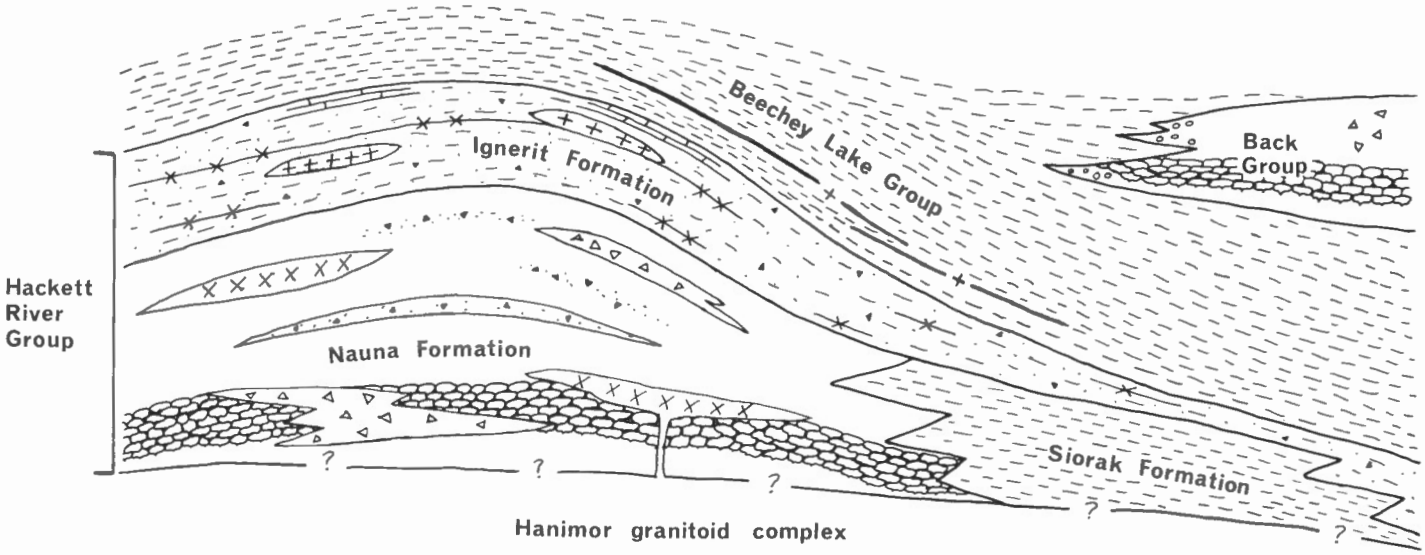


Figure 15.5. Suggested stratigraphic relationships for the Yellowknife Supergroup of the Nose-Beechey lakes map area. This is a northeast-southwest section through the northern part of the belt, with the geology to the north and south projected onto the section. Layered rocks in contact are conformable except at the base of the Back Group, where slight angular unconformities have been observed. Symbols are the same as in Figure 15.3.

The Beechey greywacke-mudstones both underlie and overlie the Back Group. The underlying rocks are thickly bedded, with grey to black argillaceous mudstone containing graded beds and rare rip-up structures. Near the Back River, where the Beechey greywacke-mudstones are thought to overlie the Back Group, the greywackes "are among the coarsest grained and thickest bedded seen anywhere in the Slave Province" (Henderson, 1975, p. 326) and they are dominantly comprised of volcanic debris. This contact of the Beechey Lake greywacke-mudstones with the Back Group may be similar to the contacts with the Hackett River Group, the Back Group contact being characterized by thin carbonaceous mudstone units and iron formations, some of which can be traced for 20 km (Henderson, 1975).

Back Group

The Back Group is named after the Back River, which flows along the southeast margin of the caldera complex. The group is a third and mostly younger succession of supracrustal rocks of the Yellowknife Supergroup. The group was informally referred to as the Back River volcanic complex by Lambert (1976, 1978) and the Back River volcanic belt by Frith et al. (1977).

The complex has a roughly elongate saucer shape and contains shallow dipping, laterally discontinuous, volcanic rocks of different composition and textural type. Towards the north the complex is thin and outliers, both round and sinuous, are present. Here the contacts with the underlying greywacke-mudstones are slightly unconformable, with rhyolite and quartz-pebble conglomerate forming part of the lower Back Group succession. Locally, volcanic rubble with clasts up to several metres can be observed.

The following description of the Back Group is based mainly on the work of Lambert (1976, 1978). The group is little deformed and metamorphosed. It comprises dominantly felsic to intermediate volcanics, including tuffs, breccias, lavas and domes, that erupted in both subaerial and subaqueous environments. The pile was built up above sea level during explosive eruptions of pyroclastics. Parts of the pile collapsed by caldron subsidence in two principal stages (Lambert, 1978). Rhyolite flows, dykes and domes are concentrated along concentric ring-fractures. Collapse breccias and lahars flank parts of the complex. Carbonate was deposited with tufa and breccia along ring-fractures and along the margins of the caldera. The units in the complex have been only slightly deformed and are gently to inwardly dipping.

The northwestern part of the complex is the most basic in composition. Here thick pillowed flows of basalt overlie dark grey to black mudstones. The contact is sharp at the base of the flows but their tops are brecciated and carbonate infilling is abundant. The north margin sediments are contorted, but in places sedimentary rocks which include banded iron formation, carbonate, and interlayered tuff and mudstone-greywacke, overlie the Back Group volcanics. The east-central side of the complex contains a unique brown oolitic carbonate.

Andesites are by far the most voluminous rock type. In places they overlie the northwest basalts. However, in the northeastern part of the complex, andesites conformably overlie Beechey Lake mudstones. Locally, slightly angular unconformities may be observed. West of Regan Lake, the base of outliers of andesite and dacite is in part conglomeratic, with rhyolite and quartz clasts.

Dacites are commonly tuffs, breccias and massive flows. Some outliers suggest that a more extensive area was originally covered by volcanics. The flows are commonly aphanitic with milk-white quartz phenocrysts in a white, pink or green groundmass.

Some tuffs and breccias may have been deposited subaerially (Lambert, 1976). The breccias contain angular fragments up to 25 cm in length in an unsorted dacitic matrix. Better sorting is evident in conglomeratic beds.

Rhyolitic domes are made up of flows and possibly intrusions of massive quartz-eye rhyolite. The margins are locally autobrecciated. Some bodies contain albite phenocrysts in a matrix of albite microlites and quartz. Quartz may or may not be present as phenocrysts. Some bodies preserve primary flow banding and locally contain carbonate, disseminated pyrite and minor Cu-Pb-Zn sulphides (Lambert, 1977).

The volcanics and underlying greywackes are cut by a multitude of gabbro, tonalite and mafic porphyry dykes,

particularly on the west side of the complex. The gabbros are steeply dipping dykes up to 1000 m wide and up to 20 km long. Composition of the dykes can vary along strike and chilled margins have been observed. Granophyric dyke centres may contain up to 25 per cent quartz and 50 per cent albite (Lambert, 1978).

The contacts between the volcanics and the sediments are complicated by deformation. The sediments are commonly highly deformed, whereas the overlying volcanics are much less disturbed. Where sediments interfinger with and overlie the volcanics, primary sedimentary structures may be preserved.

The thickness of the group is difficult to assess because it is essentially flat lying and there is little or no topographic relief. However, along the northern margin, where rocks are relatively undisturbed, the group is at least 1800 m thick.

The Hanimor Granitoid Complex

The Hanimor granitoid complex is composed of tonalitic, trondhjemitic, granodioritic and dioritic gneisses, intruded by generally more massive and less deformed bodies of granite, granodiorite and hypabyssal diabase, and granitic pegmatite. Intrusive relationships have not been observed between the tonalitic and trondhjemitic gneisses and any other rock type, either of the complex or of the supracrustal sequence. The gneissic unit is stratigraphically the lowest unit exposed in the area and the gneissic rocks are structurally and compositionally complex. The complex occurs in the core of the Hackett River gneiss dome and west of 'Aitch' Lake, near the centre of the Hackett River belt.

In section A-A' (Fig. 15.3) the underlying complex is more than 75 per cent medium-grained granodiorite with clots of hornblende or biotite in an even-grained matrix of quartz, plagioclase, and hornblende, with some perthite. The granodiorite intrudes a gneissic trondhjemite and both are intruded by gabbro dykes. The granodiorite may be related to the Regan intrusive suite, which includes granite, granodiorite and diorite that occur as plutons cutting all Archean rock units.

The trondhjemite is fine- to medium-grained and slightly porphyritic, commonly with phenocrysts of quartz up to 4 mm in diameter. The foliation is defined by streaks of biotite, commonly 5-15 per cent, in a matrix of oligoclase and quartz the two being present in about equal proportions. Hornblende may make up to 5 per cent and locally, perthitic feldspar, zircon, sphene, rutile and ilmenite, are present as accessories. The trondhjemite gneiss has not been observed cutting the Siorak Formation.

The granitoid rocks that form the basal complex west of 'Aitch' Lake underlie the narrowest part of the Hackett River greenstone belt. The complex, like the core of the Hackett River gneiss dome, is intruded by postvolcanic granodiorite and gabbroic rocks as irregular segregations and dykes.

At the contact with the volcanics, younger intrusive granitic dykelets commonly cut the volcanic rocks. Older plutonic phases, comprising diorite, tonalite and possibly granodiorite, are commonly sheared along north-south trending lineaments which tend to parallel the volcanic contact. Some tonalitic sills and plugs intrude the volcanics, but these are undeformed and more or less contemporaneous with the 'Aitch' Lake caldron subsidence event and related to late-stage acid volcanism (Frith and Roscoe, in prep.).

Older parts of the complex have not been radiometrically dated. A preliminary zircon, U-Pb determination and a Rb-Sr isochron on a younger granodiorite phase of the complex give ages of 2666 Ma and 2540 ± 130 Ma respectively (Wanless, pers. comm., 1978). The Rb-Sr age is similar to others obtained from rocks of the Regan intrusive suite, suggesting that the later granodiorite phase may be coeval.

Acknowledgments

We thank the following for their help in the preparation of this paper: Maurice Lambert provided maps, reports and comments on our treatment of the Back Group; John Henderson and Walter Fahrig critically read the paper and suggested revisions to improve the text; and Paul Kavanaugh drafted some of the figures.

References

American Commission on Stratigraphic Nomenclature
1970: Code of Stratigraphic Nomenclature; Am. Assoc. Pet. Geol. Inc., Box 979, Tulsa, Oklahoma 74101.

Baragar, W.R.A.
1966: Geochemistry of the Yellowknife volcanic rocks; Can. J. Earth Sci., v. 3, p. 9-30.

Bell, J.M.
1929: Great Slave Lake; Proc. Trans. Roy. Soc. Can., 3rd Series, v. 23, p. 5-38.

Bostock, H.H.
Geology of the Itchen Lake area, District of Mackenzie; Geol. Surv. Can., Mem 391 (also Open File no. 338). (in press)

Cameron, E.M. and Durham, C.C.
1974: Geochemical studies in the eastern Slave Structural Province, 1973; Geol. Surv. Can., Paper 74-27.

Casselman, M.J.
1977: Petrology and alteration of the Bathurst-Norsemines Central Area Deposits, Northwest Territories; unpubl. M.Sc. thesis, Carleton Univ., Ottawa, Canada.

Ewing, T.
1977: Geochemistry of the Hackett River volcanics, Northwest Territories; unpubl. M.Sc. thesis, New Mexico Institute of Mining and Technology, Socorro, New Mexico.

Franklin, J.M.
1976: Role of Laharic Breccias in genesis of volcanogenic massive sulphide deposits; in Report of Activities, Part A, Geol. Surv. Can., Paper 76-1A, p. 293-300.

Fraser, J.A.
1964: Geological notes on the northwestern District of Mackenzie, Northwest Territories; Geol. Surv. Can., Paper 63-40.

Frith, R.A. and Hill, J.D.
1975: The Geology of the Hackett-Back River Greenstone Belt – Preliminary Account; in Report of Activities, Part C, Geol. Surv. Can., Paper 75-1C, p. 367-370.

Frith, R.A., Fyson, W.K., and Hill, J.D.
1977: The Geology of the Hackett-Back River Greenstone Belt – Second Preliminary Account; in Report of Activities, Part A, Geol. Surv. Can., Paper 77-1A, p. 415-423.

Frith, R.A. and Roscoe, S.M.
Tectonic Setting and Sulphide Deposits, Hackett River Belt, Slave Province; Can. Inst. Min. Met. Bull. (in prep.).

Henderson, J.B.
1970: Stratigraphy of the Archean Yellowknife Supergroup, Yellowknife Bay-Prosperous Lake area, District of Mackenzie; Geol. Surv. Can., Paper 70-26.

1975: Sedimentological studies of the Yellowknife Supergroup in the Slave Structural Province; in Report of Activities, Part A, Geol. Surv. Can., Paper 75-1A, p. 325-330.

Henderson, J.F.
1938: Beaulieu River area, Northwest Territories; Geol. Surv. Can., Paper 38-1.

Jefferson, C.W., Padgham, W.A., Bryan, M.P.D., Royane, E.A., Shegelski, R.J., Vandor, H., and Thorstad, L.E.
1976a: Geology 76-F-15, E.G.S. Map 1976-4-preliminary edition (2 inch = 1 mile map with marginal notes); Dep. Indian Affairs and Northern Development, Ottawa.

Jefferson, C.W., Padgham, W.A., Bryan, M.P.D., Ronayne, E.A., Shegelski, R.J., Sterenberg, V.Z., Vandor, H., and Thorstad, L.E.
1976b: Geology Hackett River, 1976-F-16, E.G.S., Map 1976-4-preliminary edition (2 inch = 1 mile map with marginal notes); Dep. Indian Affairs and Northern Development, Ottawa.

Lambert, M.B.
1976: The Back River volcanic complex, District of Mackenzie; in Report of Activities, Part A, Geol. Surv. Can., Paper 76-1A, p. 363-367.

1978: The Back River Volcanic Complex – A cauldron subsidence structure of Archean age; in Current Research, Part A, Geol. Surv. Can., Paper 78-1A, p. 153-157.

Padgham, W.A., Bryan, M.P.D., Jefferson, C.W., Ronayne, E.A., and Sterenberg, V.Z.
1975a: Geology Agricola Lake, 76-G-12, E.G.S., 1975-2-preliminary edition (2 inch = 1 mile map with marginal notes), Dep. Indian Affairs and Northern Development, Ottawa.

1975b: Geology Index Lake, 76-G-13, E.G.S., 1975-2-preliminary edition, (2 inch = 1 mile map with marginal notes), Dep. Indian Affairs and Northern Development, Ottawa.

Percival, J.A.
1978: Stratigraphy, Structure and Metamorphism of the Hackett River Gneiss Dome, District of Mackenzie, N.W.T. unpubl. M.Sc. thesis, Queen's Univ.; Kingston, Ontario.

Sangster, D.F.
1972: Precambrian volcanogenic massive sulphide deposits in Canada: A review; Geol. Surv. Can., Paper 72-22, 44 p.

Tremblay, L.P.
1971: Geology of Beechey Lake map-area, District of Mackenzie, a part of the Western Canadian Precambrian Shield; Geol. Surv. Can., Mem. 365, 56 p.

1976: Geology of Northern Contwoyto Lake Area; District of Mackenzie; Geol. Surv. Can., Mem. 381, 56 p.

Wright, G.M.
1957: Geological notes on the eastern district of Mackenzie, Northwest Territories; Geol. Surv. Can., Paper 56-10.

SAMPLING OF BOTTOM SEDIMENTS IN THE EQUATORIAL PACIFIC FOLLOWING TEST MANGANESE MINING*

Gustavs Vilks
Atlantic Geoscience Centre,
Dartmouth, Nova Scotia

Stephen A. Swift
Pacific Marine Environmental Laboratory,
National Oceanic and Atmospheric Administration,
Seattle, Washington 98115

Introduction

During March and April of 1978, Ocean Management Inc. (OMI) carried out an experiment to retrieve manganese nodules from the seafloor of the Pacific Ocean south of Hawaii (Fig. 1). The manganese nodules and surface sediment were scooped up by a collecting unit on the bottom of the ocean and a mixture of bottom water, sediment, and nodules was pumped to the surface through a pipe of the drill ship SEDCO 445.

The effect of the mining activity on the environment was monitored by members of the Deep Ocean Mining Environmental Study (DOMES) project, which is administered by the Pacific Marine Environmental Laboratory of NOAA in Seattle, Washington. The oceanographic surveys associated with the monitoring were carried out from the NOAA ship OCEANOGRAPHER.

During the mining operations, OCEANOGRAPHER monitored the extent and characteristics of the suspended sediment plume spreading from the mining vessel and from the seabottom collection. Resuspended material was collected and oceanographic parameters measured within the euphotic surface zone and close to the bottom as part of a study of plume dispersal patterns and mechanisms. Post-mining operations consisted primarily of a systematic collection of benthic faunas, which will be compared with the base line information obtained prior to the mining. This report is a preliminary assessment of the nature of sediments collected during the post-mining phase.

During the initial phase of DOMES the oceanography of the northeastern tropical Pacific was studied to establish a comprehensive base line data set against which post-mining surveys could be statistically compared (Ozturgut et al., 1978). The mining site (Fig. 1) lies within the eastward flowing North Equatorial Counter Current just south of a divergence zone at about 10°N. Nutrient concentrations in the wind mixed layer (40-50 m thick) are comparable to values at the equator (Montgomery and Stroup, 1962), but productivity within the euphotic zone (110-120 m thick) is much less (Koblentz-Mishke, et al., 1970). Concentration of suspended particulate matter in the surface water is highest at 50-80 m (in the pycnocline) where there is a maximum in the chlorophyll a (a measure of phytoplankton standing stock) vertical profile. The small amount of particulate matter found below 200 m (<10-20 µg/L) is fine calcareous and organic debris derived from the breakup of fast settling zoo plankton fecal pellets. Within the bottom 400 m the 10 µg/L while temperature and salinity show no significant change. Baker et al. (1978), using geochemical evidence, suggested that the SPM was mostly resuspended bottom sediment. Near bottom currents (measured for 143 days in 1976 at 6 m off the bottom) averaged 3.2 cm s^{-1} to the northwest. Maximum recorded speeds of 20-25 cm s^{-1} were probably sufficient to erode fine grained bottom sediments.

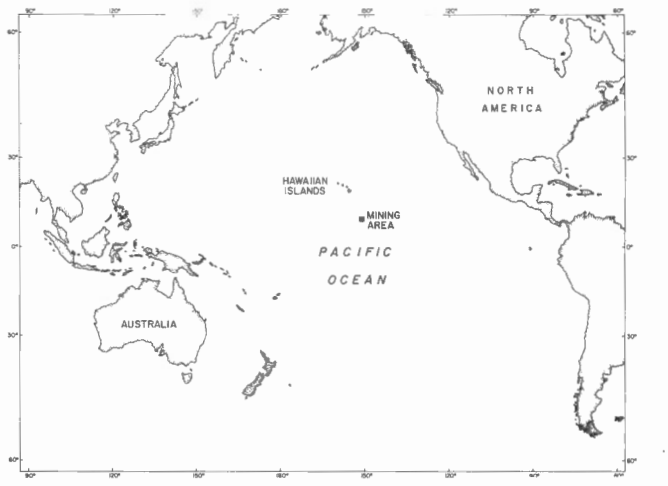


Figure 1. Index map.

The water depth at the mining site ranges from 4600 to 5300 m. The average relief of the abyssal hills is 400 m; slopes are commonly less than 5° (but ranging up to as steep as 36°); and their axial trend is to the north and northeast. Crustal age is 75-80 Ma (van Andel et al., 1975). According to Piper et al. (1977), the average sediment thickness is about 150 m, high angle faulting of sediments is present, and subsurface acoustic reflectors reach the surface along the slopes of the abyssal hills. The basic sediment type is a Quaternary brown silliceous clay with significant amounts of reworked Tertiary fossils. Sedimentation rates average 1-3 mm/10^3 years. Only trace amounts of calcium carboante are found in the sediments despite the fact that coccolithophorids are the dominant phytoplankton in the surface waters; the calcium carbonate compensation depth lies at about 4500 m (van Andel et al., 1975).

Methods

Sampling stations were chosen randomly within a 9x11 km rectangle, where the mining activity had taken place. The exact sampling sites were established with Accoustic Transponder Navigation (ATNAV) system using 14 reference transponders on the seafloor. The sampling-navigation array lowered from the ship consisted of a pinger and a transponder attached to the cable above a 0.5x0.5 m boxcore. At selectable intervals (3 minutes), a shipborne computer initiates an interrogation between the transponders on the sea floor and on the sampling unit. On the basis of signal travel times, the computer is programmed to plot the position of the sampler (as it descends) relative to the reference transponders on the bottom. At alternate intervals the shipborne ATNAV interrogates directly the seafloor transponders to determine the ship's position. As a result of the constant updating of the two positions, the ship can be manouvered to take bottom samples to the accuracy of ship's length from the desired locality of the seafloor 5000 m below.

Between May 18 and 28, 1978, 38 boxcores were taken in water ranging in depth from 4900 to 5300 m. In 26 cores (68%) the surface sediment was undisturbed. From these cores the uppermost 10 cm of sediment and all manganese nodules were removed for a subsequent study of benthic fauna. Observations of manganese nodule distribution and changes in sediment characteristics with depth were made in most of the 38 cores.

* Contribution No. 376 from NOAA/ERL Pacific Marine Environmental Laboratory.

From: Scientific and Technical Notes in Current Research, Part C; Geol. Surv. Can., Paper 78-1C.

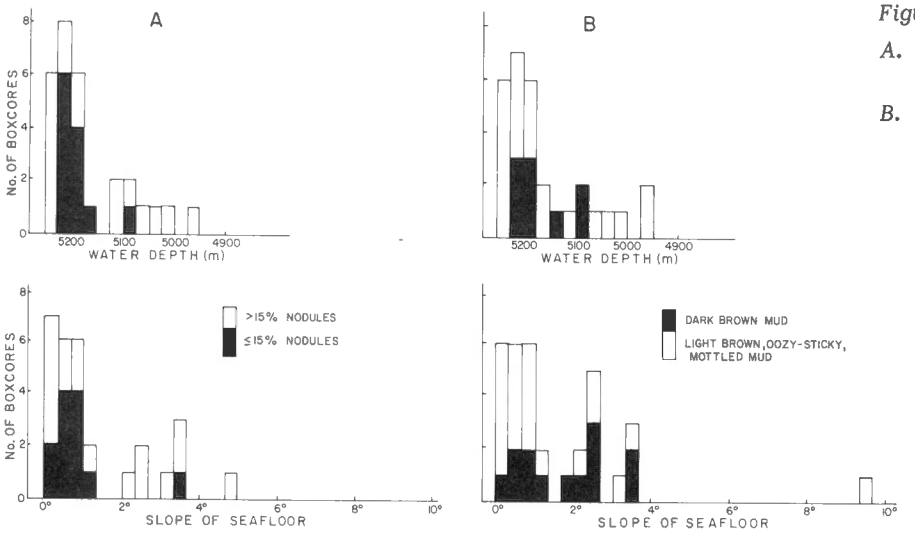


Figure 2

A. Correlation of manganese module abundance with water depth and slope of seafloor.

B. Correlation of sediment colour with water depth and slope of seafloor.

Observations

The surface layer of the sediments is light brown and on the average 10 cm thick with a range from 30 cm to a few millimetres. Sediment coarser than 74 microns is partly fibrous, brownish grey biogenic material, with no evidence of calcareous skeletons being present.

Manganese nodules were found lying on top of the surface sediment in each of the boxcores taken. Generally, the nodules are flattened ovoids, but are occasionally irregular, rounded or botryoidal. The maximum diameters range from 0.5 cm to 10 cm, with an average of approximately 4 cm. The surface of the nodules is either smooth or gritty and slightly friable.

Manganese nodules are present in higher numbers where the surface layer of the sediment is thicker than 5 cm. The nodules lie evenly distributed on the surface of the soft mud and are partly submerged. The estimated average bottom surface covered by the nodules is 25% of the 2500 cm^2 taken by each boxcore. The maximum estimated area covered by the nodules is 80% and the minimum about 1 per cent. The depth of water or the slope of the seafloor in the vicinity of the sampling site do not correlate with nodule abundance (Fig. 2A).

Only few and small benthic animals were visible on top of the sediment. Most commonly, sessile animals (sponges, foraminifera) were attached to the nodules. Occasionally the surface of the clay was covered with recognizable fecal pellets, casts or worm tubes. One boxcore contained a sea urchin and several samples included brittle stars.

The lithostratigraphy in the cores consists basically of two kinds. The more common type (23 out of 33 observations) consists of a homogeneous and oozy surface layer that grades at a depth of 10-15 cm to a more cohesive and mottled clay. Below the surface layer the colour pattern is characterized by light brown burrow infillings in a medium brown matrix. The second type has similar surface layer, but the contact between the surface and subsurface sediments is sharp with a very thin surface layer evident in a few of the cores. Below the surface the colour is dark brown and the sediment separates in fragments and is not sticky. This deeper layer contains numerous burrows, some of which are very large (5 cm in diam). The burrows are filled with lighter coloured clay in several colour zones. A light brown central zone grades to a bright yellow marginal zone that has a sharp contact with the matrix. A thin layer of black sediment separates the matrix from sediment in the burrows.

The sharp contact between the thin layer of the oozy recent sediments (missing on one core) and the semiconsolidated subsurface clays of the second type probably represent a previous period of nondeposition and erosion. After removal of the recent layer, the upper surface of the semiconsolidated clays is pitted (to depth of 1-2 cm) exposing excellent cross-sections of the burrows described above. The sharp upper contact and the comparatively high consolidation characteristics of the subsurface clays suggest a much greater age for the dark brown, dry clay of the second type.

The lithologic evidence suggests pelagic sedimentation of the now semi-consolidated dark brown unit, a period of erosion ending at least 17 000 years before present (5 cm surface ooze at 0.3 cm/1000 years from Thayer, 1977), followed by a period of normal pelagic sedimentation of the light brown unit. The occurrence of the two lithologies (Fig. 2B) suggest that the erosion occurred more frequently at the base of the abyssal hills where there are a wide range of slopes. However, these distribution patterns can be explained as well by nonuniform sedimentation since the erosional event. Winnowing of fine grained material from around the base of abyssal hills may have produced thinner deposits of post-erosion sediments in some locations, allowing the boxcore to penetrate to the much older consolidated sediments below. Detailed biostratigraphic studies of these cores are needed to describe the sequence of sedimentation events.

References

Koblentz-Mishke, O.J., Volkovinsky, V.V., and Kabanova, J.G.
1970: Plankton primary production of the world ocean, in Scientific exploration of the South Pacific Wooster, W.S., ed., Natl. Acad. Sci., Washington, p. 183-193.

Montgomery, R.B. and Stroup, E.P.
1962: Equatorial waters and currents at 150°W in July-August, 1952; Johns Hopkins Oceanographic Studies, No. 7, Baltimore, Johns Hopkins Press, 68 p.

Ozturgut, E., Anderson, G.C., Burns, R.E., Lavelle, J.W., and Swift, S.A.
Deep ocean mining of manganese nodules in the North Pacific. Pre-mining environmental conditions and anticipated mining effects; NOAA/ERL Technical Rept., U.S. Dept. of Commerce, Boulder, Colo. (in press)

Piper, D.Z., et al.
1977: Deep ocean environmental study: geology and geochemistry of DOMES Sites A, B, and C, Equatorial North Pacific; U.S. Geol. Surv., Open File Rept. 77-778.

van Andel, Tj.H., Heath, G.R., and Moore, T.C.
1975: Cenozoic history and paleoceanography of the central equatorial Pacific Ocean; Geol. Soc. Am., Mem. 143, 134 p.

SPORE FLUORESCENCE COLORATION – A RAPID MICROSCOPIC METHOD OF MATURATION ASSESSMENT

Stephen Creaney
Institute of Sedimentary and Petroleum Geology, Calgary

Introduction

Microscopic 'rank' or maturation assessment currently involves three techniques:

1) Vitrinite reflectance determination. This developed from the early work of Hoffman and Jenkner (1932) and was used by several subsequent authors to assess coal rank Seyler (1948), Broadbent and Shaw (1955), McCartney and Ergun (1958), Murchison (1958), Kötter (1960). Recently this type of work has been extended to include vitrinite contained in other sediment types (Bostick, 1970, 1971; Castaño and Sparks, 1974).

2) Transmitted light coloration of various organic matter types. This technique was initiated by Gutjahr (1966) who used the colour of spores and pollen grains in transmitted light as a rank indicator. The method was further developed by Staplin (1969) and utilized by several subsequent workers including Correia (1971), Cramer and Diez (1975), Gunther (1976), Bujak et al. (1977).

3) The most recent technique utilizes the fluorescent properties of spores during ultraviolet irradiation and was described by Ottenjahn et al. (1975). The method involves photometric measurement of the spectrum of emitted light from ultraviolet irradiated spores. Sophisticated measuring equipment is necessary (Teichmüller and Wolf, 1977) and also computer facilities for rapid data processing.

Vitrinite reflectance is the most accurate microscopic rank parameter but the technique is often limited by a paucity of first-generation vitrinite within largely marine sequences. Transmitted light coloration studies are subjective and show only subtle colour variations across the prime oil generation zone (Bujak et al., 1977). Spectral fluorescence measurements are relatively time consuming and require expensive equipment. The present study briefly outlines the results of a more approximate, rapid version of the spectral fluorescence technique.

Results

Ottenjahn et al. (1974, 1975) showed by spectral measurement that the spectral fluorescence colour of sporinite normally shifts to a longer wavelength as rank increases, i.e., the fluorescence colour of sporinite changes from green in the peat stages to brown in the medium-volatile bituminous coal stage. During the present study, 60 coal samples encompassing this rank range were examined under ultraviolet irradiation and the fluorescent colour of the spore population was simply described. The apparatus used was a Leitz MPV 2 microscope equipped with a 100 W high pressure mercury lamp and a BG 38/UGI filter combination, to produce ultraviolet radiation (365 nm). The results of this work are summarized in Figure 1. The four simple colour categories in Figure 1 are those which could be readily recognized.

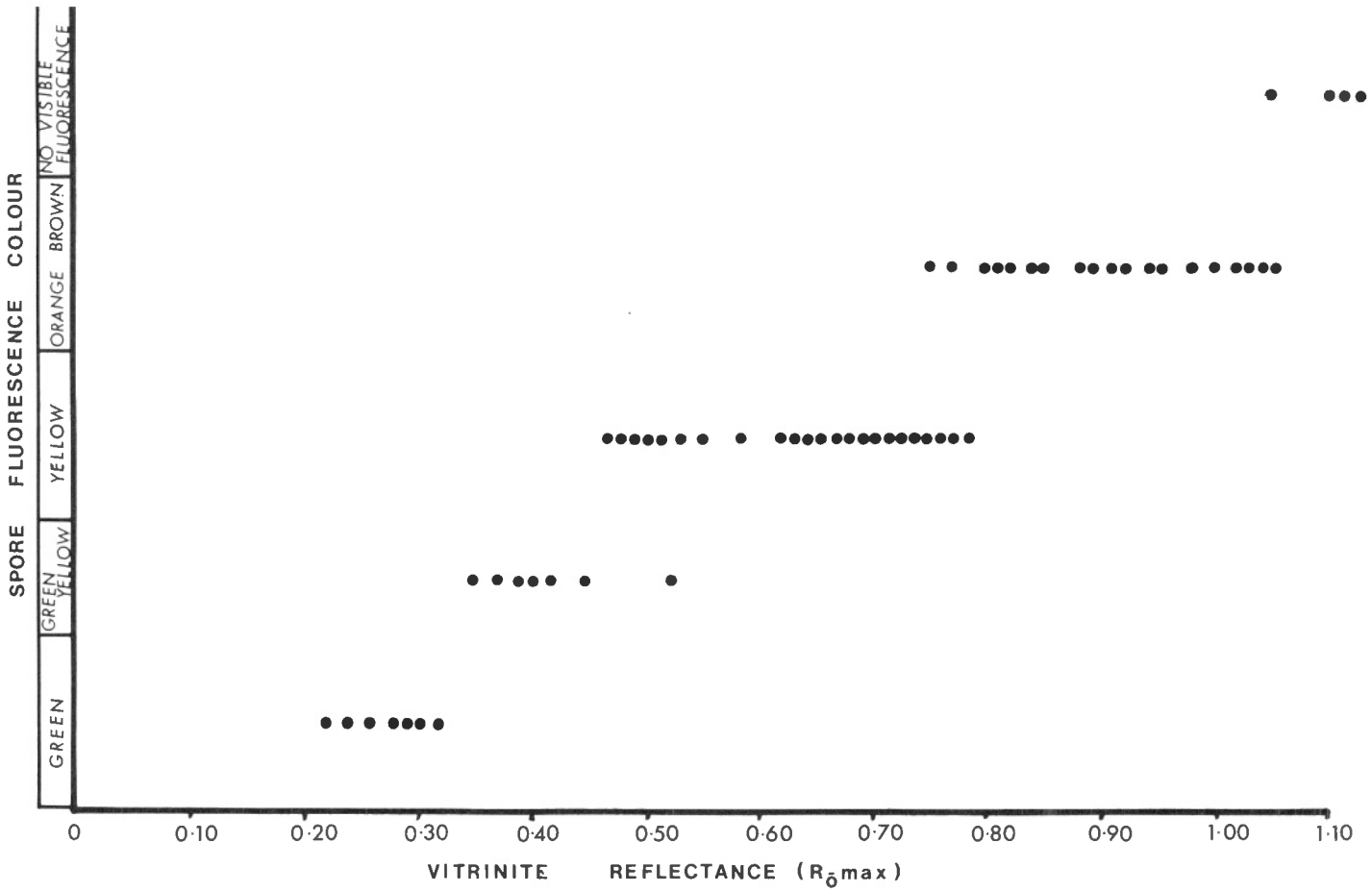


Figure 1. Results of 60 coal samples examined under ultraviolet irradiation.

From: Scientific and Technical Notes in Current Research, Part C, Geol. Surv. Can., Paper 78-1C.

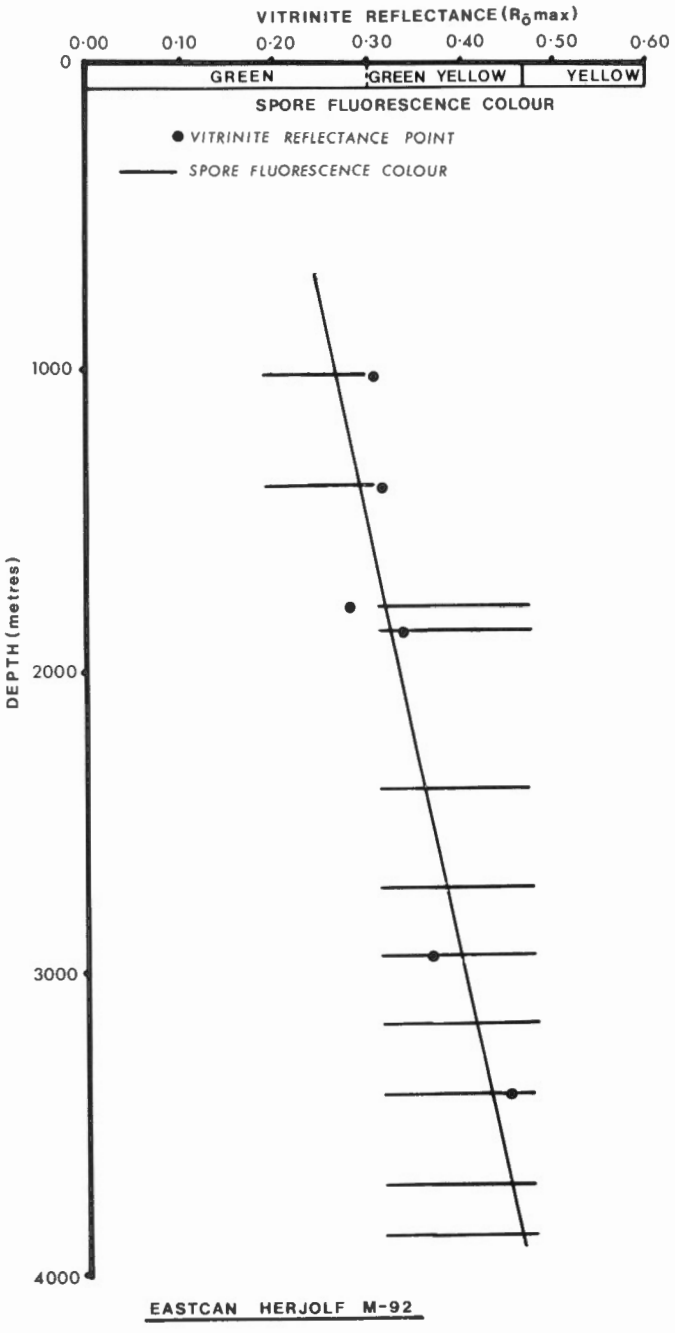


Figure 2. Results of samples exposed to ultraviolet irradation from the Eastcan Herjolf M-92 well.

Obviously simple visual assessment of colour is very subjective (Wyszecki and Stiles, 1967) but the results show good correlation with the photometrically determined results of Ottenjahn et al. (1975). Also the colour variation across this rank range is reasonably large and consequently the various stages are more easily recognized. The total disappearance of spore fluorescence at 1.05 per cent maximum vitrinite reflectance and the loss of green coloration at approximately 0.45 per cent vitrinite reflectance both agree well with previous work and allow approximate division of the oil and gas generation zone (up to 1.20 per cent vitrinite reflectance – Teichmüller and Wolf (1977)).

This type of study is currently being applied to Canadian oil and gas exploratory wells and proving useful in vitrinite deficient sequences. Figure 2 illustrates the results from the Eastcan Herjolf M-92 well (Labrador Shelf). The small amount of reflectance data that was obtained has been supported by extensive spore fluorescence coloration data. The spore colorations were determined on spores observed in relief polished "raw cuttings" samples, thus eliminating any lengthy extraction procedure. The results indicate a thick sequence of immature to marginally mature sediments (green/yellow fluorescence colour) equivalent to a vitrinite reflectance of 0.40 to 0.50 per cent.

Conclusions

The results indicate that visually assessed fluorescence coloration can provide a very useful support parameter for vitrinite reflectance in vitrinite depleted sequences. Subjective colour determinations suffer from the disadvantage of operator dependence but have the advantages of being rapid and requiring no photometer or data acquisition equipment.

References

Bostick, N.H.
1970: Measured alteration of organic particles (phytoclasts) as an indicator of contact and burial metamorphism in sedimentary rocks; Abstr. Geol. Soc. Am., v. 2, no. 2, p. 74.

1971: Thermal alteration of clastic organic matter as an indicator of contact and burial metamorphism in sedimentary rocks; Geoscience and Man, v. III.

Broadbent, S.R. and Shaw, A.J.
1955: Reflectance of coal; Fuel, Lond., v. 34, p. 385.

Bujak, J.P., Barss, M.S., and Williams, G.L.
1977: Offshore East Canada's organic type and color and hydrocarbon potential (Parts 1 and 2); Oil and Gas J., Apr. 4th and 11, 1977.

Castaño, J.R. and Sparks, D.M.
1974: Interpretation of vitrinite reflectance measurements in sedimentary rocks and determination of burial history using vitrinite reflectance and authigenic minerals; Geol. Soc. Am., Spec. Paper 153.

Correia, M.
1971: Diagenesis of sporopollenin and other comparable organic substances – application to hydrocarbon research in Sporopollenin, J. Brooks, P.R. Grant, M.D. Muir, P. Van Gijzel and G. Shaw, ed.; Academic Press, p. 569-620.

Cramer, F.H. and Diez, M.C.R.
1975: Palynological determination of organic maturity; in Advances in Organic Geochemistry 1975, R. Campos and J. Goni, ed.; Empresa Nacional Adaro de Investigaciones Mineras, Madrid.

Gunther, P.R.
1976: Palynomorph color and dispersed coal particle reflectance from three Mackenzie Delta boreholes; Geoscience and Man, v. XV, p. 35.

Gutjahr, G.C.M.
1966: Carbonization measurements of pollen grains and spores and their application; Leidse. Geol. Meded., v. 38, p. 1.

Hoffman, E. and Jenkner, A.
1932: Die Inkohlung und Ihre Erkennung in Mikrobilo; Glückauf, 68, p. 81.

Kötter, K.
1960: Die Mikroskopische Reflexionsmessung mit dem Photomultiplier und Ihre Anwendung auf die Kohlenuntersuchung; Brennst. – Chemie, v. 41, p. 263.

McCartney, J.T. and Ergun, S.
1958: Optical properties of graphite and coal; Fuel, Lond., v. 37, p. 272.

Murchison, D.G.
1958: Reflectance of vitrinite; Brennst. – Chemie, v. 39, p. 547.

Ottenjahn, K., Teichmüller, M., and Wolf, M.
1974: Spektrale Fluoreszenz-Messuneen an Sporiniten mit Auglicht-Anregung, eine Mikroskopische Methode zur Bestimmung des Inkohlungsgrades Gering Inkohlter Kohlen; Fortschr. Geol. Rheinl. u. Westf., v. 24, p. 1.

Ottenjahn, K., Teichmüller, M., and Wolf, M. (cont'd.)
1975: Spectral fluorescence measurements of sporinites in reflected light and their applicability for coalification studies; in Pétrographic Organique et Potential Pétrolier, B. Alpern, ed., p. 49, C.N.R.S., Paris.

Peters, K.E., Ishiwatari, R., and Kaplan, I.R.
1977: Color of kerogen as index of organic maturity; Bull. Am. Assoc. Petrol. Geol., v. 61, no. 4, p. 504.

Seyler, C.A.
1948: The past and future of coal – the contribution of coal petrology; Proc. S. Wales Inst. Engrs., v. 63, p. 213.

Staplin, F.L.
1969: Sedimentary organic matter, organic metamorphism and oil and gas occurrence; Bull. Can. Petrol. Geol., v. 17, p. 47.

Teichmüller, M. and Wolf, M.
1977: Application of fluorescence microscopy in coal petrology and oil exploration; J. Microscopy, v. 109, pt. 1, p. 49.

Wyszecki, G. and Stiles, W.S.
1967: Color science; John Wiley and Sons, Inc., New York, London, Sydney.

AN ORTHORHOMBIC UNIT CELL FOR TLALOCITE

A.C. Roberts
Central Laboratories and Administrative Services Division

Tlalocite $Cu_{10}Zn_6(TeO)_3\ (TeO_4)_2C\ell(OH)_{25}\cdot 27\ H_2O$ is an extremely rare mineral found at the Bambollita mine, Moctezuma, Sonora, Mexico. Originally described by Williams (1975), it has been fully characterized except for indexing of the powder diffraction pattern. With regard to the indexing, Williams states, "Attempts at indexing the pattern failed. Two axes, 12.062 Å and 16.782 Å will index most of the lines nicely, and after this much progress, failure to discover a third axis, assuming an orthorhombic cell, suggests that the mineral is monoclinic. Alternatively, as most of the remaining unindexed lines are faint, poorer d-values may account for the problem." The purpose of this short note is to report an orthorhombic cell consistent with the powder diffraction data.

The powder pattern was indexed by a combination of visual inspection of the d-spacings, the Heese-Lipson procedure and trial and error indexing. The two axes reported by Williams, 12.062 Å and 16.782 Å, were clearly present and the third axis, approximately 20.10 Å was deduced by the trial and error method. Refinement of these approximate cell parameters led to the following unit cell: a = 16.780(3) Å, b = 19.985(4) Å, c = 12.069(3) Å.

The powder data of Williams (1975) is reproduced in Table 1, together with the calculated d-spacings and miller indices related to the orthorhombic cell. The computed cell volume is 4047.32 $Å^3$. With Z = 4, the calculated density is 4.58 g/cc, in very good agreement with the value of 4.55 ± 0.1 g/cc measured by Williams.

Table 1

Orthorhombic indexing of Tlalocite*

I	d meas.	d calc.	hkℓ
10	16.787	16.780	100
8	8.394	8.390	200
1/2	5.895	5.832	031
1	5.593	5.593	300
10	4.201	4.195	400
1	4.101	4.102	302
1	3.912	3.912	103
1	3.569	3.569	213
2	3.442	3.444 3.444	402 033
6	3.355	3.356	500
1/2	3.204	3.213 3.211 3.192	440 061 511
2	3.095	3.097 3.096	252 260
1	3.026	3.017	004
2	2.969	2.970	104
1	2.830	2.836 2.835	442 053
3	2.796	2.797 2.796	600 153
2	2.700	2.699	611
3b	2.588	2.586	362
3b	2.473	2.471	180
2	2.390	2.389	105
1/2	2.329	2.328	073
3	2.110	2.109	661
2	1.860	1.860	803
2	1.817	1.817	0110
4	1.560	1.560	186

*powder data taken from Williams (1975)

indexed on an orthorhombic cell with a = 16.780(3), b = 19.985(4) and c = 12.069(3) Å.

Reference

Williams, S.A.
1975: Xocomecatlile, $Cu_3TeO_4(OH)_4$, and tlalocite, $Cu_{10}Zn_6(TeO_3)(TeO_4)_2C\ell(OH)_{25}\cdot 27\ H_2O$, two new minerals from Moctezuma, Sonora, Mexico; Min. Mag., v. 40, no. 311, p. 221-226.

From: Scientific and Technical Notes in Current Research, Part C; Geol. Surv. Can., Paper 78-1C.

OBSERVATIONS ON THE PALEOMAGNETISM OF SOME SEDIMENTS FROM ELLESMERE AND DEVON ISLANDS, DISTRICT OF FRANKLIN

R.J. Richardson
Terrain Sciences Division

Introduction

Three short lake sediment cores and twelve sediment plugs from a river section were collected from southern Ellesmere Island during the summer of 1977 as part of the project entitled "Quaternary Geochronology, Arctic Islands" (Blake, 1978). These samples were taken to study the paleomagnetic characteristics of some Holocene arctic sediments. Sampling of the lake sediments also served to test a light-weight (25 kg) gravity corer and tripod constructed for S.M. Blasco by the Technical Services Section (G.A. Meilleur, Head), Central Laboratories and Administrative Services.

The unnamed lake from which cores were recovered measures 2.8 by 1 km; it is situated 15 km west of Makinson Inlet, Ellesmere Island (Fig. 1, and see Blake, 1978, Fig. 36.2). Coring was carried out from the surface of the ice near the southeastern end of the lake (77°15'N, 82°46'W). The lake was chosen because of its proximity to base camp and because in early July it had the solid ice cover (1.8 m thick) necessary for coring. Many other lakes in the area, particularly those nearer sea level, had lost most of their ice cover because of warm weather during the early summer. The elevation of the lake (over 300 m a.s.l.), its large size relative to others in the area, and the depth of water (12 m at the coring site) probably contribute to the persistence of ice until relatively late in the season.

The sediment plugs of marine clayey silt were collected at a river section 2 km east of the base camp (Fig. 1) on Swinnerton Peninsula (Fig. 36.2 in Blake, 1978).

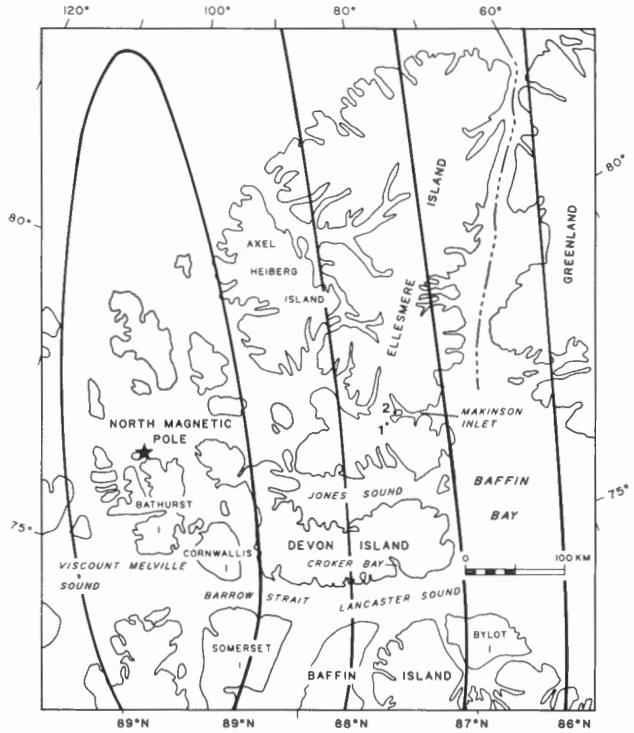


Figure 1. Map showing the location of the sample sites (1. lake site, 2. river section site), position of the North Magnetic Pole, and contours of equal magnetic inclination (based on Isoclinic Chart 1975.0, Earth Physics Branch).

From: Scientific and Technical Notes in Current Research, Part C, Geol. Surv. Can., Paper 78-1C.

Field Methods and Results

In order to obtain the lake sediment cores, several holes, spaced a few tens of centimetres apart, were bored through the lake ice using a powerdriven unit (STIHL model 4308) with an 8 cm inside diameter core barrel. The holes were joined and enlarged using an ice chisel, until a 30 to 40 cm wide hole (large enough to allow free passage of the corer's fins) was produced. Using this method it took more than two hours to cut through the 1.8 m thickness of ice. A light-weight (25 kg) Benthos-type gravity corer suspended from a tripod of all aluminum construction (to reduce weight for field use) was then dropped through the hole. A hand cranked, rachet-type winch attached to one leg of the tripod was used to recover the corer.

Three short (ca. 19 cm) cores of lake sediment were recovered in less than half an hour. The lack of significant penetration of the corer was a result of its light weight and the stiffness of the sediment. The sediments are finely laminated clayey silts having average clay and silt contents of 30% and 70%, respectively, based on six analyses (Fig. 2) with a SediGraph 5000 Particle Size Analyzer. X-radiographs (Fig. 2) show that the two cores chosen for paleomagnetic analysis (sample BS-77-25; core 2, core 3) contain identical horizons and, with the exception of the lowermost 2 cm, the sediments are undisturbed. Disturbance at the base is thought to have been caused by the core catcher.

Samples of marine clayey silt (32% clay, 68% silt; determined with a SediGraph) were obtained from the river section by pushing thin walled (2 mm thick) plastic vials (4.5 cm in diameter and 9.5 cm long) vertically into a freshly cut horizontal face. The vials then were removed by cutting away the surrounding material. The sediment plugs were oriented, with respect to north, by utilizing the National Topographic System 1:250 000 map (Vendom Fiord, 49D), prominent geographic features, and a line inscribed on the outside of each vial. Little or no disturbance of the sediments could be detected as having occurred using this easy and rapid method of sampling. A total of twelve vials were taken from the same horizon for paleomagnetic analysis although only seven were studied.

Paleomagnetic Results and Discussion

Specimens were measured at 2 cm intervals in cores 2 and 3, and the declination and inclination data are shown in Figure 2. Each specimen was measured first for natural remanent magnetism (NRM) and then remeasured after demagnetization (cleaning) in eleven peak fields of 50 to 1000 oersteds. It was found that the samples had a single component of remanent magnetization which was stable at a cleaning field of 200 oersteds. The basal 2 cm interval in both cores produced erratic data due to disturbance by the core catcher during sampling; these erratic data are omitted from Figure 2.

Declination is plotted relative to zero which is the average between the extreme east and extreme west declinations. It was not possible to orient the corer, with respect to some azimuth, during sampling. Average inclinations of six samples each from cores 2 and 3 are +66° and +65°, respectively. The plots of inclination and declination for the cores appear to be similar (Fig. 2), suggesting that the magnetic character is real.

A 4 m long core (H74-026-95) of marine sediments collected by Blake from Croker Bay, Devon Island (Fig. 1, 74°45.77'N, 83°13.2'W; see Blake and Lewis, 1975) and previously reported on by Lichti-Federovich (1976) presently is being studied in more detail. It is interesting that the top 18 cm of this core has a similar magnetic signature to those of cores 2 and 3 (Fig. 2). The average inclination from the upper six samples of the Croker Bay core is 64°, a value which is essentially the same as that for the lake cores.

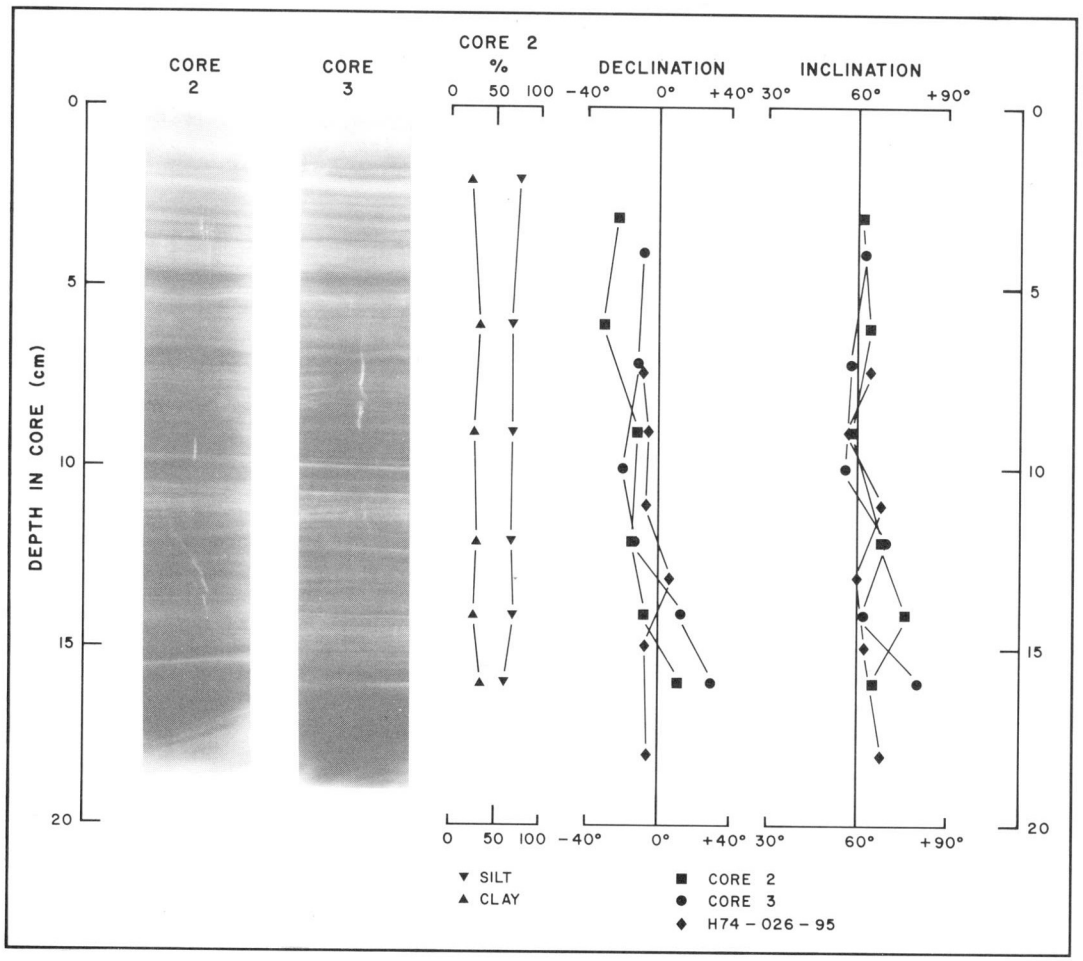


Figure 2. Inclination and declination plots of cores 2, 3, and H74-026-95 with X-radiographs of cores 2 and 3, and a plot of the silt-clay content of core 2.

A lack of organic material (including pollen[1]) in the cores has made absolute dating impossible. However, since both the lake and marine cores come from active depositional environments and since the uppermost sediment apparently was sampled in each case, it is reasonable to expect these sediments to be Holocene. Considering then the latitude of the coring sites and the present (1975) position of the magnetic pole 450 km to the west off the north coast of Bathurst Island, the inclination values are far too shallow for Holocene sediments. An inclination of +87.5° is estimated for both coring locations, from the Isoclinic Chart, 1975.0, Earth Physics Branch (Fig. 1). Assuming a geocentric axial dipole, the expected inclination for the lake sediments would be +83° and for the Croker Bay site +82°.

Three possible explanations for the discrepancy between the predicted and measured inclinations are that: 1) the sediments are older than expected, 2) they have been physically disturbed, or 3) they have a large 'inclination error'. The first possibility has already been discussed and is thought to be unlikely; however it cannot be ruled out as no dates have been obtained. The stable and similar magnetic character of the sediments, as well as the undisturbed fine layering seen in the X-radiographs in Figure 2, argues against the second possibility. The most likely conclusion is that the sediments display a significant inclination error. Not evident, however, is why the magnitude of error is so similar (±2°) for the three cores.

Verosub (1977) has discussed depositional and post-depositional processes in the magnetization of sediments. He notes that sediments from lakes and marginal seas, where sedimentation rates are commonly high, can have observed magnetizations that may represent either depositional detrital remanent magnetization (DRM), associated with various alignment errors, or postdepositional DRM, accurately recording the ambient field. Recently, Blow and Hamilton (1978), experimenting with remanent magnetism in artificially redeposited silty clays, found that for these sediments postdepositional compaction is a major factor in shallowing the observed inclination from the ambient field inclination. The low inclination values recorded by the clayey silts in the present study likely are a result of depositional DRM and compactive DRM and their associated errors. Since inclination errors can be 'locked into' a sediment because of compaction or dewatering below a critical value (Verosub, 1977), one must also be cautious about interpreting inclination data from older sediments.

Seven sediment plugs from a marine clayey silt dated at 8930 ± 100 years (GSC-2519; Blake, 1978) were analyzed in the same manner as the lake sediments. These samples, however, were oriented and gave a declination value of 314.1° and an inclination of +65.3°. The virtual geomagnetic pole (VGP) position was computed at 55.3°N, 203.4°W (near the western side of Kamchatka Peninsula) with an 8.25° radius of the 95% zone of confidence. Although these

[1] A pollen analysis of the upper 2.5 cm of core 2 produced so few grains of pollen that it was of little use even as reference for plants presently growing in the area (unpublished GSC Palynological Rep. No. 77-10, R.J. Mott).

sediments had a stable remanent magnetism (at a demagnetization field of 200 oersteds), it is not certain, because of possible locked in inclination errors, that the earth's geomagnetic field was accurately recorded. Inaccuracies inherent in the method of orientation (described earlier) also could have a considerable effect on the VGP position as could some local nondipole features of the earth's geomagnetic field at the time of deposition.

Conclusions

The light-weight gravity corer used for sampling the lake sediments was found to be too light for any significant penetration into stiff clayey silts. It did, however, prove successful in recovering short cores of the surface sediments.

Some recent sediments apparently are not accurately recording the present ambient field in the Canadian Arctic. They have inclination values which are about 22° too shallow. Inclination records from older sediments also may be suspect.

Acknowledgments

The author is indebted to W. Blake, Jr. for his assistance and advice during this study and to T. Frisch, Regional and Economic Geology Division, for providing logistical support. S.M. Blasco and J.H. Foster are thanked for providing equipment and for making many useful suggestions. W.E. Podolak performed the particle size analysis and D. Lusk, CANMET Non-destructive Testing Laboratory, produced the X-radiographs. Valuable comments on improving an earlier form of the report were made by T.W. Anderson and R.J. Mott.

References

Blake, W., Jr.
1978: Aspects of glacial history, southeastern Ellesmere Island, District of Franklin; in Current Research, Part A, Geol. Surv. Can., Paper 78-1A, p. 175-182.

Blake, W., Jr. and Lewis, C.F.M.
1975: Marine surficial geology: observations in the High Arctic, 1974; in Report of Activities, Part A, Geol. Surv. Can., Paper 75-1A, p. 383-387.

Blow, R.A. and Hamilton, N.
1978: Effect of compaction on the acquisition of a detrital remanent magnetization in fine-grained sediments; R. Astron. Soc., Geophys. J., v. 52, no. 1, p. 13-23.

Lichti-Federovich, S.
1976: A preliminary list of diatoms from sea floor sediments in Croker Bay, Devon Island, District of Franklin; in Report of Activities, Part B, Geol. Surv. Can., Paper 76-1B, p. 133-136.

Verosub, K.L.
1977: Depositional and postdepositional processes in the magnetization of sediments; Rev. Geophys. Space Phys., v. 15, no. 2, p. 129-143.

CARBON/NITROGEN (C/N) RATIOS IN SURFICIAL MARINE SEDIMENTS OF BRITISH COLUMBIA

Brian D. Bornhold
Regional and Economic Geology Division

Introduction

"The C/N ratio and the total organic matter in marine sediments vary widely between environments but one or both are usually an important, sensitive, distinctive environmental characteristic" (Goodell, 1972). The purpose of this study was to compare sediments from various marine environments in British Columbia with respect to C/N ratios and to attempt to deduce the relative contributions of marine and terrestrial organic material.

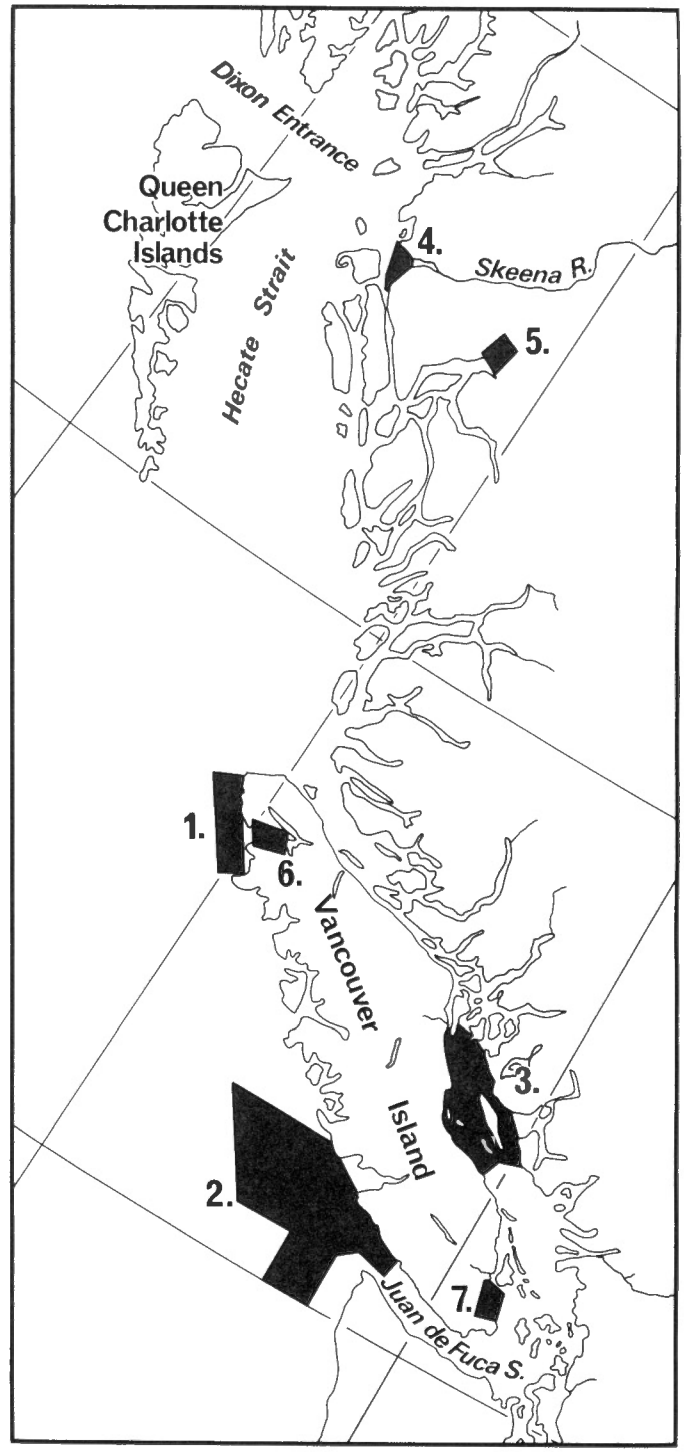
The ratio of organic carbon to nitrogen in marine sediments is a function of both the source of the organic matter and processes of decomposition. According to Deevey (1973) the biosphere, which is quantitatively dominated by woody plant tissue, has an average C/N ratio of 92.5. Within this, marine plankton range from about 5.4 to 8.3 (Fleming, 1940; Ketchum and Redfield, 1949; Harvey, 1960) with a mean of approximatley 5.7 (Fleming, 1940). C/N ratios within land plants, on the other hand, are considerably higher and vary more widely than in marine plankton: Clarke (1924) gave the C/N ratio for wood as 54.0 and Garrels et al. (1973), averaging and weighting data from many sources, suggested a value of 89. For the purposes of this paper Clarke's ratio of 54 will be used because: (1) it has been used by previous workers (Gucluer and Gross, 1964); and, (2) much of the identifiable plant material in the samples from the British Columbia coastal areas is wood.

Because amino acids and proteins, the main nitrogenous componds in organic matter, are less stable under geological conditions than hydrocarbons, C/N ratios tend to increase with age in marine sediments (e.g., Trask and Patnode, 1942; Bader, 1955). According to Degens and Mopper (1976), however, C/N ratios remain fairly constant during the early stages of diagenesis. In the present study, sedimentation rates are very high in many areas (greater than 0.5 mm/year in the fiords) and the grab sampler removes only the uppermost 7 to 8 cm or less. It has been assumed, therefore, for the purpose of this preliminary study, that the sediments are in the earliest stages of diagenesis and that their C/N ratios reflect reasonably faithfully those of their source materials. As will be seen, the C/N ratios in sediments from the areas of lowest sedimentation rate, the continental shelf, have very low C/N ratios suggesting that diagenesis even in these areas has had little effect on the C/N ratios.

Four geological environments were selected for comparison (Fig. 1): (1) open shelf (west coast of Vancouver Island); (2) enclosed shelf (northern Strait of Georgia); (3) deltaic (Skeena Delta) (Fig. 2); and, (4) fiord (Kitimat Arm, Quatsino Sound, and Saanich Inlet). With the exception of Saanich Inlet all samples were obtained by the Geological Survey. Samples from the Skeena Delta were collected by Luternauer (1976); from the northern Strait of Georgia by Clague (1975); from southwestern Vancouver Island by Milliman (1976) and Luternauer (1976); and from Kitimat Arm by Luternauer and Swan (1978). The results obtained by Gucluer and Gross (1964) were used for Saanich Inlet.

Methods

Samples containing more than about 15 per cent mud were selected for analysis since organic carbon and nitrogen levels in coarser sediments are, in general, quite low. At very low concentrations, analytical error becomes significant (Emery and Uchupi, 1972) leading to wide scatter in C/N values. All samples were dried and pulverized prior to analysis.



1. *Northwest Vancouver Island shelf*
2. *Southwest Vancouver Island shelf*
3. *Northern Strait of Georgia*
4. *Skeena Delta*
5. *Kitimat Arm*
6. *Quatsino Sound*
7. *Saanich Inlet*

Figure 1. Location map of western British Columbia showing the areas studied.

From: Scientific and Technical Notes in Current Research, Part C, Geol. Surv. Can., Paper 78-1C.

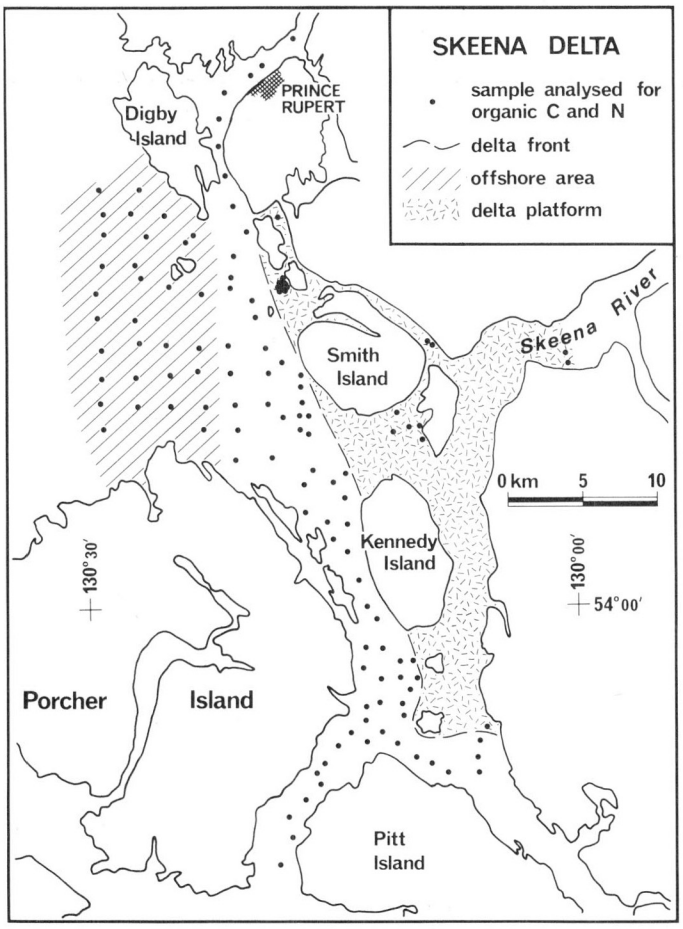


Figure 2. Location map of the Skeena Delta area and samples analysed for organic C and N.

Organic Carbon

Dried pulverized samples were boiled in HCl, to remove all carbonates, and placed on LECO crucibles. The samples were dried and analyzed using a LECO induction furnace. Every fifth sample was repeated; results were reproducible to ± 0.02 per cent.

Nitrogen

Dried pulverized samples were digested and distilled using the Kjeldahl procedure. Nitrogen was determined by titration of the liberated ammonia. Duplicate analyses were made on every fifth sample; results were reproducible to ± 0.01 per cent.

Results

The organic carbon and nitrogen results are presented in Figures 3 through 6 for each of the four environments. The mean C/N ratio and the standard deviation envelope is shown on each graph.

Open Shelf

The lowest mean C/N ratio in this study was found in samples from the open shelf area off western Vancouver Island (Fig. 3). The mean for all samples (302) was 6.10 with a standard deviation of 1.33. Within this area, ratios are somewhat, though not significantly higher (6.20) off southwestern Vancouver Island than off northwestern Vancouver Island (6.01). Organic carbon values were everywhere less than 2 per cent and nitrogen, less than 0.4 per cent.

Enclosed Shelf

Samples from the northern Strait of Georgia have a mean C/N ratio comparable to that on the open shelf, 6.16 for 124 samples; the standard deviation was 2.88. Much of the variance is contributed by a relatively few (23) samples with very low organic C and N contents, as is apparent in Figure 4. If, for example, only samples with greater than 0.1 per cent N are considered, the standard deviation diminishes to 1.30 and the mean becomes 5.53.

Organic carbon values were all less than 3.5 per cent and nitrogen, less than 0.5 per cent.

Deltaic

Samples from the vicinity of the Skeena Delta (Fig. 2) have an overall C/N ratio of 7.21 and a standard deviation of 2.33 (Fig. 5; 123 samples). C/N ratios for the offshore samples (area A, Fig. 2) have a mean of 5.93 (26 samples). Excluding these samples, the mean C/N ratio for the remaining samples increases to 7.61 and if only the samples from the delta platform are considered, the mean C/N ratio increases again to 7.77 (13 samples).

Organic carbon values are all less than 3 per cent with all but three samples falling below 1.5 per cent; nitrogen values are all less than 0.4 per cent with all but three, less than 0.3 per cent.

Fiords

Samples from Quatsino Sound (12 samples) and Saanich Inlet (19 samples) are very similar in their C/N ratios (Fig. 6), averaging 6.84 and 6.85, respectively; with standard deviations of 1.03 and 0.96. A slight trend towards higher C/N ratios with increasing organic C content in Saanich Inlet is apparent.

Saanich Inlet samples reach 5.26 per cent organic C and 0.65 per cent N. Those from Quatsino Sound are somewhat lower, less than 3.5 per cent organic C and 0.55 per cent N.

Samples from Kitimat Arm (Fig. 6) contrast markedly with those from either of the other fiords. The mean C/N ratio is 14.29 (14 samples) with a standard deviation of 4.05. Organic carbon values are less than 2 per cent and nitrogen, less than 0.12 per cent.

Discussion

The C/N ratios in samples from the west coast of Canada agree very well with results obtained elsewhere (Table 1). In general, open continental shelves are characterized by lower ratios than nearshore areas because of lower levels of terrestrial plant material in offshore sediments. Sharp (1975) showed that C/N ratios of particulate organic matter in seawater average 6.0 in oceanic waters and 7.14 in estuarine waters. He attributed this difference to the presence of detrital organic matter from higher plants in estuarine and nearshore waters.

Shelf Areas

The very low values (6.1 to 6.2) found for the open shelf off Vancouver Island and for the Strait of Georgia imply that very little organic matter from terrestrial sources is reaching these areas. Using C/N ratios of 5.7 and 54.0 for plankton and wood, respectively, the average sample from both the open shelf and the northern Strait of Georgia would contain less than 1 per cent terrestrial plant material. For the open shelf, 80 per cent of the samples contain less than 3 per cent terrestrial plant material. For the northern Strait of Georgia 80 per cent of the samples contain less than 5 per cent terrestrial organic matter.

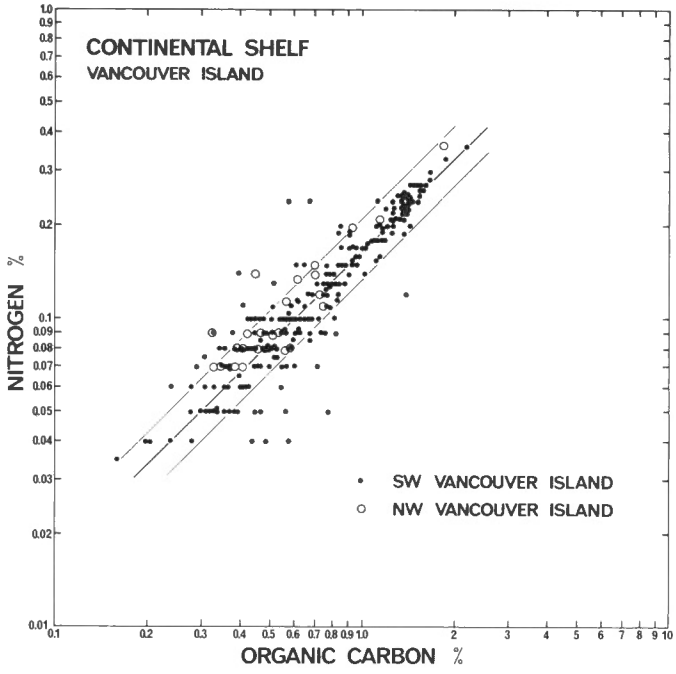


Figure 3. Graph of N versus organic C for samples from western Vancouver Island.

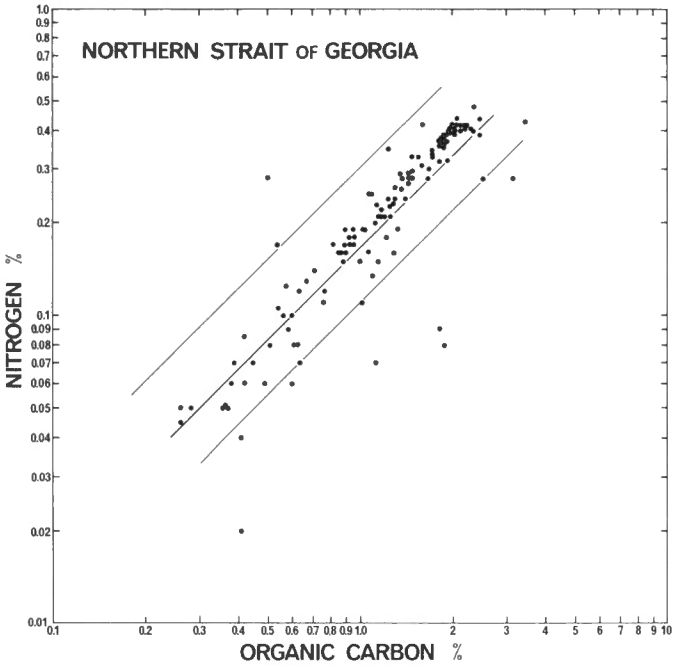


Figure 4. Graph of N versus organic C for samples from northern Strait of Georgia.

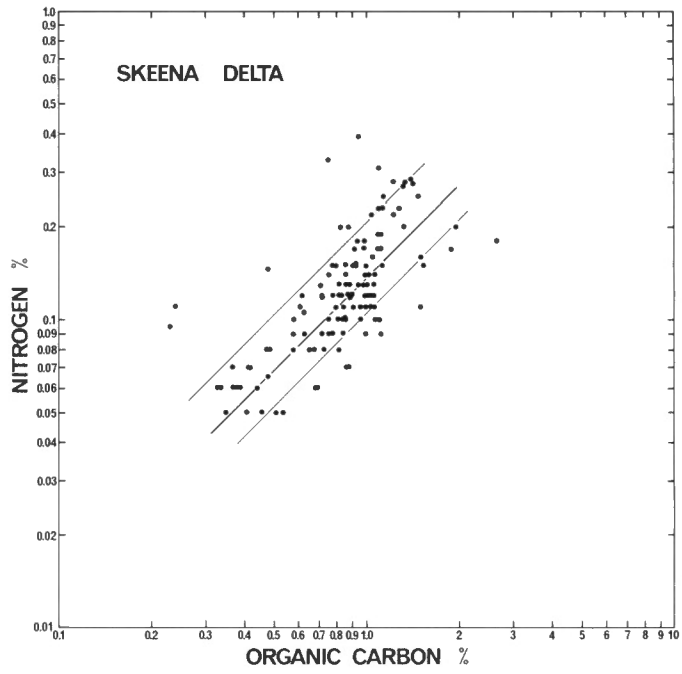


Figure 5. Graph of N versus organic C for samples from the Skeena Delta.

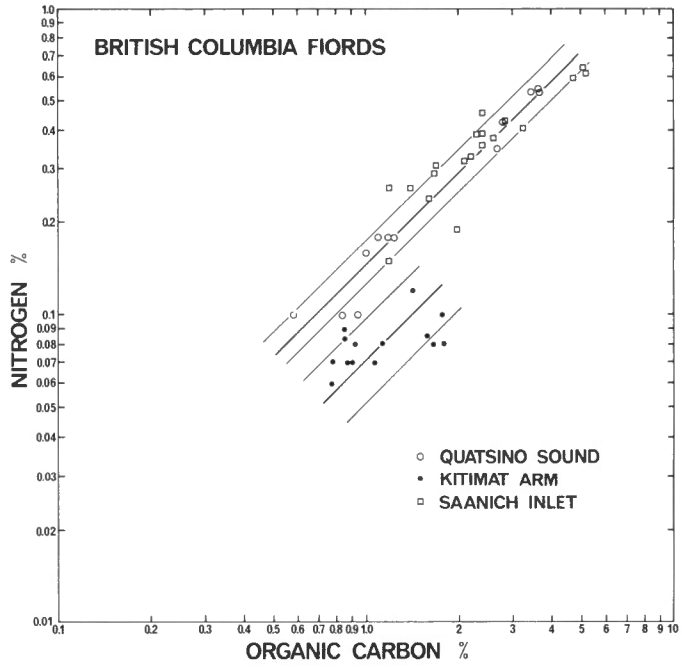


Figure 6. Graph of N versus organic C for samples from Quatsino Sound, Saanich Inlet and Kitimat Arm.

In the case of the open shelf these results are not suprising since most modern sediment is trapped within the fiords and never reaches the shelf. Thus, the only source of organic matter is marine plankton with very low C/N ratios.

The low values in the northern Strait of Georgia are somewhat unexpected, however, since the area is surrounded by high, heavily wooded terrain. A possible explanation is that few major rivers enter the Strait from Vancouver Island and most rivers on the mainland enter fiords which are trapping much of the modern detrital sediment. The occurrence of several samples with C/N ratios between 10 and 25 suggests that locally detrital plant material can make a significant contribution to the sediment.

Skeena Delta

The C/N ratios for the Skeena Delta samples are significantly higher (>99 per cent probability; Mann-Whitney U test) than those from either of the shelf areas, a result of

Table 1

C/N ratios in surface sediments

Locality	C/N Ratio	Environment	Source
Antarctic Shelf - Weddell Sea Ross Sea	4.0 7.2	open shelf	Goodell (1972)
Gulf of Paria - Central Gulf	6.8	open shelf	von Andel and Postma (1954)
Atlantic U.S. continental margin (including estuaries)	7.0	mainly open shelf	Emery and Uchupi (1972)
Southwest Africa	7.3	open shelf	Degens and Mopper (1976)
Gulf of Paria - Marginal shelf	7.6	nearshore shelf	von Andel and Postma (1954)
Buzzards Bay, Massachusetts	7.58	nearshore shelf	Roman (1978)
New York Bight	11.1	nearshore shelf	Degens and Mopper (1976)
Marine fiord	8.3	fiord	Bader (1955)
Puget Sound	9.5	fiord	Bader (1955)
Gulf of Paria - Delta platform	13.4	delta	von Andel and Postma (1954)
West Coast Vancouver Island	6.10	open shelf	this paper
Northern Strait of Georgia	6.16	enclosed shelf	this paper
Skeena Delta - Entire region Nearshore area Delta platform	7.21 7.61 7.77	delta	this paper
Quatsino Sound	6.84	fiord	this paper
Saanich Inlet	6.85	fiord	Gucluer and Gross (1964)
Kitimat Arm	14.29	fiord	this paper

proportionately higher terrestrial plant debris. The progressive decrease in mean C/N ratio from more than 7.75 on the delta platform to less than 6.00 in the offshore area near the delta reflects the greater contribution of marine plankton to the offshore sediments.

The average sample in the Skeena Delta area, however, contains less than 5 per cent detrital organic material, with 80 per cent of the samples containing less than 7 per cent. Even the sample with the highest C/N ratio (15) would contain only 15 per cent terrestrial organic material.

Fiords

C/N ratios for the sediments in Quatsino Sound and Saanich Inlet are somewhat higher than open shelf values (significantly different at 90 per cent level; Mann-Whitney U test) reflecting the expected increase in land-derived plant material. As Gucluer and Gross (1964) concluded for Saanich Inlet, however, using C/N ratios of 5.7 and 54 for plankton and wood, samples from these fiords contain less than 3 to 5 per cent terrestrially derived organic material. The slight trend toward increasing C/N ratios with increased organic C content in Saanich Inlet is probably a result of the observed increase in abundance of wood in the deeper parts of the central basin of the inlet (Gucluer and Gross, 1964).

Kitimat Arm is significantly different (>99 per cent level; Man-Whitney U test) from all of the other localities in terms of C/N ratios. The average sample contains 18 per cent land-derived plant material and one-third of the samples contain more than 25 per cent detrital plant debris.

The differences between Kitimat Arm and the other two fiords is thought to be due to differences in fluvial input. No major rivers enter either Saanich Inlet or Quatsino Sound whereas the samples from Kitimat Arm were taken at the foot of the large Kitimat River delta. In addition to the much higher fluvial input into Kitimat Arm, activities of the logging industry, particularly within the last decade, have undoubtedly affected the composition of organic matter in the inlet (Bell and Kallman, 1976). Logging in the Kitimat River valley has been intense, a pulp mill has been established at Kitimat, and much of the delta has been used as a log storage and handling area. All of these activities have led to an increased delivery of bark and wood chips to the floor of Kitimat Arm.

Even in the absence of the logging industry, however, the high C/N ratios in Kitimat Arm may not be unexpected. Anderson (1962) reports C/N ratios of over 50 from Deep Inlet, Alaska. He attributes these very high values to the tremendous fluvial influx of wood debris.

Conclusions

As von Andel and Postma (1954) and Gucluer and Gross (1964) have shown, an analysis of C/N ratios in surface sediments permits at least a preliminary assessment of the relative contributions of marine and terrestrial sources of organic matter. Clearly, the great variability of C/N ratios, particularly in terrestrial plants, precludes a precise evaluation of the amount of organic material from each source within an individual sample. Regional differences and trends can be demonstrated, however, and can provide a basis and direction for more detailed studies of organic geochemistry.

In this investigation of sediments from British Columbia waters, the following conclusions can be drawn:

(1) Despite striking differences in geographic setting between the northern Strait of Georgia and the open continental shelf off Vancouver Island, the C/N ratios are remarkably similar and indicate a very low input of terrestrial plant material.

(2) Samples from the Skeena Delta and from all of the fiords contain organic matter with significantly higher C/N ratios than either of the shelf areas.

(3) Despite major differences in the geochemical environment between Quatsino Sound and Saanich Inlet, the C/N ratios are very similar and imply a minimal input of terrestrial organic material.

(4) Sediments from Kitimat Arm, because of much greater fluvial influx, and possibly because of local logging activity, have significantly higher C/N ratios than either of the other fiords.

Acknowledgments

I am indebted to John L. Luternauer and John J. Clague of the Geological Survey who provided their samples for this study. Lesley Simpson selected and prepared the samples for analysis. Walt Cretney of the Ocean Chemistry Section, Institute of Ocean Sciences and John Luternauer critically read the manuscript and offered many helpful suggestions.

References

Anderson, N.K.
1962: Recent Sediments of Deep Inlet, Alaska, a fjord estuary; unpubl. M.S. Thesis, University of Washington, Seattle.

Bader, R.G.
1955: Carbon and nitrogen relations in surface and subsurface marine sediments; Geochim. Cosmochim. Acta, v. 7, p. 205-211.

Bell, L.M. and Kallman, R.J.
1976: The Kitimat River Estuary – Status of Environmental knowledge to 1976; Fisheries and Marine Service, Special Estuary Series No. 6, 296 p.

Clague, J.J.
1975: Quaternary geology, northern Strait of Georgia; in Report of Activities, Part A, Geol. Surv. Can., Paper 75-1A, p. 397-400.

Clarke, F.W.
1924: The data of geochemistry; U.S. Geol. Surv., Bull. 770, 841 pp.

Deevey, E.S.
1973: Sulphur, nitrogen and carbon in the biosphere; in Carbon in the Biosphere, Woodwell, G.M. and Pecan, E.V. (eds.), Tech. Info. Centre, U.S. Atomic Energy Commission, p. 182-190.

Degens, E.T. and Mopper, K.
1976: Factors controlling the distribution and early diagenesis of organic material in marine sediments; in Chemical Oceanography, v. 6, Riley, J.P. and Chester, R. (eds.), Academic Press, New York, p. 59-113.

Emery, K.O. and Uchupi, E.
1972: Western North Atlantic Ocean; Am. Assoc. Pet. Geol., Mem. 17, 532 p.

Fleming, R.H.
1940: The composition of plankton and units for reporting populations and production; Proc. Pacific Sci. Assoc., 6th Ann. Meeting, Vancouver, 1939, p. 535-540.

Garrels, R.M., Mackenzie, F.T., and Hunt, C.
1973: Chemical Cycles and the Global Environment; William Kaufmann, Los Altos, 206 p.

Goodell, H.G.
1972: Carbon/nitrogen ratio; in Encyclopedia of Geochemistry and Environmental Sciences, Fairbridge, R.W. (ed.), Van Nostrand Reinhold, New York, p. 136-142.

Gucluer, S.M. and Gross, M.G.
1964: Recent marine sediments in Saanich Inlet, a stagnant marine basin; Limnol. Oceanogr., v. 9, p. 359-376.

Harvey, H.W.
1960: The Chemistry and Fertility of Sea Waters; Cambridge University Press, 240 pp.

Ketchum, B. and Redfield, A.C.
1949: Some physical and chemical characteristics of algae growth in mass cultures; Cellular Comparative Physiol. J., v. 33, p. 281.

Luternauer, J.L.
1976: Skeena Delta sedimentation, British Columbia; in Report of Activities, Part A, Geol. Surv. Can., Paper 76-1A, p. 239-242.

1976: Geofisheries research off the west coast of Canada; in Report of Activities, Part C, Geol. Surv. Can., Paper 76-1C, p. 157-159.

Luternauer, J.L. and Swan, D.
1978: Kitimat submarine slump deposit(s): a preliminary report; in Current Research, Part A, Geol. Surv. Can., Paper 78-1A, p. 327-332.

Milliman, J.D.
1976: Sand and gravel deposits off southwestern Vancouver Island, British Columbia; in Report of Activities, Part A, Geol. Surv. Can., Paper 75-1A, p. 23-26.

Roman, M.R.
1978: Tidal resuspension in Buzzards Bay, Massachusetts II. Seasonal changes in the size distribution of chlorophyll, particulate concentration, carbon and nitrogen in resuspended particulate matter; Estuarine and Coastal Marine Sciences, v. 6, p. 47-53.

Sharp, J.H.
1975: Gross analyses of organic matter in seawater: why, how and from where; in Marine Chemistry in the Coastal Environment; Church T.M. (ed.), Am. Chem. Soc., Symposium Series 18, p. 682-696.

Trask, P.D. and Patnode, H.W.
1942: Source Beds of Petroleum; Am. Assoc. Pet. Geol., 566 pp.

von Andel, Tj. H. and Postma, H.
1954: Recent sediments of the Gulf of Paria; in Reports of the Orinoco Shelf Expedition, v. 1, Kon Nederl. Akad. Wetensch. Verh., v. 20, 245 pp.

COMPOSITION OF PYROXENE PHENOCRYSTS FROM LOWER MESOZOIC VOLCANICS, NORTH-CENTRAL BRITISH COLUMBIA

J.W.H. Monger
Regional and Economic Geology Division, Vancouver

M. Bonardi and A.G. Plant
Central Laboratories and Administrative Services Division

Introduction

This note on compositions of pyroxenes from the Upper Triassic Takla Group and the Lower Jurassic Hazelton Group in McConnell Creek map area (94D), north-central British Columbia, supplements an earlier report on these rocks by Monger (1977). The pyroxenes were studied as a means of distinguishing the upper part of the Takla Group from the overlying Hazelton Group and to see if the alkaline character of the Takla Group shown by whole-rock chemical analyses is primary or secondary. The upper formation of the Takla Group, the Moosevale Formation (Fig. 1; Monger, 1977), is an intermediate volcaniclastic unit that is chemically and lithologically similar to parts of the overlying Hazelton Group. In places there is a clear stratigraphic break between the two sequences, marked by a distinctive conglomerate. Elsewhere a contact is not obvious and the two groups appear to be gradational. Optical investigation of pyroxene compositions from both units by Jon Dudley, using the $A_1 \wedge C$ method of Ruegg (1964), indicated that Hazelton pyroxenes are generally more iron-rich than Triassic ones, and suggested a method of distinguishing the two sequences (Monger, 1977, p. 44-45). On alkali-silica plots from whole-rock analyses, the lower basaltic part of the Takla Group, known as the Savage Mountain Formation, lies partly in the sub-alkaline and partly in the alkaline field, crossing the dividing line between the two compositions proposed by Irvine and Baragar (1971), (Monger, 1977, p. 40). Although these rocks are generally nepheline normative, no minerals characteristic of

			Numbers of specimens with analysed pyroxene phenocrysts		Lithology of specimens	Number of Crystals Analysed	Total number of Analyses
LOWER JURASSIC	HAZELTON GP.	TELKWA FORMATION red, non-marine tuff, volcanic breccia and conglomerate, with local flows ranging from basalt to rhyolite and basal, polymictic conglomerate in places	80-F3-75 RW		Coarse grained augite feldspar andesite	4	4
			29a-75-RW		Feldspar augite porphyritic andesite	4	7
UPPER TRIASSIC	TAKLA GROUP	MOOSEVALE FORMATION red and green, non-marine and marine, volcanic breccia and conglomerate, typically composed of fine-grained feldspar augite porphyry and feldspar porphyry clasts, sandstone, tuff, argillite	MU75-173	173	Fine grained feldspar augite porphyry; clast from volcanic breccia	3	31
			MU75-210	210	crystal lithic tuff	2	8
			MU75-210g	210g	Fine grained feldspar augite porphyry; clast from volcanic breccia	6	10
			MU75-84	84	Crystal lithic tuff	6	6
		DEWAR FORMATION SAVAGE MOUNTAIN FORMATION mainly grey-green, grey-black, locally red, flows, pillows and massive volcanic breccia, composed mainly of basaltic, altered olivine (?), pyroxene porphyry	MU75-144a		Augite porphyry basalt	3	7
		grey-green, brown, well-bedded tuff, volcanic sandstone and argillite, with local pyroxene porphyry sills and dykes, feeders to Savage Mountain Fm.	MU73-137 (sill)		Coarse-grained augite-altered olivine (?) porphyritic basalt	4	13
						1	28 (traverse)

Figure 1. Stratigraphy, lithology, specimen identifications and numbers of specimens containing analyzed pyroxene phenocrysts.

From: Scientific and Technical Notes in Current Research, Part C; Geol. Surv. Can., Paper 78-1C.

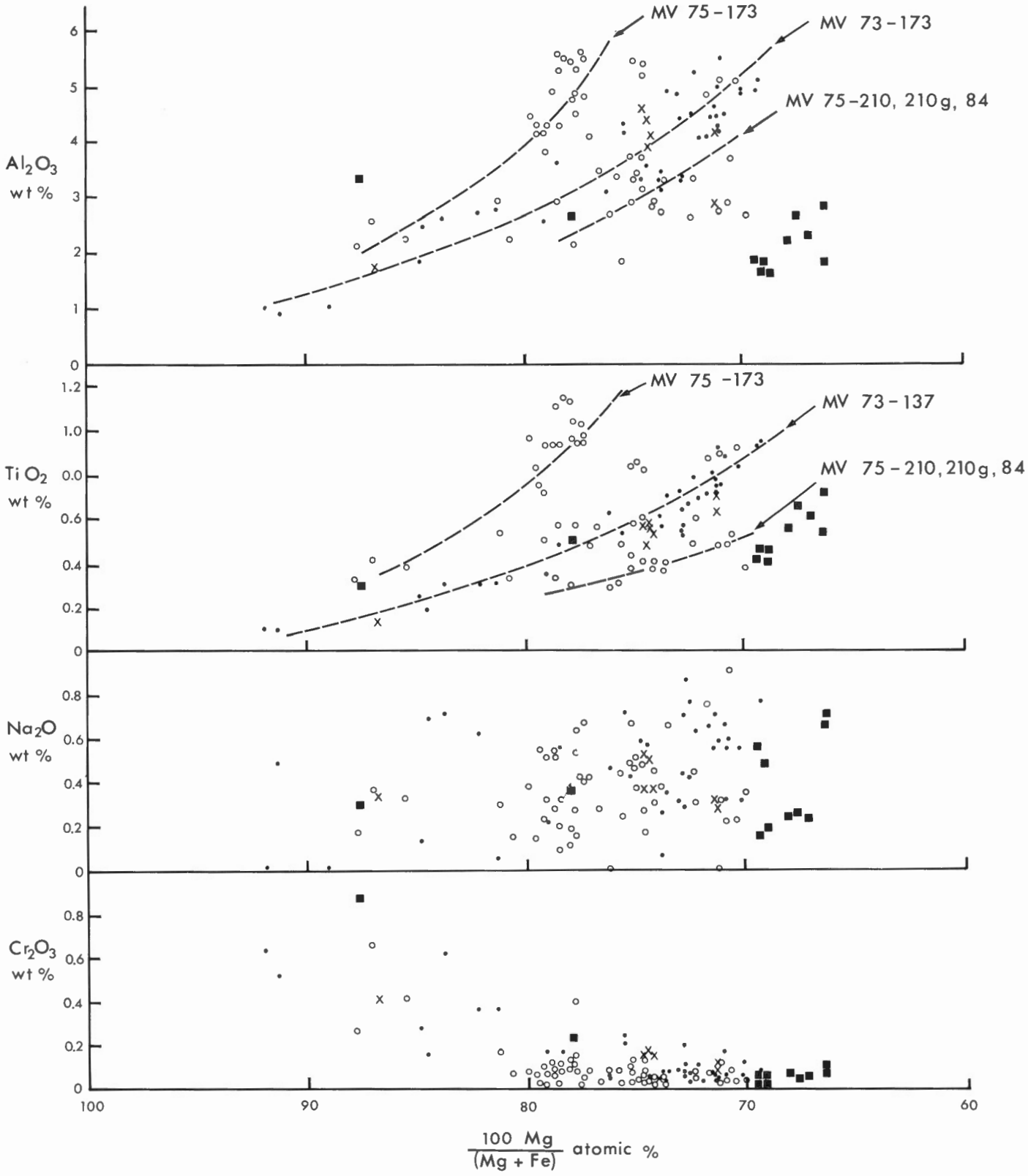


Figure 2. Variation diagram of all pyroxenes analyzed, showing certain well-defined trends.

alkaline rocks are known from them; in particular, the pyroxenes do not have the optical characteristics of the high-titanium species commonly associated with alkaline volcanics. Because the rocks are partly submarine and are of zeolite to prehnite-pumpellyite metamorphic grade, one possible reason for their partly alkaline chemistry is that alkalis were introduced during cooling or low-grade metamorphism shifting the composition towards the alkaline field. Pyroxene phenocrysts presumably recrystallized well before extrusion and are typically fresh and unaltered. Therefore they should have preserved their original composition thus indicating affinities of the magma more reliably than chemical analyses of the whole rock.

Brief descriptions of the stratigraphic units which provided the analyzed pyroxene specimens are given in Figure 1.

Method

The pyroxenes were analyzed using a Materials Analysis Company electron microprobe equipped with a Kevex energy dispersive spectrometer and automated to produce simultaneous multi-element analysis and data reduction (Plant and Lachance, 1973). Operating conditions were as follows: 20kV accelerating voltage, specimen current of 10 nanoamperes measured on a standard kaersutite, and a counting time of 100 seconds. The pyroxenes were analyzed for 10 elements, namely Si, Ti, Al, Cr, Fe, Mn, Mg, Ca, Na and K; no other elements were detected in the energy dispersive spectra. Standards used were as follows: kaersutite (Na, Mg, Al, Si, K, Ca, Ti and Fe), chromite (Cr), biotite (Mn). All analytical points were recorded on photomicrographs. With the exception of sodium, the determinations have a relative accuracy of ± 1-2 per cent for major elements and up to 5 per cent for minor elements. For sodium, the relative accuracy is ± 10 per cent.

Results

Variation of Al_2O_3, TiO_2, Na_2O and Cr_2O_3 against Mg/Mg+Fe is shown in Figure 2. Figure 3 shows Ca-Mg-Fe ratios and Figure 4, oxide variations in two intersecting traverses across the single crystal, in the photomicrograph in Figure 5. The plots have the form of those used by Irvine (1973) in a study of volcanics with a somewhat similar composition from the Lower Cretaceous of southeastern Alaska.

(1) Augite-altered olivine(?) basalt: feeder to Savage Mountain Formation: MV73-137

This specimen is from a sill intruding the lower part of the Takla Group which on the basis of its lithology and chemistry is presumed to be a feeder to the Savage Mountain Formation. Figure 2 shows a normal, consistent decrease of Al_2O_3 with TiO_2. The TiO_2 content is below 1% by weight, and in most analyses between 0.5-0.8% by weight, well below those of pyroxenes from typical alkaline basalts (1-3%) or peralkaline basalt (3-5%) (LeBas, 1964). The sodium content is generally below 1% by weight but shows no consistent variation. K_2O varies between 0.0 and 0.07% by weight, and MnO between 0.01 and 0.25% by weight. On Ca-Mg-Fe plots (Fig. 3) most examples have a composition about $Ca_{45}Mg_{40}Fe_{15}$. Some crystals show a normal variation with low iron ratios (4-8%) in the core, passing to higher ratios (14-16%) near the rim, but others, including the crystal traversed (Fig. 4 and 5), locally reverse this trend and have narrow zones with decreased iron ratios (9-11%) near the rim. The pyroxene phenocrysts lie closer to, but below, the calcic augite line of Brown (1967, p. 122) than to the augite line, and are almost entirely within the field of (groundmass) pyroxenes in alkaline rocks shown by LeBas (1964, p. 268).

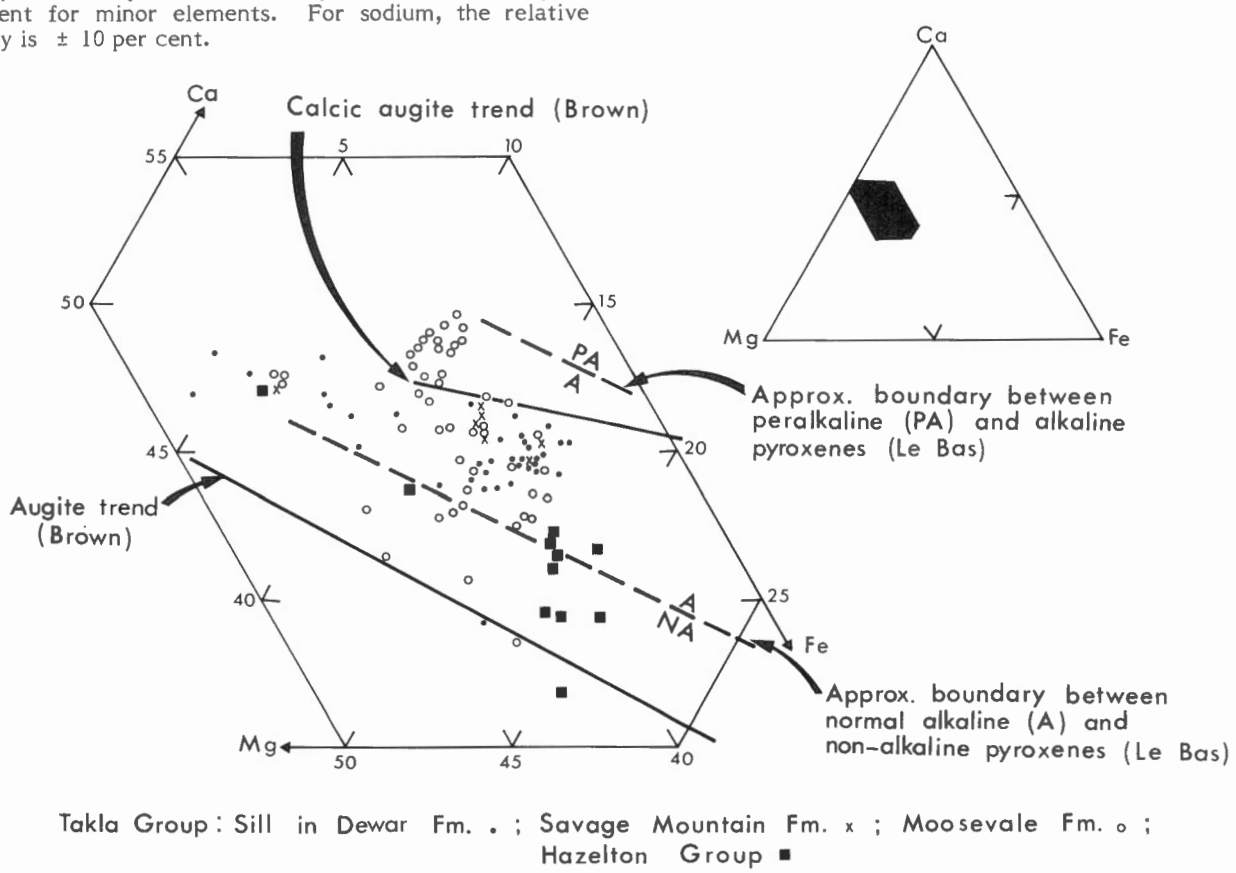


Figure 3. Ca-Mg-Fe plot of all pyroxenes analyzed, showing relationship to calcic augite and augite lines of Brown (1967) and (approximately) to peralkaline, alkaline and non-alkaline fields of LeBas (1964).

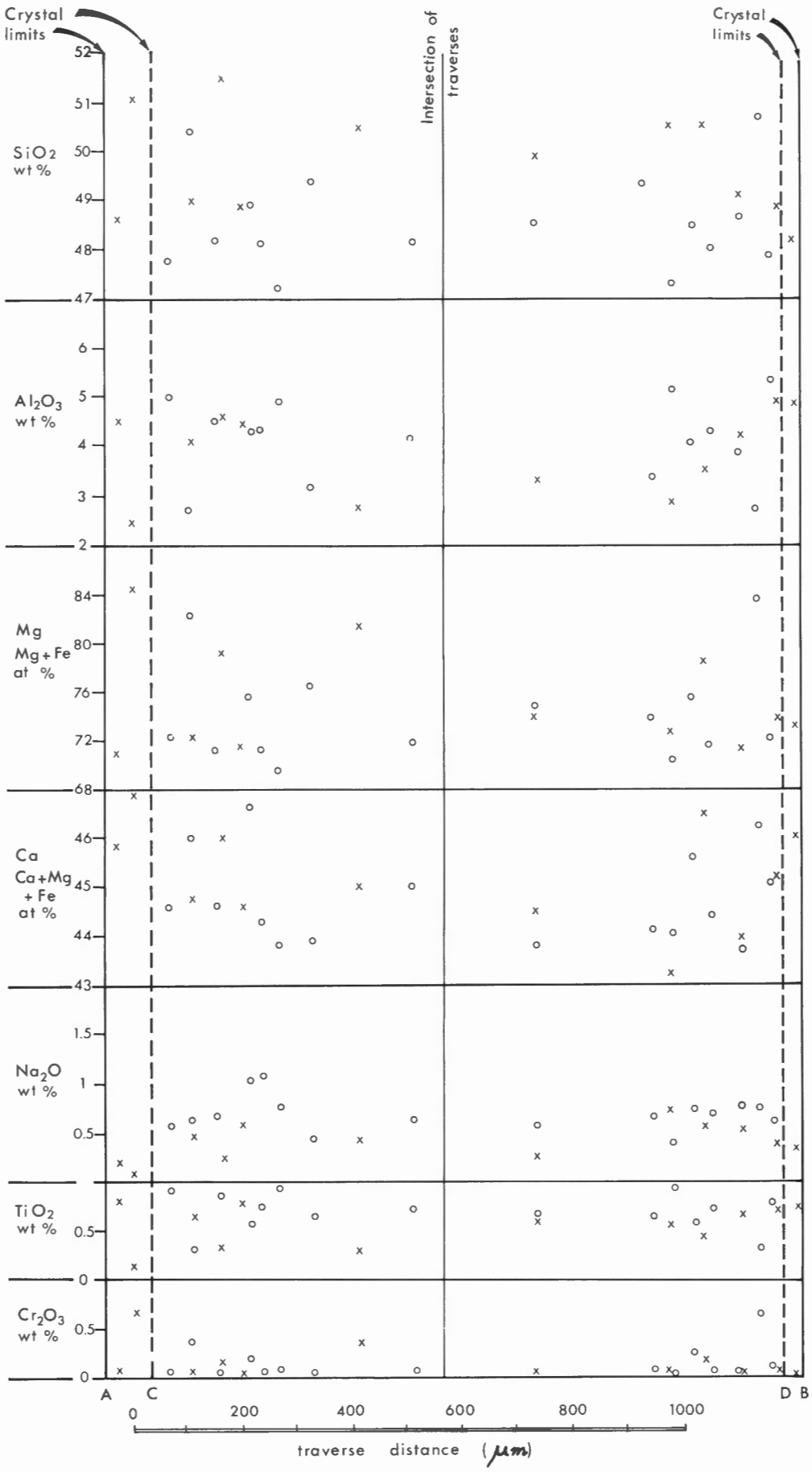


Figure 4. Variation in composition of a single crystal from two intersecting traverses aligned at about 30 to one another. Specimen MV73-137. A-B(x) and C-D(o).

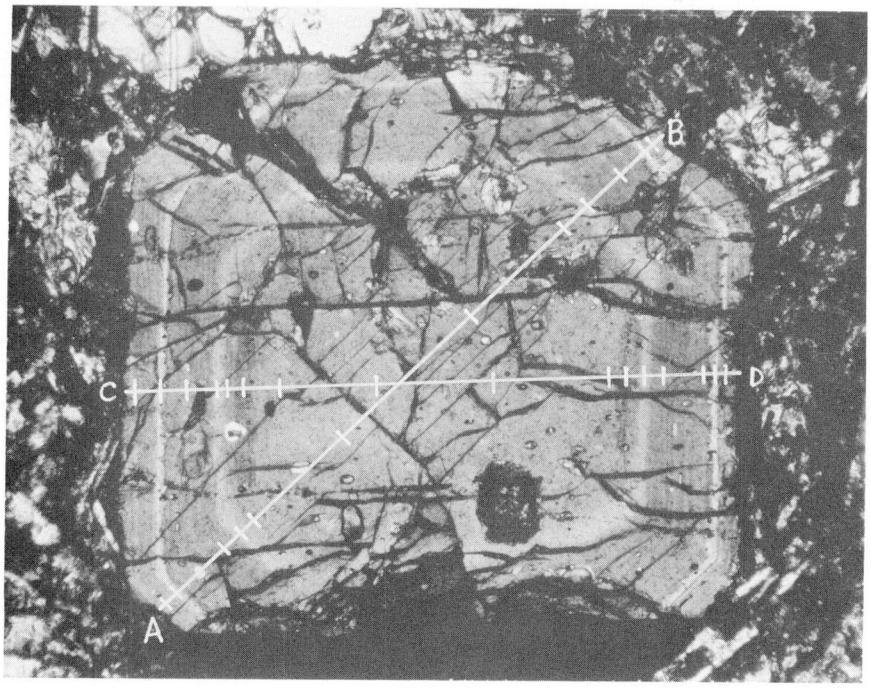


Figure 5

Photomicrograph of pyroxene from specimen MV73-137, showing traverses A-B and C-D with analysis points, the results of which are given in Figure 4. Field of view is 1.35 x 1.05 mm.

(2) Augite basalt: Savage Mountain Formation: MV73-144a

This specimen is lithologically typical of the Savage Mountain Formation and is from a sequence of submarine, locally pillowed, flows. The pyroxenes are similar to those of the sill. The Na_2O content lies well within the range shown by the sill and K_2O variation is similar, so there appear to be no added alkalis resulting from submarine extrusion, as opposed to intrusion. Iron ratio of the pyroxene rims is about 14% and cores are either 16% or about 7% FeO.

(3) Fine grained augite feldspar porphyry: Moosevale Formation: MV75-84; MV75-173; MV75-210; MV75-210g

The pyroxenes are from lithologically similar, fine grained augite feldspar porphyry clasts in volcanic breccias of the Moosevale Formation. Three, (MV75-84, 210, 210g) are compositionally similar to pyroxenes from the Savage Mountain Formation, with similar amounts of TiO_2 and Al_2O_3 and a composition of $Ca_{44}Mg_{42}Fe_{14}$, although there is more scatter. One (MV75-173), from the basal parts of the formation, is unusual in that it has higher TiO_2 (~1% vs. 0.5%) and Al_2O_3 (5% vs. 3%) contents, and an average composition of about $Ca_{49}Mg_{40}Fe_{11}$. Pyroxenes from the latter specimen lie mainly above the calcic augite line of Brown (1967) and touch the peralkaline field of LeBas (1964), although within the formation as a whole the pyroxenes show a variation from non-alkaline to alkaline fields.

(4) Fine grained augite feldspar porphyry: Telkwa Formation: 29a-75RW, 80-F3RW

These specimens are from the lowest formation of the Hazelton Group. In the field, it is generally possible to distinguish the Telkwa Formation from the Moosevale on stratigraphic characteristics, although locally and at specimen level, the two may be indistinguishable. Most pyroxenes analyzed appear to be quite distinct from those of the Takla Group. Al_2O_3 and TiO_2 vs. Mg/Mg+Fe plots are generally distinct (apart from two out of eleven analyses) and the composition of $Ca_{41}Mg_{40}Fe_{19}$ is much lower in calcium and higher in iron than Takla pyroxenes. Hazelton pyroxenes lie much closer to Brown's augite line, and are either within the field of pyroxenes from non-alkaline rocks or close to the dividing line.

Conclusions

(1) This preliminary investigation suggests that pyroxene compositions can be used to separate the Takla Group from the Hazelton Group in places where there are no other distinguishing features.

(2) The pyroxene composition indicates (as does the rock chemistry) that the Takla Group has primary alkaline affinities, although the pyroxenes are remarkably low in TiO_2 for alkali basalts.

References

Brown, G.M.
1967: Mineralogy of basaltic rocks; in Basalts, the Poldervaart treatise on rocks of basaltic composition; Interscience Publishers, v. 1, p. 103-162.

Irvine, T.N.
1973: Bridge Cove volcanics, Juneau area, Alaska: possible parental magma of Alaskan-type ultramafic complexes; Carnegie Inst. Wash. Yearb. 72, p. 478-491.

Irvine, T.N. and Baragar, W.R.A.
1971: A guide to the chemical classification of common volcanic rocks; Can. J. Earth Sci., v. 8, p. 523-548.

LeBas, M.J.
1964: The role of aluminum in igneous clinopyroxenes with relation to their parentage; Am. Jour. Sci., v. 260, p. 267-288.

Monger, J.W.H.
1977: The Triassic Takla Group in McConnell Creek map-area, north-central British Columbia; Geol. Surv. Can., Paper 76-29, 45 p.

Plant, A.G. and Lachance, G.R.
1973: Quantitative electron microprobe analysis using an energy dispersive spectrometer; Proc. Eighth Nat. Conf. on Electron Probe Analysis (New Orleans), Paper 13.

Ruegg, N.R.
1964: Use of the angle $A_1 \wedge C$ in optical determination of the composition of augite; Am. Mineral, v. 49, p. 599-606.

MULTICHANNEL REFLECTION SEISMIC SURVEY IN THE LABRADOR SEA

K. Hinz[1], H.-U. Schluter[1]; and
A.C. Grant, S.P. Srivastava, D. Umpleby, and J. Woodside
Atlantic Geoscience Centre, Dartmouth

A geophysical reconnaissance survey was carried out in the Labrador Sea-Davis Strait area between July and September 1977 by the Federal Institute for Geosciences and Natural Resources (BGR), Hannover, Germany. The lines were planned in co-operation with the Atlantic Geoscience Centre, Geological Survey of Canada, and the Greenland Geological Survey (Denmark).

The seismic, magnetic, and gravity data from 5931 km on 21 lines (Fig. 1) were recorded on magnetic tape. A 24-fold coverage technique was used with 48 seismic channels (traces), with a 2400 m streamer cable, and a 23.45 L airgun array. A fully integrated computerized satellite navigation system (INDAS III) was used for determining the position of the survey vessel. The survey was executed on the research vessel MS EXPLORA chartered from PRAKLA-SEISMOS GMBH, who served as contractor.

The seismic records from this survey were interpreted jointly by the German and Canadian scientists listed above, and the results have been reviewed at the symposium on "Crustal Properties across Passive Margins" held in Halifax, Nova Scotia, June 19-23, 1978. The proceedings of this symposium will be published in a forthcoming issue of TECTONOPHYSICS.

The original data from this survey are held by:

Dr. K. Hinz,
Director and Professor,
Bundesanstalt Fur Geowissenschaften und Rohstoffe,
Federal Institute for Geosiciences and Natural Resources,
3 Hannover 51 – Postfach 510153,
Federal Republic of Germany.

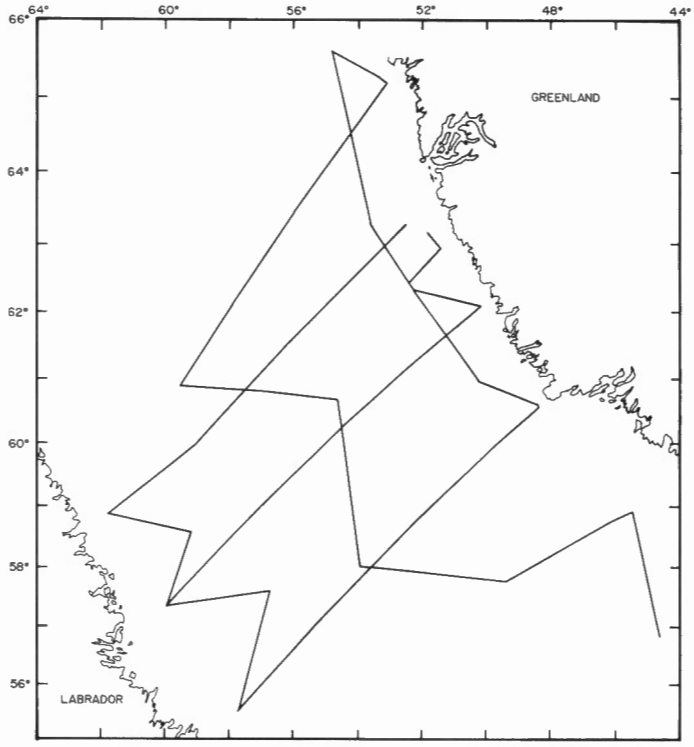


Figure 1. Location of BGR multichannel reflection seismic lines in the Labrador Sea.

[1] Federal Institute for Geosciences and Natural Resources (BGR), Hannover, (F.R.G.).

From: Scientific and Technical Notes in Current Research, Part C; Geol. Surv. Can., Paper 78-1C.

CORING OF HOLOCENE POND SEDIMENTS AT CAPE HERSCHEL, ELLESMERE ISLAND, ARCTIC ARCHIPELAGO

W. Blake, Jr.
Terrain Sciences Division

Introduction

Prior to the 1977 field season an examination of aerial photographs of the Cape Herschel peninsula, eastern Ellesmere Island, revealed the presence of a number of ponds (Fig. 1,2). Studies in the area, during July 1977 (Blake, 1977), showed that several ponds contained organic-rich sediments, despite the general sparseness of vegetation on the surrounding granitic terrane. The majority of ponds are at relatively low elevations, below the level of raised beaches and marine shells in undisturbed shallow-water deposits. Thus it was thought that if cores of the bottom sediments could be recovered, a study of diatoms might reveal the point at which the transition from marine to freshwater conditions had occurred (cf. Hyvärinen, 1969). Then, assuming that the age of the organic sediments above this transition could be determined by radiocarbon dating, it might be possible to document the passage of the shoreline and to construct an emergence curve for the Cape Herschel area.

Because the ponds on the peninsula are shallow (all of those observed in July 1977 had less than 1 m of water), it was assumed that they would freeze to the bottom each winter, and hence the easiest time to recover cores of the bottom sediments would be before the spring thaw set in. For this reason a visit to Cape Herschel was made between May 17 and 29, 1978. This note briefly describes the methods and equipment used in recovering sediment cores and gives some preliminary results.

Good weather prevailed throughout the 13 days spent at Cape Herschel, although there was considerably more cloudiness towards the end of May than during the early part of our stay. The maximum temperatures, which we recorded in the Stevenson screen at the base camp of North Water Project (cf. Müller et al., 1975), ranged from -7.7°C (May 18) to -0.6°C (May 22); minimum temperatures varied between -10.0°C (May 18 to -2.6°C (May 26).

Methods

Because the land airstrip at Cape Herschel is short, and it was rough because of the sastrugi developed there, the ski-equipped Twin Otter landed on the smooth sea ice of Rosse Bay (Fig. 2). Travel on the Cape Herschel peninsula was mainly by skidoo towing a Nansen sledge. The extremely hard packed snow made walking easy, and skis were used on only one occasion. Crampons were necessary only once, en route to the Cape Herschel plateau, where a slope too steep to be negotiated by skidoo was encountered.

Coring was carried out with a SIPRE (CCREL)-type auger powered by a 6 h.p. gasoline motor and equipped with a reduction gear box (Stihl model 4308). This unit allows recovery of 7.6 cm (3 inch)-diameter cores, and the core barrels used can accommodate increments up to 40 cm in length. The corer is equipped with tungsten carbide teeth which make it possible to penetrate inorganic sediments. Aluminum extension rods are 1 m in length.

A four-man team proved to be the ideal size to operate this coring unit. Two people could lift or apply leverage on the handles attached to the motor while the third connected and disconnected the extension rods, helped with core extrusion, and provided extra weight on the handles (Fig. 3,4). The fourth person logged and packed core increments as they were extruded.

Upon recovery of a core notes were made of the length of each increment, colour changes, and the presence of special features such as ice lenses, shell fragments, etc. Each increment was wrapped individually in lightweight aluminum foil, the top and bottom were marked, and then it was placed in a plastic bag. In some cases, the cores were packed directly in an insulated box, otherwise they were kept in the shade prior to their return to base camp. Despite the relatively warm air temperatures, the cores were preserved frozen by storing them deep within a snowbank. For transport to the large walk-in freezer in Resolute, Coleman 40-quart insulated boxes were used, as well as some individual plastic core containers manufactured by CESSCO, Toronto, following a design by J.J. Veillette, these containers utilize an inner and an outer section of PVC tubing, and each one can accommodate core increments totalling 30 cm in length (Veillette and Nixon, 1976). Four of these containers fitted into a new lightweight and disposable plastic box (available from Technical Field Support Services). The same method of packing was utilized in shipping the cores south.

Results

Five ponds were cored successfully on Cape Herschel peninsula (Fig. 2). In three other ponds, one on the plateau and two fairly close to sea level, no sediment was encountered on top of the rocky bottom. Because, as anticipated, all ponds were frozen to the bottom, it was possible to recover the watery surface sediment; in fact, a break occurred in each core approximately 0.5 to 2.0 cm above the uppermost sediment, and the contact could be seen through the clear ice. Details of the numbers of cores recovered, as well as of ice and sediment thicknesses, are summarized in Table 1.

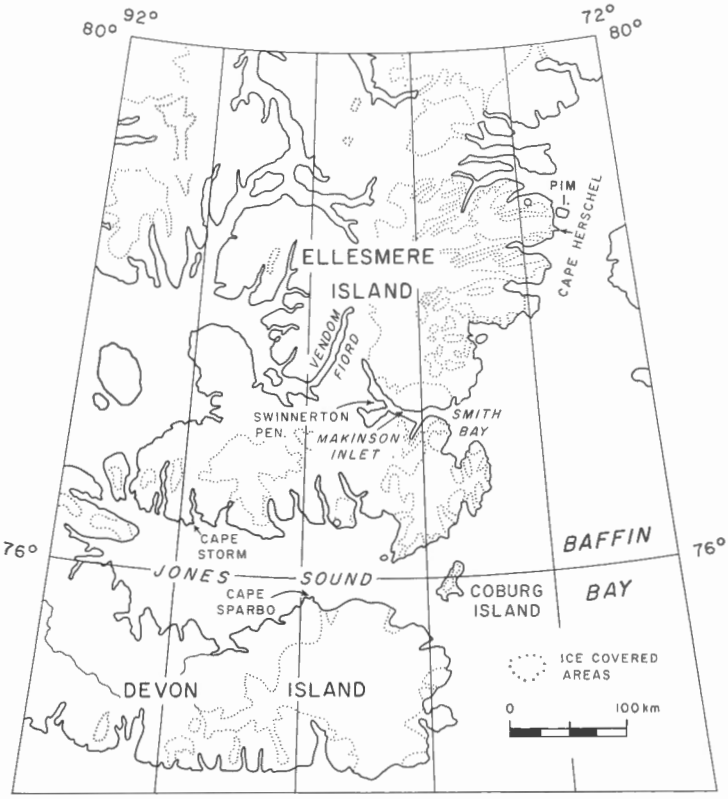


Figure 1. Location map, southeastern Ellesmere Island.

From: Scientific and Technical Notes in Current Research, Part C, Geol. Surv. Can., Paper 78-1C.



Figure 2. Details of the Cape Herschel peninsula showing locations of the ponds referred to in the text (Table 1). Enlargement of aerial photograph A-16607-10, taken from an altitude of ca. 9100 m, July 5, 1959; courtesy National Air Photographic Library, Energy, Mines and Resources, Ottawa.



Figure 3. Coring operations underway at pond 23 (cf. Figure 2), May 22, 1978. View northward across Rosse Bay towards Pim Island (GSC-175227).

Ice lenses and stringers were fairly abundant, especially in the lower portions of cores in which organic-rich sediments appear to be predominant (e.g., ponds 4, 23, and 26) or in cores characterized by inorganic sediments (ponds 27 and 32; in the former, ice lenses were up to 0.8 cm thick).

Most of the core increments have been X-radiographed, and one of these is reproduced as Figure 5 (pond 23 in Table 1 and Figure 2). This shallow pond at 33 m a.s.l. between two beach ridges is known to have been under the sea until only a few thousand years ago, for aragonitic shells of the marine pelecypod **Mya truncata**, in sand underlying a pocket of raised beaches some 0.7 km to the south and at approximately 52 m a.s.l., are 7210 ± 90 years old (GSC-2525).

Preliminary diatom analysis has been carried out on the basal increments of cores from the five ponds, and none show a distinct assemblage of marine littoral diatoms such as those found in one of the ponds on the

Table 1

Summary of coring results, Cape Herschel Peninsula

	Pond designation (Fig. 2)[1]				
	4	23	26	27	32
Number of cores	8	15	20	1	1
Snow thickness (cm)	40	50	0	0	125
Ice thickness (cm)	11	11	24 to 51	95	11
Maximum thickness of sediments (cm)	104	35	59	50	141
Approximate elevation a.s.l.[2] (m)	58	33	3	19	82

[1] Numbers correspond to sample numbers at the same localities.

[2] Determined by levelling with a Wild NK-10 level, using the flat surface of the ice foot to represent high tide level.



Figure 4. Close-up view of coring at pond 4, showing details of the core barrels, a 1 m-long aluminum extension rod, and the Stihl motor unit. At this site only 11 cm of ice were encountered above 1 m of sediment. May 18, 1978 (GSC-175271).

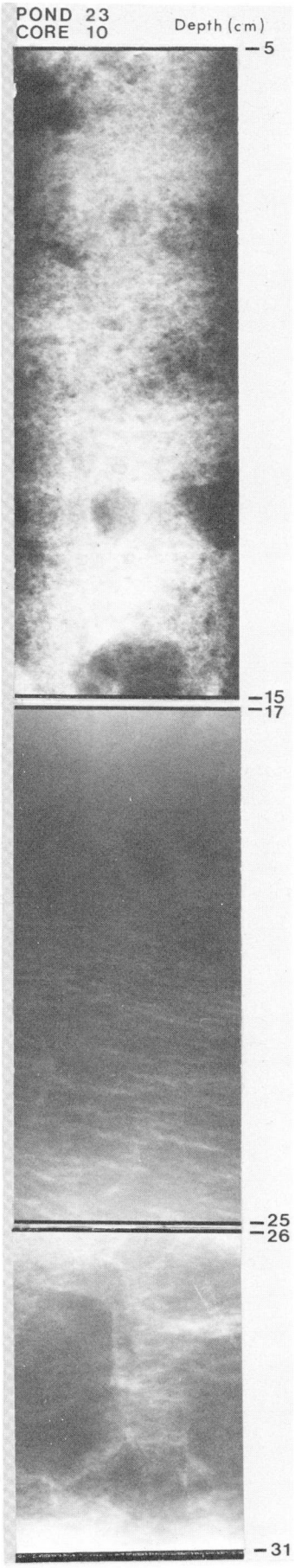


Figure 5.

X-radiograph (exposure 32) of core 10 from pond 23. Note the faint banding in the core increment at 5 to 15 cm depth, the thin ice lenses at 20 to 25 cm depth, and the rock fragments lower down (base of core at 31 cm).

peninsula west of pond 26 (Fig. 2). In this pond, which is so low that it presumably receives an influx of sea water during spring tides, **Diploneis interrupta**, **Navicula digito-radiata**, and **Scoliopleura tumida** occur. All are characteristic of zones subject to tidal action, and the last two also occur, for example, in present-day intertidal sediments at Cape Storm, southern Ellesmere Island (S. Lichti-Federovich, unpublished GSC Diatom Reports 78-7 and 78-20). None of these marine littoral diatoms have been found in core 10 from pond 23; on the contrary, the three samples extracted from depths of 14 to 31 cm in this core show a dominance of **Epithemia sorex**, suggesting an early postemergence freshwater stage or brackish water stage (unpublished GSC Diatom Report 78-21). Although Hyvärinen (1968) reported this species as abundant in the lower sediments of two lakes on Bjørnøya, Svalbard, which he concluded had not been inundated by the sea during Holocene time, Eronen (1974) listed **Epithemia sorex** as one of the brackish water species typical of the Mastogloia phase of the Baltic Sea along the coast of Finland (cf. Alhonen, 1971). It also has been reported among the freshwater-brackish diatoms occurring in the lower lacustrine deposits (above marine beds) of a basin near the coast of southwestern Norway (H. Håkansson in Anundsen, 1978). According to Remane and Schlieper (1971) **Epithemia sorex** is one of a group of freshwater diatoms that are able to withstand salinities of up to about 3 °/oo.

Studies of the diatom flora in the ponds on Cape Herschel peninsula are continuing, and it is hoped that the cores from ponds 4, 23, and 26 contain sufficient organic material that radiocarbon age determinations can be carried out.

Acknowledgments

Logistical support was provided by the Polar Continental Shelf Project (G.D. Hobson, Director). F. Alt and F.P. Hunt of the Polar Continental Shelf Project staff were particularly accommodating in Resolute. Assistance in the field was provided by J.P. Bridgland, R.J. Richardson, and P.B. Smith. In addition we are indebted to K. Schroff, ETH, Zürich, Switzerland, for his help upon our arrival at Cape Herschel. K. Meliske, of the Non-Destructive Testing Laboratory, CANMET, allowed us access to darkroom facilities and instructed us in the correct procedures of developing our X-radiographs. S. Lichti-Federovich provided the information on diatoms from Cape Herschel reported in this paper, and B.G. Craig commented on the manuscript.

References

Alhonen, P.
1971: The stages of the Baltic Sea as indicated by the diatom stratigraphy; Acta Bot. Fennica, v. 92, p. 1-18.

Anundsen, K.
1978: Marine transgression in Younger Dryas in Norway; Boreas, v. 7, p. 49-60.

Blake, W., Jr.
1977: Glacial sculpture along the east-central coast of Ellesmere Island, Arctic Archipelago; in Report of Activities, Part C, Geol. Surv. Can., Paper 77-1C, p. 107-115.

Eronen, M.
1974: The history of the Litorina Sea and associated Holocene events; Soc. Sci. Fenn., Commentat. Phys.-Math., v. 44, No. 4, p. 79-195.

Hyvärinen, H.
1968: Late-Quaternary sediment cores from lakes on Bjørnøya; Geogr. Ann., Ser. A, v. 50, p. 235-247.

1969: Trullvatnet: A Flandrian stratigraphical site near Murchisonfjorden, Nordaustlandet, Spitsbergen; Geogr. Ann., Ser. A, v. 51, p. 42-45.

Müller, F., Blatter, H., and Kappenberger, G.
1975: Temperature measurement of ice and water surfaces in the North Water area using an airborne radiation thermometer; J. Glaciol., v. 15, p. 241-250.

Remane, A. and Schlieper, C.
1971: Biology of Brackish Water; E. Schweizerbart'sche Verlagshandlung, Stuttgart, 372 p.

Veillette, J.J. and Nixon, M.F.
1976: Permafrost coring equipment; in Report of Activities, Part A, Geol. Surv. Can., Paper 76-1A, p. 269.

IMPLEMENTATION OF AN INTERACTIVE SYSTEM FOR COMPUTER PROCESSING OF GEOLOGICAL IMAGES

A.G. Fabbri, T. Kasvand[1], and J.H. Stray[2]
Regional and Economic Geology Division

Introduction

A system of programs for interactive processing of images of geological nature has been designed as part of multidisciplinary efforts in the fields of geology and pattern recognition. Applications of image processing techniques to mineral exploration problems and to the analysis of geologic textures are being developed as in Agterberg and Fabbri (1978) and Fabbri and Kasvand (1978).

A part of the system which is written in FORTRAN and is compatible with the departmental CDC CYBER 74 computer is now available. It allows computations and interactive displays, via a Tektronix 4014-1 video terminal, of the results of transformation of geological binary (0-1) images obtained by optical or mechanical scanning, or by manual digitization.

An associated picture file management system for image processing provides information on picture data, such as headings with names and dimensions, and comments on the history of processing of each image. By means of a simplified conversational language, logical operations between images or picture element neighbourhood transformations can be computed by algorithms designed for arrays of up to 1080 x 1080 bits. These computations e.g., for autocorrelation and cross-correlation, provide measures of geometrical attributes of binary images and of relationships between images.

Geometrical probability and pattern recognition concepts can be directly applied to such images, which represent valuable data bases for different applications ranging from the study of map patterns to the analysis of micrographic materials.

The present version of the interactive system operates under the NOS/BE operating software on the Cyber 74 computer of the Computer Science Centre of the Department. It utilizes the Plot 10 Advanced Graphing II Tektronix software for the Tektronix 4014 graphic terminals.

In order to minimize response time and resident memory requirements, it was necessary to segment the program package into several overlays, each executing at less than 70 000 octal words.

From an operational point of view, pictures are treated as data files. The programs allow the selection of options and calls to various subprograms which generate new pictures as output files. The latter can be used as input data for further processing. Plotting subprograms for graphic display on the video terminal can be called as well as routines which modify the picture data into input files for other display devices. Hard copies of the text of the interactive conversation and of the binary images displayed can be obtained by means of a Tektronix 4631 hard copy unit.

The processing of binary pictures in which each picture element corresponds to one bit of a computer word (in an "on" or an "off" state representing a "0" or a "1" respectively) requires bit manipulation. All character and bit manipulation in the system is carried out uitlizing routines from the EMR program library EMRLIB. The direct access I/O is accomplished using the random access routines of the Cyber 74. Specialized file handling routines were written to allow sequential file searching of the picture data files.

[1] National Research Council, Canada

[2] Computer Science Centre, Energy, Mines and Resources

From: Scientific and Technical Notes in Current Research, Part C; Geol. Surv. Can., Paper 78-1C.

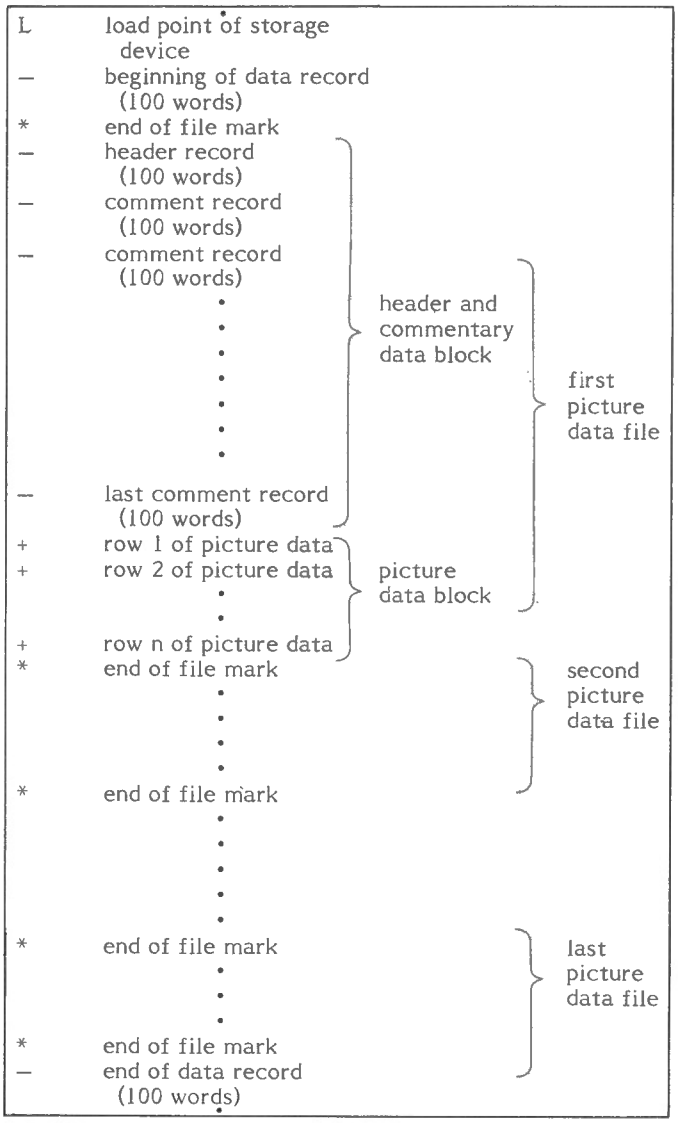


Figure 1.

Picture Storage and Processing

For optimum processing speeds, the picture data organization depends on the nature of the picture processing algorithms. Fortunately, most algorithms process the pictures systematically, starting for example, from the top left corner of the pictures and ending at the bottom right corner. The pictures can then be stored as very large two-dimensional matrices, in which each element and a certain number of its intermediate neighbours or the corresponding elements in other picture matrices are used in the computation. For minimizing storage, only a strip across the picture is stored in core. The width of the strip corresponds to the number of rows of input picture data which are used in a given algorithm. The minimum strip consists of one row of picture elements.

The picture data is represented as matrices of integer or one bit binary numbers of up to 1080 x 1080 elements. These are stored row by row in a sequential manner. Each row of picture data represents one logical record.

In order to allow pictures of varying sizes to be processed by the system, and to have the ability to include a commentary on which processing algorithms have been applied, each picture has a set of header records. The first header record (of 100 words) contains information about picture size, data type etc. The subsequent header records consist of comments. At least one comment line is added by each main program which has processed the picture. In this way a running commentary is obtained so that it is possible to trace what has been done to a given picture. Experience has indicated that these comments can be very valuable afterwards. The picture data is thus structured as shown in Figure 1.

Organization of I/O Picture Data

Up to five physically or operationally independent storage devices (discs) may be used simultaneously. Each picture is referred to by a number or numeric label. Consequently, pictures stored on physical device number 1 are to be numbered 100, 101, 102..., etc. Those stored on device number 2 are labelled 200, 201, 202..., etc. A similar procedure is applied to devices 3, 4 and 5. It is the responsibility of the user to know which label number corresponds to which picture. However, during the initial phase of a session, a procedure can be followed whereby all picture labels and the corresponding header and comments can be listed in order to assist in identifying the labels.

Each physically independent unit can serve either as an input or an output storage device. A physical unit cannot, however, be used in more than one role at the same time, since the storage is sequential.

Conversational Structure

The system expects the user to specify three different classes of interaction: (a) define I/O picture numbers, (b) define the running parameters for a given subprogram, and (c) call the particular program. When the program completes execution, the control returns to the user.

The conversational system is kept to a bare minimum by referring only to parameter addresses and the corresponding values. Consequently, a description of the program and a list of its parameter addresses and possible values must be used during the interaction. The subprograms themselves are also called by numbers which are explained in the description. Some subprograms present various options to the user and require a response. These are explained in detail and in plain language.

The system attempts to be as helpful as possible. At the beginning of a run, in which one or more existing picture files are available, a procedure reads the headers of all the existing files and creates a table which contains all information for file availability (input or output) on all five storage devices. If during a processing step the user tries to read a nonexistent picture file or tries to overwrite existing data, the system simply generates error messages and returns control to the user, without ruining the picture data or aborting. Only the last picture on a physical device can be erased.

In general, the system and its subprograms try to protect themselves against a careless user by checking as much input data as possible. However, the system is also forgiving since a detected error will only generate an error message (usually a program name followed by a number) and return control to the user, instead of returning control to the operating system of the computer. Thus, during a normal run the system does not allow an abort to occur

System Philosophy

The modern equivalent of the old Chinese proverb about a picture being equal to a thousand words is; "A picture is worth a million computer words". Since at present computers do not usually have central memories of this size, and it should be remembered that several processed versions of a picture may have to be accessible simultaneously, one of the basic problems in picture processing on a general purpose digital computer is the organization of the picture data. This system represents an attempt to simplify this problem as much as possible.

Conclusions

This interactive computer processing system has been adapted to a multi-user environment, however it still provides capabilities which resemble those of an image analyzer. The processing is slow in comparison to an image analyzer, but it does allow continuous development of programs while it avoids capital investments in special hardware. Its only requirement is a graphic terminal in order to display pictures on which decisions are made for further processing.

A detailed documentation of the algorithms used and a user's guide are under preparation by the authors.

References

Agterberg, F.P. and Fabbri, A.G.

1978a: Spatial correlation of stratigraphic units quantified from geological maps; Computers and Geoscience.

1978b: Statistical treatment of tectonic and mineral deposit data; Bull. Global Tectonics and Metallogeny; Am. Univ., Washington, D.C., v. 1, no. 1, p. 16-29.

Fabbri, A.G. and Kasvand, T.

1978: Picture processing of geological images; in Current Research, Part B, Geol. Surv. Can., Paper 78-1B, p. 169-174.

THE EFFECT ON VITRINITE REFLECTANCE OF ELEVATED TEMPERATURES DURING SAMPLE PREPARATION

D.L. Marchioni
Institute of Sedimentary and Petroleum Geology, Calgary

Introduction

An investigation of vertical and lateral rank variation as expressed by mean maximum vitrinite reflectance is in progress as the initial part of a study of the petrography of the lignite deposit at Hat Creek, south-central British Columbia. Preliminary determinations indicated an increase from 0.25% to 0.53% for this parameter over the thickness of the deposit (300 m). To provide meaningful results for a comparative rank study involving coals of such low rank, within a deposit in which vertical changes are relatively small, it is clear that all sources of error, however small, needed to be investigated and either eradicated or at least quantified.

The usual method of preparing particulate coal samples for microscopic analyses at the Institute of Sedimentary and Petroleum Geology (and at other laboratories) is by mixing the coal and a thermoplastic powder into a mould and forming a pellet by subjecting the mixture to heat and pressure. The equipment used at the Institute generates temperatures up to 110°C for a period of approximately 20 minutes. An alternative method, common to many laboratories, is to use liquid epoxy or polyester resins as the mounting medium. Some of these compounds also generate heat when hardening after the addition of a catalyst but in most cases temperature increase can be held to low levels by the selection of a suitable resin. This latter method is used in response to the known behaviour of coal to extraneous heating and to the frequent warnings in the literature concerning 'overheating' of samples during drying and pellet preparation (e.g. International Commission for Coal Petrology, 1971, 1973; A.S.T.M. Standards, 1977). There are few quantitative data available on the effects of the laboratory heating of coal samples on their vitrinite reflectance and the temperatures considered excessive vary from 50°C to 100°C.

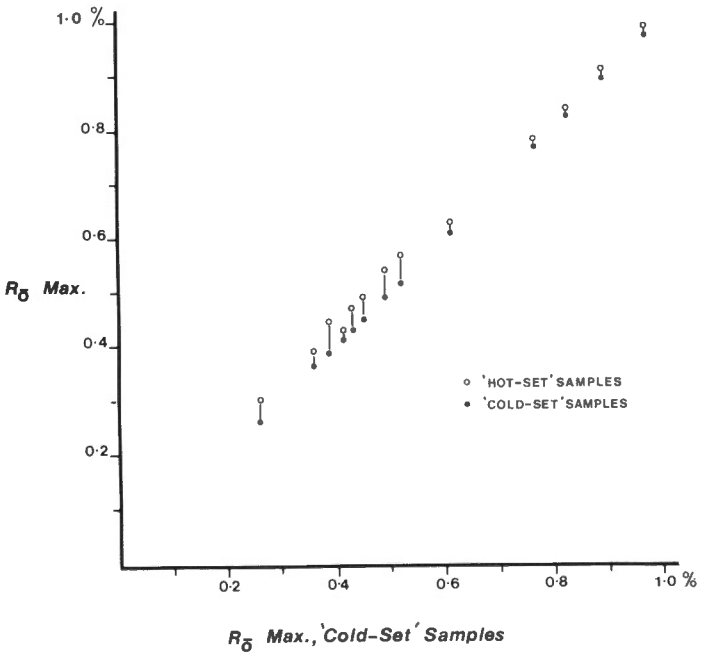


Figure 1. Plot of R_o max. of paired 'cold-set' and 'hot-set' pellets. The R_o max. of the 'cold-set' samples has been used as the basis for comparison and is plotted on the abscissa.

Based on the methods of paleotemperature determination of Huck and Karweil (1955), it appears that the Hat Creek lignites have never been subjected to temperatures in excess of 70°C. Although the heating produced during the 'thermoplastic' mounting procedure is of short duration, it was considered possible, especially in view of the significantly lower paleotemperatures involved, that anomalous vitrinite reflectance values may result. The aim of this investigation was to determine if there was an increase in vitrinite reflectance in samples prepared by the 'thermoplastic' method over those prepared in cold-setting resins, to quantify such variations, and to determine if they warranted changes in sample preparation technique.

Method and Results

Seven samples of Hat Creek lignite and six other western Canadian coals were selected to provide a range of rank between mean maximum vitrinite reflectances (R_o max.) of 0.25% and 1.0%. All of these coals had maximum paleotemperatures of 60°C to 95°C. In each case, samples were crushed to pass a 20 mesh sieve and then two splits of a volume suitable for the preparation of a particulate pellet were obtained by riffling. One split was then mounted by the 'thermoplastic' process and the other in a cold-setting resin. The resin used was found to increase in temperature by only 3°C above room temperature during hardening. Both pellets were then polished by the same procedure and then stored in a desiccator.

Thirty determinations were made of maximum vitrinite reflectance on each pellet, according to a standard procedure. In all cases, the pellets which had been heated revealed mean reflectance values higher than those set without heating. Figure 1 shows the R_o max. of all pairs of pellets, plotted against the R_o max. of the cold-set sample in each case (horizontal axis). The graph shows disparities ranging from 0.015% to 0.05% between the same coal mounted by the two different processes. Harrison (1965) and Thomas and Damberger (1976) found that reflectance increased as samples of the same coal were subjected to progressive drying. It is possible that the higher reflectances recorded here may be due to the loss of pore moisture by the imposition of high temperatures during moulding. Reflectance discrepencies are highest in the 0.25% to 0.50% range of R_o max. where natural moisture content would also be highest. Alternatively, the variation may be due to more fundamental changes in the chemical-physical nature of vitrinite, as in the normal processes of coalification, primarily in response to heating.

Over the range of R_o max. from 0.25% to 1.0%, the relationship between the two sets of samples is expressed by the equation:

$$y = 0.9759x + 0.0444 \text{ (correlation coefficient} = 0.9918);$$

where y = R_o max. of a sample prepared by the 'thermoplastic' process

and x = R_o max. of the same coal mounted in a cold-setting resin.

Vitrinite reflectance determinations were repeated on three pairs of pellets by members of the Coal Technology Section and, while the absolute value of R_o max. varied by ±0.01%, the discrepancy between samples of the same coal was identical for each operator.

From: Scientific and Technical Notes in Current Research, Part C, Geol. Surv. Can., Paper 78-1C.

The above relationship indicates an increase in R_o max. of relatively low rank coals (high volatile bituminous and lower) by approximately 0.03% by heating to 110°C during sample preparation. While this appears to be quite a small error, it should be noted that the range of reflectance values determined on individual pellets of Hat Creek coal is generally less than 0.13% and R_o max. is repeatable to ± 0.01%. At this level of accuracy and in view of the small range of reflectance within the deposit (0.30%), this source of error is considered significant. In terms of a comparative rank study, it is particularly significant that the discrepancy is not constant. It was decided that all samples of Hat Creek lignite prepared for reflectance analyses would be mounted in cold-setting resin as would other coals used in detailed rank studies. For most industrial applications, this error is not significant and would have little effect on calculations of other chemical and physio-chemical parameters of the coal or on any decisions likely to be made during exploration or assessment of potential.

References

American Society for Testing and Materials
1977: 1977 Annual book of A.S.T.M. standards; Part 26, Standard D2797.

Harrison, J.A.
1965: Effect of moisture content on reflectance values of coal; Fuel, v. 44, p. 225-228.

Huck, G. and Karweil, J.
1955: Physikalisch-chemische Probleme der Inkohlung; Brennst. Chem., v. 36, p. 1-11.

International Committee for Coal Petrology
1963, 1971: International handbook of coal petrography; Centre National de la Récherce Scientifique, Paris (2nd ed., 1963; suppl. to 2nd ed., 1971).

Thomas, J., Jr. and Damberger, H.H.
1976: Internal surface area, moisture content and porosity of Illinois coals: variations with coal rank; Ill. State Geol. Surv., Circ. 493.

NOTE TO CONTRIBUTORS

Submissions to the *Discussion* section of *Current Research* are welcome from both the staff of the Geological Survey and from the public. Discussions are limited to 6 double-spaced typewritten pages (about 1500 words) and are subject to review by the Chief Scientific Editor. Discussions are restricted to the scientific content of Geological Survey reports. General discussions concerning branch or government policy will not be accepted. Illustrations will be accepted only if, in the opinion of the editor, they are considered essential. In any case no redrafting will be undertaken and reproducible copy must accompany the original submissions. Discussion is limited to recent reports (not more than 2 years old) and may be in either English or French. Every effort is made to include both *Discussion* and *Reply* in the same issue. *Current Research* is published in January, June and November. Submissions for these issues should be received not later than November 1, April 1, and September 1 respectively. Submissions should be sent to the Chief Scientific Editor, Geological Survey of Canada, 601 Booth Street, Ottawa, Canada, K1A 0E8.

CARMANVILLE MAP AREA, NEWFOUNDLAND; THE NORTHEASTERN END OF THE APPALACHIANS – DISCUSSION

W.D. Brückner
Department of Geology, Memorial University of Newfoundland, St. John's, Newfoundland, A1B 3X5

Manuscript received June 13, 1978

As the Carmanville area straddles the tectono-stratigraphic Zones F and G, or Botwood and Gander zones, of the northeastern Appalachians (Williams et al., 1972, 1974), the detailed study of its complex bedrock geology is of considerable general interest. The compact progress report on work in this area by Pickerill et al. (1978) clearly shows that much new information has been gathered recently despite the frustrating extensive cover of thick regolith and bog, and of dense forest. The new observations and inferences concerning the plutonic bodies, and the history of penetrative deformation and metamorphic changes, are especially praiseworthy. Yet the report also has aspects that call for a few critical comments. I shall deal with them under two headings.

Nomenclature

Pickerill et al. have assigned the nonintrusive rocks south of the Ragged Harbour Fault and west of the gneissic Flinns Tickle complex, i.e. the units 3 to 5 of their sketch map, to the "Gander Lake Group as defined by Kennedy and McGonigal" (1972) and those on the northwest side of the fault, i.e. their units 7 to 11, to the "Davidsville Group", also following Kennedy and McGonigal (1972), apart from a significant boundary correction in the northeast.

The term "Gander Lake Group" was introduced by Jenness (1958, 1963) in order to adapt the "Gander Lake Series" of Twenhofel (1947) to the recommendations of the American Commission of Stratigraphic Nomenclature (1956, 1961). This group, with the type section alongside Gander Lake, contained all nonintrusive rocks that underlie the area bounded roughly by Gander Bay in the northwest and Bonavista Bay in the southeast. Subsequently, Kennedy and McGonigal (1972) subdivided the rocks of this very broad group into three parts: (1) a "gneissic terrane" to the southeast and east (in the Carmanville area represented by the Flinns Tickle complex of Pickerill et al.); (2) a "metasedimentary terrane" in the central part of the region; and (3) a "sedimentary and volcanic terrane" to the northwest. They also assigned formal names to subdivisions (2) and (3), calling them the Gander Lake Group and Davidsville Group, respectively. Yet as restriction of a group name to only one of several subdivisions of the sequence which originally had that name contravenes a stipulation of the nomenclature commission just mentioned (1970, article 14(b)), I suggested at once that a name other than Gander Lake Group be chosen for the "metasedimentary terrane" (Brückner, 1972). Jenness (1972) also expressed concern about Kennedy and McGonigal's new divisions and interpretations, mentioning among several reasons that emphasis seemed to have been given to structural rather than stratigraphic criteria (op. cit., p. 1781). Faced with such critical statements, Kennedy and McGonigal quietly abandoned their incorrect and confusing redefinition of the Gander Lake Group, and their metasedimentary terrane was henceforth called the "Gander Group" (see e.g. McGonigal, 1972; Uzuakpunwa, 1973; Kennedy and Blackwood, 1974; Kennedy, 1975; Blackwood and Kennedy, 1975; Blackwood, 1977, 1978). It is most unfortunate, therefore, that Pickerill et al. have chosen to resurrect Kennedy and McGonigal's incorrect redefinition of the Gander Lake Group.

A further confusion results from the correction Pickerill et al. found necessary to make to the boundary between the (incorrectly redefined) Gander Lake Group and the Davidsville Group. In 1977, Currie and Pajari, two of Pickerill's co-authors, had cautiously spoken of the Gander and Davidsville "sequences", instead of "groups"; and because of the boundary correction, rocks of their Gander sequence have now become "metamorphosed equivalents of the Davidsville Group" (Pickerill et al., 1978, p. 210).

Clearly, such nomenclature confusion calls for rectification. It may suffice to explicitly reject again Kennedy and McGonigal's Gander Lake Group and to abandon explicitly Currie and Pajari's Gander sequence as well, adding concurrently a statement that the units 3 to 5 in the map legend of Pickerill et al. should have been assigned to the Gander Group as used since 1972 by other workers in the general region. It may be better, however, to use neither Gander Lake nor Gander again as names for stratigraphic or structural/metamorphic subdivisions in the tectono-stratigraphic Zones F and G of northeastern Newfoundland, and to introduce instead new, preferably still informal, names.

Furthermore, the term Davidsville Group should also be abandoned because "the gross structure and hence the stratigraphy" of the rocks currently assigned to this group "is imperfectly understood" (Pickerill et al., 1978, p. 211). The assumption that an allochthonous sheet (possibly an equivalent to the "Davidsville Nappe" of Uzuakpunwa, 1976) is present in the Carmanville area makes it clear that the stratigraphy of Kennedy and McGonigal's "sedimentary and volcanic terrane" is more complex than is thought at present (see below). Obviously, therefore, the use of a formal stratigraphic name is still inappropriate.

Interpretation of the "Sedimentary and Volcanic Terrane"

Despite their uncertainty about "the gross structure and ... stratigraphy", Pickerill et al. seem to be confident in assigning, in both text and map legend, definite consecutive stratigraphic positions to their units 6 (Gander River ultramafic belt) and 7 to 11 (Davidsville Group). Their map, however, appears to contradict this concept. For example, one band of unit 9 (conglomerate) lies between the (mainly shaly) units 10 and 11; another band of unit 9 lies inside unit 11; and neither band makes contact with unit 8 (olistostrome). Unit 8, moreover, touches unit 7 (mainly volcanics) only in the northwestern part of the area whereas another band of unit 8 lies within rocks of unit 11; and in the west, unit 8 has an even stranger relationship to units 7, 10, and 11. The field relationships, mention of an allochthonous sheet, and remarks on the significance of unit 8 (op. cit., p. 214) rather suggest that the true mutual relationships of the units 6 to 11 differ considerably from those given in the text and map legend.

The key to a more appropriate interpretation obviously is unit 8, which Currie and Pajari (1977) have already stated is "not a stratigraphic unit". In 1972, I found from personal observation that this unit is not an olistostrome consistent with the original definition of this term by Flores (1955), i.e. a mappable deposit of chaotic composition resulting from large-scale mass-wasting in a semifluid state, interbedded between "normal" strata of a sedimentary sequence. Instead, it is a "mélange" exhibiting the characteristic properties of

From: Discussions and Communications in Current Research, Part C; Geol. Surv. Can., Paper 78-1C.

"zones of chaotic structure" that lie beneath and between allochthonous tectonic slices such as have been found and described, e.g., in the West Newfoundland klippe (or "Humber Arm Allochthon") by Brückner (1966), Comeau (1972), Williams (1975), and others. Thus, where it is not strongly affected by metamorphism, unit 8 lacks diagenetic cementation of its constituent clasts whereas genuine olistostromes always show diagenetic changes closely matching those exhibited by the "normal" (i.e. non-chaotic) strata below and above them. (For other characteristics of "zones of chaotic structure", their association with flysch sequences, and the inferred mode of their origin and emplacement, see Brückner, 1975.)

By analogy with the clear relationships within the "Humber Arm Allochthon" (and of course also with those in other orogen segments containing "mélange" zones), the bands of unit 8 discernible in the Carmanville area should be interpreted as "zones of chaotic structure" that separate transported, allochthonous sheets or slices from one another and from an authochthonous terrane beneath them (although the latter may not be exposed or identifiable). By suggesting that an allochthonous sheet may be present, Pickerill et al. clearly were on the right track, but they should have gone further. Other transported sheets or slices no doubt exist in the area, and even the Gander River ultramafic belt with its strangely disrupted nature (see maps by Jenness, 1958) would seem to be an allochthonous body composed of mélange with "knockers" floating in it. Like the Bay-of-Islands ophiolite slabs crowning the West Newfoundland klippe, this belt probably represents relics of the uppermost transported slice of the region, and if so, it cannot be "continuous at depth" as assumed by Pickerill et al. (1978, p. 210). (Incidentally, the belt of much disrupted ultramafics and related rocks along the Baie Verte lineament in the tectono-stratigraphic Zone C (Fleur de Lys Zone) of Newfoundland (Williams et al., 1977; Williams and St. Julien, 1978) seems to represent a comparable (though also tectonically torn) allochthonous unit of "knockers" and mélange.)

Once they are mapped in detail, each of the transported slices separated by mélange zones should be found to have its individual stratigraphic sequence, probably with little differences existing between slices composed of shale-greywacke (flysch) sequences (units 10 and 11), and with a great contrast to be noted where a flysch-sequence slice, and one consisting of volcanics and related rocks (unit 7), are juxtaposed. In the course of the tectono-stratigraphic reassessment suggested, the stratigraphic position, mode of emplacement, and clast source(s) of the unit 9 conglomerate(s) would probably become identifiable more clearly as well.

By analogy with the geotectonic-environmental development inferred for the Humber Arm Allochthon (and similar examples), uplift and partial erosive dissection and disintegration of the terranes involved, continuing during subsequent gravity sliding and gradual stacking of transported slices derived from them, would have begun at some distance to the northwest. Penecontemporaneously, the finer-grained eroded material would gradually have been deposited farther southeast as the Arenig-to-Caradocian flysch sequence that now constitutes the bulk of the sedimentary terrane northwest of the Ragged Harbour Fault. Larger bodies formed by mass-wasting, however, would have become trapped between the moving slices and tectonically redistributed to form the intervening "zones of chaotic structure". Although starting from a misinterpretation of unit 8, Pickerill et al. (1978, p. 214) did visualize a somewhat comparable mega-tectonic development. I feel confident, however, that a modified interpretation such as suggested above can be established despite the difficulties arising (beside scarcity of exposures) from the effects of a second orogeny, intrusion of plutons, and concomitant metamorphism throughout the tectono-stratigraphic zones of which the Carmanville area is part.

References

American Commission on Stratigraphic Nomenclature

1956: Report 4 — Nature, usage and nomenclature of rock-stratigraphic units; Am. Assoc. Pet. Geol. Bull., v. 40, p. 2003-2014.

1961: Code of stratigraphic nomenclature; Am. Assoc. Pet. Geol. Bull., v. 45, p. 645-665.

1970: Code of stratigraphic nomenclature (2nd ed.); Am. Assoc. Pet. Geol., 21 p.

Blackwood, R.F.

1977: Geology of the Hare Bay area, northwestern Bonavista Bay; Newfoundland Dep. Mines, Energy; Min. Dev. Div. Rep. 77-1, p. 7-14.

1978: Northeastern Gander Zone, Newfoundland; Newfoundland Dep. Mines, Energy; Min. Dev. Div. Rep. 78-1, p. 72-79.

Blackwood, R.F. and Kennedy, M.J.

1975: The Dover Fault: western boundary of the Avalon Zone in northeastern Newfoundland; Can. J. Earth Sci., v. 12, p. 320-325.

Brückner, W.D.

1966: Stratigraphy and structure of west-central Newfoundland: Geol. Mineral. Assoc. Can., Ann. Mtg., Halifax, Nova Scotia; Guidebook, Geology of parts of Atlantic Provinces, p. 137-155.

1972: The Gander Lake and Davidsville Groups of northeastern Newfoundland: new data and geotectonic implications: discussion; Can. J. Earth Sci., v. 9, p. 1778-1779.

1975: Origin of "Zones of Chaotic Structure" in certain orogenic belts: IXth Int. Congr. Sedimentology, Nice; theme 4, v. 1, p. 33-39.

Comeau, R.L.

1972: Transported slices of the coastal complex, Bay of Islands, western Newfoundland; unpubl. M.Sc. thesis, Memorial University of Newfoundland, St. John's, Newfoundland, 105 p.

Currie, K.L. and Pajari, G.E., Jr.

1977: Igneous and metamorphic rocks between Rocky Bay and Ragged Harbour, northeastern Newfoundland; in Report of Activities, Part A, Geol. Surv. Can., Paper 77-1A, p. 341-345.

Flores, G.

1955: Discussion: IVth World Petroleum Congr. Proc., sect. I, v. 1, p. 120-121.

Jenness, S.E.

1958: Geology of the Gander River ultrabasic belt, Newfoundland; Geol. Surv. Newfoundland, Rep. 11, 58 p.

1963: Terra Nova and Bonavista map-areas, Newfoundland; Geol. Surv. Can., Mem. 327, 184 p.

1972: The Gander Lake and Davidsville Groups of northeastern Newfoundland: new data and geotectonic implications: discussion; Can. J. Earth Sci., v. 9, p. 1779-1781.

Kennedy, M.J.

1975: Repetitive orogeny in the northeastern Appalachians — new plate models based upon Newfoundland examples; Tectonophysics, v. 28, p. 39-87.

Kennedy, M.J. and Blackwood, R.F.
1974: Polydeformed metamorphic belts on the southeastern and northwestern margins of the Newfoundland Central Mobile Belt; Geol. Mineral. Assoc. Can., Ann. Mtg., St. John's, Newfoundland, Fieldtrip Manual B-7, 52 p.

Kennedy, M.J. and McGonigal, M.H.
1972: The Gander Lake and Davidsville Groups of northeastern Newfoundland: new data and geotectonic implications; Can. J. Earth Sci., v. 9, p. 452-459.

McGonigal, M.H.
1972: The Gander and Davidsville Groups: major tectonostratigraphic units in the Gander Lake area, Newfoundland; unpubl. M.Sc. thesis, Memorial University of Newfoundland, St. John's, Newfoundland, 121 p.

Pickerill, R.K., Pajari, G.E., Jr., Currie, K.L., and Berger, A.R.
1978: Carmanville map area, Newfoundland; the northeastern end of the Appalachians; in Current Research, Part A, Geol. Surv. Can., Paper 78-1A, p. 209-216.

Twenhofel, W.H.
1947: The Silurian of eastern Newfoundland with some data relating to physiography and Wisconsin glaciation of Newfoundland; Am. J. Sci., v. 245, p. 65-122.

Uzuakpunwa, A.B.
1973: Structural studies of the Gander and Davidsville Groups in the Carmanville – Ladle Cove areas, Newfoundland; unpubl. M.Sc. thesis, Memorial University of Newfoundland, St. John's, Newfoundland, 141 p.

1976: The emplacement of the Middle Ordovician Davidsville Nappe, northeastern Newfoundland: its bearing on the plate tectonic evolution of Newfoundland Appalachians; Geol. Soc. Am., Abstr., v. 8, p. 290-291.

Williams, H.
1975: Structural succession, nomenclature, and interpretation of transported rocks in western Newfoundland; Can. J. Earth Sci., v. 12, p. 1874-1894.

Williams, H., Kennedy, M.J., and Neale, E.R.W.
1972: The Appalachian structural province; in Price, R.A., and Douglas, R.J.W. (editors): Tectonic styles in Canada; Geol. Assoc. Can., Spec. Paper 11, p. 181-261.

1974: The northeastward termination of the Appalachian orogen; in Nairn, A.E.M., and Stehli, F.G. (editors): The ocean and basins and margins; v. 2, p. 79-123.

Williams, H., Hibbard, J.P., and Bursnall, J.T.
1977: Geological setting of asbestos-bearing ultramafic rocks along the Baie Verte lineament, Newfoundland; in Report of Activities, Part A, Geol. Surv. Can., Paper 77-1A, p. 351-360.

Williams, H. and St. Julien, P.
1978: The Baie Verte – Brompton line in Newfoundland and regional correlations in the Canadian Appalachians; in Current Research, Part A, Geol. Surv. Can., Paper 78-1A, p. 225-229.

From: Discussions and Communications in Current Research, Part C; Geol. Surv. Can., Paper 78-1C.

CARMANVILLE MAP AREA, NEWFOUNDLAND; THE NORTHEASTERN END OF THE APPALACHIANS – REPLY

R.K. Pickerill, G.E. Pajari
University of New Brunswick, Fredericton, New Brunswick, E3B 5A3

K.L. Currie
Geological Survey of Canada, Ottawa, Ontario, K1A 0E8

A.R. Berger
Memorial University of Newfoundland, St. John's, Newfoundland, A1B 3X5

Introduction

The policy and general philosophy of this Geological Survey of Canada Publication is perhaps best summarized in the anonymous introduction to Paper 74-1 Part A which states that... "Many of the conclusions presented in this publication are based on a preliminary assessment of the data collected and are subject to confirmation or revision" ... In our report (Pickerill et al., 1978) we presented the pertinent observations of our mapping in the summer of 1977 in the Carmanville map area, northeastern Newfoundland, research which is still incomplete and is still being continued. The criticisms raised by Brückner are essentially twofold: stratigraphic nomenclature and interpretation of the sedimentary and volcanic terrane. Since the preliminary report was neither an appropriate nor sufficient vehicle for discussion of these involved problems we welcome this opportunity to expand our previous statements.

Stratigraphic Nomenclature

Many differences exist in stratigraphic philosophy; some are national or regional, others are the result of differing professional backgrounds and others are a result of the problems faced (Hedburg, 1972a). This is hardly surprising as stratigraphy is a dynamic science and new concepts are continually being evolved. Lithostratigraphic units, those with which we are concerned here, are objective or observational units and irrespective of their rank in classification are characterized by a distinctive lithologic type or package of lithologic types. Because, in part, this particular research program was formulated under the auspices of the International Geological Correlation Programme (IGCP), our stratigraphic nomenclature was employed using guidelines proposed by the International Subcommission on Stratigraphic Classification (ISSC). The lithostratigraphic guidelines were published in 1970 (ISSC Report 3) and subsequently summarized in Hedburg (1972b, 1976).

The nomenclatural problems and their historical development in this part of northeastern Newfoundland have been succinctly summarized by Brückner. Essentially he recommends that both terms Gander Lake Group and Davidsville Group of Kennedy and McGonigal (1972a) and ourselves (Pickerill et al., 1978; Pajari and Currie, 1978; Pajari et al., in press) be abandoned, the former because it contravened Article 14(b) of the Code of the American Commission on Stratigraphic Nomenclature and the latter because we had stated that "...the gross structure and hence the stratigraphy of the Davidsville Group is imperfectly understood...". We will therefore consider each of these in turn.

Gander Lake Group

When Kennedy and McGonigal (1972a) defined the Gander Lake Group for their 'metasedimentary terrane' or 'lower division' of Jenness' (1958) tripartite Gander Lake Group they undoubtedly contravened the Code of the

American Commission on Stratigraphic Nomenclature, as Brückner (1972) correctly pointed out. The immediate discussion raised by Brückner (1972) and Jenness (1972) was defended by Kennedy and McGonigal (1972b) who, furthermore, continued to utilize Gander Lake Group in their original sense. Subsequent workers, however 'quietly abandoned' this incorrect and confusing definition and, instead, adopted the term Gander Group (e.g. Kennedy and Blackwood, 1974; Blackwood and Kennedy, 1975; Kennedy, 1975, 1976). This 'quiet abandonment' and subsequent adoption of an alternative nomenclature contravenes all known stratigraphic codes because "...the revision or redefinition of an established stratigraphic unit requires as much justification as the establishment of a new unit..." (ISSC 5•5 – Hedburg, 1972b). Since the establishment of a formal stratigraphic division requires definition and publication in a 'recognized scientific medium', which has thus far not been attempted, adopting the term Gander Group as used since 1972 (as recommended by Brückner) simply creates more confusion and contravenes, even further, acceptable stratigraphic codes because, for example, ISSC 5•4 suggests that "priority...of a defined unit should be respected". In our report (Pickerill et al., p. 209, 1978) we made it perfectly clear that we had adopted Gander Lake Group in the sense of Kennedy and McGonigal, thus avoiding the improper usage of 'Gander Group' as a recognizable stratigraphic unit but also implying that Kennedy and McGonigal's definition, although erroneous, was still the most recently formalized. It may well be, as Brückner suggests, that eventually we will revise the stratigraphic terminology once our research is complete – until that time we are forced to adopt the lesser of the two evils.

Davidsville Group

Kennedy and McGonigal (1972a) defined the Davidsville Group as a distinctive assemblage of lithofacies found between the Gander Lake Group to the southeast and the Silurian Botwood and Indian Island groups to the northwest, encompassing the 'middle' and 'upper units' of Jenness' (1958) Gander Lake Group. Though Jenness (1972) suggested the term should be rejected his reasoning was unsound and subsequent workers in a variety of geological disciplines have continued its adoption (e.g. Kennedy and Blackwood, 1974; Kennedy, 1975, 1976; Bell et al., 1977; Rast et al., 1976; Strong and Dickson, 1978; etc.). More recently two of us (Pajari and Currie, 1978) examined the term in detail and concurred that it was a useful stratigraphic description for the assemblage of black, green and maroon slates, greywackes and conglomerates and basal volcanic rocks in this area.

Brückner's main objection stems from our statement that "the gross structure and hence the stratigraphy is imperfectly understood". This statement still remains true but when we made it (Pickerill et al., 1978, p. 211), we were referring to a more detailed stratigraphic understanding within the Davidsville Group – because of this we made no attempt to refine the stratigraphy and merely designated lithologic units numerically. The internal stratigraphy is extremely complex, but this still does not preclude assignation of the total distinctive package to the Davidsville Group.

Usually, if there are conflicts in stratigraphic terminology it is often necessary to fall back on the test of usage. If a term is not useful it will die out and, moreover, leaving the decision to the test of usage avoids any suggestion of unjust suppression. As Hedburg (1972b) points out, "Priority of a properly proposed, named and defined unit should be respected... the critical factors should always be the usefulness of the unit, the adequacy of its description, the freedom from ambiguity, and the suitability for widespread application" (ISSC 5•4). We, as apparently others, believe that the term Davidsville Group, fulfills all these prerequisites and is a clearly suitable and applicable term and therefore prefer to retain it.

Interpretation of the Sedimentary and Volcanic Terrane

The assumption that our numerically designated units in Pickerill et al. (1978) were consecutive stratigraphic units was incorrect. In fact it is specifically stated in both text and map legend that this is not the case although "as far as possible map units (were) fitted into their appropriate chronological position" (Blackadar et al., 1975). The criticism of Brückner (1978) therefore rests on his misunderstanding that numerical units represented both a chronostratigraphy and lithostratigraphy sensu stricto, whereas the former by necessity sensu lato.

Brückner's major criticism is directed towards our interpretation of unit 8 as an olistostrome and claims that "...it is a 'mélange' exhibiting the characteristic properties of 'zones of chaotic structure' that lie beneath and between allochthonous tectonic slices...". We agree that unit 8 is a mélange but not that it is a 'zone of chaotic structure' as defined by Brückner (1966, 1975). By stating that mélanges occurred in definitive tectonic positions in association with nappes and tectonic slides Brückner (ibid.), perhaps inadvertently, introduced certain genetic (tectonic) implications as to the origin of zones of chaotic structure! We have subsequently presented (Pajari et al., in press) a detailed description and evidence to substantiate our general conclusion that the mélange unit 8 is sedimentary and not tectonic in origin, and the reader is referred to this paper for a more detailed appraisal. Admittedly, the distinction between the two can be difficult since both tend to be associated with trench slopes at active convergent plate margins (e.g. Dickinson, 1971, 1973; Seely et al., 1974; White and Klitgord, 1976), where olistostromes can subsequently undergo a mélanging process by moving into the subduction zone or, alternatively, mélanged terrain exposed on a trench inner slope can fail gravitationally to form an olistostrome (see Moore et al., 1976). Nevertheless, the following general observations lead us to conclude that the mélange is sedimentary in origin:-

1) Contrary to the preliminary observation of Currie and Pajari (1977) that the mélange was not a stratigraphic unit, more detailed mapping has revealed that it does occupy a definitive stratigraphic position in the upper part of the Davidsville Group.
2) The mélange is overlain and underlain by deep-water marine sediments of approximately the same age.
3) Underlying sediments exhibit soft-rock (hydroplastic) deformation features.
4) The argillaceous matrix of the mélange exhibits soft-rock deformation.
5) Blocks within the mélange have rotated around inconstant axes during the movement of the mass.
6) The deformation style exhibited by the mélange is inconsistent with a tectonic origin. Moreover, upper and lower contacts are not bounded by shear surfaces (see Hsü, 1974).

These observations are consistent with the original definition of an olistostrome by Flores (1955) and are criteria commonly employed in their recognition (see Abbate et al., 1970). Furthermore, unit 8 only represents the presently known distribution of the 'matrix' of the mélange, where both pelitic matrix and chaotically ordered but recognizable olistoliths can be discerned. Further mapping, particularly to the southwest, may reveal other 'matrix' horizons and it may well be that the Davidsville Group in toto is a mega-mélange, as suggested by Williams (1978, pers. comm.).

There is no direct evidence to suggest that the mélange separates and is associated with allochthonous sheets or slices, as Brückner suggests. Indeed, his presupposition that allochthonous slices similar to the Bay-of-Islands ophiolite slabs and Humber Arm Allochthon is probably erroneous. For example, he states that the Gander River ultramafic belt "probably represents relics of the uppermost transported slice ...and cannot be continuous at depth as assumed by Pickerill et al. (1978, p. 210)". However, geophysical studies conducted by H.G. Miller in conjunction with ourselves clearly demonstrate that this belt is, in fact, continuous at depth and underlies the Davidsville Group.

In our opinion, attempts to model the Carmanville area by analogy to the Humber Arm Allochthon, or by analogy to any other area for that matter, are premature. When the present study is complete we hope that it will define a tectonic model appropriate to this region. In times when the geologic model has attained its peak in popularity, as particularly exemplified in Newfoundland, we can only hope that it is the model and not the geology that is discarded when the two disagree.

References

Abbate, E., Bortolotti, V., and Passerini, P.
1970: Olistostromes and olistoliths; in Development of the Northern Apennines Geosyncline, G. Sestini (Ed.); Sediment. Geol., v. 4, p. 521-558.

Bell, K., Blenkinsop, J., and Strong, D.F.
1977: The geochronology of some granitic bodies from eastern Newfoundland and its bearing on Appalachian evolution; Can. J. Earth Sci., v. 14, p. 456-476.

Blackadar, R.G., Dumych, H., and Griffin, P.J.
1975: Guide to authors – A guide for the preparation of geological maps and reports; Geol. Surv. Can., Misc. Rep. 16, 199 p.

Blackwood, R.F. and Kennedy, M.J.
1975: The Dover Fault: Western boundary of the Avalon Zone in northeastern Newfoundland; Can. J. Earth Sci., v. 12, p. 320-325.

Brückner, W.D.
1966: Stratigraphy and structure of west-central Newfoundland. Geol. Mineral. Assoc. Can., Ann. Mtg., Halifax, Nova Scotia; Guidebook, Geology of parts of Atlantic Provinces, p. 137-155.

1972: The Gander Lake and Davidsville groups of northeastern Newfoundland: New data and geotectonic implications: Discussion; Can. J. Earth Sci., v. 9, p. 1778-1779.

1975: Origin of "Zones of Chaotic Structure" in certain orogenic belts; IXth Int. Congr. Sedimentology, Nice; Theme IV, p. 33-39.

1978: Carmanville map area, Newfoundland; the northeastern end of the Appalachians – Discussion; in Current Research, Part C, Geol. Surv. Can., Paper 78-1C.

Currie, K.L. and Pajari, G.E., Jr.
1977: Igneous and metamorphic rocks between Rocky Bay and Ragged Harbour, northeastern Newfoundland; in Report of Activities, Part A, Geol. Surv. Can., Paper 77-1A, p. 341-345.

Dickinson, W.R.
1971: Clastic sedimentary sequences deposited in shelf, slope and trough settings between magmatic arcs and associated trenches; Pacific Geol., v. 3, p. 15-30.

Dickinson, W.R. (cont'd.)
1973: Widths of modern arc-trench gaps proportional to past duration of igneous activity in associated magmatic arcs; J. Geophys. Res., v. 78, p. 3376-3389.

Flores, G.
1955: Discussion of paper by E. Beneo; in Fourth World Pet. Congr., Sect. 1, p. 121-122.

Hedburg, H.D. (ed.)
1972a: Introduction to an International Guide to Stratigraphic Classification, Terminology, and Usage; Lethaia, v. 5, p. 283-295.

1972b: Summary of an International Guide to Stratigraphic Classification, Terminology, and Usage; Lethaia, v. 5, p. 297-323.

1976: International Stratigraphic Guide. A Guide to the Stratigraphic Classification, Terminology and Procedure; International Subcommission on Stratigraphic Classification (ISSC); John Wiley and Sons, 200 p.

Hsü, K.
1974: Mélanges and their distinction from olistostromes; in Modern and Ancient Geosynclinal Sedimentation, R.H. Dott, Jr. (Ed.); Soc. Econ. Paleontol. Mineral., Spec. Publ. 19, p. 321-333.

ISSC Report 3
1970: Preliminary report on Lithostratigraphic Units; 24th Int. Geol. Congr. (Canada), 30 p.

Jenness, S.E.
1958: Geology of the Lower Gander River ultrabasic belt; Geol. Surv. Newfoundland, Rep. 14, 58 p.

1972: The Gander Lake and Davidsville Groups of Northeastern Newfoundland: New Data and Geotectonic Implications: Discussion; Can. J. Earth Sci., v. 9, p. 1779-1781.

Kennedy, M.J.
1975: Repetitive orogeny in the northeastern Appalachians – new plate models based upon Newfoundland examples; Tectonophysics, v. 28, p. 39-87.

1976: Southeastern margin of the northeastern Appalachians: Late Precambrian orogeny on a continental margin; Geol. Soc. Am. Bull., v. 87, p. 1317-1325.

Kennedy, M.J. and Blackwood, R.F.
1974: Polydeformed metamorphic belts on the southeastern and northwestern margins of the Newfoundland Central Mobile Belt: Geol. Mineral. Assoc. Can., Ann. Mtg., St. John's, Newfoundland; Fieldtrip Manual B-7, 52 p.

Kennedy, M.J. and McGonigal, M.H.
1972a: The Gander Lake and Davidsville Groups of northeastern Newfoundland: New Data and Geotectonic Implications; Can. J. Earth Sci., v. 9, p. 453-459.

1972b: The Gander Lake and Davidsville Groups of northeastern Newfoundland: New Data and Geotectonic Implications: Reply; Can. J. Earth Sci., v. 9, p. 1781-1783.

McKerrow, W.S. and Cocks, L.R.M.
1977: The location of the Iapetus Ocean suture in Newfoundland; Can. J. Earth Sci., v. 14, p. 488-495.

Moore, D.G., Curray, J.R., and Emmel, F.J.
1976: Large submarine slide (olistostrome) associated with Sundra Arc subduction zone, northeast Indian Ocean; Marit. Geol., v. 21, p. 211-226.

Page, B.M.
1978: Franciscan mélanges compared with olistostromes of Taiwan and Italy; in K.L. Burns and R.W.R. Rutland (Eds.). Structural Characteristics of Tectonic Zones; Tectonophysics, v. 47, p. 223-246.

Pajari, G.E., Jr., Pickerill, R.K., and Currie, K.L.
The nature, origin and significance of the Carmanville Mélange, northeastern Newfoundland; Can. J. Earth Sci., v. 16. (in press)

Pajari, G.E., Jr. and Currie, K.L.
1978: The Gander Lake and Davidsville Groups of northeastern Newfoundland: a re-examination; Can. J. Earth Sci., v. 15, p. 708-714.

Pickerill, R.K., Pajari, G.E., Jr., Currie, K.L., and Berger, A.R.
1978: Carmanville map area, Newfoundland; the northeastern end of the Appalachians; in Current Research, Part A, Geol. Surv. Can., Paper 78-1A, p. 209-216.

Rast, N., Kennedy, M.J., and Blackwood, R.F.
1976: Comparison of some tectonostratigraphic zones in the Appalachians of Newfoundland and New Brunswick; Can. J. Earth Sci., v. 13, p. 868-875.

Seely, D.R., Vail, P.R., and Walton, G.G.
1974: Trench Slope Model; in Geology of Continental Margins, C.A. Burke and C.L. Drake (Eds.), p. 249-260.

Strong, D.F. and Dickson, W.L.
1978: Geochemistry of Paleozoic granitoid plutons from contrasting tectonic zones of northeast Newfoundland; Can. J. Earth Sci., v. 15, p. 145-156.

White, R.S. and Klitgord, K.
1976: Sediment deformation and plate tectonics in the Gulf of Oman; Earth Planet. Sci. Lett., v. 32, p. 199-209.

AUTHOR INDEX

	Page
Balkwill, H.R.	35
Blake, W., Jr.	119
Bonardi, M.	113
Bornhold, B.D.	108
Brückner, W.D.	127
Christie, K.W.	1
Clowes, R.M.	29
Conaway, J.G.	19
Creaney, S.	101
Eade, K.E.	7
Fabbri, A.G.	123
Fahrig, W.F.	1
Freda, G.	1
Frith, R.A.	89
Geldsetzer, H.H.J.	43
Grant, A.C.	118
Haimila, N.E.	35
Heywood, W.W.	79
Hills, L.V.	63
Hinz, K.	118
Hunter, J.A.	13
Judge, A.S.	13
Kasvand, T.	123
Lynch, S.	29
MacAulay, H.A.	13
Marchioni, D.L.	125
Monger, J.W.H.	113
Neave, K.G.	13
Pajari, G.E.	129
Percival, J.A.	89
Pickerill, R.K.	129
Plant, A.G.	113
Poulton, T.P.	39
Richard, S.H.	23
Richardson, R.J.	105
Roberts, A.C.	49, 104
Schluter, H.-U.	118
Srivastava, S.P.	118
Stray, J.H.	123
Swift, S.A.	99
Tan, J.T.	63
Tella, S.	71, 79
Thorleifson, A.J.	29
Tipnis, R.S.	75
Umpleby, D.	118
Vilks, G.	99
Vincent, J.-S.	53
Woodside, J.	118